

# Scientific Drilling

Reports on Deep Earth Sampling and Monitoring



**Towards an integrated system  
understanding for the Early Jurassic**

**1**

**Sediments from a glacially  
overprinted valley in Switzerland**

**27**

**Effects of drilling tools on sediment  
lithification and physical properties**

**43**

**Poor Man's Line Scan**

**55**

**Drilling Pliocene lakes in western  
North America**

**61**

**Drilling Nicaraguan Lakes: bridging  
continents and oceans**

**73**

**Planning for the Lake Izabal Basin  
Research Endeavor**

**85**

**Mission-specific platform approaches  
to assessing natural hazards**

**101**

**Deep-time Arctic climate archives**

**113**

Dear Reader,

We are thrilled to announce that, after 18 years, our journal *Scientific Drilling* is listed for the first time with an impact factor (1.2) in the Web of Science from Clarivate Analytics. The Editorial Board is very grateful to all the authors, reviewers, and Copernicus Publications for their dedicated work in contributing to the success of our journal and for reaching this important milestone. We look forward to publishing more exciting, innovative, and open-access research from all fields of scientific marine, continental, and ice drilling.

The focus of this issue of *Scientific Drilling* (Vol. 32) is on paleoclimate archives with two Scientific Reports on drilling activities in Europe and five Workshop Reports on various drilling targets in North and Central America, the high-Arctic Svalbard Archipelago, and the use of mission-specific platforms to assess natural hazards. The volume also includes a Scientific Report on the effect of coring on carbonate properties and a Technical Development paper on a low-cost alternative for producing drill core scans.

A paper – Drilling for the Early Jurassic Earth System and Timescale (**p. 1**) – reports initial results on a fully integrated and astronomically calibrated timescale for this incisive period in Earth's history. Results from drilling glacially overdeepened valley sediments in the northern Alpine foreland (**p. 27**) help to better understand past, ongoing and future changes in the pan-Alpine area. **P. 43** highlights the importance of carefully considering the choice of sampling techniques when planning marine carbonate sediment sampling programmes and interpreting subsequent analyses.

The PlioWest workshop report (**p. 61**) selected optimal drill sites in the western USA to resolve contradicting observations between a Pliocene that was warmer and largely wetter than today. At the NicaBRIDGE workshop (**p. 73**), scientists discussed scientific drilling in Nicaraguan lakes to obtain long lacustrine sediment records. At the LIBRE workshop (**p. 85**), scientists discussed ways to gain maximum information on seismicity and environmental change in the northern Neotropics. The SVALCLIME workshop (**p. 113**) focused on geological records preserved on the Svalbard Archipelago to elucidate deep-time climate change events from the late Precambrian to the Paleogene. Finally, the **p. 101** workshop report defined questions about natural hazards to be tested with IODP mission-specific platforms.

Scientific progress is often driven by new technologies or access to facilities. In this issue, the **p. 55** technical development article describes how to use smartphone technique as a centrepiece of a low-cost drill-core scanner to be manufactured as a DIY project. With this issue we also send a very warm welcome to the new editor Nadine Hallmann and send our sincere gratitude to the outgoing editor Jan Behrmann.

We wish our readers some inspiring and relaxing time with this issue of *Scientific Drilling*.

With best regards,  
the editors of *Scientific Drilling*

**Ulrich Harms, Thomas Wiersberg, Nadine Hallmann,  
Tomoaki Morishita, and Will Sager**

## Aims & scope

**Scientific Drilling (SD)** is a multidisciplinary journal focused on bringing the latest science and news from the scientific drilling and related programmes to the geosciences community. *Scientific Drilling* delivers peer-reviewed science reports from recently completed and ongoing international scientific drilling projects. The journal also includes reports on engineering developments, technical developments, workshops, progress reports, and news and updates from the community.

## Editorial board

Ulrich Harms (editor in chief),  
Thomas Wiersberg, Nadine Hallmann,  
Will Sager, and Tomoaki Morishita



[sd-editors-in-chief@mailinglists.copernicus.org](mailto:sd-editors-in-chief@mailinglists.copernicus.org)

## Additional information



ISSN 1816-8957 | eISSN 1816-3459

### Copernicus Publications

Bahnhofsallee 1e  
37081 Göttingen  
Germany  
Phone: +49 551 90 03 39 0  
Fax: +49 551 90 03 39 70

[editorial@copernicus.org](mailto:editorial@copernicus.org)  
[production@copernicus.org](mailto:production@copernicus.org)

<https://publications.copernicus.org>

View the online library or learn  
more about *Scientific Drilling* on:  
**[www.scientific-drilling.net](http://www.scientific-drilling.net)**

**Cover figure:** The JET (p. 1) Drill Rig in action at night (Photograph by Jim Riding).

**Insert 1:** A biostratigraphically significant ammonite (Photograph by Amy Elson) from Prees Core, JET project (p. 1).

**Insert 2:** The Permian-Triassic research drilling in Deltadalen, Svalbard using a helicopter-transportable drill rig. Photograph by Sverre Planke (p. 113).



## Science Reports

- 1** **Initial results of coring at Prees, Cheshire Basin, UK (ICDP JET Project); towards an integrated stratigraphy, timescale, and Earth system understanding for the Early Jurassic**  
S. Hesselbo et al.
- 27** **Drilling into a deep buried valley (ICDP DOVE): A 252 m long sediment succession from a glacial overdeepening in northwestern Switzerland**  
S. Schaller et al.
- 43** **Coring tools have an effect on lithification and physical properties of marine carbonate sediments**  
D. De Vleeschouwer et al.

## Technical Developments

- 55** **Poor Man's Line Scan – a simple tool for the acquisition of high-resolution, undistorted drill core photos**

## Workshop Reports

- 61** **Workshop report: PlioWest – drilling Pliocene lakes in western North America**
- 73** **Workshop on Drilling the Nicaraguan Lakes: Bridging Continents and Oceans (NICA-BRIDGE)**
- 85** **Planning for the Lake Izabal Basin Research Endeavor (LIBRE) continental scientific drilling project in eastern Guatemala**
- 101** **MagellanPlus Workshop: Mission-specific platform approaches to assessing natural hazards that impact society**
- 113** **Deep-time Arctic climate archives: High-resolution coring of Svalbard's sedimentary record – SVALCLIME, a workshop report**



# Initial results of coring at Prees, Cheshire Basin, UK (ICDP JET project): towards an integrated stratigraphy, timescale, and Earth system understanding for the Early Jurassic

Stephen P. Hesselbo<sup>1</sup>, Aisha Al-Suwaidi<sup>2</sup>, Sarah J. Baker<sup>3</sup>, Giorgia Ballabio<sup>4</sup>, Claire M. Belcher<sup>3</sup>, Andrew Bond<sup>5</sup>, Ian Boomer<sup>6</sup>, Remco Bos<sup>7</sup>, Christian J. Bjerrum<sup>8</sup>, Kara Bogus<sup>1</sup>, Richard Boyle<sup>3</sup>, James V. Browning<sup>9</sup>, Alan R. Butcher<sup>10</sup>, Daniel J. Condon<sup>11</sup>, Philip Copestake<sup>12</sup>, Stuart Daines<sup>3</sup>, Christopher Dalby<sup>1</sup>, Magret Damaschke<sup>11</sup>, Susana E. Damborenea<sup>13</sup>, Jean-Francois Deconinck<sup>14</sup>, Alexander J. Dickson<sup>5</sup>, Isabel M. Fendley<sup>15</sup>, Calum P. Fox<sup>16</sup>, Angela Fraguas<sup>17</sup>, Joost Frieling<sup>15</sup>, Thomas A. Gibson<sup>1</sup>, Tianchen He<sup>18</sup>, Kat Hickey<sup>1</sup>, Linda A. Hinnov<sup>19</sup>, Teuntje P. Hollaar<sup>1,3</sup>, Chunju Huang<sup>20</sup>, Alexander J. L. Hudson<sup>1</sup>, Hugh C. Jenkyns<sup>15</sup>, Erdem Idiz<sup>15</sup>, Mengjie Jiang<sup>1</sup>, Wout Krijgsman<sup>7</sup>, Christoph Korte<sup>8</sup>, Melanie J. Leng<sup>11</sup>, Timothy M. Lenton<sup>3</sup>, Katharina Leu<sup>21</sup>, Crispin T. S. Little<sup>22</sup>, Conall MacNiocaill<sup>15</sup>, Miguel O. Manceñido<sup>13</sup>, Tamsin A. Mather<sup>15</sup>, Emanuela Mattioli<sup>23</sup>, Kenneth G. Miller<sup>9</sup>, Robert J. Newton<sup>23</sup>, Kevin N. Page<sup>1</sup>, József Pálffy<sup>24,25</sup>, Gregory Pieńkowski<sup>26,†</sup>, Richard J. Porter<sup>1</sup>, Simon W. Poulton<sup>22</sup>, Alberto C. Riccardi<sup>13</sup>, James B. Riding<sup>11</sup>, Ailsa Roper<sup>22</sup>, Micha Ruhl<sup>27</sup>, Ricardo L. Silva<sup>28</sup>, Marisa S. Storm<sup>29</sup>, Guillaume Suan<sup>23</sup>, Dominika Szűcs<sup>1</sup>, Nicolas Thibault<sup>8</sup>, Alfred Uchman<sup>30</sup>, James N. Stanley<sup>9</sup>, Clemens V. Ullmann<sup>1</sup>, Bas van de Schootbrugge<sup>7</sup>, Madeleine L. Vickers<sup>31</sup>, Sonja Wadas<sup>21</sup>, Jessica H. Whiteside<sup>32</sup>, Paul B. Wignall<sup>22</sup>, Thomas Wonik<sup>21</sup>, Weimu Xu<sup>4</sup>, Christian Zeeden<sup>21</sup>, and Ke Zhao<sup>20</sup>

<sup>1</sup>Camborne School of Mines, Department of Earth and Environmental Sciences, University of Exeter, Penryn Campus, Penryn, Cornwall, TR10 9FE, UK

<sup>2</sup>Department of Earth Sciences, Khalifa University of Science and Technology, P.O. Box 12333, Abu Dhabi, UAE

<sup>3</sup>Department of Geography, Laver Building, University of Exeter, North Park Road, Exeter, EX4 4QE, UK

<sup>4</sup>School of Earth Sciences and SFI Research Centre in Applied Geosciences (iCrag), University College Dublin, Dublin 4, Ireland

<sup>5</sup>Centre of Climate, Ocean and Atmosphere, Department of Earth Sciences, Royal Holloway University of London, Surrey, TW20 0EX, UK

<sup>6</sup>Geosciences Research Group, School of Geography, Earth and Environmental Sciences, University of Birmingham, Birmingham, B15 2TT, UK

<sup>7</sup>Department of Earth Sciences, Utrecht University, Marine Palynology and Paleooceanography, Princetonlaan 8a, 3584, CB, Utrecht, the Netherlands

<sup>8</sup>Department of Geosciences and Natural Resource Management, University of Copenhagen, Øster Voldgade 10, 1350 Copenhagen-K, Denmark

<sup>9</sup>Department of Earth and Planetary Sciences, Rutgers, the State University of New Jersey, 610 Taylor Road, Piscataway, NJ 08854-8066, USA

<sup>10</sup>Geological Survey of Finland, Espoo, 02151, Finland

<sup>11</sup>British Geological Survey, Keyworth, Nottingham, NG12 5GG, UK

<sup>12</sup>Merlin Energy Resources Ltd., Newberry House, Ledbury, Herefordshire, HR8 2EJ, UK

<sup>13</sup>División Paleozoología Invertebrados, Facultad de Ciencias Naturales y Museo, Universidad Nacional de La Plata, Argentina, CONICET, Paseo del Bosque S/N 1900, La Plata, Argentina

<sup>14</sup>Biogeosciences, UMR 6282, UBFC/CNRS, Université Bourgogne Franche-Comté, 6 Boulevard Gabriel, 21000 Dijon, France



- <sup>15</sup>Department of Earth Sciences, University of Oxford, Oxford, OX1 3AN, UK
- <sup>16</sup>Biogeochemistry Center, Japan Agency for Marine–Earth Science and Technology,  
2-15 Natsushima-cho Yokosuka 237-0061, Japan
- <sup>17</sup>Dpto. Biología y Geología, Física y Química Inorgánica y Grupo de Investigación en Dinámica  
de la Tierra y Evolución del Paisaje (Dynamical), ESCET, Universidad Rey Juan Carlos,  
C/Tulipán s/n, 28933 Móstoles, Madrid, Spain
- <sup>18</sup>College of Oceanography, Hohai University, 1 Xikang Road, Nanjing, Jiangsu, 210098, China
- <sup>19</sup>Department of Atmospheric, Oceanic, and Earth Sciences,  
George Mason University, Fairfax, VA 22030, USA
- <sup>20</sup>State Key Laboratory of Biogeology and Environmental Geology, School of Earth Sciences,  
China University of Geosciences, Wuhan, China
- <sup>21</sup>Leibniz Institute for Applied Geophysics (LIAG), Stilleweg 2, 30655 Hanover, Germany
- <sup>22</sup>School of Earth and Environment, University of Leeds, Leeds, LS2 9JT, UK
- <sup>23</sup>Univ Lyon, UCBL, ENSL, UJM, CNRS, LGL-TPE, 69622 Villeurbanne, France
- <sup>24</sup>Department of Geology, Eötvös Loránd University, Pázmány Péter sétány 1/C, Budapest 1117, Hungary
- <sup>25</sup>HUN-REN-MTM-ELTE Research Group of Palaeontology,  
Pázmány Péter sétány 1/C, Budapest 1117, Hungary
- <sup>26</sup>Polish Geological Institute–National Research Institute, Rakowiecka 4, 00-975, Warsaw, Poland
- <sup>27</sup>Department of Geology and SFI Research Centre in Applied Geosciences (iCrag),  
Trinity College Dublin, The University of Dublin, Dublin, Ireland
- <sup>28</sup>Department of Earth Sciences, Clayton H. Riddell Faculty of Earth, Environment, and Resources, University  
of Manitoba, 230 Wallace Building, 125 Dysart Road, Winnipeg, Manitoba, R3T 2N2, Canada
- <sup>29</sup>NIOZ Royal Netherlands Institute for Sea Research, Department of Marine Microbiology and  
Biogeochemistry, P.O. Box 59, 1790 AB, Den Burg (Texel), the Netherlands
- <sup>30</sup>Faculty of Geography and Geology, Jagiellonian University, Gronostajowa 3a, 30-087, Kraków, Poland
- <sup>31</sup>Centre for Earth Evolution and Dynamics (CEED), University of Oslo,  
P.O. Box 1028 Blindern, 0315 Oslo, Norway
- <sup>32</sup>Department of Geological Sciences, San Diego State University, San Diego, CA 92182-1010, USA
- †deceased, 19 April 2023

**Correspondence:** Stephen P. Hesselbo (s.p.hesselbo@exeter.ac.uk) and Clemens V. Ullmann  
(c.ullmann@exeter.ac.uk)

Received: 16 May 2023 – Revised: 30 August 2023 – Accepted: 22 September 2023 – Published: 26 October 2023

**Abstract.** Drilling for the International Continental Scientific Drilling Program (ICDP) Early Jurassic Earth System and Timescale project (JET) was undertaken between October 2020 and January 2021. The drill site is situated in a small-scale synformal basin of the latest Triassic to Early Jurassic age that formed above the major Permian–Triassic half-graben system of the Cheshire Basin. The borehole is located to recover an expanded and complete succession to complement the legacy core from the Llanbedr (Mochras Farm) borehole drilled through 1967–1969 on the edge of the Cardigan Bay Basin, North Wales. The overall aim of the project is to construct an astronomically calibrated integrated timescale for the Early Jurassic and to provide insights into the operation of the Early Jurassic Earth system. Core of Quaternary age cover and Early Jurassic mudstone was obtained from two shallow partially cored geotechnical holes (Prees 2A to 32.2 m below surface (m b.s.) and Prees 2B to 37.0 m b.s.) together with Early Jurassic and Late Triassic mudstone from the principal hole, Prees 2C, which was cored from 32.92 to 651.32 m (corrected core depth scale). Core recovery was 99.7 % for Prees 2C. The ages of the recovered stratigraphy range from the Late Triassic (probably Rhaetian) to the Early Jurassic, Early Pliensbachian (Ibex Ammonoid Chronozone). All ammonoid chronozones have been identified for the drilled Early Jurassic strata. The full lithological succession comprises the Branscombe Mudstone and Blue Anchor formations of the Mercia Mudstone Group, the Westbury and Lillstock formations of the Penarth Group, and the Redcar Mudstone Formation of the Lias Group. A distinct interval of siltstone is recognized within the Late Sinemurian of the Redcar Mudstone Formation, and the name “Prees Siltstone Member” is proposed. Depositional environments range from playa lake in the Late Triassic to distal offshore marine in the Early Jurassic. Initial datasets compiled from the core include radiography, natural gamma ray, density, magnetic susceptibility, and X-ray fluorescence (XRF). A full suite of downhole logs was also run. Intervals of organic carbon enrichment occur in the Rhaetian (Late Triassic) Westbury Formation and in the earliest Hettangian and

earliest Pliensbachian strata of the Redcar Mudstone Formation, where up to 4 % total organic carbon (TOC) is recorded. Other parts of the succession are generally organic-lean, containing less than 1 % TOC. Carbon-isotope values from bulk organic matter have also been determined, initially at a resolution of  $\sim 1$  m, and these provide the basis for detailed correlation between the Prees 2 succession and adjacent boreholes and Global Stratotype Section and Point (GSSP) outcrops. Multiple complementary studies are currently underway and preliminary results promise an astronomically calibrated biostratigraphy, magnetostratigraphy, and chemostratigraphy for the combined Prees and Mochras successions as well as insights into the dynamics of background processes and major palaeo-environmental changes.

## 1 Introduction

### 1.1 Late Triassic and Early Jurassic Earth and solar system history

The Early Jurassic Earth System and Timescale scientific drilling project (JET) aims to construct a fully integrated and astronomically calibrated timescale for this epoch. This was a time in Earth's history,  $\sim 200$ – $175$  Ma, when important physical, chemical, and biological elements of the modern Earth system first emerged, for example as expressed in the initial phases of Atlantic Ocean opening (e.g. Torsvik and Cocks, 2017) or the rapid evolution of marine organisms, including planktonic primary carbonate producers (e.g. Knoll and Follows, 2016; Antell and Saupe, 2021; Riding et al., 2023). At the same time, other elements of the Earth system had distinctly Mesozoic characteristics, such as generally warm climate states, the presence of extensive epicontinental seaways susceptible to water mass stratification and anoxia, and short-lived episodes of massive flood basalt volcanism (e.g. Hesselbo et al., 2020a; Remírez and Algeo, 2020; Ruhl et al., 2022).

The interactions between the atmosphere, hydrosphere, biosphere, and lithosphere over Late Triassic to Early Jurassic time have become a focus of much scientific study over the last couple of decades, particularly for the prominent environmental changes that characterize the Triassic–Jurassic transition at  $\sim 201$  Ma and the Toarcian Oceanic Anoxic Event at  $\sim 183$  Ma (e.g. Capriolo et al., 2022; Ruhl et al., 2022, and references therein), and much has been learned about the driving processes for mid-Mesozoic climate change, extinction, and evolution. However, the diverse Early Jurassic biostratigraphic, astrochronologic, magnetostratigraphic, and chemostratigraphic schemes have, for the most part, remained poorly integrated with each other and have lacked accurate numerical calibration, leaving many uncertainties with regard to the rates and relative timing of key Earth system processes (e.g. Hesselbo et al., 2020a; Al-Suwaidi et al., 2022). Although astrochronologic studies, which make use of stable orbital cycles, have been used to great advantage recently, incompatible interpretations for the Early Jurassic are not uncommon (see e.g. Ruhl et al., 2016; Weedon et al., 2019; Storm et al., 2020); additionally, be-

cause astronomical models cannot accurately constrain orbital histories earlier than the Cenozoic, the pre-Cenozoic rock record is itself crucial for extending knowledge of solar system orbital history into the deep past (Kent et al., 2018; Olsen et al., 2019).

Using a new integrated stratigraphic framework, the JET project aspires to document and quantify the influence of the principal internal and external forcing factors on the Earth system during the Early Jurassic, for both the major palaeo-environmental events and the more stable “background” states between them.

### 1.2 Site selection, related borehole records, and regional context

The initial focus for this project was on obtaining a new core from the Llanbedr (Mochras Farm) site in the Cardigan Bay Basin (Hesselbo et al., 2013), where previous drilling in the late 1960s had recovered a  $\sim 1.3$  km thick Mesozoic succession comprising the Rhaetian (Late Triassic), Hettangian, Sinemurian, Pliensbachian, and Toarcian (Early Jurassic) stages, overlain by  $\sim 0.6$  km of Cenozoic deposits (Wood and Woodland, 1968; Woodland, 1971; Fig. 1). The Early Jurassic mudstone succession at Mochras was found to be biostratigraphically complete at the ammonite zonal level (Woodland, 1971; Dobson and Whittington, 1987; Copestake and Johnson, 2014). The borehole proved to be of great value for understanding UK Jurassic palaeo-geography and basin history, but although the original recovery is calculated as 97.6 % for the Jurassic, only 59.1 % is preserved as core slabs at the British Geological Survey (BGS) National Core Repository, the remainder being either kept as discrete fossil specimens or placed into bags of coarse fragments ( $\sim 20$  mm diameter) representing 5 ft (i.e.  $\sim 1.5$  m) stratigraphic intervals (Storm et al., 2020). Although much work has been carried out on the legacy Mochras core as part of the JET project (Percival et al., 2016; Ruhl et al., 2016; Baker et al., 2017; Xu et al., 2018a, b; Deconinck et al., 2019; Storm et al., 2020; Hollaar et al., 2021, 2023; Menini et al., 2021; Munier et al., 2021; Pieńkowski et al., 2021; Damaschke et al., 2022; Ruhl et al., 2022; Ullmann et al., 2022; Paulsen and Thibault, 2023), the poor physical state of the lower half of the core (Hettangian and Sinemurian) means any signal of orbital cy-



cles at the fundamental precession scale has been lost, with preserved intact core slabs to a very large degree restricted to the Pliensbachian and Toarcian stages of the cored interval. Similarly, there are no downhole wireline logs for the lower half of the Jurassic succession.

The Mochras site proved to be very challenging on account of its exceptional present-day setting and infrastructural constraints that would have been beyond a practical financial budget to contend with. Because of these considerations at Mochras, a site at Prees, in the neighbouring Cheshire Basin, was selected as an alternative. The Prees site has the principal advantage that the prime stratigraphic targets lie at shallower depths in an environmentally and logistically straightforward location.

The drilled site at Prees represents a similar overall tectonic and depositional setting to Mochras (Penn, 1987; Evans et al., 1993; Tappin et al., 1994; Warrington, 1997; Plant et al., 1999; Fig. 1), Prees being situated within a SW–NE-oriented half-graben called the Wem–Audlem Sub-basin, ~3.2 km NW of the bounding faults of the Wem–Red Rock fault system on its south-eastern margin (Evans et al., 1993; Mikkelsen and Floodpage, 1997).

Two boreholes drilled previously in the Cheshire Basin – “offset wells” – provide a solid stratigraphic background for the Prees location: Wilkesley (Grid Reference SJ 363864 341438), drilled by the British Geological Survey in 1959–1960 to a depth of 1686 m and in its upper part recovering a succession from the Early Jurassic to the Early Triassic, and Prees 1 (Grid Reference SJ 355727 334474), drilled in 1972–1973 by Trend Petroleum for Shell to a depth of 3829 m and penetrating Jurassic to Silurian strata (Fig. 1). Wilkesley was part of an exploration programme that proved salt deposits within the Triassic, and Prees 1 was an exploration well for hydrocarbon resources in possible Triassic and Permian sandstone reservoirs. A shallow borehole at Platt Lane (Grid Reference SJ 351400 336450), drilled for the British Geological Survey in 1959 to 113 m, provides additional core and stratigraphic data around the Triassic–Jurassic boundary. Late Triassic and Jurassic strata were not cored in Prees 1. Although the Hettangian at Wilkesley was fully cored, the core was subsequently broken up, with only hand samples retained at 1 ft (i.e. ~30 cm) intervals together with a series of registered fossil specimens (these latter with significant potential to yield further biostratigraphic, lithological, geochemical, and mineralogical information).

The Hettangian and earliest Sinemurian in the Wilkesley borehole comprise medium- to dark-grey calcareous mudstone with silty mudstone and argillaceous limestone (Poole and Whiteman, 1966). Based on the Prees 1 well completion log together with our examination of cuttings, the entire Early Jurassic succession at Prees was inferred to comprise calcareous mudstone and siltstone with subordinate limestone, a very similar lithological succession to Mochras (Woodland, 1971; Hesselbo et al., 2013; Ruhl et al., 2016;

Xu et al., 2018a; Ullmann et al., 2022). Pyrolysis data from Prees 1 cuttings and the Wilkesley core show organic matter maturity to be similar to Mochras, lying on the boundary between immature and mature (Appendix A). Marine calcareous fossils are common in the early Hettangian at Wilkesley, including ammonites, and these have previously allowed a highly resolved ammonite biostratigraphy to be constructed (Donovan in Poole and Whiteman, 1966; Plant et al., 1999). The ammonite succession provides a remarkable record of early recovery faunas after the end-Triassic mass extinction and includes shells with nacreous preservation, i.e. aragonite (Bloos and Page, 2000). A record of foraminifers has also been compiled from the Late Triassic and Early Jurassic of Wilkesley (Copestake, 1989; Copestake and Johnson, 1989).

In total, six exploration wells have been drilled for conventional oil and gas targets in the Cheshire Basin, and all have proven to be dry, likely as a result of the absence of a suitable source rock, particularly in the south of the basin where Prees is located, and due to a lack of closed structures for the early drilled wells (Mikkelsen and Floodpage, 1997; Plant et al., 1999).

## 2 Methods

### 2.1 Drilling and logging

Two shallow cored boreholes were drilled for geotechnical characterization of the site between December 2019 and January 2020. These are designated “Prees 2A” (drilled to 32.2 m below surface, m.b.s.) and “Prees 2B” (drilled to 37 m b.s.). Drilling and logging operations for the principal borehole, Prees 2C, were carried out from 22 October 2020 to 1 January 2021. Prees 2C reached a total depth (TD) of 651.32 m corrected core depth (m.c.c.d.) (see Sect. 2.7 for a description of depth scales for Prees 2C). The primary parameters for the cored boreholes are summarized in Table 1. Full details of the drilling and logging operations are provided in the Operations Report (Hesselbo et al., 2023).

Downhole geophysical data for Prees 2C were acquired by the logging contractor in two runs, from 240 to 33 m depth on 16 November 2020 and for the remainder of the hole after drilling was completed (28 and 29 December 2020). The probes successfully run from ~240 m to the surface were Spectral Gamma Ray, Density, Neutron Porosity, Focused Electric Log, 4-Arm Caliper, Mud Temperature/Conductivity, Full Wave Sonic, and Acoustic TelevIEWer. The probes successfully run from TD to 240 m were Spectral Gamma Ray, Density, Neutron Porosity, Induction Log, 4-Arm Caliper, Mud Temperature/Conductivity, Full Wave Sonic, and Acoustic TelevIEWer.

### 2.2 Seismic reflection data

The Prees site lies in a region characterized by relatively good seismic coverage including a 1970s vintage low-fold

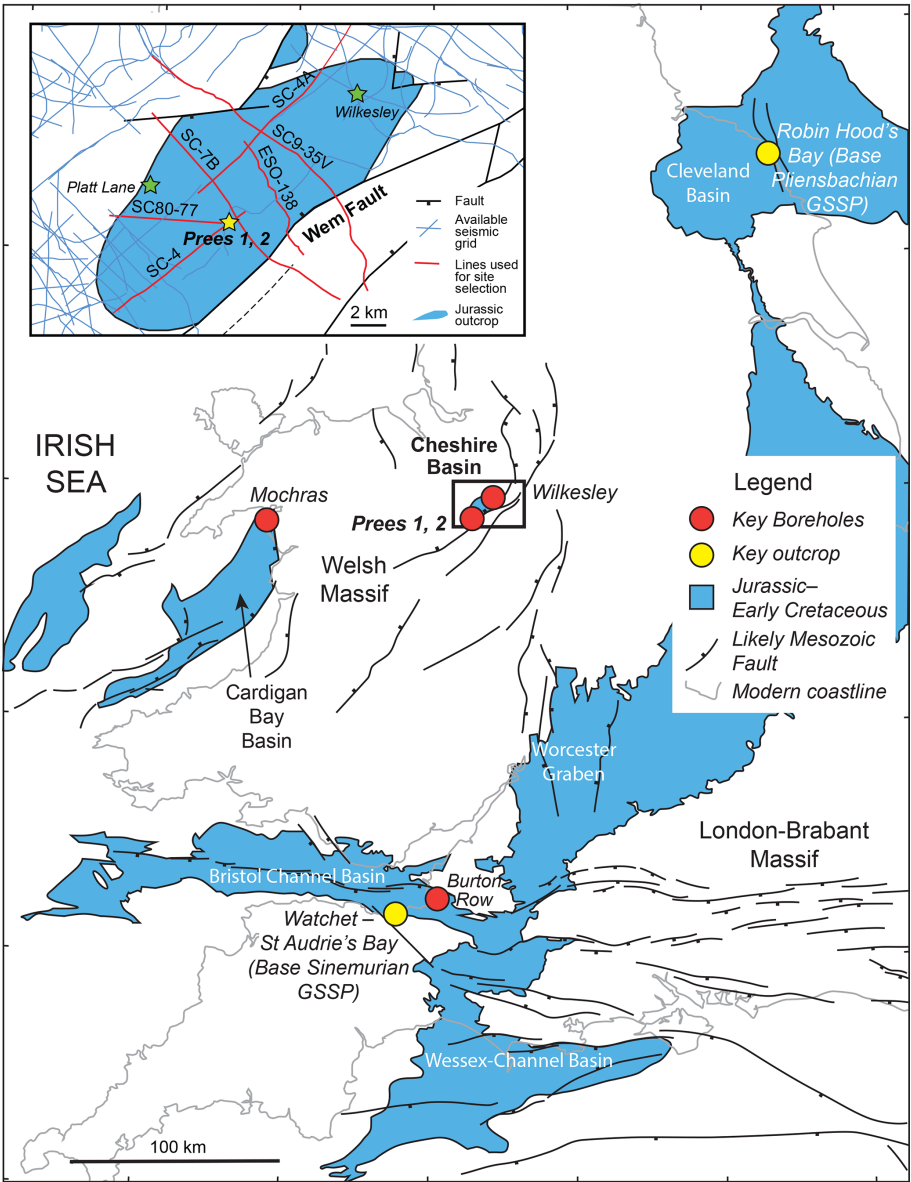


**Figure 1.** Geological map of Jurassic–Early Cretaceous strata in the southern UK area, showing the locations of the Prees 1 and Prees 2 wells (main map and inset) in relation to the Mochras, Burton Row, Platt Lane, and Wilkesley boreholes as well as outcrop Early Jurassic GSSP sites. The Prees Jurassic outlier (main map and inset) sits in the southern part of the Cheshire Basin. The main figure is based on a BGS 1 : 1 500 000 series tectonic map of the UK, Ireland, and adjacent areas, Sheet 1 (Pharaoh, 1996). The inset is based on data in the UK Onshore Geophysical Library (<http://ukogl.org.uk>, last access: 6 October 2023). The depositional and tectonic settings of Prees are broadly comparable to Mochras but differ in detail. Green stars in the inset give offset well locations.

**Table 1.** Principal parameters for Prees 2 boreholes. OS: Ordnance Survey; WGS84: World Geodetic System 1984; OD: Ordnance Datum; SOBI: Single Onshore Borehole Index; m: metres below surface (Prees 2A and 2B); m c.c.d.: metres corrected core depth (Prees 2C). Refer to Sect. 2.7 for a description of the depth scales. Note: n/a – not applicable.

Name	OS grid reference	Latitude (WGS84)	Longitude (WGS84)	Ground level (m, OD)	Rig floor datum (m)	Final depth (m b.s. or m c.c.d.)	SOBI number
Prees 2A	SJ 55569 34483	52.905933	−2.662053	86.63	n/a	32.2	SJ53SE/52
Prees 2B	SJ 55574 34490	52.905996	−2.661980	86.63	n/a	37.0	SJ53SE/51
Prees 2C	SJ 55559 34478	52.905887	−2.662201	86.48	4.58	651.32	SJ53SE/53



dynamite grid and a denser grid of vibroseis acquired in the late 1970s and 1980s (Mikkelsen and Floodpage, 1997). For site selection, the relevant seismic lines (Fig. 1 inset) were obtained and re-processed where possible. Two seismic reflection profiles were used to help determine the optimum drill site location and provide a basinal context, SC-&B and SC4 (Fig. 1). Line SC-7B is oriented NW–SE, passing 0.5 km from Prees 1 (Figs. 1 and 2). Line SC-7B was acquired in 1970 using a dynamite source with a shot point spacing of approximately 60 to 120 m. Vertical geophones with a spacing of about 60 m were used as receivers, and the recording length was 5 s at a sampling rate of 2 ms. In addition to a recording filter of 12 to 96 Hz, the original processing included, for example, true amplitude recovery, static and dynamic corrections, velocity field determination from NMO curves, stacking, and predictive deconvolution.

More modern seismic processing methods were applied to the dataset to improve the imaging quality, especially of the Jurassic formations. Since the raw data of profile SC-7B were not available, only the post-stack data were used. We applied a frequency–wavenumber filter to eliminate disturbing effects of noisy frequencies, which cover the primary reflections. Spectral balancing was then applied to compensate for frequency attenuation, especially at higher frequencies, to obtain a higher-resolution image of the subsurface. Then the data were slightly smoothed with a non-linear smoothing filter to facilitate the interpretation of the horizons. A finite-difference (FD) time migration was applied to correct the positions of dipping reflectors, collapse diffractions, and further increase spatial resolution. Finally, the data were converted from the time domain to the depth domain to allow joint interpretation of the seismic and borehole data.

### 2.3 Core processing at the drill site

For Prees 2C, the core was obtained at 6 m lengths with a nominal diameter of 97 mm and a hole size of 161.9 mm. A 7 m long plastic liner was used for all core runs. At the drill site the metal core barrel was transported from the rig floor to the core processing area, where the core catcher was removed and any core therein retained in a short section of liner. The core in its liner was then removed from the core barrel onto a series of trestles, where the position of the top of the core was located through the liner and the liner cut at that point. The core was then pushed from the top to the bottom of the liner, and any excess liner was trimmed to fit. Plastic end-caps were then used to mark the top (blue) and bottom (white) of the entire recovered core, which was then marked up into sections 1 m long from the top, with the bottom section generally being less than 1 m in length. In cases where coherent core catcher sections were obtained, these were combined with the bottom section prior to marking up and section cutting.

Each core section was then individually cut with a rock saw and flushed with water whilst still in the liner to re-

move most drilling fluid from the outer core surfaces and from within fractures (except the first few cores, down to ~83 m b.s., for which this cleaning was carried out in the BGS National Core Repository). Samples of drilling fluid were retained at intervals for later geochemical analysis. Cleaned core sections were then capped using blue and white end-caps and carried into the core description lab. Each core section was given a rudimentary description and a sample chip was taken from the bottom to form the basis of initial analyses for organic carbon isotopes, carbonate and organic carbon content, and elemental abundances at ~1 m resolution, with a total sample set of 625. All drilling, core processing, and sample data were then entered into the mDIS (the International Continental Scientific Drilling Program (ICDP)'s Drilling Information System Goes Mobile). Core sections were boxed on site and stored in a container until they were transported to the National Core Repository in Keyworth at 2- to 3-week intervals.

Core and core section identification follows standard ICDP and BGS protocols. ICDP identification is based on the following format: project\_code\_site number\_hole letter\_core number\_section number (e.g. for the JET project, Hole Prees 2C, Core 10, Sect. 3, the formulation is 5065\_1\_C\_10\_3). Each core section was also assigned a BGS core box number in the following manner. As an example, the core box number CB00354103 was assigned for a whole round, with the same number retained for the Archive half derived from this when slabbed (see below).

### 2.4 Core processing and scanning at the National Core Repository and Core Scanning Facility (multi-sensor core logger, XRF, optical imagery, photography)

Core curation at the BGS National Core Repository was carried out in parallel with drilling, and all whole round sections that were shipped from the drill site were curated with the designation of the future Archive halves. Once whole round-core scanning was completed, the core sections were cut into half-cores and re-boxed, and the Working halves were curated as subsamples of the whole rounds with assigned core box numbers 1000 higher than the respective Archive half (e.g. CB00355103 for Archive half CB00354103). Curation was finalized in August 2021.

Whole round X-ray radiography was carried out using a Geotek X-ray computed tomography (CT) system at the BGS Core Scanning Facility. Whole round sections that were long enough (ca. 50 cm or longer) were scanned in the liner at three angles (0, 45, and 90°) at scan rates approximating 7 min per metre. Resulting radiographic images were post-processed to optimize contrast and greyscale spread to best highlight structural elements such as fractures as well as fossils, burrows, and nodules.

Whole round sections were then scanned using a Geotek multi-sensor core logger (MSCL). Three types of analysis (gamma density GD, magnetic susceptibility MS, and natural

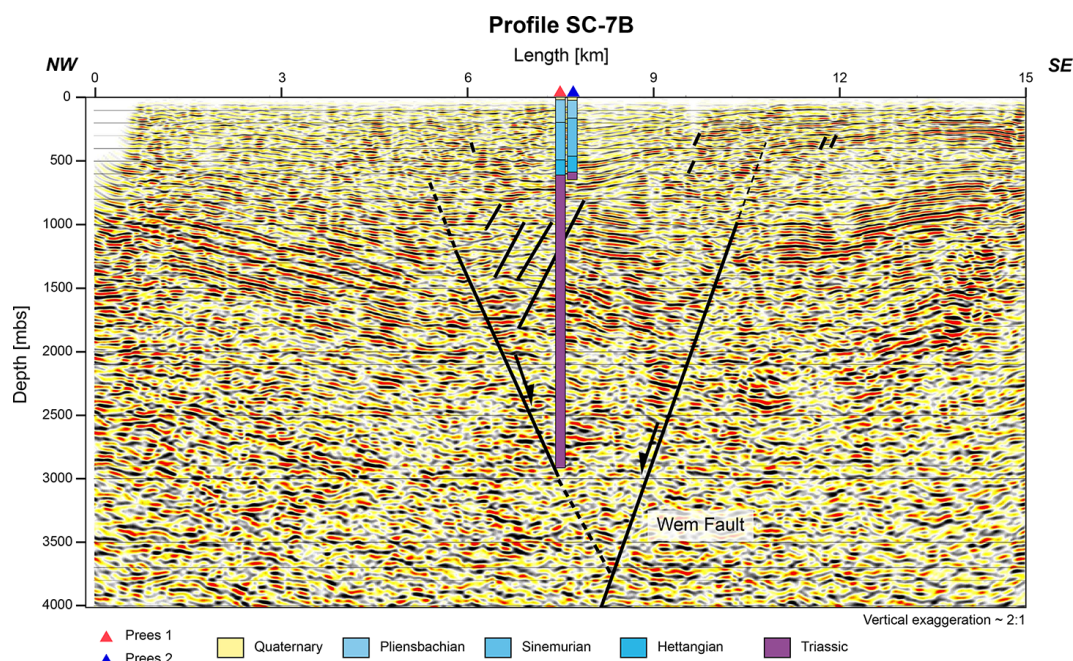


**Figure 2.** Migrated and depth-converted section of profile SC-7B oriented NW (left)–SE (right) (see Fig. 1 inset). The Prees 1 and Prees 2 boreholes are projected onto the seismic line. The stratigraphic units are colour-coded to match Fig. 3. Note the change in subsidence style equivalent to a depth of about 800 m at Prees, using assumed time–depth parameters, which likely corresponds to a level within the Late Triassic. Prees 1 also drilled Permian, Carboniferous, and Silurian age strata below the Triassic (not shown).

gamma-ray emission NG) were carried out at a step size of 2 cm. Data were integrated for 10 s for GD and MS and for 30 s averaging of the signal of three detectors for NG.

Core slabbing was undertaken after completion of MSCL work in batches of 28 core sections (one pallet) to avoid premature drying and development of fractures. Working and Archive halves were designated at this point, with the Archive half retaining the original core box number. After sawing of the sections, they were washed and covered with tissue to draw out saline pore liquids and avoid salt crust formation. Sections below depths of  $\sim 80$  m required multiple rounds of rinsing and salt removal before they could be further scanned due to very high sodium chloride content.

High-resolution core photographs were taken for both the Archive and Working halves using a semi-automated layout on a scanning station at the BGS National Core Repository using a digital camera. Data were immediately uploaded to the BGS system for quality control.

Core-scanning XRF data were acquired for Archive half core sections using an Itrax core-scanning system capable of automatically processing up to five sections. Analyses were carried out in 1 cm increments with 10 s integration for each increment and peak areas were quantified using a single, preliminary model fit to the data. Image data were also acquired using this instrument.

Samples for palaeo-magnetic study were marked in 50 cm intervals on the Working half and cut using rock-sawing equipment. The sample sizes are  $\sim 3 \times 3 \times 3$  cm with orien-

tation marks scratched on the surface using a steel preparation pin (results from analysis of these samples will be presented elsewhere).

## 2.5 Macrofossil sampling and identification

Macrofossil sampling was undertaken on the Working half of the core, with fossils selected from inspection of bedding planes on a centimetre-by-centimetre basis in mudstone lithology. Ammonite samples dominated, and a subset of other macrofossil material specimens was also set aside. Sampling for ammonites was prioritized, and a representative selection of other macrofossil material specimens was also set aside. Each ammonite recovered was identified to the most refined taxonomic level possible, and these identifications form the basis for the biochronostratigraphic framework.

## 2.6 Carbon isotopes, total organic carbon, and calcium content

Bulk rock samples were crushed and ground at the BGS National Environmental Isotope Facility, generating subsamples of different size fractions. Coarse material was retained for palynological work, and fine-grained powders were split into subsamples for decarbonation and subsequent organic carbon ( $C_{org}$ ) isotope analysis and subsamples for bulk geochemical analysis. Powdered and homogenized samples were de-



carbonated using a 5 % HCl solution and then neutralized through repeated dilutions with deionized water before finally being dried in a freeze drier. These samples were then analysed using an Elementar Vario ISOTOPE cube elemental analyser (EA) coupled to an Isoprime precisiON isotope-ratio mass spectrometer (IRMS) with an onboard centrION continuous-flow interface system.

Carbon-isotope data are reported in delta ( $\delta$ ) notation per mil (‰) relative to the international reference VPDB (Vienna Pee Dee Belemnite). Carbon-isotope ratios were corrected using a two-point calibration comprising the organic analytical standard B2162 (*Spirulina* algae, Elemental Microanalysis Ltd.;  $-18.7$ ‰, in-house value) and a laboratory working standard (BROC3,  $-27.6$ ‰). The reference materials BROC3 and B2162 have been calibrated for  $\delta^{13}\text{C}$  using IAEA-CH-6 ( $-10.5$ ‰), USGS54 ( $-24.4$ ‰), USGS40 ( $-26.4$ ‰), and B2174 (urea, Elemental Microanalysis Ltd.;  $-36.5$ ‰). BROC3 (41.3 %C and 4.9 %N) was used to calculate the carbon elemental content of samples. The within-run sample repeat average external precision ( $1\sigma$ ) for carbon content was  $<0.1$  wt %, and the within-run standards' average external precision ( $1\sigma$ ) for  $\delta^{13}\text{C}$  was  $<0.1$ ‰.

Finely powdered bulk rock splits were analysed for bulk geochemical composition at the University of Exeter's Penryn campus using an Olympus portable XRF scanner (p-XRF) in "geochem" mode, employing 40 and 10 kV beams for 60 s each. Ca data were used to estimate carbonate content and were calibrated by determination of  $\text{CO}_2$  emissions of a subset of 24 samples using a Sercon 20–22 gas source isotope ratio mass spectrometer at the University of Exeter's Penryn campus. The  $\text{CaCO}_3$  content thus derived was then used to correct carbonate-free TOC values to true values. For simplicity, calculation of  $\text{CaCO}_3$  assumes that neither siderite nor dolomite is present (which is known not to be strictly the case).

## 2.7 Core depth scales

The depth scales for the two shallow holes, Prees 2A and Prees 2B, are simply metres below surface (Table 1). The Prees 2C depth model for the core is more complex and is summarized in "Prees\_Depth\_Model.xlsx" (Supplementary Data File 1 in the Supplement). Depths for the Prees 2C core were initially assigned from information recorded in the daily drilling reports. These drillers' depths were reported as metres below floor of the drill rig (m b.r.f.) for each drilled interval (core run), which was typically 6 m. Drillers' depths were then converted into metres below surface by subtracting the measured 4.58 m offset between the rig floor and surface (Table 1) from the reported m b.r.f. value. Depth information for the top depth of individual core sections cut from the full core run was then assigned by adding the distance of the top of a core section from the top of the respective core run. The depth assignments (m b.s.) for core sections resulting from

this were reported to the BGS for core curation and are thus also the curated depths for the core.

The drillers' depth assumes the top depth of each core run to be equivalent to the length of the coring string in the hole at the beginning of the core run. In the majority of cases, the extracted amount of core was nearly equivalent to the drilled interval but, depending on the effectiveness of the core catcher, deviations of a few to several tens of centimetres commonly occurred. Where material from a previously incompletely extracted core run (e.g. Core 94) was recovered (Core 95), the above assumption leads to an apparent core gap above the longer core (between cores 94 and 95) and an apparent core overlap below (between cores 95 and 96) at the curated depths.

Given that the entire length of extracted core from 50 to 650 m depth taken together deviates by only a few tens of centimetres from the drilled length, the amount of extracted core can guide depth correction. Corrected model depths have thus been constructed, and this new depth scale is denoted by m c.c.d. This is the depth scale that should normally be used for reporting any finalized data for the Prees 2C core.

A small number of assumptions was made for construction of the "metres corrected core depth" (m c.c.d.) scale. The top depths of Core runs 1 and 2 were taken to be correct as there was significant core fragmentation and core loss in Core run 1. Core run 2 recovered 5.25 m of material as opposed to a reported drilling progress of 5.20 m, so the top depth of Core run 3 of 38.92 m b.s. was shifted down by 5 cm to 38.97 m c.c.d. Core runs 4 to 6 retained their initial depth assignments as Core runs 3 to 5 all yielded significantly less material than the reported drilling progress, and the retrieved material was still heavily fractured.

With the start of Core run 6, core material was largely intact and material recovery typically within a few centimetres of the reported drilling progress. The m c.c.d. scale from this point onwards is thus anchored at an assumed correct top depth of Core run 6 where 49.92 m b.s. = 49.92 m c.c.d. From this point downwards, the top of the subsequent core run is calculated by adding the recovered length of the previous core run to the top depth of the previous core run. For example, for Core run 7, the corrected depth of 54.48 m c.c.d. derives from the top of Core run 6 of 49.92 m c.c.d., with the length of the recovered core from Core run 6 being 4.56 m (54.48 m c.c.d. = 49.92 m c.c.d. + 4.56 m). This system was followed up to (and including) Core run 98 with a top depth of 571.77 m c.c.d.

Core run 98 was characterized by significant failure of recovery due to core catcher malfunction but also additional unconstrained core loss. Further coring problems occurred in Core run 106, where core integrity and recovery were compromised over an interval of ca. 1.07 m due to failure of drilling fluid circulation and a melted liner. In order to accommodate the known core loss at these points, a new depth anchor was set at the top of Core run 106 based on the reported core top position at 603.42 m b.s. = 603.42 m c.c.d.

Core top depths for Core runs 99–105 were then calculated by subtracting the lengths of individual core runs from this anchor point. For example, the top depth of Core run 105 of 597.20 m c.c.d. derives from the top depth of Core run 106 of 603.42 m c.c.d. and the recovered length of Core run 105 of 6.22 m ( $597.20 \text{ m c.c.d.} = 603.42 \text{ m c.c.d.} - 6.22 \text{ m}$ ). This procedure results in an assumed core loss of 8 cm in Core run 98 (base Core run 98 = 573.13 m c.c.d.; top Core run 99 = 573.21 m c.c.d.), which is compatible with observations.

The remaining part of the corrected depth model is then based on the assumption that the top depth of Core run 107 is correct, i.e. 604.49 m b.s. = 604.49 m c.c.d. This assumption results in a core loss of 43 cm within Core run 106, which appears realistic given observations during coring. The TD of the core according to the length of the remaining Core runs 107 to 114 is 651.32 m c.c.d. This figure contrasts with a value of 651.45 m b.s. and suggests a residual core loss of 13 cm at the bottom of the hole.

The top depths of individual core sections were assigned in the same way as in the curated depth scale, i.e. by adding the distance between the section top and the core run top to the top depth of the core run. For example, for Core 90, the run starts at 531.46 m c.c.d. The top depth of section 1 in this run is thus also 531.46 m c.c.d. Given the length of section 90\_1 being 99 cm in this core run, the top depth of section 90\_2 is 532.45 m c.c.d. ( $531.46 \text{ m c.c.d.} + 0.99 \text{ m}$ ). The section top of section 90\_3 is 533.45 m c.c.d. given the length of section 90\_2 of 1.00 m ( $533.45 \text{ m c.c.d.} = 531.46 \text{ m c.c.d.} + 0.99 \text{ m} + 1.00 \text{ m}$ ), and so forth.

The total core loss from Core runs 6 to 114 is thus  $8 + 43 + 13 \text{ cm} (= 64 \text{ cm})$  in the range from 49.92 to 651.32 m c.c.d., yielding a core recovery of 99.89 % in this interval and an overall core recovery from 32.92 m c.c.d. to a TD of 99.68 %.

## 2.8 Visual core description

Visual core descriptions were carried out on the Archive half core slabs at the National Core Repository to provide sample context for interpretation of depositional environments as well as diagenetic and structural history. Each core section was described at  $\sim 1 \text{ cm}$  resolution on a proforma document into which the Archive core photograph had been inserted. Visual core descriptions were then used as a basis for construction of a summary graphic log at a scale of  $3 \text{ mm} = 10 \text{ m}$ . In order to control for subjectivity in descriptions, carbonate enrichment and grey shade were adjusted using Ca count data and grey-scale data from core-scanning optical images (Sect. 2.4, 2.6).

## 3 Results and initial interpretation

### 3.1 Tectonic context

Although the Prees site is clearly in an overall extensional half-graben setting within the Cheshire Basin (Evans et al., 1993; Plant et al., 1999), the latest Triassic and Early Jurassic stratal geometries are significantly different from the bulk of the Triassic and Permian in the same location.

The main structural features in seismic profile SC-7B (Fig. 2) are a NW-dipping and SW–NE-striking major normal fault (offset about 600 m) in the south and a SE-dipping and SW–NE-striking antithetic normal fault in the north. The major normal fault is the well-known Wem Fault (see Fig. 1; Evans et al., 1993; Plant et al., 1999). An imbricate system of minor synthetic normal faults is observed between the two larger faults. The Jurassic deposits above the Permian–Triassic half-graben form a small-scale synformal basin possibly created by the downward movement of the normal fault blocks along the large antithetic and smaller synthetic normal faults, although a role for salt migration in the underlying Triassic cannot be ruled out (e.g. Hodgson et al., 1992).

As is the case for the Prees 1 drilling site, the Jurassic succession of Hettangian to Pliensbachian age appears to be tectonically undisturbed, and the borehole is located through the deepest part of the synformal structure. The thickest Jurassic succession clearly occurs at the projected location of the Prees 2 well, where it is not affected by seismically imageable faults.

Due to uncertainties in our initial time–depth conversion, the precise level at which the change in tectonic style occurs is not known; however, the Late Triassic age lithostratigraphy is complete (i.e. all formations and members of the Rhaetian age Penarth Group are present), and therefore any missing strata related to the change in subsidence style must be restricted to a level lower in the Late Triassic strata than recovered in the Prees 2C core, likely at the base of the Branscombe Mudstone (Table 2) or below. Interpretation of Line SC-7B is supported by interpretation of Line SC9-35V, which is parallel and lies  $\sim 4 \text{ km}$  to the NW. Line ESO-138 is of poor quality and does not yield any additional constraint on Jurassic stratigraphy or structure.

Line SC-4 is a SW–NE-oriented line along the axis of the basin, with Prees situated at the north-eastern end (Fig. 1). This profile confirms the general tilt of the Jurassic succession in a north-easterly direction along the axis of the basin. Line SC80-77 also approaches the Prees location at its eastern end, with the profile being oblique across the basin structure (Fig. 1). This line confirms that a reduced thickness of Jurassic strata occurs to the NW of the Prees 2 drill site and confirms the antithetic geometry of the subsidiary fault shown in Fig. 2.

**Table 2.** Lithostratigraphy of Prees 2 cores. Note: n/a – not applicable.

Group	Formation	Member	Age (epoch, age)	Depth to top of unit (m c.d.)	Unit thickness (m)	ICDP code 5065_1_ (Hole_Core_ Section_Depth; cm)	BCS core box no. (archive)	Unit top	Summary description of unit
n/a	n/a	n/a	Pleistocene	0.30	23.92	n/a	n/a	Thin soil 30 cm recorded	Diamictic, clay, sand and gravel
Lias	Redcar Mud- stone	n/a	E. Jurassic; L. Sinemurian– E. Pliensbachian	24.22	172.75	B_1_1_72cm	CB00352862	Unconformable; the top of the formation is weathered and deformed down to ~25.75 m.	Dark-grey, massive to faintly laminated mudstone and marl; carbonate concretions throughout, including sideritic and septarian; macro and trace fossils abundant at intervals; organic enriched in the lower part, ~143 to 196 m depth; intense fracturing from the unit top to ~50 m.
Penaarth	Lilstock	Prees	E. Jurassic; E.–L. Sinemurian	196.90	89.25	C_31_2_49cm	CB00354191	Downward transition of dark-grey mudstone to bioturbated fine to very fine sandstone or siltstone.	Pale-grey, buff bioturbated fine to very fine sandstone and siltstone intercalated with medium- to dark-grey mudstone; low carbonate content
		n/a	E. Jurassic; Hettangian– E. Sinemurian	286.29	306.04	C_47_1_63cm	CB00354289	Downward transition of > 1 m thick very fine sandstone or siltstone beds to the marl or mudstone with siltstone beds (< 1 m)	Dark-grey, massive to faintly laminated mudstone and marl; sparse carbonate concretions, including sideritic and septarian; macro and trace fossils abundant at intervals; organic enriched in organic matter below 560 m c.d.; lowest (~51 m dark-grey planar, wavy, and crinkly laminated silty limestone and mudstone
Penaarth	Lilstock	Langport	L. Triassic; Rhaetian	592.33	0.18	C_104_2_13cm	CB00354625	Sharp downward change from dark-grey, faintly laminated mudstone of the overlying formation to laminated grey mudstone	Pale-olive green or grey faintly laminated limestone and laminated mudstone with scattered bioclasts and thin beds or laminae of siltstone at the base
		Cotnam	L. Triassic; Rhaetian	592.51	5.52	C_104_2_31cm	CB00354625	Sharp downward change to a pale-grey/buff siltstone/limestone complex bedset	Dark-grey to pale-olive green mudstone and grey to pale-olive green siltstone and silty limestone, convolute bedding common; heterolithic way to lenticular bedding common; scours; the top of the unit comprises pale-grey and pale-brown silt and limestone beds, including a series of pale-grey millimetre-scale silt and limestone laminae and microbially silty limestone
Mercia Mudstone	Blue Anchor	Westbury	L. Triassic; Rhaetian	598.03	7.79	C_105_1_83cm	CB00354630	Sharp downward change to massive dark-grey mudstone	Dark-grey massive to laminated (including crinkly) mudstone; occasional thin limestone, siltstone, bivalve shell, and fossiliferous (phosphatic) arenaceous beds ("bone beds"), locally cross-stratified, convoluted, or pyritic
		Branscombe Mudstone	L. Triassic; Rhaetian	605.82	14.52	C_107_2_34cm	CB00354642	Thin dark-grey to black arenaceous mudstone with phosphatic nodules of overlying formation resting sharply on green-grey argillaceous limestone and mudstone	Pale green to grey mudstone or siltstone with occasional beds of grey to black-brown dolomitic mudstone and yellowish-grey laminated (planar, wavy, and crinkly) brecciated dolostone with desiccation cracks; bioturbation common
Mercia Mudstone	Blue Anchor	Branscombe Mudstone	L. Triassic; Rhaetian	620.34	30.98	C_109_6_00cm	CB00354658	Top of the highest consistent occurrence of medium red-brown calcareous mudstone beds	Calcareous mudstone and siltstone, red-brown with common grey-green patches, spots, and thin beds that are commonly carbonate-cemented



### 3.2 The Late Triassic, Early Jurassic, and Quaternary successions at Prees and regional correlation

Cores of Quaternary sand and diamict and Early Jurassic mudstone were obtained from the two shallow geotechnical holes drilled for site investigation (Prees 2A to 32.2 m b.s. and Prees 2B to 37.0 m b.s.). A core of Early Jurassic and Late Triassic mudstone was obtained from the principal hole Prees 2C from 32.92 to 651.32 m c.c.d. (see Sect. 2.7 for a discussion of the depth scales for Prees 2C). A summary of the lithostratigraphy of the Prees 2 cores is provided in Table 2 and Fig. 3, and a graphic compilation of key core-based datasets is presented in Fig. 4. A graphical summary of the downhole logging data is provided in Fig. 5. A synopsis of the overall lithological succession and a comparison to previously known lithostratigraphy are given below, working stratigraphically up from the base of the cored succession.

#### 3.2.1 Mercia Mudstone Group, Branscombe Mudstone Formation

The Branscombe Mudstone Formation of the Mercia Mudstone Group occurs from the base of the core up to 620.34 m c.c.d. The formation comprises calcareous red-brown mudstone and siltstone, with common grey-green patches, spots, and thin beds, particularly towards the top of the unit (Figs. 3, 6, 7). There are occasional occurrences of pale-grey or brown laminated and micro-brecciated carbonate beds. Burrow mottling and trace fossils occur sporadically. The lithology is similar to that described from limited outcrops and previous cores in the region (previously referred to as the Brooks Mill Mudstone – Warrington et al., 1999; Howard et al., 2008), except that anhydrite and gypsum nodules are absent or very rare. An ephemeral lake and playa depositional environment is inferred. The age of the formation is Late Triassic (likely Rhaetian). The unit has notably low downhole resistivity values (Fig. 5) possibly related to saline pore fluids.

#### 3.2.2 Mercia Mudstone Group, Blue Anchor Formation

The Blue Anchor Formation, 14.52 m thick, is a pale-green to grey mudstone or siltstone with occasional beds of grey to black-brown dolomitic mudstone and yellowish-grey laminated (planar, wavy, and crinkly) brecciated dolostone with desiccation cracks. Bioturbation structures and trace fossils are common (Figs. 3, 6, 7). The formation ranges up to 605.82 m c.c.d., where a sharp junction with the overlying formation is observed (Fig. 7). Elsewhere in the UK, the depositional environment of the formation has been interpreted as evaporitic lacustrine passing up into shallow marine and representing the initial regional transgression in the Rhaetian (Mayall, 1981). As for the Branscombe Mudstone, this unit of the Mercia Mudstone Group also has notably low downhole resistivity values (Fig. 5) possibly related to the presence of saline pore fluid. Three distinct cycles in a number

of downhole and core log parameters (e.g. gamma, density, sonic; Figs. 4, 5) denote very well-developed  $\sim 5$  m scale sedimentary cycles.

#### 3.2.3 Penarth Group, Westbury Formation

The Westbury Formation, 7.79 m thick, comprises dark-grey massive to laminated (including crinkly) mudstone with local thin limestone and siltstone beds, bivalve shell beds, and fossiliferous (phosphatic) arenaceous beds (“bone beds”); locally, cross-laminated, convoluted, or pyritic strata are observed (Figs. 3, 6, 7). The formation is relatively enriched in organic matter (up to  $\sim 4\%$  TOC). The lithofacies at Prees is typical of the Westbury Formation across the entire UK region and was deposited in a restricted shallow marine setting (e.g. MacQuaker, 1999; Swift, 1999; Hesselbo et al., 2004). The age assignment is late Rhaetian. The relatively high gamma-ray signature reflects high clay and low carbonate content, and sonic velocities are low (Figs. 4, 5).

#### 3.2.4 Penarth Group, Lilstock Formation

The Lilstock Formation, 5.70 m thick, comprises dark-grey to pale olive-green mudstone and grey to pale olive-green siltstone and silty limestone, with common convolute bedding. Heterolithic wavy to lenticular bedding occurs with scours. The top of the unit comprises pale-grey or pale-brown silt or limestone beds, including a series of pale-grey millimetre-scale silt or limestone laminae and possibly microbial silty limestone (Figs. 3, 6, 7). The upper 18 cm are composed of pale olive-green or grey faintly laminated limestone and laminated mudstone beds with scattered bioclasts and thin beds or laminae of siltstone at the base. This bed is identified as the “Langport Member”, whilst the underlying bulk of the formation is identified as the “Cotham Member” (following the practice reported in Warrington et al., 1999).

We note that Penn (1987) and Warrington et al. (1999, their Fig. 23) indicated a thicker Langport Member in the Prees 1 well, with a top depth that corresponds to  $\sim 586$  m c.c.d. in Prees 2, but this seems to be based on an over-simplified interpretation of the geophysical log data, which show a distinct gamma-ray low and sonic velocity high associated at Prees with carbonate-rich and relatively organic-matter-rich shales at the base of the Lias Group (Figs. 3–5).

The depositional environment of the Cotham Member in the general area of the UK and Ireland is interpreted as marginal marine, commonly coastal in view of the extensively observed desiccation cracks and localized oolitic limestones (e.g. Hesselbo et al., 2004), although neither of these features is observed in the Prees core. The convolute bedding has been much commented upon and is interpreted as representing regionally widespread seismically induced liquefaction (Mayall, 1983; Simms, 2007; Lindström et al., 2015; Laborde-Casadaban et al., 2021). The Langport Member is understood to have been deposited in a marine environment,

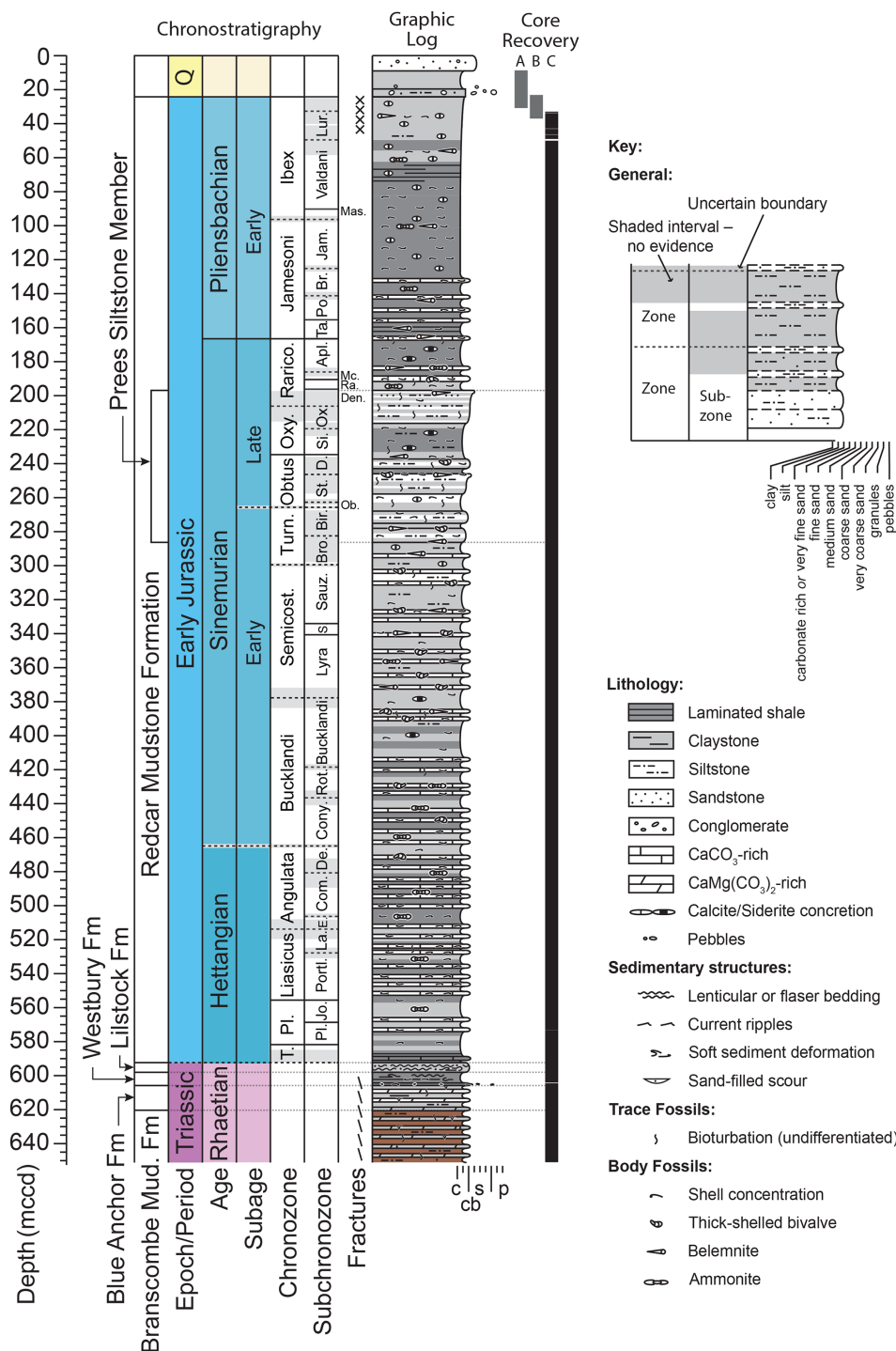


**Figure 3.** Summary graphic log for the recovered succession. The Branscombe Mudstone and the Blue Anchor Formation are at the top of the Mercia Mudstone Group, the Westbury Formation and the Lilstock Formation together comprise the Penarth Group, and the Redcar Mudstone here is the lowest formation of the Lias Group. Cores for the A and B site investigation holes are not yet fully documented. Abbreviations for ammonoid chronozones and subchronozone in alphabetical order – Apl.: Aplanatum; Br.: Brevispina; Bro.: Brooki; Bir.: Birchi; Com.: Complanata; Cony.: Conybeari; D.: Denotatus; Da.: Davoei; De.: Depressa; Den.: Densinodulum; E.: Extranodosa; Jam.: Jamesoni; Jo.: Johnstoni; La.: Laqueus; Lias.: Liasicus; Lur.: Luridum; Mc.: Macdonnelli; Mas.: Masseanum; Ob.: Obtusum; Ox.: Oxynotum; Pl.: Planorbis; Po.: Polymorphus; Portl.: Portlocki; Ra.: Raricostatoidea; Rarico.: Raricostatum; Rot.: Rotiforme; Sauz.: Sauzei; S.: Scipionium; Semicost.: Semicostatum; Si.: Simpsoni; St.: Stellare; T.: Tilmanni; Ta.: Taylori; Turn.: Turneri. Hybrid grain-size scale – c: clay; s: sand; p: pebble; cb: carbonate.

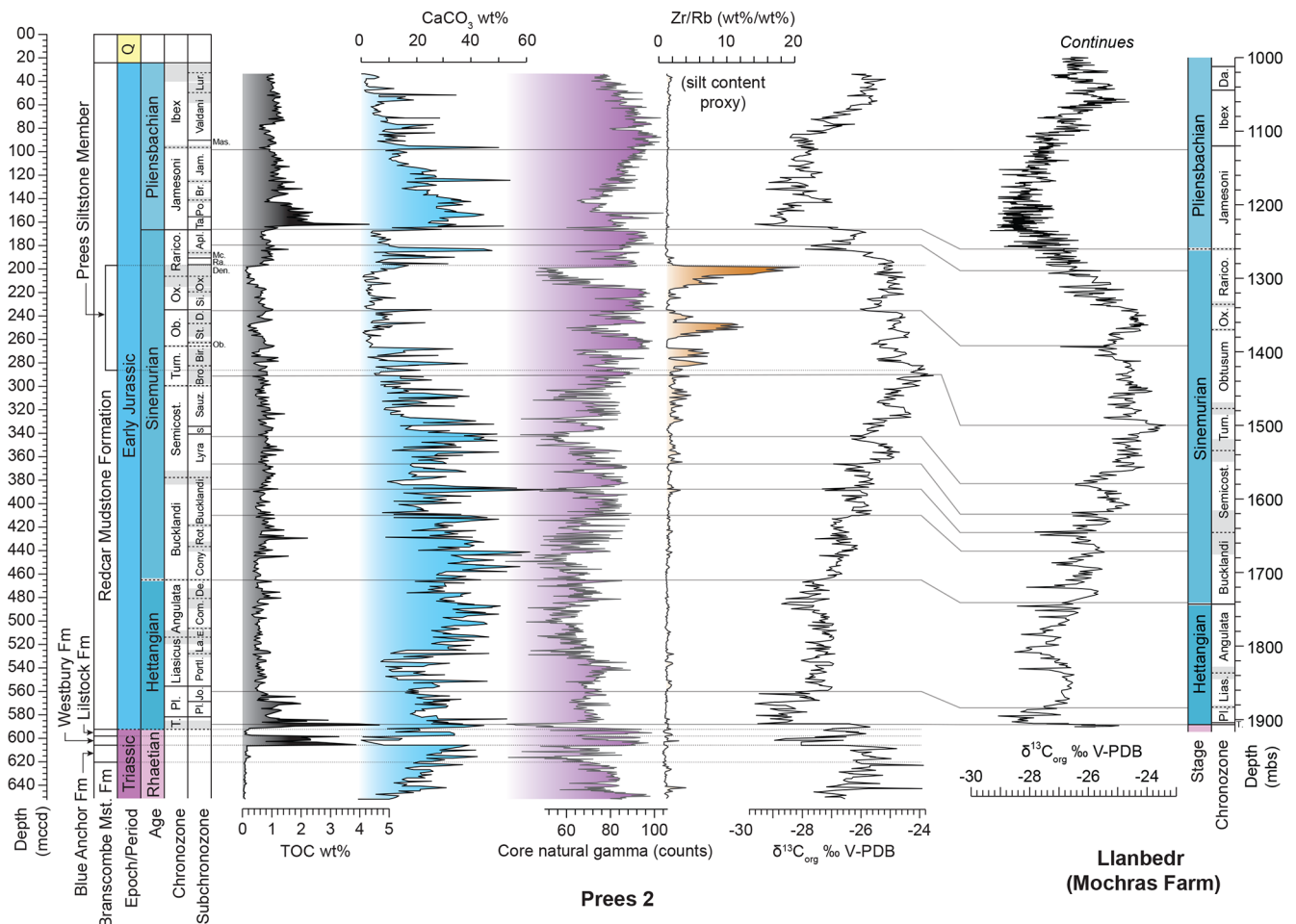


**Figure 4.** Summary of the succession in the Prees 2 cores and proposed correlation with the equivalent succession in the Llanbedr (Mochras Farm) borehole based on carbon-isotope stratigraphy (note the different scales used for Prees versus Mochras). Correlation lines are based on both negative and positive carbon-isotope excursions within constraints imposed by ammonite biostratigraphy. The lithological succession of the Lias Group at Prees most closely matches that of the Cleveland Basin, and thus the Redcar Mudstone Formation is adopted as the principal lithostratigraphic unit in the Cheshire Basin (Cox et al., 1999). The Prees member is defined herein. m.c.c.d.: metres corrected core depth. See Fig. 3 for abbreviations of ammonoid chronozones and subchronozone. The carbon-isotope record ( $\delta^{13}\text{C}_{\text{org}}$ ), TOC, and  $\text{CaCO}_3$  data are at  $\sim 1$  m stratigraphic resolution and are based on bulk samples. The core gamma ray is at a smoothed resolution of 20 cm. Mochras  $\delta^{13}\text{C}_{\text{org}}$  from Storm et al. (2020). Data shown in this figure are tabulated in Supplementary Data Files 4–6 together with additional elements determined by p-XRF.

and in the area of the UK and Ireland it may have been deposited in a carbonate ramp to offshore shelf setting (Hesselbo et al., 2004; Jeram et al., 2021). The age assignment for both members at Prees is the latest Rhaetian (see Sect. 3.4.1).

### 3.2.5 Lias Group, Redcar Mudstone Formation

This formation, 568 m thick in Prees 2 and truncated below the Quaternary, comprises dark-grey massive to faintly laminated mudstone and marl. Carbonate concretions occur throughout, including sideritic and septarian varieties. Macrofossils and trace fossils are abundant at many levels, and organic matter is relatively enriched at around 590 m.c.c.d. (earliest Hettangian) and 160 m.c.c.d. (earliest

Pliensbachian) (Figs. 3, 6, 7). The earliest Hettangian part of the formation at Prees,  $\sim 5$  m, comprises a distinctive dark-grey,  $> 4\%$  TOC, planar, wavy, and crinkly laminated silty limestone or mudstone lithofacies, similar to some levels within the Westbury Formation at Prees. The high carbonate content in this basal unit is responsible for a markedly low downhole and core gamma-ray signature (Figs. 4, 5).

The bulk of the strata recovered in the Prees 2 cores is referred to as the Lias Group, but the formation names most appropriately used are a matter for discussion because of the previous lack of a complete record of the lower Lias Group from the Cheshire Basin (Cox et al., 1999). Names adopted could be chosen from the schemes for the south-western UK or north-eastern England. Herein we use the



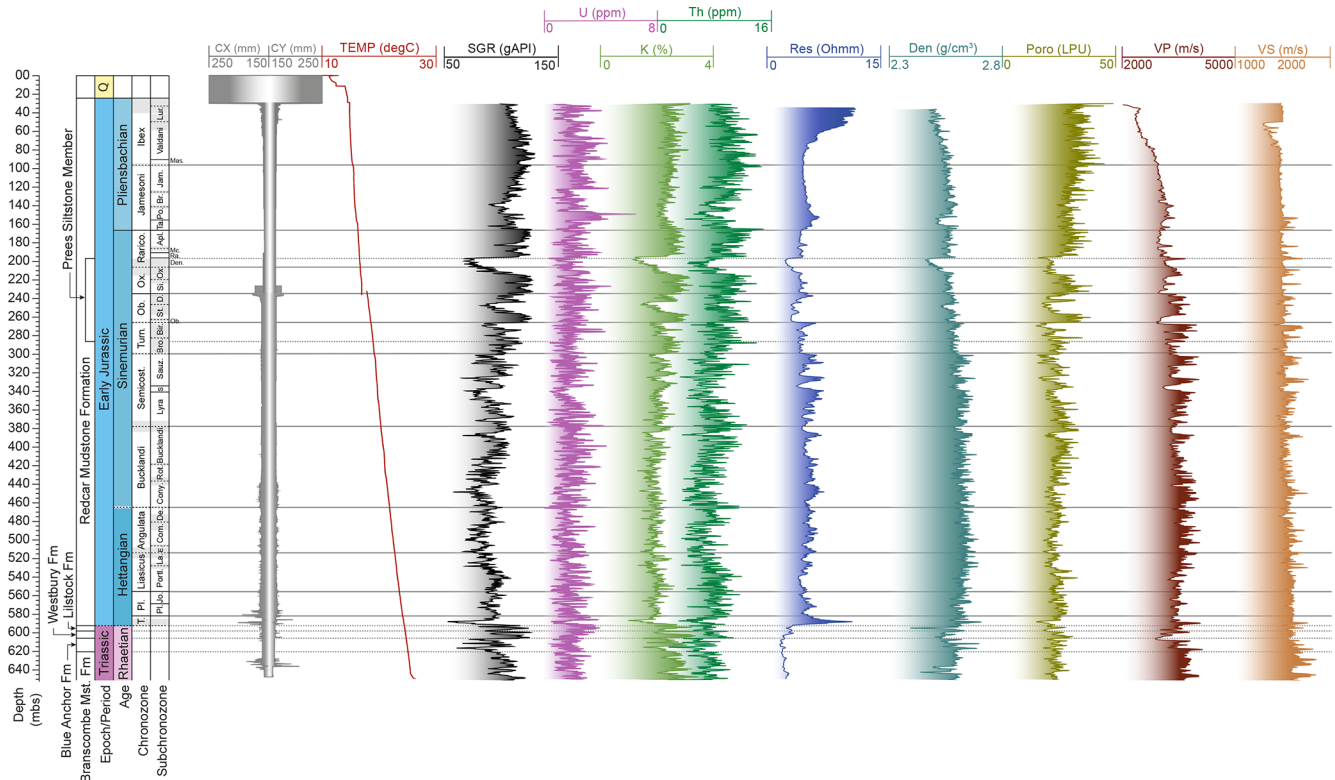


**Figure 5.** Summary of the downhole logging data from Prees 2C plotted against metres below the surface (m.b.s.). Note that the m.b.s. scale used for downhole logs generally differs only at most a few tens of centimetres from the m.c.d. scale, except potentially at the two locations where core loss was significant, in the lowest Redcar Mudstone Formation and in the lowest Westbury Formation (see Fig. 3). From left to right: caliper (CX/CY, mm); temperature (TEMP, °C); spectral gamma ray (SGR (total), gAPI, U, ppm, K, %, Th, ppm); resistivity (Res, Ohm); density (Den, g cm<sup>-3</sup>); porosity (Poro, limestone porosity units LPU); sonic velocity (P-wave (VP), S-wave (VS), m s<sup>-1</sup>).

formational name from the Cleveland Basin (Redcar Mudstone) on the basis of overall greater similarity to the Early Jurassic cropping out on the coast of north-eastern England (Yorkshire–Teesside, Cleveland Basin; Powell, 2010) compared to successions from south-western and central England and Wales (Wessex Basin, Bristol Channel Basin, and Worcester Graben; Old et al., 1987, 1991; Brandon et al., 1990; Gaunt et al., 1992; Hesselbo and Jenkyns, 1995; Warrington and Ivimey-Cook, 1995; Berridge et al., 1999).

Between 286.29 and 196.90 m.c.d., in the Late Sinemurian interval, a distinctive unit occurs comprising pale grey-buff bioturbated fine to very fine sandstone and siltstone, intercalated with medium- to dark-grey mudstone and with a low carbonate content (generally < 10 %). This sub-unit is designated the “Prees Siltstone Member” herein and is correlative in time with the similarly silty and sandy Siliceous Shale Member of the Cleveland Basin Redcar Mudstone succession (e.g. Powell, 2010; Hesselbo et al., 2020b). Other similarities to the Redcar Mudstone include calcareous mudstone beds in the lower part (up to the middle of the Sinemurian, ~ 340 m.c.d.), pyritic shales around the Sinemurian–Pliensbachian boundary (~ 200–150 m.c.d.), and nodular sideritic mudstones in the Pliens-

bachian (~ 100 m.c.d. and above). The lower, more calcareous part of the recovered succession at Prees has some distinct lithological and palaeontological similarities to the Blue Lias Formation of the south-western UK but lacks the characteristic fully developed limestone beds or periodically occurring finely laminated black shale beds with high (5 %–10 %) TOC content (see for example Fig. 6d). (If Blue Lias and Charmouth Mudstone names were to be adopted instead, as might be required for a nationally or supranationally applicable scheme, then, accepting a broader lithological definition for Blue Lias, the boundary between formations would lie at ~ 340 m.c.d., and the Prees Siltstone Member could be extended down to the base of the Charmouth Mudstone thus defined.) The lithostratigraphic subdivisions of the Lias Group at Prees are all clearly evident in all the core and downhole geophysical log datasets, with gamma-ray logs being influenced strongly by both carbonate and quartz silt and sand content (Figs. 4, 5).

In line with most other lower Lias Group occurrences, the succession at Prees is interpreted as being deposited in an offshore, hemipelagic, marine setting subject to periods of basin restriction and affected by wave and distal storm processes (Hallam, 1960; Weedon, 1986; van Buchem et al.,



**Figure 6.** Typical lithofacies of Jurassic and Triassic lithological units. **(a)** Redcar Mudstone Formation, medium-grey argillaceous and siliceous mudstone with common shell debris, silty and shelly laminae and beds and red-weathering (sideritic) nodules, likely hiatus at 18 cm depth, CB00354003, 5065\_1\_C\_2\_3, 35.72–36.72 m c.c.d., Pliensbachian, ?Ibex Chronozone. **(b)** Redcar Mudstone Formation, medium- to dark-grey pyritic calcareous argillaceous mudstone, CB00354134, 5065\_1\_C\_23\_1, 146.79–147.79 m c.c.d., Pliensbachian, Jamesoni Chronozone. **(c)** Redcar Mudstone Formation, Prees Siltstone Member, pale- to medium-grey-buff bioturbated argillaceous siltstone CB00354205, 5065\_1\_C\_33\_2, 208.52–209.52 m c.c.d., Sinemurian, Oxynotum, or Raricostatum Chronozone. **(d)** Redcar Mudstone Formation, dark-grey pyritic argillaceous calcareous mudstone, CB00354454, 5065\_1\_C\_74\_2, 442.43–443.43 m c.c.d., Sinemurian, Bucklandi Chronozone. **(e)** Redcar Mudstone Formation, dark-grey and pale-grey pyritic argillaceous calcareous mudstone, CB00354531, 5065\_1\_C\_86\_4, 510.48–511.48 m c.c.d., Hettangian, Liasicus, or Angulata Chronozone. **(f)** Lilstock Formation, Cotham Member, medium-pale grey-green heterolithic mudstone with siltstone or very fine sandstone laminae and lenses, cross-laminated, with discrete levels of convolute bedding, CB00354628, 5065\_1\_C\_104\_5, 595.19–596.19 m c.c.d., Rhaetian. **(g)** Westbury Formation, dark-grey heterolithic mudstone with crinkly siltstone and carbonate laminae, with discrete levels of bioturbation structures and convolute bedding, CB00354632, 5065\_1\_C\_105\_3, 599.20–600.19 m c.c.d., Rhaetian. **(h)** Blue Anchor Formation. Grey-green calcareous argillaceous mudstone and siltstone, bioturbated, CB00354655, 5065\_1\_C\_109\_3, 617.35–618.35 m c.c.d., ?Rhaetian. All panels are Itrax optical images.

1994; Weedon et al., 2017). This setting contrasts with the Lias at Mochras, Cardigan Bay Basin, which is interpreted as having been deposited below the influence of storm processes and instead subject to contour currents and related sediment transport (Pieńkowski et al., 2021). Downhole and core gamma-ray logs provide an excellent record of metre-

scale lithological cyclicity through most of the Redcar Mudstone (Figs. 4, 5).





**Figure 7.** Key boundaries of Jurassic and Triassic chronostratigraphic and lithostratigraphic units, marked with a red arrow head. **(a)** Sinemurian–Pliensbachian stage boundary: pale-grey bioturbated shelly calcareous mudstone rests sharply at 166.80 m c.c.d. on pale- to medium-grey shelly pyritic mudstone, carbonate-cemented in the top 9 cm; CB00354157, 5065\_1\_C\_26\_2, 166.31–167.31 m c.c.d. **(b)** Top Prees Siltstone Member, Densinodulum Subchronozone, Raricostatum Chronozone, transition of dark-grey pyritic argillaceous mudstone downward at 196.90 m c.c.d. into bioturbated fine to very fine sandstone or siltstone, CB00354191, 5065\_1\_C\_31\_2, 196.41–197.41 m c.c.d. **(c)** Base Prees Siltstone Member, Turner Chronozone, transition downward at 286.29 m c.c.d. of pale-grey bioturbated siltstone into medium-grey argillaceous siliceous mudstone, CB00354289, 5065\_1\_C\_47\_1, 285.66–286.66 m c.c.d. **(d)** Top Lilstock Formation and Langport Member, top Cotham Member, Rhaetian; the top Langport Member has a sharp downward change from dark-grey, faintly laminated argillaceous mudstone of an overlying formation to medium-grey heterolithic laminated siltstone, limestone, and mudstone (592.33 m c.c.d.). The top Cotham Member is marked by a sharp downward change to a pale-grey or buff siltstone or limestone partly stromatolitic bedset (592.51 m c.c.d.); CB00354625, 5065\_1\_C\_104\_2, 592.20–593.19 m c.c.d. **(e)** Top Westbury Formation, Rhaetian, sharp downward change at 598.03 m c.c.d. from medium- to dark-grey convolute bedded silty mudstone to massive dark-grey argillaceous mudstone; CB00354630, 5065\_1\_C\_105\_1, 597.20–598.20 m c.c.d. **(f)** Top Blue Anchor Formation, ?Rhaetian, thin dark-grey to black arenaceous mudstone with phosphatic nodules of an overlying formation resting sharply at 605.82 m c.c.d. on green-grey argillaceous limestone and mudstone, CB00354642, 5065\_1\_C\_107\_2, 605.48–606.43 m c.c.d. **(g, h)** Top Branscombe Mudstone Formation, ?Rhaetian, top of the first consistent occurrence at 620.34 m c.c.d. of medium red-brown patches in an otherwise massive grey-green calcareous mudstone, CB00354657, 5065\_1\_C\_109\_5, 619.35–620.34 m c.c.d. and CB00354658, 5065\_1\_C\_109\_6, 620.34–621.33 m c.c.d. All panels are Itrax optical images.

### 3.2.6 Quaternary diamict

The lowest unit within the Quaternary succession is a red-brown diamict comprising a clay-silt matrix and abundant matrix-supported subangular to subrounded mudstone and

carbonate clasts that range in colour from white through to dark grey and dark brown. The clast sizes range up to medium pebbles. The thickness of the diamict unit is estimated to be ~4.72 m and its base is at 24.22 m b.s. However, the upper 1.38 m of the Lias Group (from 25.60 to



24.22 m b.s.) comprises a highly disturbed mudstone breccia in a mud matrix that may alternatively also be regarded as part of the Quaternary succession.

### 3.2.7 Quaternary clay, sand, and gravel

The upper part of the Quaternary succession comprises pebbly sand at the base (1.4 m) passing up into 6.8 m of gravelly clay and 11 m of medium sand. This unit is interpreted as part of the deltaic infill of the glacial Lake Prees (Chiverrell et al., 2021).

## 3.3 Fractures

### 3.3.1 Hydrofractures in the Lias Group

The uppermost Lias in Prees 2A and Prees 2B proved difficult to recover as fully intact cores. This is likely due to fine-scale fracture networks, particularly in the upper  $\sim 7$  m below the Quaternary deposits. Fractures in the strata underlying ice sheets are a widely observed phenomenon (e.g. Phillips et al., 2013; Philips and Hughes, 2014) and have been described as hydrofracture systems (Benn and Evans, 2010). At Prees, the top 1.38 m comprises dislocated angular fine pebbles and granules of mudstone in a mudstone matrix. Below this level (25.60 m b.s.), the mudstone remains in place but is highly fractured in multiple orientations down to at least 31 m b.s. Below this level the cores show common mostly bedding-parallel fracturing, but it is difficult to distinguish between natural fracture networks and those induced by drilling. The hydrofracture system at Prees is likely the result of loading by the ice mass that formed the land-terminating lobe of the Irish Sea Glacier, which was at its maximum extent during the Late Pleistocene Last Glacial Maximum ( $26.5 \pm 1.8$  ka), terminating at the glacial Lake Morville,  $\sim 45$  km SSE of Prees (Chiverrell et al., 2021).

### 3.3.2 Subvertical fractures in the Mercia Mudstone and Penarth Group

Both mineralized and unmineralized subvertical fractures occur commonly in the Triassic succession at Prees. Most cores from the Westbury Formation downwards (Core 105, 600 m c.c.d.) are affected by these fractures (Fig. 8). The fracture faces dip steeply ( $\sim 85^\circ$ ), but their compass orientation has yet to be determined. Mineralization appears to depend on host lithology in a similar manner to what is observed at Mochras (see Ullmann et al., 2022). The dense occurrence of these fractures within the Late Triassic succession suggests a relationship with the change in tectonic style at the inception of the Late Triassic to Early Jurassic sag basin. Drilling operations data (drilling fluid loss into the formation) show that these fractures remain open in the subsurface in the present day and will have significance for the sealing properties of the Mercia Mudstone Group in the

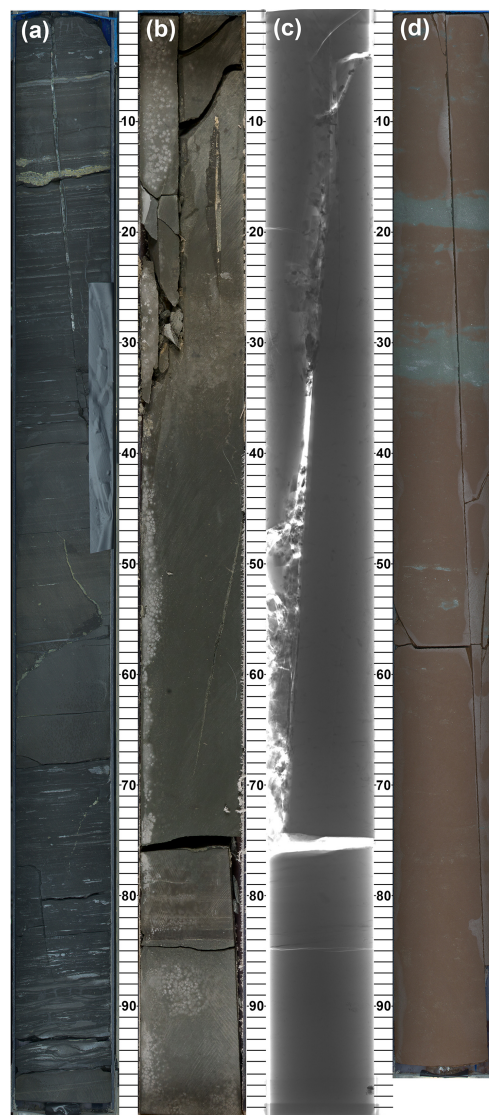


**Figure 8.** Subvertical fractures, Late Triassic. (a) Westbury Formation, subvertical mineralized fracture with millimetre-scale offset, Itrax optical image, CB00354641, 5065\_1\_C\_107\_1, 604.49–605.48 m c.c.d. (b) Blue Anchor Formation, subvertical mineralized fracture, core-lab photograph, CB00354644, 5065\_1\_C\_107\_4, 607.37–608.37 m c.c.d. (c) Blue Anchor Formation, subvertical mineralized fracture, X radiograph of the whole round, CB00354644, 5065\_1\_C\_107\_4, 607.37–608.37 m c.c.d. (d) Branscombe Mudstone Formation, subvertical unmineralized fracture, Itrax optical image, CB00354678, 5065\_1\_C\_112\_6, 638.23–639.20 m c.c.d.

Cheshire Basin and in related tectonic settings (see e.g. Al-Najdi and Worden, 2023).

### 3.4 Stratigraphic correlation and depositional history

#### Ammonite chronostratigraphy and carbon-isotope stratigraphy

Ammonite chronostratigraphy combined with carbon-isotope stratigraphy presently provides the principal means of regional correlation of the Jurassic strata in Prees 2 cores (Fig. 3). Chronozones can be derived from Jurassic ammonoid biozones as discussed by Page (2017). Particular emphasis is placed on identification of ammonite taxa indicative of chronozones and subchronozones and biohorizons if possible, following the biostratigraphic and chronostratigraphic scheme of Page (2003, 2009, 2010a, b) and Weedon et al. (2017, 2019), and the results are summarized here in Fig. 3 and in Supplementary Data File 2. Assignment of intervals of the core that lie between the highest and lowest markers for the chronozones and subchronozones is uncertain (i.e. there is no ammonite evidence for which zone or subzone these strata belong to), and such intervals are indicated by grey shading in the graphics.

Fossils characteristic of almost all ammonite-based chronozones and subchronozones for the cored stratigraphy are recognized at Prees. Biostratigraphic characterization is particularly good for the Hettangian and Early Sinemurian (Figs. 3–5; Supplementary Data File 2). All Late Sinemurian subchronozones are also present, but the boundaries of these subdivisions are less well defined than for the strata below, and their thicknesses are evidently quite reduced in some cases (e.g. the *Raricostatoides* Subchronozone of the *Raricostatum* Chronozone; Figs. 3–5; Supplementary Data File 2). The Early Pliensbachian ammonite-based zonation is again well defined, except in the top 35 m (Ibex Chronozone).

Carbon-isotope stratigraphy based on analysis of bulk organic matter has proven to be particularly useful for local to regional and, potentially, even global correlations to help refine those based on ammonite chronostratigraphy (e.g. Al-Suwaidi et al., 2022). Although it is broadly acknowledged that the finer details of carbon-isotope curves may be due to factors under local controls, such as mixing of different organic matter components with their individual carbon-isotopic compositions (e.g. Suan et al., 2015; Fox et al., 2022), consistent patterns in different, sometimes very distant basins are nevertheless well established. Figure 4 shows a correlation between Prees 2C, based on new data, and the basal Hettangian–Early Pliensbachian of Mochras using the carbon-isotope stratigraphy of Storm et al. (2020); all correlations shown are consistent with the ammonite biostratigraphy (see Supplementary Data File 3 for refinements to the previously published ammonite chronostratigraphy for Mochras; Page in Copestake and Johnson, 2014). No doubt further tie lines could be proposed. A noteworthy feature of the carbon-isotope curve of Prees (166.70–165.90 m.c.c.d.) is the abrupt negative excursion at the Sinemurian–Pliensbachian boundary, which supports the de-

termination of a hiatus at 166.80 m.c.c.d. based on sedimentological and ichnological observations (Fig. 7). The fairly prominent negative carbon-isotope excursion in Mochras at about 1310 m in the lower part of the *Raricostatum* Zone may be missing at another hiatus in Prees, possibly at the top of the Prees Siltstone Member, where there is a very strongly expressed transgressive surface.

Recognition of the Triassic–Jurassic boundary away from the GSSP at Kuhjoch in Austria is currently challenging due to the very rare occurrence elsewhere of the primary marker taxon, *Psiloceras spelae* (von Hillebrandt et al., 2013). In Prees, the lowest ammonite fossil in the succession, a possible psiloceratid fragment, lies at 583.57 m.c.c.d., which is 8.76 m above the lithostratigraphical base of the Lias Group (Redcar Mudstone Formation), and there are no other age-diagnostic fossils recovered yet from these basal Lias mudstones. The presence of confirmed *Psiloceras erugatum* (Phillips), however, only 0.07 m higher at 583.50 m.c.c.d., represents the lowest *Psiloceras* species recorded in the UK and Irish Jurassic (Bloos and Page 2000) – placing this latter level in Prees definitely in the upper part of the basal Jurassic Tilmanni Chronozone (Page, 2010a, equivalent to the Hn2 biohorizon in Weedon et al., 2017, 2019).

Recently, Jeram et al. (2021) reviewed correlations of UK basal Jurassic successions with reference to a newly published high-resolution carbon-isotope record from Larne, Northern Ireland; these authors discuss three possible correlations based on carbon-isotope stratigraphy. Here we follow the practice of several recent authors (Korte et al., 2019; Ruhl et al., 2020) who identify a secondary negative carbon-isotope excursion lying between the “initial” and “main” carbon-isotope excursions of Hesselbo et al. (2002). In lieu of further biostratigraphic data from other fossil groups, this correlation likely places the Triassic–Jurassic boundary in Prees 2C close to the junction between the Lilstock Formation and Redcar Mudstone Formation (between 592.78 and 592.19 m.c.c.d., lithostratigraphically at 592.33 m.c.c.d.), but the possibility remains that the system boundary lies higher in the succession (possibly as high as ~589 m.c.c.d.) pending study of higher-resolution carbon-isotope datasets and palynology. We interpret the isotopically light  $\delta^{13}\text{C}_{\text{org}}$  values at the top of the Cotham Member of the Lilstock Formation as representing the “initial” negative carbon-isotope excursion of Hesselbo et al. (2002). Records of lower ammonites in the UK and Irish successions, including *Neophyllites lavernockensis* Hodges, as reported from the uppermost Lilstock Formation in South Wales (Hodges, 2021), would likely be of the latest Triassic age, lying as they do below the base of the Lias and below those features of the carbon-isotope curves generated from bulk organic matter samples that signify the base of the Jurassic (see e.g. Korte et al., 2019, and references therein).

#### 4 Summary and research prospects

The data presented here provide the stratigraphic framework and depositional context for multiple ongoing studies into Early Jurassic Earth history and Earth system processes. The succession recovered in the Prees cores spans the Late Triassic mass extinction event and its aftermath, and each ammonite chronozone and subchronozone through to the Early Pliensbachian Ibex Chronozone is represented. The recovered Lias succession is predominantly argillaceous and shows the greatest similarity to the lower Lias Group in the Cleveland Basin, which lies  $\sim 200$  km to the NE. The prospects of determination of orbital cycles look to be very good based on clearly evident 1 m scale lithological cyclicity (Figs. 6e, 7c), which finds strong expression in both the high-resolution core-scanning data and the downhole log datasets (Figs. 4, 5). The 1 m cycles likely represent precession and form the principal building blocks for construction of an astrochronology.

A carbon-isotope curve based on bulk organic matter at  $\sim 1$  m resolution presented here is used to correlate with the Llanbedr (Mochras Farm) borehole in the adjacent Cardigan Bay Basin. The generated carbon-isotope stratigraphy corroborates curves at comparable resolution generated from bulk organic matter and fossil wood at Mochras (Storm et al., 2020) and from bulk organic matter, wood, and macrofossil carbonate in adjacent north-western European basins (e.g. Hesselbo et al., 2020b; Ullmann et al., 2022). The Hettangian and Sinemurian stages are already notable for the parallel progressive decrease in oxygen-isotope values of benthic macrofossils whilst organic matter  $\delta^{13}\text{C}_{\text{org}}$  increases, suggesting that regional seawater temperature is not directly related to global carbon burial (e.g. Hesselbo et al., 2020c). New environmental palaeo-proxy data to be generated from the core can be used to test, amongst other hypotheses, whether opening of the Hispanic oceanic corridor to the west may have driven tropical Tethyan waters further north into the north-western European basins (e.g. Ruvalcaba Baroni et al., 2018).



## Appendix A: Organic matter characterization and thermal maturity in Mochras, Prees 1, and Wilkesley

Pyrolysis data were generated using a Vinci Rock-Eval 6 instrument (Behar et al., 2001) at the Department of Earth Sciences, University of Oxford, and the results are shown in Fig. A1 (see also Supplementary Data File 5).

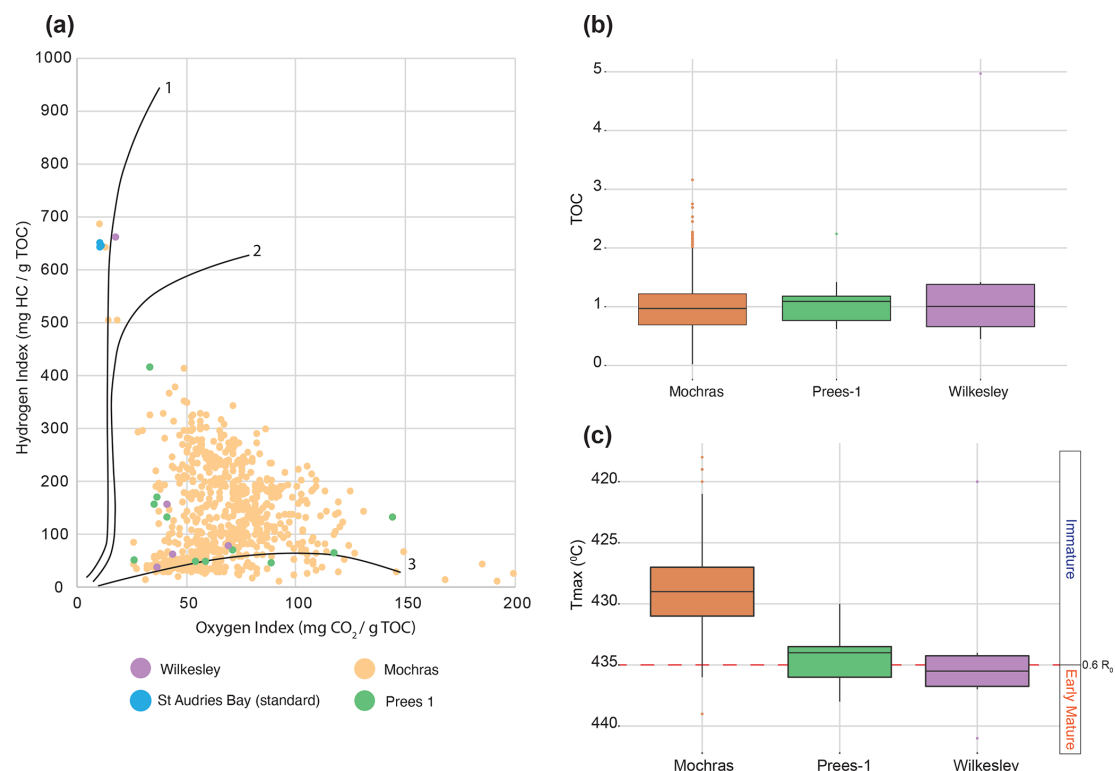


**Figure A1.** Rock-Eval 6 pyrolysis data. **(a)** Pyrolysis data presented in a van Krevelen diagram showing the organic matter types of the studied Prees 1 cuttings compared to Wilkesley and Mochras core samples, with outcrop samples from St Audries Bay, south-western England, used as standards. The Rock-Eval data for Prees 1 ( $n = 11$ ) and Wilkesley ( $n = 5$ ) indicate a Type-3 to mixed Type-2–Type-3 kerogen source (see e.g. Espitalié et al., 1977); one sample from the Wilkesley borehole plots is in the Type-1 zone. There is some uncertainty as to the representative nature of this distribution due to the small sample set. In addition, the small sample set from the Prees 1 and Wilkesley boreholes plots close to the large dataset ( $n = 910$ ) from the Mochras borehole (Storm et al., 2020). **(b)** TOC box-and-whisker plots showing organic matter quantity. The box plots for Prees 1, Wilkesley, and Mochras have comparable ranges in TOC, with a median value close to 1 wt %. **(c)** Tmax box-and-whisker plots for thermal maturity (see Evenick, 2021, for a recent review). The range of Tmax values reported across the three wells is narrow and the differences in average Tmax relatively small, indicating practically the same to very marginally deeper burial for Prees 1 and Wilkesley compared to Mochras. The average Tmax recorded for Wilkesley just surpasses the Tmax = 435 °C mature-to-immature transition equivalent to vitrinite reflectance  $R_0$  values approaching 0.6.

**Data availability.** Full core scan data (<https://doi.org/10.5285/91392f09-25d4-454c-aece-56bde0dbf3ba>, BGS Core Scanning Facility, 2022) will be available after 1 November 2024 via the Natural Environment Research Council (NERC) National Geoscience Data Centre (<https://webapps.bgs.ac.uk/services/ngdc/accessions/index.html#>, last access: 12 October 2023). Downhole logging data (<https://doi.org/10.5880/ICDP.5065.001>, Wonik, 2023) will be made available via the ICDP (<https://www.icdp-online.org/projects/by-continent/europe/jet-uk/>, last access: 12 October 2023).

The JET Operational Report is published as Hesselbo et al. (2023); full information about the operational dataset, the logging dataset, data availability and the explanatory remarks is available on the ICPD-JET project website: <https://www.icdp-online.org/projects/by-continent/europe/jet-uk/> (last access: 12 October 2023).

A subset of data, additional biostratigraphic tables, and vector graphics files for Figs. 3–5 are included as the Supplement. Supplementary Data File 1 tabulates the corrected depth scale for Prees 2C. Supplementary Data File 2 summarizes the ammonite-based chronostratigraphy of the Prees 2 cores (ammonite identifications by Kevin N. Page). Supplementary Data File 3 summarizes the ammonite-based chronostratigraphy for the Hettangian to Early Pliensbachian of the Llanbedr (Mochras Farm) borehole (updated by Kevin N. Page). Supplementary Data File 4 tabulates the organic carbon-isotope ratios, TOC, and carbonate content of low-resolution samples taken at the Prees drill site; TOC and carbonate data are calculated using calibration based on portable XRF (Supplementary Data File 5) and a gas source isotope ratio mass spectrometer (Supplementary Data File 6). Supplementary Data File 5 tabulates portable XRF results for bulk rock powders of low-resolution samples taken at the Prees drill site; uncertainties stated in the table are given for the fit to the raw data and do not reflect the true reproducibility of the data. Empty fields indicate values under the detection limit. Sample SSK116001 acted as a repeat sample which was measured 70 times over the course of the data acquisition to determine the repeatability and drift of the instrument. LE stands for “light elements”. Supplementary Data File 6 tabulates gas source isotope ratio mass spectrometry (GS-IRMS) data (oxygen- and carbon-isotope ratios of carbonate as well as carbonate content calculated as calcite) for a set of 24 samples covering the entire core length and reflecting a representative spread of carbonate content. Comparison of GS-IRMS data with p-XRF data was used to create a calibration curve to calculate the carbonate (and TOC) content of all low-resolution samples. Supplementary Data File 7 tabulates pyrolysis data (Rock-Eval 6) for Prees 1 well cuttings and Wilkesley borehole samples. Supplementary Data File 8 contains vector graphics files (.svg) for Figs. 3–5.

**Sample availability.** Samples will be available on request to the British Geological Survey National Geological Repository after 1 November 2024.

**Supplement.** The supplement related to this article is available online at: <https://doi.org/10.5194/sd-32-1-2023-supplement>.

**Author contributions.** All the authors contributed to the investigation. The project was conceptualized by SPH, CJB, CMB, JVB, DJC, SD, AJD, AF, LAH, CH, WK, CK, CTSL, CM, EM, RJN, KGM, JP, GP, SWP, JBR, MR, MSS, GS, NT, CVU, BvdS, TW, and WX. Additional funding was acquired by SPH, CMB, DJC, SD, HCJ, MJL, TML, CTSL, CM, RJN, JP, GP, SWP, JBR, AU, CVU, BvdS, PBW, and TW. SPH, CVU, RLS, and JBR developed and co-ordinated the project methodology. SPH and CVU created the original draft manuscript. All the authors contributed to review and editing. KH and KB were project administrators.

**Competing interests.** The contact author has declared that none of the authors has any competing interests.

**Disclaimer.** Publisher’s note: Copernicus Publications remains neutral with regard to jurisdictional claims made in the text, published maps, institutional affiliations, or any other geographical representation in this paper. While Copernicus Publications makes every effort to include appropriate place names, the final responsibility lies with the authors.

**Acknowledgements.** We enthusiastically thank the ICDP Operations Support Group for continued help and advice over many years. The professional input of all the project contractors, Zetland Group, Zenith Energy, Marriott Drilling Group, Fox (Owmbly) Ltd, Excellence Logging, and Robertson Geo, is all gratefully acknowledged. We thank the landowners, Grafton Beddoes & Sons, for access and hospitality. David J. Smith (BGS Edinburgh) provided hugely valued advice in the initial stages of this project. Staff at the BGS National Geological Repository and Core Scanning Facility, British Geological Survey, Keyworth, are warmly thanked for their long-standing support. Emma Cieslak-Jones and Connor O’Keeffe are thanked for helping with palaeontological collections and curation. Contributions to core processing at the drill site by Amy Elson and Libby Robinson are gratefully acknowledged, as is input at the original JET workshop from Hemmo Abels, Joachim Blau, Linhao Fang, Adam Robinson, Charlotte Sweeney, Christian Meister, and Ken Williford. We also thank Simon Holford and Jonathan Turner for their advice and encouragement. Daniel J. Condon, Margaret Damaschke, Melanie J. Leng, and James B. Riding all publish with the approval of the Executive Director, British Geological Survey (NERC). This project would not have been possible without the sustained support of Helen Butler, Chrysten Cole, Sam Barker, Hugh McCann, and Ruth Banyard (University of Exeter). John Cope, Mike Sumbler, and Mick Oates are thanked for their discussion of the lithostratigraphy. Reviewers Paul Olsen and Sietske Batenburg provided very helpful comments on the manuscript.

**Financial support.** This research has been supported by the ICDP, the Natural Environment Research Council (grant no. NE/N018508/1 to Stephen P. Hesselbo, Clemens V. Ullmann, Claire M. Belcher, Timothy M. Lenton, Robert J. Newton, Crispin T. S. Little, Simon W. Poulton, and Paul B. Wignall), the German Research Foundation (grant no. 398741931 to Thomas Wonik), the Hungarian Scientific Research Fund (grant no. NN

128702 to József Pálffy), the National Science Centre, Poland (Opus 13, grant no. 2017/25/B/ST10/02235 to Gregory Pieńkowski and Alfred Uchman), and the Polish Geological Institute (grant no. 62.9012.2016.00.0 to Gregory Pieńkowski).

**Review statement.** This paper was edited by Thomas Wiersberg and reviewed by Sietske Batenburg and Paul Olsen.

## References

- AlNajdi, N. and Worden, R. H.: Porosity in mudstones and its effectiveness for sealing carbon capture and storage sites, in: *Enabling Secure Subsurface Storage in Future Energy Systems*, edited by: Miocic, J. M., Heinemann, N., Edlmann, K., Alcalde, J., and Schultz, R. A., *Geol. Soc. Lond. Spec. Publ.*, 528, 339–357, <https://doi.org/10.1144/SP528-2022-84>, 2023.
- Al-Suwaidi, A. H., Ruhl, M., Jenkyns, H. C., Damborenea, S. E., Manceñido, M. O., Condon, D. J., Angelozzi, G. N., Kamo, S. L., Storm, M., Riccardi, A. C., and Hesselbo, S. P.: New chronostratigraphic constraints on the Lower Jurassic Pliensbachian–Toarcian Boundary at Chacay Melehue (Neuquén Basin, Argentina), *Sci. Rep.*, 12, 4975, <https://doi.org/10.1038/s41598-022-07886-x>, 2022.
- Antell, G. S. and Saupe, E. E.: Bottom-up controls, ecological revolutions and diversification in the oceans through time, *Curr. Biol.*, 31, R1237–R1251, 2021.
- Baker, S. J., Hesselbo, S. P., Lenton, T. M., and Belcher, C. M.: Charcoal evidence that rising atmospheric oxygen terminated Early Jurassic ocean anoxia, *Nat. Commun.*, 8, 15018, <https://doi.org/10.1038/ncomms15018>, 2017.
- Behar, F., Beaumont, V., and Pentead, H. L. De B.: *Rock-Eval 6 Technology: Performances and Developments*, *Oil & Gas Science and Technology – Rev. IFP*, 56, 111–134, <https://doi.org/10.2516/ogst:2001013>, 2001.
- Benn, D. and Evans, D. J. A.: *Glaciers and Glaciation*, 2nd edn., Routledge, London, 816 pp., <https://doi.org/10.4324/9780203785010>, 2010.
- Berridge, N. G., Pattison, J., Samuel, M. D. A., Brandon, A., Howard, A. S., Pharaoh, T. C., and Riley, N. J.: *Geology of the country around Grantham*, Memoir of the British Geological Survey, Sheet 127 (England and Wales), ISBN 0118845306, 1999.
- BGS Core Scanning Facility: Prees-2C Core Scanning Dataset, NERC EDS National Geoscience Data Centre [data set], <https://doi.org/10.5285/91392f09-25d4-454c-aece-56bde0dbf3ba>, 2022.
- Bloos, G. and Page, K.: The basal Jurassic ammonite succession in the North-West European Province – review and new results, in: *Advances in Jurassic Research 2000*, edited by: Hall, R. L. and Smith, P. L., *Proceedings of the Fifth International Symposium on the Jurassic System*, Vancouver, Canada, 12–25 August 1998, GeoResearch Forum, Trans Tech Publications, Zürich, 6, 27–40, ISBN 0878498443, ISBN 9780878498444, 2000.
- Brandon, A., Sumblar, M. G., and Ivimey-Cook, H. C.: A revised lithostratigraphy for the Lower and Middle Lias (Lower Jurassic) east of Nottingham, England, *P. Yorks. Geol. Soc.*, 48, 121–141, 1990.
- Capriolo, M., Mills, B. J. W., Newton, R. J., Corso, J. D., Dunhill, A. M., Wignall, P. B., and Marzoli, A.: Anthropogenic-scale CO<sub>2</sub> degassing from the Central Atlantic Magmatic Province as a driver of the end-Triassic mass extinction, *Global Planet. Change*, 209, 103731, <https://doi.org/10.1016/j.gloplacha.2021.103731>, 2022.
- Chiverrell, R. C., Thomas, G. S. P., Burke, M., Medialdea, A., Smedley, R., Clark, M. B., C., Duller, G. A. T., Fabel, D., Jenkins, G., Ou, X., Roberts, H. M., and Scourse, J.: The evolution of the terrestrial-terminating Irish Sea glacier during the last glaciation, *J. Quaternary Sci.*, 36, 752–779, 2021.
- Copestake, P.: Triassic, in: *Stratigraphical Atlas of Fossil Foraminifera*, edited by: Jenkins, D. G. and Murray, J. W., 2nd edn., Ellis Horwood, Chichester, 97–124, ISBN 9780853122104, 1989.
- Copestake, P. and Johnson, B.: The Hettangian to Toarcian (Lower Jurassic), in: *Stratigraphical Atlas of Fossil Foraminifera*, 2nd edn., Ellis Horwood Ltd., Chichester, UK, edited by: Jenkins, D. G. and Murray, J. W., 129–188, ISBN 9780853122104, 1989.
- Copestake, P. and Johnson, B.: Lower Jurassic Foraminifera from the Llanbedr (Mochras Farm) Borehole, North Wales, UK, *Palaeontological Society Monograph*, Publ. 641, v. 167 (part), 1–403, <https://doi.org/10.1080/02693445.2013.11963952>, 2014.
- Cox, B. M., Sumblar, M. G., and Ivimey-Cook, H. C.: A formational framework for the Lower Jurassic of England and Wales (onshore area), *British Geological Survey Research Report RR/99/01*, 1–28, 1999.
- Damaschke, M., Fellgett, M. W., Howe, M. P. A., and Watson, C. J.: Unlocking national treasures: The core scanning approach, in: *Core Values: the Role of Core in Twenty-first Century Reservoir Characterization*, edited by: Neal, A., Ashton, M., Williams, L. S., Dee, S. J., Dodd, T. J. H., and Marshall, J. D., *Geol. Soc. Lond. Spec. Publ.*, 527, <https://doi.org/10.1144/SP527-2022-58>, 2022.
- Deconinck, J.-F., Hesselbo, S. P., and Pellenard, P.: Climatic and sea-level control of Jurassic (Pliensbachian) clay mineral sedimentation in the Cardigan Bay Basin, Llanbedr (Mochras Farm) borehole, Wales, *Sedimentology*, 66, 2769–2783, 2019.
- Dobson, M. R. and Whittington, R. J.: The geology of Cardigan Bay, *P. Geologist. Assoc.*, 98, 331–353, 1987.
- Espitalié, J. J., Laporte, L., Madec, M., Marquis, F., Leplat, P., Paulet, J., and Bouitefeu, A.: Méthode rapide de caractérisation des roches mères, de leur potentiel pétrolier et de leur degré d'évolution, *Rev. I. Fr. Pétrol.* 32, 23–45, 1977.
- Evans, D. J., Rees, J. G., and Holloway, S.: The Permian to Jurassic stratigraphy and structural evolution of the Cheshire Basin, *J. Geol. Soc. London*, 150, 857–870, 1993.
- Evenick, J. C.: Examining the relationship between Tmax and vitrinite reflectance: An empirical comparison between thermal maturity indicators, *J. Nat. Gas Sci. Eng.*, 91, 103942021, <https://doi.org/10.1016/j.jngse.2021.103946>, 2021.
- Fox, C. P., Whiteside, J. H., Olsen, P. E., Cui, X., Summons, R. E., Idiz, E., and Grice, K.: Two-pronged kill mechanism at the end-Triassic mass extinction, *Geology*, 50, 448–453, 2022.
- Gaunt, G. D., Fletcher, T. P., and Wood, C. J.: *Geology of the country around Kingston upon Hull and Brigg*, Memoir of the British Geological Survey, Sheets 80 and 89 (England and Wales), ISBN 0118843990, 1992.



- Hallam, A.: A sedimentary and faunal study of the Blue Lias of Dorset and Glamorgan, *Philos. T. Roy. Soc. Lond.* B243, 1–44, 1960.
- Hesselbo, S. P. and Jenkyns, H. C.: A comparison of the Hettangian to Bajocian successions of Dorset and Yorkshire, in: *Field Geology of the British Jurassic*, edited by: Taylor, P. D., *Geol. Soc. Lond. Spec. Publ.*, 105–150, ISBN 1897799411, 1995.
- Hesselbo, S. P., Robinson, S. A., Surlyk, F., and Piasecki, S.: Terrestrial and marine extinction at the Triassic–Jurassic boundary synchronized with major carbon-cycle perturbation: a link to initiation of massive volcanism?, *Geology*, 30, 251–254, 2002.
- Hesselbo, S. P., Robinson, S. A., and Surlyk, F.: Sea-level change and facies development across potential Triassic–Jurassic boundary horizons, south west Britain, *J. Geol. Soc. London*, 161, 365–379, 2004.
- Hesselbo, S. P., Bjerrum, C. J., Hinnov, L. A., MacNiocaill, C., Miller, K. G., Riding, J. B., van de Schootbrugge, B., and the Mochras Revisited Science Team: Mochras borehole revisited: a new global standard for Early Jurassic earth history, *Sci. Dril.*, 16, 81–91, <https://doi.org/10.5194/sd-16-81-2013>, 2013.
- Hesselbo, S. P., Ogg, J. G., and Ruhl, M.: The Jurassic Period, in: *Geologic Time Scale 2020*, edited by: Gradstein, F. M., Ogg, J. G., Schmitz, M. D., and Ogg, G. M., Elsevier, 955–1021, ISBN 978-0-12-824360-2, 2020a.
- Hesselbo, S. P., Hudson, A. J. L., Huggett, J. M., Leng, M. J., Riding, J. B., and Ullmann, C. V.: Palynological, geochemical, and mineralogical characteristics of the Early Jurassic Liasidium Event in the Cleveland Basin, Yorkshire, UK, *Newsl. Stratigr.*, 53, 191–211, 2020b.
- Hesselbo, S. P., Korte, C., Ullmann, C. V., and Ebbesen, A.: Carbon and oxygen isotope records from the southern Laurusian Seaway following the Triassic–Jurassic boundary: parallel long-term enhanced carbon burial and seawater warming. *Earth-Sci. Rev.*, 203, 103131, <https://doi.org/10.1016/j.earscirev.2020.103131>, 2020c.
- Hesselbo, S. P., Ullmann, C. V., Silva, R. F. L., et al.: Early Jurassic Earth System and Timescale scientific drilling project (JET) – Operational Report, International Continental Scientific Drilling Program (ICDP), <https://doi.org/10.48440/ICDP.5065.001>, 2023.
- Hodges, P.: A new ammonite from the Penarth Group, South Wales and the base of the Jurassic System in SW Britain, *Geol. Mag.*, 158, 1109–1114, 2021.
- Hodgson, N. A., Farnsworth, J., and Fraser, A. J.: Salt-related tectonics, sedimentation and hydrocarbon plays in the Central Graben, North Sea, UKCS, in: *Exploration Britain: Geological insights for the next decade*, edited by: Hardman, R. F. P., *Geol. Soc. Lond. Spec. Publ.*, 67, 31–63, 1992.
- Hollaar, T. P., Baker, S. J., Hesselbo, S. P., Deconinck, J.-F., Mander, L., Ruhl, M., and Belcher, C. M.: Wildfire activity enhanced during phases of maximum orbital eccentricity and precessional forcing in the Early Jurassic, *Communications Earth & Environment*, 2, 247, <https://doi.org/10.1038/s43247-021-00307-3>, 2021.
- Hollaar, T. P., Hesselbo, S. P., Deconinck, J.-F., Damaschke, M., Ullmann, C. V., Jiang, M., and Belcher, C. M.: Environmental changes during the onset of the Late Pliensbachian Event (Early Jurassic) in the Cardigan Bay Basin, Wales, *Clim. Past*, 19, 979–997, <https://doi.org/10.5194/cp-19-979-2023>, 2023.
- Howard, A. S., Warrington, G., Ambrose, K., and Rees, J. G.: A formational framework for the Mercia Mudstone Group (Triassic) of England and Wales, British Geological Survey Research Report, RR/08/04, 2008.
- Jeram, A. J., Simms, M. J., Hesselbo, S. P., and Raine, R.: Carbon isotopes, ammonites and earthquakes: Key Triassic–Jurassic boundary events in the coastal sections of south-east County Antrim, Northern Ireland, UK, *P. Geologist. Assoc.*, 132, 702–725, 2021.
- Kent, D. V., Olsen, P. E., Rasmussen, C., Lepre, C., Mundil, R., Irmis, R. B., Gehrels, G. E., Giesler, D., Geissman, J. W., and Parker, W. G.: Empirical evidence for stability of the 405-kiloyear Jupiter–Venus eccentricity cycle over hundreds of millions of years, *P. Natl. Acad. Sci. USA*, 115, 6153–6158, 2018.
- Knoll, A. H. and Follows, M. J.: A bottom-up perspective on ecosystem change in Mesozoic oceans, *P. R. Soc. B*, 283, 20161755, <https://doi.org/10.1098/rspb.2016.1755>, 2016.
- Korte, C., Ruhl, M., Pálffy, J., Ullmann, C. V., and Hesselbo, S. P.: Chemostratigraphy across the Triassic–Jurassic boundary, in: *Chemostratigraphy Across Major Chronological Boundaries*, edited by: Sial, A. N., Gaucher, C., Ramkumar, M., and Ferreira, V. P., John Wiley & Sons, Inc and AGU Books, *Geophysical Monograph*, 240, 185–210, 2019.
- Laborde-Casadaban, M., Homberg, C., Schnyder, J., Borderie, S., and Raine, R.: Do soft sediment deformations in the Late Triassic and Early Jurassic of the UK record seismic activity during the break-up of Pangea?, *P. Geologist. Assoc.*, 132, 688–701, 2021.
- Lindström, S., Pedersen, G. K., van de Schootbrugge, B., Hansen, K. H., Kuhlmann, N., Thein, J., Johansson, L., Petersen, H. I., Alwmark, C., Dybkjær, K., Weibel, R., Erlström, M., Nielsen, L. H., Oschmann, W., and Tegner, C.: Intense and widespread seismicity during the end-Triassic mass extinction due to emplacement of a large igneous province, *Geology*, 43, 387–390, 2015.
- MacQuaker, J. H. S.: Aspects of the sedimentology of the Westbury Formation, in: *Fossils of the Rhaetian Penarth Group*, edited by: Swift, A. and Martill, D. M., The Palaeontological Association, London, 39–48, ISBN 090170265X, 1999.
- Mayall, M. J.: The late Triassic Blue Anchor Formation and the initial Rhaetian transgression in south-west Britain, *Geol. Mag.*, 118, 377–384, 1981.
- Mayall, M. J.: An earthquake origin for synsedimentary deformation in a late Triassic (Rhaetian) lagoonal sequence, southwest Britain, *Geol. Mag.*, 120, 613–622, 1983.
- Menini, A., Mattioli, E., Hesselbo, S. P., Ruhl, M., and Suan, G.: Primary versus carbonate production in the Toarcian, a case study from the Llanbedr (Mochras Farm) borehole (Wales), *Geol. Soc. Lond. Spec. Publ.*, 514, 59–81, 2021.
- Mikkelsen, P. W. and Floodpage, J. B.: The hydrocarbon potential of the Cheshire Basin, in: *Petroleum Geology of the Irish Sea and Adjacent Areas*, edited by: Meadows, N. S., Trueblood, S. E., Hardman, M., and Cowan, G., *Geol. Soc. Lond. Spec. Publ.*, 124, 16–183, 1997.
- Munier, T., Deconinck, J.-F., Pellenard, P., Hesselbo, S. P., Riding, J. B., Ullmann, C. V., Bougeault, C., Mercuzot, M., Santoni, A.-L., Huret, É., and Landrein, P.: Million-year-scale alternation of warm–humid and semi-arid periods as a mid-latitude climate mode in the Early Jurassic (late Sinemurian, Laurusian Seaway), *Clim. Past*, 17, 1547–1566, <https://doi.org/10.5194/cp-17-1547-2021>, 2021.

- Old, R. A., Sumbler, M. G., and Ambrose, K.: Geology of the country around Warwick, Memoir of the British Geological Survey, Sheet 184 (England and Wales), ISBN 0118844016, 1987.
- Old, R. A., Hamblin, R. J. O., Ambrose, K., and Warrington, G.: Geology of the country around Redditch, Memoir of the British Geological Survey, Sheet 183 (England and Wales), ISBN 0118844776, 1991.
- Olsen, P. E., Laskar, J., Kent, D. V., Kinney, S. T., Reynolds, D. J., Sha, J., and Whiteside, J. H.: Mapping Solar System chaos with the Geological Orrery, *P. Natl. Acad. Sci. USA*, 116, 10664–10673, 2019.
- Page, K. N.: The Lower Jurassic of Europe – its subdivision and correlation, in: *The Jurassic of Denmark and adjacent areas*, edited by: Ineson, J. and Surlyk, F., *Geol. Surv. Den. Greenl.*, 1, 23–59, 2003.
- Page, K. N.: High resolution ammonite stratigraphy of the Charmouth Mudstone Formation (Lower Jurassic: Sinemurian-Lower Pliensbachian) in south-west England (UK), *Volumina Jurassica*, 7, 19–29, 2009.
- Page, K. N.: Stratigraphical Framework, in: *Fossils from the Lower Lias of the Dorset Coast*, edited by: Lord, A. R. and Davis, P. G., *Palaeontological Association Field Guide to Fossils*, 13, 33–53, ISBN 1444337742, 2010a.
- Page, K. N.: Ammonites, in: *Fossils from the Lower Lias of the Dorset Coast*, edited by: Lord, A. R. and Davis, P. G., *Palaeontological Association Field Guide to Fossils*, 13, 169–261, ISBN 1444337742, 2010b.
- Page, K. N.: From Opper to Callomon (and beyond!): Building a high-resolution ammonite-based biochronology for the Jurassic System, *Lethaia*, 50, 336–355, 2017.
- Penn, I. E.: Geophysical logs in the stratigraphy of Wales and adjacent offshore and onshore area, *P. Geologist. Assoc.*, 98, 275–314, 1987.
- Percival, L. M. E., Cohen, A. S., Davies, M. K., Dickson, A. J., Hesselbo, S. P., Jenkyns, H. C., Leng, M. J., Mather, T. A., Storm, M. S., and Xu, W.: Osmium-isotope evidence for two pulses of increased continental weathering linked to Early Jurassic volcanism and climate change, *Geology*, 44, 759–762, 2016.
- Pharaoh, T. C.: Tectonic map of Britain, Ireland and adjacent areas. Sheet 1. 1 : 500 000, British Geological Survey, Keyworth, UK, ISBN XBIT1, 1996.
- Phillips, E. and Hughes, L.: Hydrofracturing in response to the development of an overpressurised subglacial meltwater system during drumlin formation: an example from Anglesey, NW Wales, *P. Geologist. Assoc.*, 125, 296–311, 2014.
- Phillips, E., Everest, J., and Reeves, H.: Micromorphological evidence for subglacial multiphase sedimentation and deformation during overpressurized fluid flow associated with hydrofracturing, *Boreas*, 42, 257–469, 2013.
- Pieńkowski, G., Uchman, A., Ninard, K., and Hesselbo, S.P.: Ich-nology, sedimentology, and orbital cycles in the hemipelagic Early Jurassic Laurasian Seaway (Pliensbachian, Cardigan Bay Basin, UK), *Global Planet. Change*, 207, 103648, <https://doi.org/10.1016/j.gloplacha.2021.103648>, 2021.
- Plant, J. A., Jones, D. G., and Haslam, H. W. (Eds.): *The Cheshire Basin: basin evolution, fluid movement and mineral resources in a Permo-Triassic rift setting*, the British Geological Survey, Keyworth, Nottingham, 263 pp., ISBN 0852723334, 1999.
- Paulsen, M. and Thibault, N.: On the occurrence of rare nannoliths (calcareous nannofossils) in the Early Jurassic and their implications for the end-Triassic mass extinction, *Pap. Palaeontol.*, 9, e1489, <https://doi.org/10.1002/spp2.1489>, 2023.
- Poole, E. G. and Whiteman, A. J.: Geology of the country around Nantwich and Whitchurch. Memoirs of the Geological Survey of Great Britain (England and Wales), Sheet 122, HMSO, London, ISBN 0118807668, 1966.
- Powell, J. H.: Jurassic sedimentation in the Cleveland Basin: a review, *P. Yorks. Geol. Soc.*, 58, 21–72, 2010.
- Remfrez, M. N. and Algeo, T. J.: Carbon-cycle changes during the Toarcian (Early Jurassic) and implications for regional versus global drivers of the Toarcian oceanic anoxic event, *Earth-Sci. Rev.*, 209, 103283, <https://doi.org/10.1016/j.earscirev.2020.103283>, 2020.
- Riding, J. B., Fensome, R. A., Soyer-Gobillard, M.-O., and Medlin, L. K.: A review of the dinoflagellates and their evolution from fossils to modern, *Journal of Marine Science and Engineering*, 11, 1, <https://doi.org/10.3390/jmse11010001>, 2023.
- Ruhl, M., Hesselbo, S. P., Hinnov, L., Jenkyns, H. C., Xu, W., Storm, M., Riding, J. B., Minisini, D., Ullmann, C. V., and Leng, M. J.: Astronomical constraints on the duration of the Early Jurassic Pliensbachian Stage and global climatic fluctuations, *Earth Planet. Sc. Lett.*, 455, 149–165, <https://doi.org/10.1016/j.epsl.2016.08.038>, 2016.
- Ruhl, M., Hesselbo, S. P., Al-Suwaidi, A., Jenkyns, H. C., Damborenea, S. E., Manceñido, M., Storm, M., Mather, T., and Riccardi, A.: On the onset of Central Atlantic Magmatic Province (CAMP) volcanism, environmental and carbon-cycle change at the Triassic–Jurassic transition (Neuquén Basin, Argentina), *Earth-Sci. Rev.*, 208, 103229, <https://doi.org/10.1016/j.earscirev.2020.103229>, 2020.
- Ruhl, M., Hesselbo, S. P., Jenkyns, H. C., Xu, W., Silva, R. L., Matthews, K. J., Mather, T. A., Mac Niocaill, C., and Riding, J. B.: Reduced plate movement controlled onset and timing of Early Jurassic (Toarcian) Karoo-Ferrar large igneous province volcanism and global environmental change, *Sci. Adv.*, 8, eabo0866, <https://doi.org/10.1126/sciadv.abo0866>, 2022.
- Ruvalcaba Baroni, I., Pohl, A., van Helmond, N. A., Papadomanolaki, N. M., Coe, A. L., Cohen, A. S., van de Schootbrugge, B., Donnadieu, Y., and Slomp, C. P.: Ocean circulation in the Toarcian (Early Jurassic): a key control on deoxygenation and carbon burial on the European Shelf, *Paleoceanography and Paleoclimatology*, 33, 994–1012, <https://doi.org/10.1029/2018PA003394>, 2018.
- Simms, M. J.: Uniquely extensive soft-sediment deformation in the Rhaetian of the UK: evidence for earthquake or impact? *Palaeogeogr. Palaeoclimatol.*, 244, 407–423, 2007.
- Storm, M. S., Hesselbo, S. P., Jenkyns, H. C., Ruhl, M., Ullmann, C. V., Xu, W., Leng, M. J., Riding, J. B., and Gorbatenko, O.: Orbital pacing and secular evolution of the Early Jurassic carbon cycle, *P. Natl. Acad. Sci. USA*, 117, 3974–3982, 2020.
- Suan, G., van de Schootbrugge, B., Adatte, T., Fiebig, J., and Oschmann, W.: Calibrating the magnitude of the Toarcian carbon cycle perturbation, *Paleoceanography*, 30, 495–509, 2015.
- Swift, A.: Stratigraphy (including biostratigraphy), in: *Fossils of the Rhaetian Penarth Group*, edited by: Swift, A. and Martill, D. M., *The Palaeontological Association, London*, 161–167, ISBN 090170265X, 1999.

- Tappin, D. R., Chadwick, R. A., Jackson, A. A., Wingfield, R. T. R., and Smith, N. J. P.: Geology of Cardigan Bay and the Bristol Channel, United Kingdom Offshore Regional Report, British Geological Survey, HMSO, 107 pp., ISBN 0118845063, 1994.
- Torsvik, T. and Cocks, L. R. M.: *Earth History and Palaeogeography*. Cambridge University Press, Cambridge, UK, 317 pp., <https://doi.org/10.1017/9781316225523>, 2017.
- Ullmann, C. V., Szűcs, D., Jiang, M., Hudson, A. J. L., and Hesselbo, S. P.: Geochemistry of macrofossil, bulk rock, and secondary calcite in the Early Jurassic strata of the Llanbedr (Mochras Farm) drill core, Cardigan Bay Basin, Wales, UK, *J. Geol. Soc. London*, 179, jgs2021-018, <https://doi.org/10.1144/jgs2021-018>, 2022.
- Van Buchem, F. S. P., McCave, I. N., and Weedon, G. P.: Orbitally induced small-scale cyclicity in a siliciclastic epicontinental setting (Lower Lias, Yorkshire, UK), in: *Orbital Forcing and Cyclic Sequences*, edited by: de Boer, P. L. and Smith, D. G., *Int. As. Sed.*, 19, 345–66, 1994.
- von Hillebrandt, A., Krystyn, L., Kürschner, W. M., Bonis, N. R., Ruhl, M., Richoz, S., Schobben, M. A. N., Urlichs, M., Bown, P. R., Kment, K., McRoberts, C. A., Simms, M., and Tomasovych, A.: The Global Stratotype Sections and Point (GSSP) for the base of the Jurassic System at Kuhjoch (Karwendel Mountains, Northern Calcareous Alps, Tyrol, Austria), *Episodes*, 36, 162–198, 2013.
- Warrington, G.: The Penarth Group-Lias Group succession (Late Triassic-Early Jurassic) in the East Irish Sea Basin and neighbouring areas: a stratigraphical review, in: *Petroleum Geology of the Irish Sea and Adjacent Areas*, edited by: Meadows, N. S., Trueblood, S. E., Hardman, M., and Cowan, G., *Geol. Soc. Lond. Spec. Publ.*, 124, 33–46, 1997.
- Warrington, G. and Ivimey-Cook, H. C.: The Late Triassic and Early Jurassic of coastal sections in west Somerset and South and Mid-Glamorgan, in: *Field Geology of the British Jurassic*, edited by: Taylor, P. D., *Geol. Soc. Lond. Spec. Publ.*, 9–30, ISBN 1-897799-41-1, 1995.
- Warrington, G., Wilson, A. A., Jones, N. S., Young, S. R., and Haslam, H. W.: Stratigraphy and Sedimentology, in: *The Cheshire Basin: Basin Evolution, Fluid Movement and Mineral Resources in a Permo-Triassic Rift Setting*, edited by: Plant, J. A., Jones, D. G., and Haslam, H. W., *Keyworth, British Geological Survey*, 10–40, ISBN 0852723334, 1999.
- Weedon, G. P.: Hemipelagic shelf sedimentation and climatic cycles: the basal Jurassic (Blue Lias) of South Britain, *Earth Planet. Sc. Lett.*, 76, 321–35, 1986.
- Weedon, G. P., Jenkyns, H. C., and Page, K. N.: Combined sea-level and climate controls on limestone formation, hiatuses and ammonite preservation in the Blue Lias Formation, South Britain (uppermost Triassic – Lower Jurassic), *Geol. Mag.*, 155, 1117–1149, 2017.
- Weedon, G. P., Page, K. N., and Jenkyns, H. C.: Cyclostratigraphy, stratigraphic gaps and the duration of the Hettangian Stage (Jurassic): insights from the Blue Lias Formation of southern Britain, *Geol. Mag.*, 156, 1469–1509, 2019.
- Wonik, T.: Downhole logging data of the ICDP Scientific Drilling Project “Early Jurassic Earth System and Time Scale (JET)”, GFZ Data Services [data set], <https://doi.org/10.5880/ICDP.5065.001>, 2023.
- Wood, A. and Woodland, A.: Borehole at Mochras, West of Llanbedr, Merionethshire, *Nature*, 219, 1352–1354, 1968.
- Woodland, A. (Ed.): *The Llanbedr (Mochras Farm) Borehole*. Institute of Geological Sciences, Report 71/18, 1–116, ISBN 118802135, 1971.
- Xu, W., Ruhl, M., Jenkyns, H. C., Leng, M. J., Huggett, J. M., Minisini, J. M., Ullmann, C. V., Riding, J. B., Weijers, J. W. H., Storm, M. S., and Hesselbo, S. P.: Evolution of the Toarcian (Early Jurassic) carbon-cycle and global climatic controls on local sedimentary processes (Cardigan Bay Basin, UK), *Earth Planet. Sc. Lett.*, 484, 396–411, 2018a.
- Xu, W., MacNiocaill, C., Ruhl, M., Jenkyns, H. C., Riding, J. B., and Hesselbo, S. P.: Magnetostratigraphy of the Toarcian Stage (Lower Jurassic) of the Llanbedr (Mochras Farm) Borehole, Wales: basis for a global standard and implications for volcanic forcing of palaeoenvironmental change, *J. Geol. Soc. London* 175, 594–604, 2018b.



# Drilling into a deep buried valley (ICDP DOVE): a 252 m long sediment succession from a glacial overdeepening in northwestern Switzerland

Sebastian Schaller<sup>1,2</sup>, Marius W. Buechi<sup>1,2</sup>, Bennet Schuster<sup>3,1,2</sup>, and Flavio S. Anselmetti<sup>1,2</sup>

<sup>1</sup>Institute of Geological Sciences, Universität Bern, Baltzerstr. 1+3, 3012 Bern, Switzerland

<sup>2</sup>Oeschger Centre for Climate Change Research, Universität Bern,  
Hochschulstrasse 4, 3012 Bern, Switzerland

<sup>3</sup>Institute of Earth and Environmental Sciences, University of Freiburg,  
Tennenbacher Str. 4, 79106 Freiburg, Germany

**Correspondence:** Sebastian Schaller (sebastian.schaller@geo.unibe.ch)

Received: 17 March 2023 – Revised: 12 July 2023 – Accepted: 9 August 2023 – Published: 26 October 2023

**Abstract.** The modern Alpine landscape and its foreland were strongly impacted by the numerous glacier advance and retreat cycles during the Middle-to-Late Pleistocene. Due to the overall erosive character of each glaciation cycle, however, direct traces of older glaciations tend to be poorly preserved within the formerly glaciated domains of the pan-Alpine area. Nevertheless, sediments of older glaciations may occur hidden under the modern surface in buried glacially overdeepened troughs that reach below the normal level of fluvial erosion (fluvial base level). These sedimentary archives, partly dating back to the Middle Pleistocene period, are of great scientific value for reconstructing the timing and extent of extensive Alpine glaciation, paleoclimate, and paleoenvironmental changes in the past and help to better understand ongoing and future changes in the pan-Alpine area. Therefore, the International Continental Scientific Drilling Program (ICDP) project DOVE (Drilling Overdeepened Alpine Valleys) targets several of these glacial overdeepened sedimentary basins to recover their sedimentary infills. In the frame of the DOVE project, a 252 m long drill core of unconsolidated Quaternary sediments was recovered in northern Switzerland from an over 300 m deep glacially overdeepened structure (“Basadingen Trough”) formed by the former Rhine Glacier lobe system. The recovered sedimentary succession was divided into three stratigraphic units on the basis of lithological and petrophysical characteristics. The lowest unit, deposited below the fluvial base level, consists of an over 200 m thick succession of glacial to (glacio)lacustrine sediments and contains remains of possibly two glaciation cycles. Overlying this lowermost succession, an ~37 m thick fluvial-to-glaciofluvial gravel deposit occurs, which correlates to a locally outcropping Middle Pleistocene formation (“Buechberg Gravel Complex”). The sediment succession is capped by an ~11 m thick diamictic succession interpreted as the subglacial till from the later extensive glaciation, including the regional glaciation during the Last Glacial Maximum. The recovered sediment succession thus supports the proposed multi-phase origin of trough formation and its infill.

## 1 Introduction

The global marine isotope records reveal the changes in the global temperature and ice volumes during the Quaternary. This geological period is dominated by glacial–interglacial cycles, each including stadial–interstadial higher-frequency fluctuations (Lisiecki and Raymo, 2005). Further, the marine

isotope records show a global shift in the periodicity from ca. 41 to 100 ka and an increase in the amplitude of the temperature and ice volume during the Middle Pleistocene climatic transition (MPT) between 1250 and 700 ka (Ruddiman et al., 1986; Clark et al., 2006). During each glacial–interglacial cycle, ice sheets grew in the polar areas as well as in mountainous areas (including the Alps), and glaciers advanced into



the lowlands from where they retreated again with the onset of the next interglacial. While the last glaciation left prominent traces in the Alpine landscape (e.g., erratic blocks and side and end moraines), traces of previous glaciations often became obscured and eroded as advancing glaciers modified the overridden landscape drastically.

During extensive glaciation of the Alpine foreland, numerous glacially overdeepened troughs were eroded by subglacial processes below the fluvial base level, i.e., below the lowest fluvial channels terminating downstream with adverse slopes (e.g., Cook and Swift, 2012; Alley et al., 2019). Upon deglaciation, the troughs were refilled with sediments and, in most cases, eventually completely buried. Like this, the valley fills remained at least partially protected from subsequent glacial and fluvial erosion and therefore contain relatively complete or multi-phase archives extending through several glacial cycles (Preusser et al., 2010; Ellwanger et al., 2011; Pomper et al., 2017; Buechi et al., 2018). Therefore, these overdeepened valley fills represent some of the most valuable land-based sedimentary archives in glacial landscapes for reconstructing glacial history over multiple glaciations. They thus contribute significantly to reconstructing the glaciation history preceding the last glacial cycle in areas such as the Alps and its foreland, as shown in several case studies (Dehnert et al., 2012; Fiebig et al., 2014; Buechi et al., 2018; Schwenk et al., 2022). These studies profited from new developments in dating methods, especially luminescence dating and cosmogenic nuclide burial dating, which allow researchers to establish an absolute chronology of those archives, which is a prerequisite for understanding and reconstructing the local-to-regional glaciation history into a broader context. On a regional scale, the onset of increased glacial erosion (Haeuselmann et al., 2007; Valla et al., 2011) and the beginning formation of overdeepened structures during the MPT have been proposed for the Alpine region at that time (e.g., Schlüchter, 2004; Ellwanger et al., 2011). The initial concept with four proposed Alpine glaciations (Penck and Brückner, 1909) has been replaced by a scenario with ca. 15 proposed glaciations (Preusser et al., 2011). Furthermore, it has been documented that regional the glacial dynamics and extents also vary strongly inside the pan-Alpine area. For example, it is postulated that at around ca. 65 ka, the glaciers in the western Alps reached their last maximum of extension (e.g., Gribenski et al., 2021), while it is postulated that glaciers barely reached into the inner Alpine valleys in the Eastern Alps (Ivy-Ochs et al., 2008). Such asymmetry and asynchronicity can be related to many local, regional, and global factors such as topography, climate change (including temperature and precipitation), and ice dynamics (e.g., Reber and Schlunegger, 2016; Spötl et al., 2021).

All these studies also underline the potential and justify the significant logistical and financial effort to drill, document, and analyze these overdeepened troughs and their sediment fill. Besides their unique scientific value as sedimentary archives, understanding overdeepened structures is also cru-

cial for applied aspects such as the longtime safety of nuclear waste disposal sites, groundwater reservoirs, natural hazards, and large-scale underground transportation infrastructure.

## Project DOVE

In the frame of the International Continental Scientific Drilling Program (ICDP) project Drilling Overdeepened Alpine Valleys (DOVE), the sedimentary infill of several overdeepened troughs are targeted with the overarching goal of quantifying the proposed asymmetry in the extent and timing of the Alpine glaciations in the pan-Alpine area and their implications for the paleoclimate, paleolandscape, and paleoenvironmental evolution back to the Middle Pleistocene. A detailed overview of the DOVE project is provided in Anselmetti et al. (2022). The project seeks to achieve these goals by combining the following: (i) a series of new drill cores, (ii) analyzing existing drill cores, and (iii) geophysical surveys across overdeepened troughs. The project is grouped into two phases: Phase I covers the northern and northeastern parts of the Alps (Switzerland, Germany, and Austria) and comprises three drill cores from the former Rhine Glacier area (ICDP Site 5068\_1, TANN, IGSN (International Generic Sample Number): ICDP5068EH70001; ICDP Site 5068\_2, BASA, IGSN: ICDP5068EH40001; and ICDP Site 5068\_6, GAIS, IGSN: ICDP5068EHG0001; Fig. 1a), one from the former Isar-Loisach Glacier area (ICDP Site 5068\_3, SCHA, IGSN: ICDP5068EHC0001), one from the former Salzach Glacier area (ICDP Site 5068\_4, FREI, IGSN: ICDP5068EHD0001), and one from the former Traun Glacier area (ICDP Site 5068\_5, BADA, IGSN: ICDP5068EHE0001) (Anselmetti et al., 2022). It is planned to cover the southern and western parts of the Alps (Slovenia, Italy, and France) in Phase II (Anselmetti et al., 2022). The comparison and integration of data in Phase I will occur in several steps: (i) the data of the individual drill cores will be individually analyzed and integrated into the local context; (ii) the sites will be integrated into their extended regional system, e.g., the individual glacier lobes; and (iii) an overall synthesis of Phase I in the northern Alps will be accomplished. Eventually, the same steps are planned for Phase II for the southern and western areas. Finally, the overall DOVE synthesis and integration over the entire pan-Alpine area will be achieved. This study represents the first step on this path and presents the results of the ICDP site 5068\_2 (BASA), where the first ICDP drill core was recovered on Swiss territory (Fig. 1a and b).

## 2 Study area

The study area is located in the southwestern part of the former Rhine Glacier lobe and inside the proposed Most Extensive Glaciation (MEG) during the Middle Pleistocene and the Last Glacial Maximum (LGM, Fig. 1a). Previous studies have documented a dendritic pattern of overdeepenings

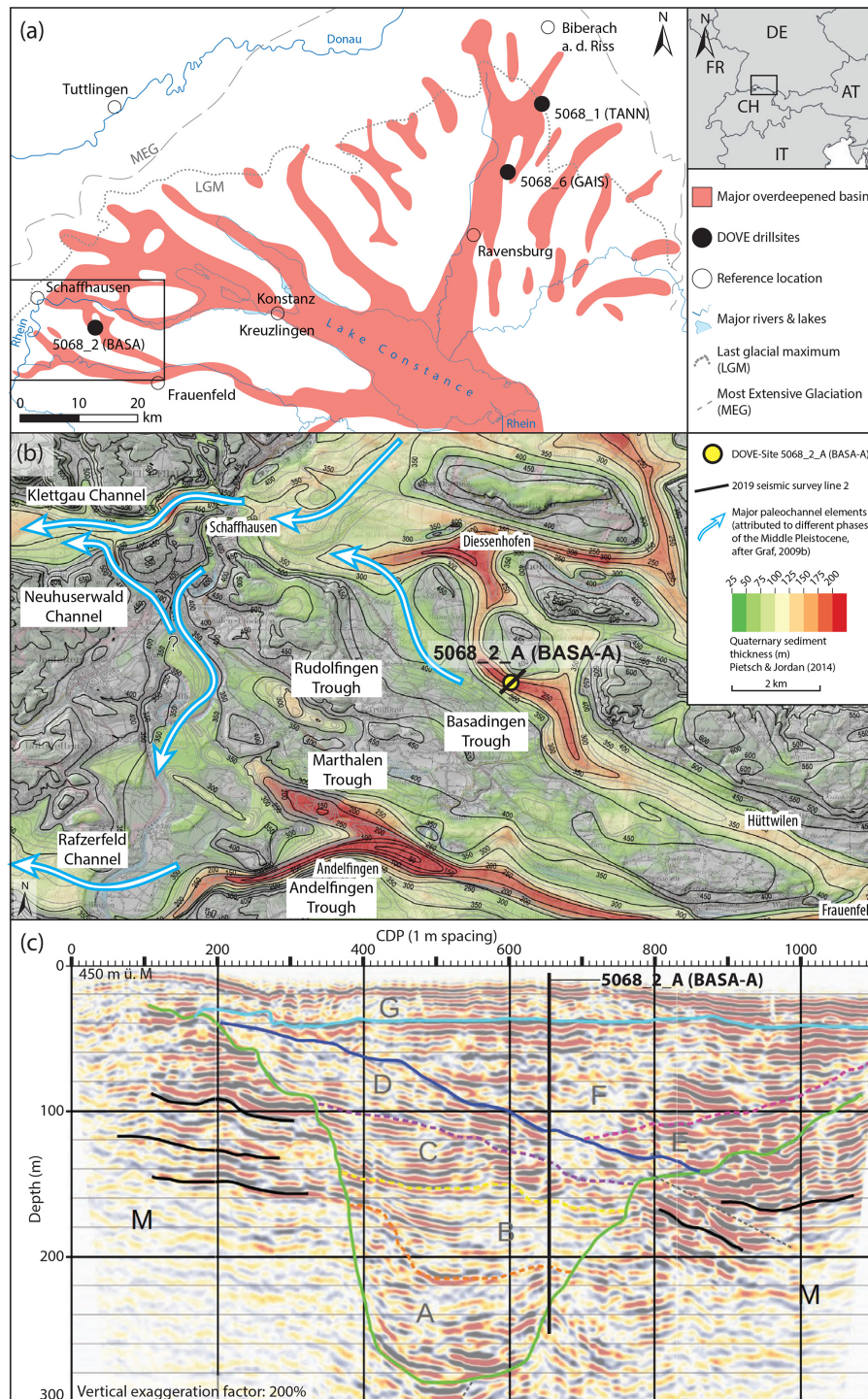


**Figure 1.** (a) Overview of the overdeepened systems within the former Rhine paleoglacier lobe (modified from Ellwanger et al., 2011). Extents of the Rhine Glacier during the Most Extensive Glaciation (MEG) and of the Last Glacial Maximum (LGM) and two DOVE Phase 1 sites: 5068\_1 (TANN), 5068\_2 (BASA), and 5068\_6 (GAIS) are indicated. (b) Regional overview of the overdeepened system of the southwestern branch of the Rhine Glacier, including the thickness of the Quaternary sediments (Pietsch and Jordan, 2014), the postulated local Middle Pleistocene paleochannels (Graf, 2009b), the indicated DOVE site 5068\_2 (BASA), and trace of the seismic line. (c) Pre-drilling interpretation of the seismic line across the Basadingen Trough (Brandt, 2020): M represents the molasse bedrock; the green line represents the outline of trough; A–G represent the stratified unconsolidated Quaternary filling with indicated potential erosional (solid lines) and internal boundaries (dashed lines); solid black lines in M represent prominent and potential continuous reflections; dashed black lines represent assumed faults; the black vertical line represents drill hole 5068\_2-A (BASA-A) with predicted bedrock at ~240 m depth. Note that the final drilling depth of 252 m did not penetrate bedrock but ended in coarse (basal) sediments.



within the footprint of the Rhine Glacier (Fig. 1a). Geometrically, these overdeepened basins appear to have a common root in the Alpine Rhine valley and the partially filled basin of Lake Constance (e.g., Keller and Krayss, 1993; Cohen et al., 2018; Ellwanger et al., 2011; Fabbri et al., 2021; Schaller et al., 2022). From this root, several overdeepened basins branch into side systems and even further distal overdeepenings (Fig. 1a). While the origin of this pattern is not fully understood, regional studies indicate that the formation of these overdeepenings did not all occur at the same time but during different glaciations (e.g., Graf, 2009a, b; Ellwanger et al., 2011; Müller, 2013).

In the surroundings of the drill site, with a terrain elevation at the drill site of  $\sim 445$  m above sea level (m a.s.l.), several parallel to partly cross-cutting bedrock overdeepenings have been detected in bedrock surface maps compiled from variably abundant drillings and geophysical data (Fig. 1b; e.g., Müller, 2013; Pietsch and Jordan, 2014). The bedrock overdeepenings, including the Basadingen Trough, reach over 300 m below the modern topography and are mainly incised into the Neogene siltstones and sandstones of the Molasse basin (mainly Upper Marine Molasse, OMM, and Lower Freshwater Molasse, USM; Hofmann and Hantke, 1964; Hofmann, 1967). The bedrock maps also reveal characteristic adverse slopes at the termini of the individual overdeepenings. At the surface, the considerable bedrock relief due to overdeepening glacial erosion is buried by younger glacial or glaciofluvial sediments (Graf, 2009b; Müller, 2013).

The transition from the overdeepened to non-overdeepened (fluvial) domain is an important physical process boundary for the interpretation of the erosional and depositional processes. The lowest fluvial outlet of the study area is the Klettgau fluvial paleochannel and lies at  $\sim 340$  m a.s.l. just west of Schaffhausen. Considering this minimal fluvial base level, the erosional and depositional processes below  $\sim 100$  m core depth have occurred in an overdeepened position and, thus, most likely in a subglacial-to-lacustrine setting. Higher values for the fluvial base level at the drill site – but with larger uncertainties – can be estimated from the highest elevations reached by the adverse slopes. Based on the base maps of the lowest fluvial gravels (“Buechberg Gravel Complex”, Middle Pleistocene; Müller, 2013), Graf (2009b) and Müller (2013) convincingly show that the lowest Pleistocene base (LPB) level gently rises to the east and reaches  $\sim 370$  m a.s.l. at the lowest known basal contact of the gravel formation. The base map reveals a strong topography of this basal boundary surface, which lies between 390 and 400 m a.s.l. around the drill site.

As part of the drill site selection process, two closely spaced seismic cross-sections over the Basadingen Trough were acquired using an acoustic signal source with a frequency between 20 and 240 Hz, a shot-point spacing of 4 m, and a receiver spacing of 2 m (Brandt, 2020, Fig. 1c). The time-to-depth conversion of the two lines

was based on the stacking velocity model, assuming velocities of  $\sim 2500$  m s $^{-1}$  for bedrock and between  $\sim 1400$  and  $\sim 2100$  m s $^{-1}$  for the sedimentary infill. The use of the rather simplified velocity model may have caused some uncertainties in the time–depth conversion of the seismic data. Both lines indicate a nearly 300 m deep bedrock incision and an infill which was interpreted to be a complex stratified geometry with a major cross-cutting unconformity separating a deep and narrow structure from a broad and shallow depression. This pattern suggests a multi-phase infill history during at least two glaciation cycles, as was earlier proposed by Müller (2013) based on existing flush drillings.

### 3 Methods

#### 3.1 Drilling and downhole operations

Drilling operations were conducted by a private contractor (Fretus AG, Bad Zurzach, Switzerland) between 25 May and 10 November 2021 (Fig. 2a–d). A final depth of 252 m was reached using a combined approach of percussion drilling (Düsterloh hammer) to a depth of 57 m and, below, a triple-tube core-barrel system (CSK-146 wireline diamond-coring system). Bedrock, initially predicted for  $\sim 240$  m (Fig. 1c), could not be reached due to geotechnically challenging sediments, loss of drilling fluid in the hole, and related technical difficulties at the final depth of 252 m. The  $> 12$  m underestimation of Quaternary sediment thickness is likely related to uncertainties in (i) the seismic velocities and/or (ii) the interpretation of the deeper reflections. A total of 278 core sections with a core diameter of 104 mm and lengths between 0.1 and 1 m were recovered in opaque PVC liners. The liners had a standard length of 1 m and were only cut if the length of the nominal drilled section was  $< 1$  m. The liners were not cut in the case of core loss, and this space was not compensated with filler material. Consequently, the quality of those sections may have suffered due to some remobilizations, especially in cases of low internal cohesion. However, since the main reason for the core loss was mobilization and/or flushing during the drilling itself, those sections were of poor quality anyway. A total recovery of  $\sim 94\%$  was reached, from which  $\sim 11\%$  was disturbed to the degree that it lost its internal structure. Water inflow was registered at depths of 3–4 and 10–11 m. The local groundwater table was reached at a depth of  $\sim 29.5$  m, which remained stable during the entire drilling operation. Significant drilling-fluid losses occurred in gravel-dominated sections between 93–108 and 141–143 m and below 250 m. They represent the major technical and lithological challenges encountered during the drilling operation. For stabilizing and reducing the drilling resistance inside the drill hole, the drill hole was telescoped several times by using different casing diameters and a flushing agent consisting of water mixed with additions of biodegradable polymers and bentonite. After the completion of the drilling activities, a broad downhole wireline logging

campaign was executed by the Leibniz Institute for Applied Geophysics (LIAG). After completion of the wireline logging, the drill hole was refilled with intervals of gravel, bentonite, and concrete according to governmental regulations. A detailed technical overview of the drilling and logging operations; core quality; the technical parameters, such as borehole geometry, used casings, and the applied refilling scheme is provided in the DOVE operational report (DOVE-Phase 1 Scientific Team et al., 2023a).

## 3.2 Core handling, description, and analysis

### 3.2.1 On-site core-related workflow

After recovery, the liners were sealed and labeled with section ID and driller depth. Each core section was weighed for a preliminary approximation of recovery. In parallel to the drilling campaign,  $p$ -wave velocity (will not be further considered due to poor quality), wet bulk density, magnetic susceptibility, and natural gamma radiation of each core section were measured in the field laboratory (Fig. 3) with a Geotek multi-sensor core logger (MSCL) (Geotek Limited, Davenport, Northants, UK) at a resolution of 5 mm. The core sections were stored in labeled standard-sized wooden boxes for better handling. Later, they were brought in batches to the Institute of Geological Sciences, University of Bern, to be stored in the cooling room until the initial core description (ICD). In parallel to recovering, the fine-grained and sandy sediments were strategically sampled for noble-gas pore-water analyses (16 samples) and microbiological investigations of the deep biosphere (60 samples).

### 3.2.2 Off-site core-related workflow

During the ICD, each core section was cut, opened, and split lengthwise into an archive half for non-destructive analyses and a working half for invasive sampling. Complete processing of the working half was performed under red-light conditions to prevent light contamination, potentially hampering the use of optically stimulated luminescence (OSL) dating. The following work was conducted on each archive half. A high-resolution line scan was obtained, and each section was sedimentologically described and documented in a log sheet. The focus of these descriptions was on the following: (i) the dominant grain size, (ii) type and thickness of bedding, (iii) color, (iv) contacts between different beds, (v) secondary sedimentary structure, (vi) quality of the core section, and (vii) an overview of clast lithology and morphology. Furthermore, where applicable, undrained shear strength ( $c'_u$ ) and undrained uniaxial compressive strength ( $q'_u$ ) were measured at 25, 50, and 75 cm section depth with a pocket vane shear tester and a pocket penetrometer. A final total depth was defined based on the observations of core quality from the ICD and the driller's top depth of each section. Depth is addressed as meters total depth (mtd) when discussing the entire sediment succession or as centimeter section depth

(cmsd) when aiming for individual core sections. Based on the combined findings from the ICD, 14 sedimentary lithotypes were defined and described (Table 1). The whole sediment succession was assigned to the best-fit lithotype. Eventually, the stratigraphic succession was subdivided into three main stratigraphic units (A–C).

In addition, X-ray computed tomography (CT) images of 49 selected core sections were taken with a medical X-ray CT scanner at the Institute of Forensic Medicine, University of Bern. Systematically, 231 samples for grain-size distribution, geochemical analyses (e.g., total inorganic carbon, TIC, and total organic carbon, TOC), and potential additional investigations were taken from each working half at 50 cmsd whenever possible (sample spacing  $\sim 1$  m). These samples were freeze-dried, and the mean water content at each position was derived from the corresponding weight differences between the three wet and dry subsamples. Furthermore, smear slides have been taken from interesting silt- and clay-rich sections.

Further, based on the line scans, samples were taken for a first screening of pollen content (31 samples), luminescence dating (22 samples), cosmogenic nuclide burial dating (2 samples), and geotechnical analyses (23 samples). After completing the ICD and the sampling campaign, the core halves were sealed in lightproof black foil, stored in standard-sized wooden boxes, labeled according to the ICDP guidelines, and brought to a commercial cooled storage facility, which serves as a temporary repository during the active DOVE Phase I (Anselmetti et al., 2022). For further information on the curated samples, analysis, and data, see the operational dataset (DOVE-Phase 1 Scientific Team et al., 2023b) and explanatory remarks (DOVE-Phase 1 Scientific Team et al., 2023c).

### 3.2.3 Carbon analysis (organic matter and carbonate content)

Total carbon (TC), nitrogen, sulfur, and total inorganic carbon (TIC) were analyzed from the fine fraction ( $< 63 \mu\text{m}$ ) using a Thermo Scientific FLASH 2000 elemental analyzer (Thermo Fischer, Waltham, MA, USA). Total organic carbon (TOC) was derived as the differences between TC and TIC. Weight percent of carbonates ( $\text{CaCO}_3$ ) and organic matter were calculated using a stoichiometrically simplified approach from TIC and TOC through multiplication with 8.3 and 1.8, respectively (Meyers and Teranes, 2001). This approach does not consider potential down-core changes in carbonate phases (i.e., dolomite / carbonate ratio). Nevertheless, it allows for a quantitative approximation of the total lithological constituents.

### 3.2.4 MSCL data processing

MSCL data were processed in five steps: (i) data of empty sections of liners, representing core loss, were removed; (ii) a baseline correction was applied to the corresponding mag-



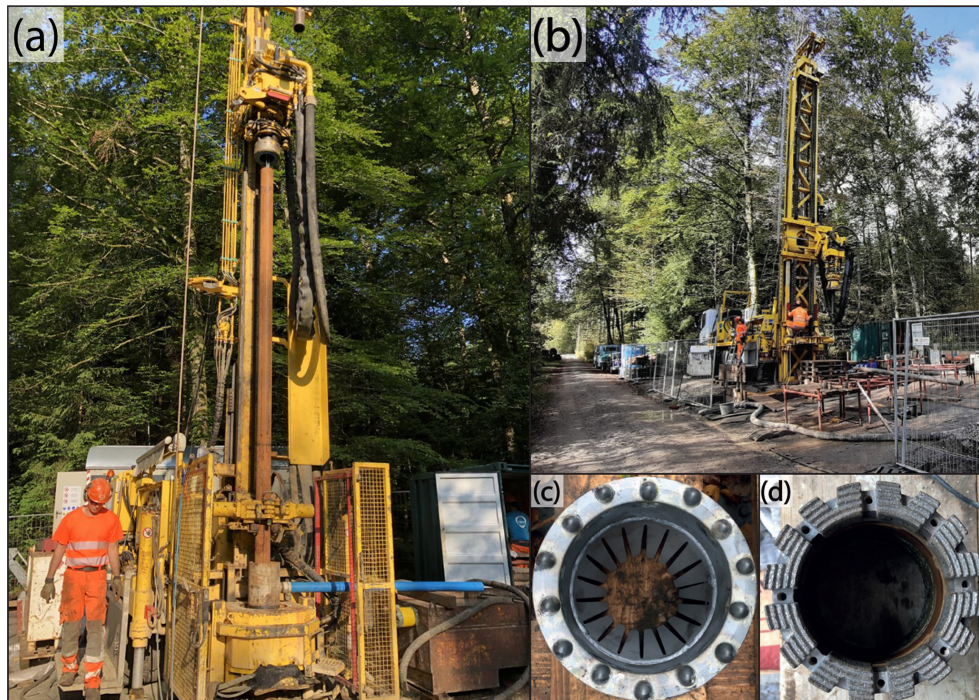


**Figure 2.** (a) Drill rig used from 0 to 228 mtd (meters total depth); (b) drill rig used from 228 to 252 mtd; (c) drill bit used during percussion-hammer coring to a depth of 57 mtd; and (d) diamond and hard-metal drill bit used during rotary drilling below 57 mtd (photos by Sebastian Schaller).



**Figure 3.** Field lab near the drill site containing the MSCL scanner (photo by Sebastian Schaller).

netic susceptibility data to correct potential systematic shifts in the data (subtraction of the average of the calibration data between 0.5 and 15 cm of each measurement cycle); (iii) low-density data ( $< 1.5 \text{ g cm}^{-3}$ ), considered heavily disturbed sections, were excluded from the density log; (iv)  $p$ -wave velocity data with an amplitude of 0, representing poor data quality, were excluded from the  $p$ -wave data (As the overall

data quality of the  $p$ -wave data is low,  $p$ -wave-velocity values are not further presented or discussed.); (v) the depth of the cleaned MSCL logs was corrected with the actual depth; and (vi) the data from the uppermost and lowermost centimeter in each section were considered likely disturbed and thus excluded.

## 4 Results

### 4.1 Core lithologies





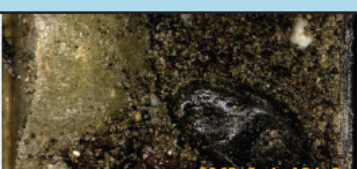
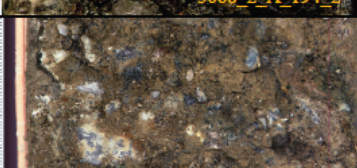

The 252 m long sediment succession was divided into 14 sedimentological lithotypes (Fig. 4). Table 1 provides an overview of these 14 defined lithotypes, including description and interpretation of the depositional environment, along with a representative core-section line scan. Figure 5 displays a composition of detailed line scans, CT scans, and the key lithotypes of 10 selected core sections.

### 4.2 Lithostratigraphic units

Based on the succession of the 14 endmember lithotypes (Table 1), the recovered succession (Fig. 4) was grouped into three lithostratigraphic units (A, B, and C), with Unit A containing five subunits (A1–A5). These units are briefly characterized from bottom to top.



**Table 1.** Colors and lithocodes of the individual lithotypes with description and interpretations. The line-scan image shows a representative core section (origin of line scan is indicated in the lower-right corner of core photos); scale is in centimeters.





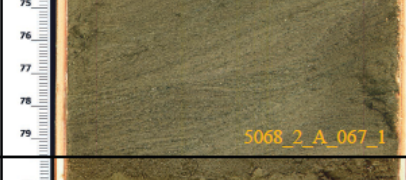


Description		Interpretation	Core photo	
Diamicts				
Dmm	<b>Matrix-supported massive:</b> Massive matrix-supported with isolated fine to coarse gravel clasts in a silty to sandy matrix with isolated cobbles (0-40 % clasts, 60-100 % matrix). Crudely bedded in decimeter- to meter-scale by a slight variation in matrix composition and/or in clast size and number. Beige color, many fresh striations, poorly sorted, subangular to subrounded.	i) Subglacial till (Evans et al., 2006) or ii) terrestrial or subaqueous cohesive debris flows with glacial sediment sources (Mulder and Alexander, 2001; Eyles et al., 1983).	26 27 28 29 30	 5068_2_A_004_1
Dms	<b>Matrix-supported stratified diamict:</b> Matrix supported with fine to coarse gravel clasts in a massive sandy to partly silty matrix (0-40 % clasts, 60-100 % matrix), stratified into centimeter- to decimeter-scale beds by oriented but mostly isolated clasts. Beige to grey-beige color, few striations, poorly sorted, subangular to (sub)rounded.	Proximal hyperconcentrated density flow deposits (Mulder and Alexander, 2001).	47 48 49 50 51	 5068_2_A_112_1
Dcn	<b>Clast-supported massive diamict:</b> Massive clast-supported, fine to coarse gravel with isolated cobbles with a silty matrix with variable sand content (60-80 % clasts, 20-40 % matrix). Sometimes crudely bedded by a slight variation in matrix composition and dominant clast size. Poorly sorted, beige matrix color, striations, subangular to subrounded.	i) subglacial below or above the fluvial base level (Evans et al., 2006), or ii) glaciofluvial deposits solely above the fluvial base level (Eyles et al., 1983).	60 61 62 63 64	 5068_2_A_092_1
Mcc	<b>Mud-clast conglomerate:</b> Mixture of beige to beige-brown clay chips with a variable medium to coarse gravel content (0->50%) in a grey-beige to brownish medium sandy matrix (5-80 % clasts, 20-95 % matrix). Mud clasts show partially internal structures and rounding of various degrees (subangular to rounded).	Fine lacustrine sediments, rounding indicates transportation upon reworking, eroded by subaqueous mass movements or other subaqueous events with high erosive potential (e.g., Li et al., 2017). The individual gravel content may indicate the type of event, i.e., a high content may indicate a delta collapse as source event.	82 83 84 85 86	 5068_2_A_186_2
Gravels				
Gms	<b>Massive to crudely bedded sandy gravel:</b> Massive medium to coarse (partly fine) gravel, with few isolated sand layers, with little to no silt and isolated cobbles (75-80 % clasts, 20-25 % matrix). Crudely bedded by variation in clast size and number and slight variation in matrix composition, moderately to well sorted, beige to beige-brownish matrix color, (sub)rounded to well rounded.	i) Fluvial to glaciofluvial deposits (over the fluvial base level; Eyles et al., 1983) or ii) subglacial to glaciolacustrine deposits, e.g., high concentration channelized density flows in a subaqueous glacial fan system (below the fluvial base level; Eyles et al., 1983).	12 13 14 15 16	 5068_2_A_194_2
Gmf	<b>Massive to crudely bedded silty sandy gravel:</b> Massive medium to coarse gravel, partly sandy, silty with isolated cobbles (75-80 % clasts, 20-25 % matrix). Crudely bedded by variations in clast size and number and slight variations in matrix composition, moderately to well sorted, brownish-reddish to brownish matrix color, (sub)rounded to well rounded, with some cementations and oxidations.	Fluvial to glaciofluvial deposits (Eyles et al., 1983), in the range of current groundwater fluctuations, leads to cementation and oxidations of clasts.	44 45 46 47 48	 5068_2_A_014_1
Fines				
Fm	<b>Massive clay/silt:</b> Massive clay and silt, little sandy, only very few isolated gravel clasts (C: <1 %, M: >99 %). Partially laminated by intercalating sand laminae resulting in a centimeter- to decimeter-scaled bedding, rarely mottled by soft clasts, with some isolated drop stones, well to very well sorted, beige to grey beige, partly slightly brownish.	i) Deposited in calm states of the lake, i.e., (glacio)lacustrine background sedimentation (Leemann and Niessen, 1994). ii) the very top of a concentrated density flows event (Mulder and Alexander, 2001); or iii) very distal from the sediment source or low energy turbidity deposits (Te, Bouma 1962).	15 16 17 18 19	 5068_2_A_169_1

#### 4.2.1 Unit A: 252.00–47.75 mtd

Unit A consists of primarily sand-dominated sediments (Fig. 5c–j) intercalated by several-meter-thick gravel-dominated beds (Fig. 4). The sand-dominated successions

can be distinguished and categorized into three types: (i) stacked massive sandy beds with low clay and silt content (Table 1; *Sm* and *Sh*), partially separated by clay caps (*Fm*), and intercalated by isolated minor gravel beds (*Gms*) or gravel-rich sections (*SGm*); (ii) fine-to-medium sand beds

Table 1. Continued.

Description		Interpretation	Core photo
Sands			
<i>Sm</i>	<b>Massive sand:</b> Massive fine to medium sand, occasionally coarse sandy, with little to no silt and only isolated gravel clasts (<5 % clasts, >95 % matrix). Crudely bedded in decimeter- to meter-scale by a slight variation in silt content and dominant grain-size fraction, well to very well sorted, greyish-beige to brownish-beige, rarely mottled with soft clasts.	Hyperconcentrated density flow deposits (Mulder and Alexander, 2001).	
<i>SGm</i>	<b>Massive sand and gravel mix:</b> Massive mix of fine to medium sand and gravel, with little to no silt (5–60 % clasts, 40–95 % matrix). Partly centimeter- to decimeter-scale bedded by oriented clasts, moderately to well sorted, subrounded to well rounded, greyish-beige to brownish-beige.	Base of concentrated density-flow deposits, very proximal to sources, or high-energy events (Mulder and Alexander, 2001).	
<i>Sh</i>	<b>Bedded sand:</b> Bedded fine to medium sand, with variable silt content and few isolated gravel clasts (<5 % clasts, >95 % matrix). Bedded in centimeter- to decimeter-scale by a variation in silt content and dominant grain-size fraction, fining up to a massive appearance, well to very well sorted, greyish-beige to brownish-beige.	i) (Massive) hyperconcentrated density flow deposits (Mulder and Alexander 2001), more distal to the source or with less energy, or ii) (stratified) turbidity deposits (Ta; Bouma, 1962; Mulder and Alexander, 2001).	
<i>Sl</i>	<b>Laminated sand:</b> Laminated fine to medium sand with variable silt content, with few isolated clay laminae and isolated gravel clasts (<1 % clasts, >99 % matrix), laminated in millimeter- to centimeter-scale by variations in silt content and dominant grain-size fraction. Individual laminae are fining-up to massive, partially mica-rich, well to very well sorted, greyish-beige to brownish-beige, with partially reddish colors.	Distal or low-energy turbidite deposit (Tb, Ta; Bouma, 1962).	
<i>Sc</i>	<b>Cross-bedded sand:</b> Cross-bedded fine to medium sand, partially silty, with isolated clay laminae and very few isolated gravel clasts (<1 % clasts, >99 % matrix). Cross-bedded in centimeter- to decimeter-scale with internal millimeter-scaled laminae, individual laminae are fining up, partly mica-rich, well to very well sorted, greyish-beige to brownish-beige, occasionally of reddish color.	Distal or low energy turbidity deposit (Tc; Bouma, 1962).	
<i>Sil</i>	<b>Irregularly bedded sand, silt, and clay:</b> Silt and clay to coarse sand, with individual gravel clasts (0–10 % clasts, 90–100 % matrix). Irregular in centimeter- to sub-decimeter-scale bedded to laminated, individual lamina/beds are mostly well-sorted and are massive to partly fining-up, partially deformed, with internal erosive contacts, with high contrast, greyish beige to brownish beige.	Stacked successions of different types of density-flow deposits, likely formed under highly variable energy conditions, possibly in cross-cutting subaquatic channel systems.	
<i>Sd</i>	<b>Deformed mix of sand, silt, and clay:</b> Strongly folded and bent mix of originally laminated to bedded sand, clay, and silt with isolated gravel clasts (<1 % clasts, >99 % matrix). Traces of slumps and dehydration structures, ductile deformed, beige to brownish beige.	i) Deformed syn- or postdepositionally by i) rapid loading and dewatering or, ii) mass movements, or iii) glaciotectionics (Evans, 2018).	

with a higher clay and silt content, thin-bedded (*Sh*) to laminated (*Sl*) and partially cross-bedded (*Sc*), and with isolated clay laminae (*Fm*); and (iii) massive sand (*Sm*, *Sh*, *Sl*, and *Sil*) interbedded to intercalated with mostly centimeter-to-decimeter-scaled partly stratified beds of sand and gravel mix (*SGm*), massive gravel beds (*Gms*), and stratified (*Dms*) or massive diamictic (*Dmm*) beds. The sandy successions, in parts, show traces of ductile deformations (Table 1; *Sd*, e.g.,

boudinage, flame structures, folding, and dewatering structures) and some brittle deformation (e.g., small-scale faults). The bases of the rather massive sandy or gravel-rich beds partially show erosive contacts, which may contain rip-up clasts (*Mcc*).

The gravel-dominated beds within Unit A can be further divided into two types: (i) more diamictic beds (Table 1; *Dcm*) with a silt-rich matrix, steeply inclined beds,



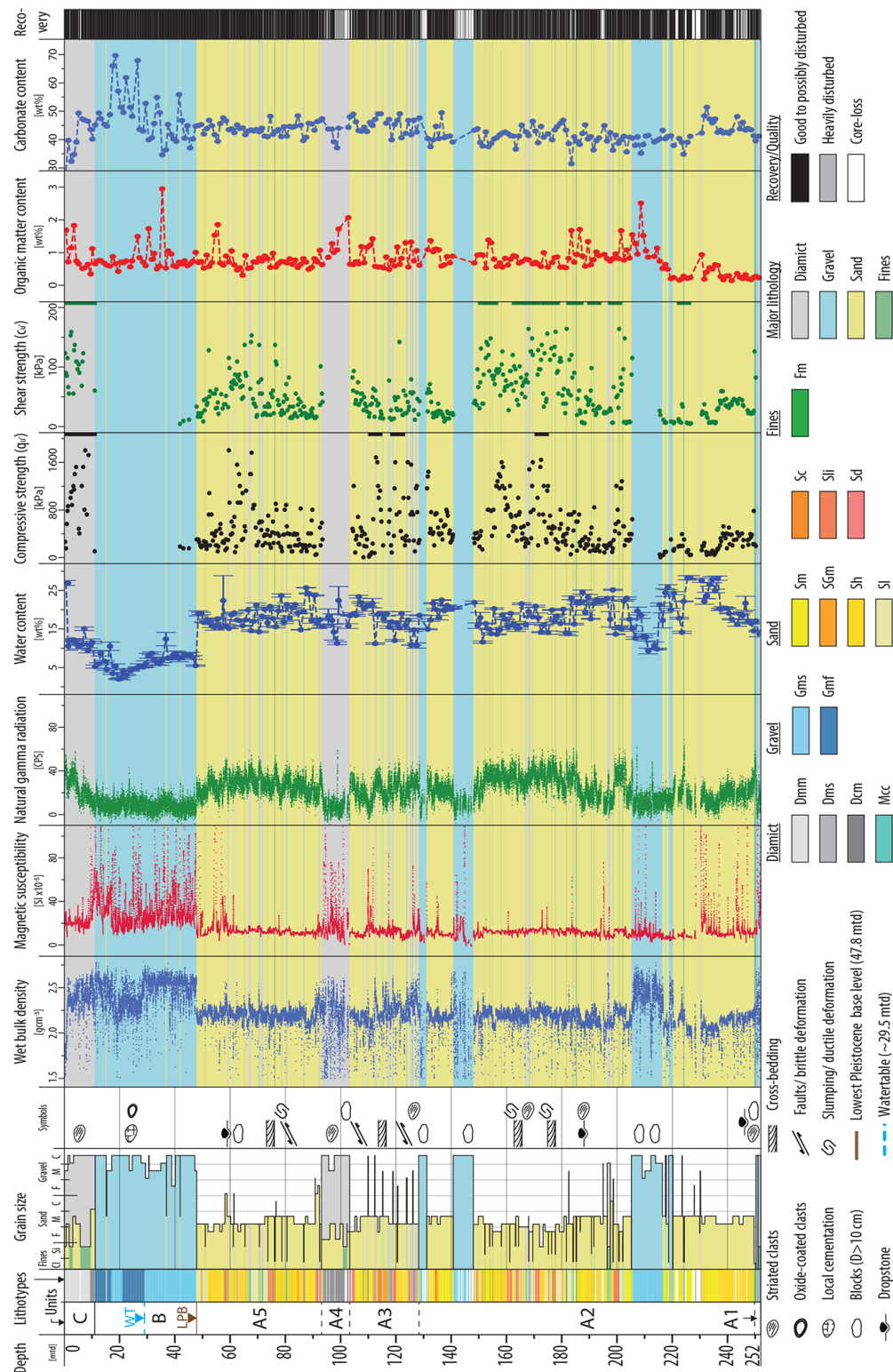


**Figure 4.** Lithological and petrophysical data versus depth. Columns from left to right: depth-scale [mtd], stratigraphic units (labeled with A1–A5, B, and C; WT = water table; LPB = lowest Pleistocene base level), lithotypes, dominant grain size with indicated main lithotypes, symbols of prominent observations, wet bulk density ( $\text{g cm}^{-3}$ ), magnetic susceptibility ( $\text{SI} \times 10^{-5}$ ), natural gamma radiation (CPS, counts per second), water content with indicated standard deviation (wt%), undrained uniaxial compressive strength ( $q_u'$ ) (kPa), undrained shear strength ( $c_u'$ ) (kPa), organic matter content (wt%), carbonate content (wt%), and the recovery. Main lithotypes are indicated as semi-transparent color codes over the plot's entire width.

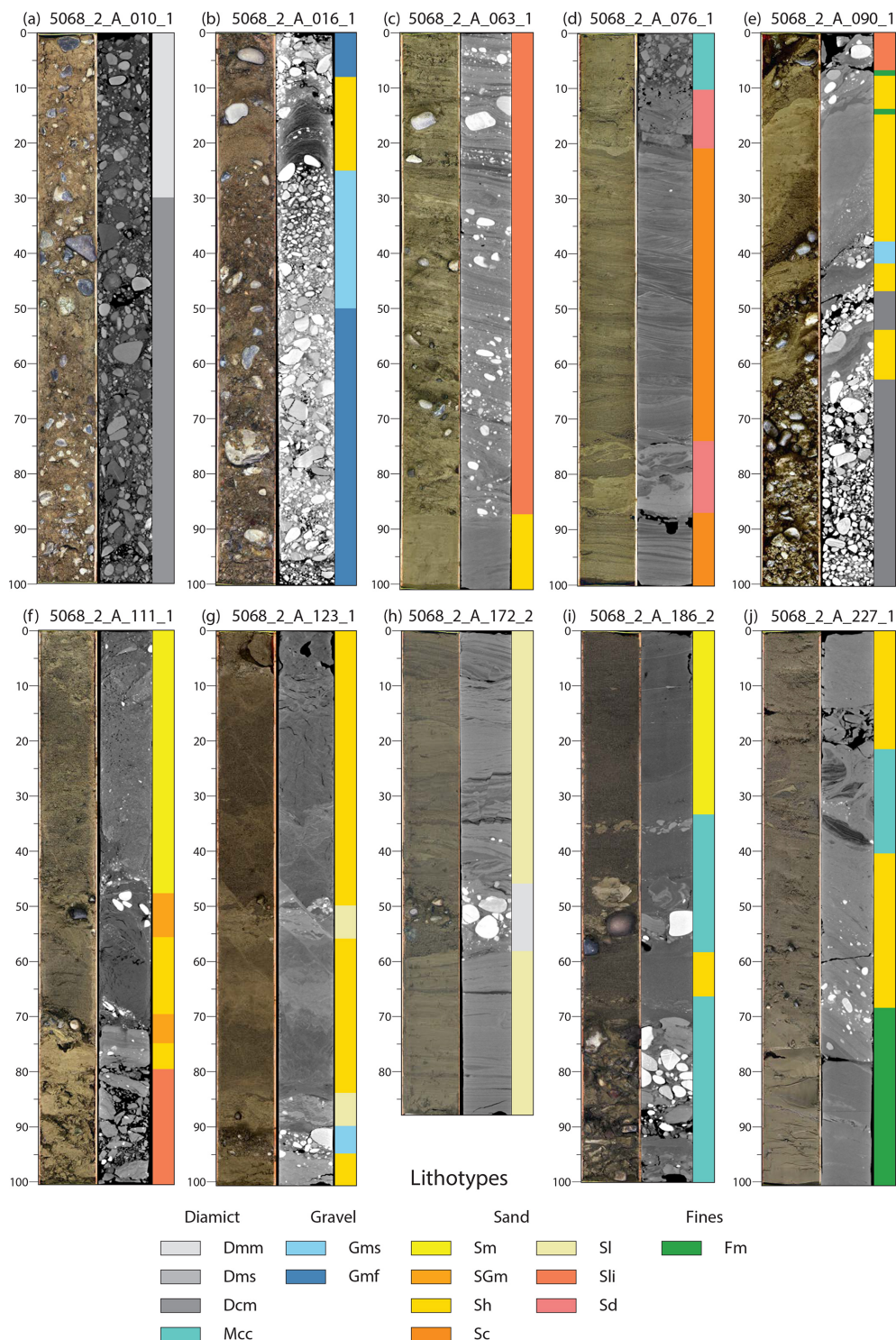


**Figure 5.** CT and line scans of selected representative core sections with corresponding lithotypes. Each core section is labeled at the top; the scale is in centimeter section depth (cmsd) and shows the following from left to right: line scan, CT scan, and lithotypes. The color code for the lithotypes is given at the bottom. Shown core sections from left to right are the following: (a) 5068\_2\_A\_010\_1 (9–10 mtd), (b) 5068\_2\_A\_016\_1 (15–16 mtd), (c) 5068\_2\_A\_063\_1 (58–59 mtd), (d) 5068\_2\_A\_076\_1 (74–75 mtd), (e) 5068\_2\_A\_090\_1 (93–94 mtd), (f) 5068\_2\_A\_111\_1 (111–112 mtd), (g) 5068\_2\_A\_123\_1 (122–123 mtd), (h) 5068\_2\_A\_172\_2 (182–182.88 mtd), (i) 5068\_2\_A\_186\_2 (196–197 mtd), and (j) 5068\_2\_A\_227\_1 (249–250 mtd).

and, in parts, including striated and bullet-shaped clasts and (ii) gravel beds (*Gms*) with better clast rounding, low silt and clay content, and a primarily sandy matrix. The base of Unit A (> 249.7 mtd) is built by a succession of diamictic beds with a massive dropstone-rich ~ 0.5 m thick clay bed on top (*Fm*; Fig. 5j). Several larger Molasse bedrock fragments and clasts with glacial striations occur in this diamictic succession. Additionally, some coarse-grained sections have a high permeability as large volumes of fluids were lost during drilling.

Over the entire Unit A, the sandy sections generally show lower density and magnetic susceptibility values and higher natural gamma values than gravelly ones (Fig. 4). Organic matter content varies between 0.5 % and 1 % except from some isolated peaks of up to 2 % in the sandy sections and a drop to nearly 0 % below 217 mtd. The carbonate content ranges between ~ 40 % and 50 %.

#### 4.2.2 Unit B: 47.75–11.00 mtd

Unit B consists of a succession of decimeter-to-meter-thick beds of sandy (Table 1; *Gms*) to partly silty (*Gmf*) gravel with isolated sand beds. The gravel beds are well sorted to locally moderately sorted with a clast-size range from fine to coarse gravel with some cobbles, and clasts are mostly (sub-)rounded to well-rounded. The groundwater table separates the succession of Unit B into the following: (i) below ~ 29.5 mtd, constantly water saturated and with a sand-rich and silt-and-clay-poor matrix, and (ii) above ~ 29.5 mtd, affected by the fluctuation of the groundwater table, with local cementations and oxide-covered clasts and a partly silt- and clay-enriched matrix (Fig. 5b). The section generally has a high density with stepwise changes above the groundwater table, high but noisy magnetic susceptibility values, and low natural gamma values (Fig. 4). Furthermore, Unit B has a low organic matter content of ~ 1 % and a highly variable carbonate content between 35 % and 65 %.

#### 4.2.3 Unit C: 11.00–0.00 mtd

The uppermost unit consists mainly of a massive to crudely bedded, poorly sorted, silty to partly sandy matrix-supported diamict (Table 1; *Dmm*; Fig. 5a) with a clast-size range from fine gravel up to cobbles and a frequent appearance of striated and/or bullet-shaped/flat-iron-shaped clasts. A general fining-up trend occurs in the clast size together with a decrease in clast content from ~ 80 % to > 5 %, supported by the up-core decreasing trend of the density values and the negatively corresponding natural gamma log (Fig. 4). The uppermost ~ 1 m shows an increasing level of organic matter, decalcification, signs of bioturbation, and a humus layer on its very top.

## 5 Interpretation and discussion

### 5.1 Interpretation of depositional environment

#### 5.1.1 Unit A (252.00–47.75 mtd): overdeepened basin fill

The sediments of Unit A were deposited in an overdeepened setting in a clastic-dominated glacial, glaciolacustrine, or lacustrine environment. The thick, stacked succession of current and mass-movement-dominated lithotypes suggests that the overdeepening was the depocenter and dominated by fast accumulation forming deltaic or basin-floor fan systems (Table 1). In such a setting, the observed lithotype association with thick sandy successions (mainly *Sm* and *Sh*), interbedded gravels (*Gms*), and gravelly diamicts (*Dms*, *Dcm*, and *Mcc*) may be interpreted as an externally forced system driven by allogenic or autogenic processes. In the case of an autogenic endmember, the activity and proximity of the sediment influx from the glacier or rivers exert the dominant controls defining the primary sediment and energy source (e.g., Lønne, 1995; Fitzsimons and Howarth, 2018). Thus the changes in the grain-size distribution and the thickness of the bedding may represent changes in the glacier's position. However, since these energy changes are not instantaneous but occur gradually over a longer time, other processes are needed to explain the frequently observed grain-size variations. Alternatively, accumulation on proximal basin-floor fan systems is associated with considerable lateral facies variability, reflecting allogenic changes of the deposition on basin-floor fans (Lønne, 1995; Fitzsimons and Howarth, 2018). This would partly suppress the sedimentary traces of the glacial proximity-related long-term depositional environmental changes, especially the potential shift from a glaciolacustrine towards a more lacustrine regime. Nevertheless, with an increasing distance of the glacier, the dominant depositional environment will evolve from a direct glacial, via a glaciolacustrine, to a lacustrine one, which may even develop into a warm lake state until the next glacial advance will reverse the evolution (e.g., Fitzsimons and Howarth, 2018; Dehnert et al., 2012; Anselmetti et al., 2022). On the basis of these processes, the succession of depositional environments of Unit A is subdivided into five subunits (from bottom to top, A1–A5):

- *Subunit A1* (> 249.7 mtd). The basal diamictic succession (Table 1; *Dmm*, *Dcm*, and *Fm*) is interpreted as proximal, submarginal to possibly subglacial deposits, emplaced in close proximity to a glacier grounded in the deep trough. The interpretation is supported by the pervasive occurrence of striated clasts and the strongly inclined bedding, indicating glaciotectonic processes. The large number of local bedrock fragments in the basal succession indicates proximity to the bedrock surface. The succession shows similar properties to the basal sediments encountered by Dehnert et al. (2012), Buechi



et al. (2017), and Schwenk et al. (2022). These deposits were also interpreted by them as ice-contact sediments at the transition to glaciolacustrine deposition. This transition is represented in the recovered sediment succession by a massive clay bed (Fig. 5j).

- *Subunit A2 (249.7–0128.7 mtd)*. This section is interpreted to have been deposited in a glaciolacustrine setting and consists of the following: (i) thick to medium bedded sand-dominated hyperconcentrated to concentrated density-flow deposits (Table 1; *Sm* and *Sh*; Mulder and Alexander, 2001); (ii) massive gravel-dominated beds, likely high-concentration channelized density-flow deposits (*Gms*), originating from a subaqueous glacial fan system (Eyles et al., 1983); and (iii) a succession of rather thin-bedded to laminated sands of likely turbiditic origin (*Sl* and *Sc*; Mulder and Alexander, 2001; Bouma, 1962). This turbiditic succession separates the partially interbedded sand-dominated and gravel-dominated density-flow deposits into a lower and upper succession, and the latter is terminated by a massive gravel bed. Since these sharp changes in grain size and bedding, frequently observed in this unit, are likely directly related to the flow energy, they may also indicate a lateral variation of the glacier outlet or local subaquatic channel-levee patterns along the submerged proglacial front. Thus, the long-term grain-size evolution controlled by glacier proximity is superimposed by higher-frequency changes caused by local variations in this highly dynamic setting of the glacier front. Therefore, it is unclear if the laminated to partially cross-bedded succession represents a rather lacustrine environment with a more distal-located glacier or a low-energy endmember of the lateral changing depositional system.
- *Subunit A3 (128.7–103.2 mtd)*. The succession of tightly interbedded sand (Table 1; *Sh*) and gravel (*Gms*) beds shows a partially diamictic character (*Dms*, *Mcc*, and *Sl*). These gravel-rich beds possibly represent slumps and subaquatic mass movements originating on unstable slopes of the rapidly infilling basin (e.g., deltas). The collapse of these unstable slope deposits could be linked to increased sediment flux caused by increased fluvial activity (e.g., glacial outburst floods), an advancing glacial front, or even earthquake shaking. The section shows traces of likely glaciotectionic overprinting (*Sd*, ductile and brittle deformation structures). Further, the top contact of this succession is built by a strongly ductile deformed and/or folded sand bed (*Sd*).
- *Subunit A4 (103.2–91.0 mtd)*. This upper diamictic succession (Table 1; *Dcm*) is similar to the basal one of Subunit A1 but lacks a massive clay bed on top (Fig. 5e and 5j). The upper diamict is also interpreted as subglacial deposits, possibly representing another period of

ice contact or at least ice proximity. The sharp and high-frequency changes in grain size of the diamict's top (*Sl*, *Dcm*, and *Fm*) indicate a partially high-energy but unstable environment. This transition is possibly related to pulsing channelized glacial meltwater outbursts that prevented the deposition of a massive clay bed here.

- *Subunit A5 (91.0–47.7 mtd)*. Subunit A5 is similar to the lower glaciolacustrine section of Subunit A2. However, the overall absence of the massive gravel beds indicates a shift to a more glaciolacustrine-to-lacustrine environment where the depositional energy was lower. Moreover, the succession shows some sections enriched in dropstones (Fig. 5c), pointing to a distal ice-contact lake environment. The whole sediment succession of Unit A is sharply cut off by the sediments of Unit B.

### 5.1.2 Unit B (47.75–11.00 mtd): fluvial gravel

The sediments of Unit B are interpreted as fluvial-to-glaciofluvial gravels (Table 1; *Gms* and *Gmf*). On the basis of the geographical and stratigraphic position, they are correlated with the local gravel formation “Buechberg Gravel Complex”, which also covers the surrounding areas and is interpreted as a Middle Pleistocene advance gravel (Graf, 2009b; Müller, 2013). Further, the relief of the contact surface between Unit A and Unit B indicates a strong fluvial erosion of the former top sediments of Unit A during the deposition of the gravels of Unit B (see Sect. 2 “Study area”; Graf, 2009b; Müller, 2013).

### 5.1.3 Unit C (11.00–0.00 mtd): glaciogenic diamicts

The sediments of Unit C are interpreted as a subglacial till and associated glaciogenic diamicts (Table 1; *Dmm* and *Dcm*). This interpretation is supported by the following: (i) the high density and consolidation; (ii) the diamictic texture (e.g., Evans et al., 2006; Evans, 2018); (iii) the abundance of fresh traces of direct ice-contact transportation (e.g., striated and/or bullet-shaped clasts, e.g., Evans et al., 2006; Evans, 2018); and (iv) the stratigraphic position. As the drill site is located within the LGM extent of the former Rhine Glacier (Fig. 1a), at least the upper part, if not all of Unit C, was emplaced during the LGM glaciation (Birrfield glaciation). Alternatively, the lower parts of Unit C may have been emplaced during earlier glaciations that reached the area, e.g., during MIS6 (Beringen glaciation, e.g., Müller, 2013; where MIS represents marine isotope stage). However, a clear unconformity was not observed in the recovered diamicts.

## 5.2 Implications for glacial history

Assuming that each glacial cycle may have left glacial deposits behind, the two diamictic deposits (Subunits A1

and A4) encountered in an overdeepened position may indicate the presence of at least two glacial sedimentary sequences within Unit A with a sequence boundary between  $\sim 103$  and 91 mtd (Subunit A4). This interpretation is supported by the presence of glaciotectionic deformations and pressure-related dewatering structures between 128.7–103.2 mtd (Subunit A3), which may have been caused by an overriding glacier during a next glacial cycle. The postulated glacial sequence boundary potentially coincides with the depth of a prominent erosive discontinuity observed in the seismic data (solid dark blue line in Fig. 1c; Brandt, 2020). This coincidence supports the interpretation that a second glacier advance is documented in the upper part of the Basadingen Through, which apparently eroded more into the width while not removing the deeper basin fill. Future age constraints will place these successions in the context of the marine isotope stages.

Since the whole succession of Unit A was deposited mostly under glacial to glaciolacustrine conditions, the lack of a significant amount of clay- and silt-rich glaciolacustrine background sediments (*Fm*) has been rather surprising. This disparity may be explained by either of the following: (i) no considerable amount of such sediments were deposited since the accommodation space was quickly filled by the sandy and gravelly sediments or (ii) they were eroded after deposition as a former presence is at least indicated by the occurrence of mud-clast conglomerates (*Mcc*, rich in clay and silt rip-up clasts). Likely, both processes may have acted together in the assumed high-energy and clastic-dominated glaciolacustrine environment.

In addition to the lack of fine-grained glaciolacustrine deposits, the absence of the fine-grained interstadial/interglacial lacustrine deposits is likely explained by the following: (i) the possibility that the lake never developed such a state as it became rapidly filled in late glacial periods, (ii) by cold and/or short interstadials, or (iii) if deposited initially they were eroded during the next glacial advance. In the case of the proposed lower glacial cycle below 103.2 mtd, the first or second case may apply since the observed increased appearance of diamictic slumps and subaquatic mass-movement deposits between 128.7–103.2 mtd may indicate a rapid glacial readvance after a short interstadial. However, in the case of the proposed upper cycle, the third explanation might act since at least its top was eroded to a certain degree by the overlying gravels of Unit B. Based on these observations, the proposed lower cycle may be, even if not completely preserved, at least more complete than the proposed upper cycle.

However, the existence of such significant “cold” or “warm” lacustrine deposits can not be ruled out for the whole Basadingen Trough since (i) this observation is only based on information from one drill hole; (ii) the assumed highly variable depositional environment; and (iii) due to possible spatial effects, which may impact the probability of local accu-

mulation of such deposits (e.g., subaquatic channels or subaquatic deltas).

The overlying gravels and tills of Units B and C are documenting the glaciation history after the filling of the trough. The gravels of Unit B document the presence of a glacier upstream of the drill site on at least one occasion before it was covered at least once again during the LGM advance of the Rhine Glacier. Whether more than one glacial cycle is preserved in Units B and C, as suggested by Graf (2009b) and Müller (2013), will be addressed with the planned geochronological analysis.

## 6 Summary and outlook

The proposed complex based on seismic data, possibly multi-phase sedimentary fill of the Basadingen Trough (Fig. 1c; Anselmetti et al., 2022; Brandt, 2020), is fully supported by the drilled and recovered succession, even though the bedrock, predicted at  $\sim 240$  m, was not reached with the final depth of 252 m. It is currently unclear if this is due to an inaccurate identification of the bedrock reflection or to an inaccurate velocity model. Analyzing the vertical seismic profile (VSP) will reveal more details on the bedrock's location. However, the appearance of cobble-sized freshwater molasse fragments indicates the nearby occurrence of the bedrock contact. A first correlation of the drilled succession with the seismic interpretation indicates the coincidence of the glacial depositional sequence at  $\sim 103$  mtd or  $\sim 340$  m a.s.l. with the seismic sequence boundary (Figs. 1c and 4; Brandt, 2020), indicating that the Rhine Glacier advanced over the upper part of the Basadingen Trough at that time. This pattern further supports the sedimentary succession's proposed multi-phase origin in at least two glacial cycles (Anselmetti et al., 2022). Furthermore, the lacustrine (overdeepened) character of the sediments of Subunit A5 indicates a higher fluvial base level at that time, as was proposed by Graf (2009b) and Müller (2013).

Upcoming correlations of seismic, wireline, and core data will help to establish a robust model of the evolution of the Basadingen Trough. The systematical correlation and characterization of the sedimentological core properties with the extended geophysical and geochemical dataset will refine the definition of glacial sequence stratigraphy that can eventually be dated by the planned geochronological data. This will contribute to the understanding of the local and regional glaciation history, the formation of overdeepenings in the Alpine foreland, and (within the context of DOVE) glaciation and landscape evolution of the Alps.

**Data availability.** The DOVE operational dataset is published under <https://doi.org/10.5880/ICDP.5068.001> (DOVE-Phase 1 Scientific Team et al., 2023b) together with the operational report (DOVE-Phase 1 Scientific Team et al., 2023a) and the explanatory remarks (DOVE-Phase 1 Scientific Team et al., 2023c).

Information on the project and the data is also available on the ICDP DOVE project website: <https://www.icdp-online.org/projects/by-continent/europe/dove-switzerland>.

**Sample availability.** IGSNs are assigned to the hole and sample material; samples are available upon request; for further information, see the operational dataset (Dove-Phase 1 Scientific Team et al., 2023b) and the operational report (DOVE-Phase 1 Scientific Team et al., 2023a).

**Author contributions.** SS served as the leading drill site geologist during the drilling operation, had the lead in the ICD, analyzed the data, and was the main author of the paper with the support of FSA and MWB. BS helped as a substitute drill site geologist and contributed substantially to the ICD. MWB and FSA organized the drilling campaign, operated as substitute drill site geologists, provided support and advice for SS during the drilling operation and the ICD, and provided significant scientific input to the paper as part of their role as PhD supervisors of SS. All authors approved the text and the figures.

**Competing interests.** The contact author has declared that none of the authors has any competing interests.

**Disclaimer.** Publisher's note: Copernicus Publications remains neutral with regard to jurisdictional claims in published maps and institutional affiliations.

**Acknowledgements.** We are grateful for continuing support of the International Scientific Continental Drilling Program (ICDP), including the ICDP Operational Support Group for providing the on-site MSCL scanner and the database management tool “mDis”. We acknowledge the tremendous effort of the drilling company, Fretus AG, in particular the drilling crew (Juan Gonzalez, Marek Bajcura, Joaquim Teixeira) for providing us with high-quality drill cores, as well as the technical staff of LIAG, who assisted with the seismic pre-site surveys and the downhole logging. Further, we acknowledge the strong support by the members of the Bürgergemeinde Basadingen-Schlattingen, the members of the Jagdgesellschaft Hegi Belzhalden, the local inhabitants, the involved services of the political community Basadingen-Schlattingen, and the Canton of Thurgau. A special thanks goes to Luka Seslak (our technical drilling consultant), Julijana Gajic, Patrizia Ruffiner (for processing and analyzing the TIC and TOC samples), Kim Lemke (for core transport and support on the drill site), and to the whole DOVE science team for their effort to make this project happen and for keeping it running.

**Financial support.** This research has been supported by the ICDP, the Deutsche Forschungsgemeinschaft (DFG, grant nos. KR2073/3-1, BU 2467/1-2, GA749/5-1, BU 2467/3-1,

BU 3894/2-1, BU 3894/3-1, and PR 957/6-1), Nagra, ENSI, LGRB, LFU, LIAG, BOKU Vienna, and University of Bern.

**Review statement.** This paper was edited by Nadine Hallmann and reviewed by Bernd Wagner and Pierre Dietrich.

## References

- Alley, R. B., Cuffey, K. M., and Zoet, L. K.: Glacial erosion: status and outlook, *Ann. Glaciol.*, 60, 1–13, <https://doi.org/10.1017/aog.2019.38>, 2019.
- Anselmetti, F. S., Bavec, M., Crouzet, C., Fiebig, M., Gabriel, G., Preusser, F., Ravazzi, C., and DOVE scientific team: Drilling Overdeepened Alpine Valleys (ICDP-DOVE): quantifying the age, extent, and environmental impact of Alpine glaciations, *Sci. Drill.*, 31, 51–70, <https://doi.org/10.5194/sd-31-51-2022>, 2022.
- Bouma, A. H.: *Sedimentology of some Flysch deposits: a graphic approach to facies interpretation*, Elsevier, Amsterdam, the Netherlands, <https://lib.ugent.be/catalog/rug01:000978747> (last access: 21 September 2023), 1962.
- Brandt, A. C.: *Erkundung des alpinen, glazial-übertieften Basadingen-Beckens mithilfe von P-Wellen-Seismik*, BSc thesis, Leibniz Universität Hannover, unpublished, 2020.
- Buechi, M. W., Frank, S. M., Graf, H. R., Menzies, J., and Anselmetti, F. S.: Subglacial emplacement of tills and meltwater deposits at the base of overdeepened bedrock troughs, *Sedimentology*, 64, 658–685, <https://doi.org/10.1111/sed.12319>, 2017.
- Buechi, M. W., Graf, H. R., Haldimann, P., Lowick, S. E., and Anselmetti, F. S.: Multiple Quaternary erosion and infill cycles in overdeepened basins of the northern Alpine foreland, *Swiss J. Geosci.*, 111, 133–167, <https://doi.org/10.1007/s00015-017-0289-9>, 2018.
- Clark, P. U., Archer, D., Pollard, D., Blum, J. D., Rial, J. A., Brovkin, V., Mix, A. C., Pisias, N. G., and Roy, M.: The middle Pleistocene transition: characteristics, mechanisms, and implications for long-term changes in atmospheric pCO<sub>2</sub>, *Quaternary Sci. Rev.*, 25, 3150–3184, <https://doi.org/10.1016/j.quascirev.2006.07.008>, 2006.
- Cohen, D., Gillet-Chaulet, F., Haeberli, W., Machguth, H., and Fischer, U. H.: Numerical reconstructions of the flow and basal conditions of the Rhine glacier, European Central Alps, at the Last Glacial Maximum, *The Cryosphere*, 12, 2515–2544, <https://doi.org/10.5194/tc-12-2515-2018>, 2018.
- Cook, S. J. and Swift, D. A.: Subglacial basins: Their origin and importance in glacial systems and landscapes, *Earth-Sci. Rev.*, 115, 332–372, <https://doi.org/10.1016/j.earscirev.2012.09.009>, 2012.
- Dehnert, A., Lowick, S. E., Preusser, F., Anselmetti, F. S., Drescher-Schneider, R., Graf, H. R., Heller, F., Horstmeyer, H., Kemna, H. A., Nowaczyk, N. R., Züger, A., and Furrer, H.: Evolution of an overdeepened trough in the northern Alpine Foreland at Niederweningen, Switzerland, *Quaternary Sci. Rev.*, 34, 127–145, <https://doi.org/10.1016/j.quascirev.2011.12.015>, 2012.
- DOVE-Phase 1 Scientific Team, Anselmetti, F. S., Beraus, S., Buechi, M. W., Buness, H., Burschil, T., Fiebig, M., Firla, G., Gabriel, G., Gegg, L., Grelle, T., Heeschen, K., Kroemer, E., Lehne, C., Lu'thgens, C., Neuhuber, S., Preusser, F., Schaller, S., Schmalfuss, C., Schuster, B., Tanner, D. C.,

- Thomas, C., Tomonaga, Y., Wieland-Schuster, U., and Wonik, T.: Drilling Overdeepened Alpine Valleys (DOVE) – Operational Report of Phase 1, (ICDP Operational Report), GFZ German Research Centre for Geosciences, Potsdam, 70 pp., <https://doi.org/10.48440/ICDP.5068.001>, 2023a.
- DOVE-Phase 1 Scientific Team, Anselmetti, F. S., Beraus, S., Buechi, M. W., Buness, H., Burschil, T., Fiebig, M., Firla, G., Gabriel, G., Gegg, L., Grelle, T., Heeschen, K., Kroemer, E., Lehne, C., Lüthgens, C., Neuhuber, S., Preusser, F., Schaller, S., Schmalfuss, C., Schuster, B., Tanner, D. C., Thomas, C., Tomonaga, Y., Wieland-Schuster, U., and Wonik, T.: Drilling Overdeepened Alpine Valleys (DOVE) – Operational Dataset of DOVE Phase 1, GFZ Data Services [data set], <https://doi.org/10.5880/ICDP.5068.001>, 2023b.
- DOVE-Phase 1 Scientific Team, Anselmetti, F. S., Beraus, S., Buechi, M. W., Buness, H., Burschil, T., Fiebig, M., Firla, G., Gabriel, G., Gegg, L., Grelle, T., Heeschen, K., Kroemer, E., Lehne, C., Lüthgens, C., Neuhuber, S., Preusser, F., Schaller, S., Schmalfuss, C., Schuster, B., Tanner, D. C., Thomas, C., Tomonaga, Y., Wieland-Schuster, U., and Wonik, T.: Drilling Overdeepened Alpine Valleys (DOVE) – Explanatory remarks on the operational dataset, ICDP Operational Dataset – Explanatory Remarks, GFZ German Research Centre for Geosciences, Potsdam, 34 pp., <https://doi.org/10.48440/ICDP.5068.002>, 2023c.
- Ellwanger, D., Wieland-Schuster, U., Franz, M., and Simon, T.: The Quaternary of the southwest German Alpine Foreland (Bodensee-Oberschwaben, Baden-Württemberg, Southwest Germany), *E&G Quaternary Sci. J.*, 60, 22, <https://doi.org/10.3285/eg.60.2-3.07>, 2011.
- Evans, D.: Till: A Glacial Process Sedimentology, John Wiley & Sons, Chichester, 383 pp., <https://doi.org/10.1002/9781118652541>, 2018.
- Evans, D. J. A., Phillips, E. R., Hiemstra, J. F., and Auton, C. A.: Subglacial till: Formation, sedimentary characteristics and classification, *Earth-Sci. Rev.*, 78, 115–176, <https://doi.org/10.1016/j.earscirev.2006.04.001>, 2006.
- Eyles, N., Eyles, C. H., and Miall, A. D.: Lithofacies types and vertical profile models; an alternative approach to the description and environmental interpretation of glacial diamict and diamictite sequences, *Sedimentology*, 30, 393–410, <https://doi.org/10.1111/j.1365-3091.1983.tb00679.x>, 1983.
- Fabbri, S. C., Affentranger, C., Krastel, S., Lindhorst, K., Wessels, M., Madritsch, H., Allenbach, R., Herwegh, M., Heuberger, S., Wieland-Schuster, U., Pomella, H., Schwesternmann, T., and Anselmetti, F. S.: Active Faulting in Lake Constance (Austria, Germany, Switzerland) Unraveled by Multi-Vintage Reflection Seismic Data, *Front. Earth Sci.*, 9, 670532, <https://doi.org/10.3389/feart.2021.670532>, 2021.
- Fiebig, M., Herbst, P., Drescher-Schneider, R., Lüthgens, C., Lomax, J., and Doppler, G.: Some remarks about a new Last Glacial record from the western Salzach foreland glacier basin (Southern Germany), *Quatern. Int.*, 328–329, 107–119, <https://doi.org/10.1016/j.quaint.2013.12.048>, 2014.
- Fitzsimons, S. and Howarth, J.: Chapter 9 – Glaciolacustrine Processes, in: *Past Glacial Environments (Second Edition)*, edited by: Menzies, J. and van der Meer, J. J. M., Elsevier, 309–334, <https://doi.org/10.1016/B978-0-08-100524-8.00009-9>, 2018.
- Graf, H. R.: Stratigraphie und Morphogenese von frühpleistozänen Ablagerungen zwischen Bodensee und Klettgau, *E&G Quaternary Sci. J.*, 58, 12–54, <https://doi.org/10.3285/eg.58.1.02>, 2009a.
- Graf, H. R.: Stratigraphie von Mittel- und Spätpleistozän in der Nordschweiz. Beiträge zur Geologischen Karte der Schweiz (N.F.), 168, Landesgeologie, Swisstopo, 2009b.
- Gribenski, N., Valla, P. G., Preusser, F., Roattino, T., Crouzet, C., and Buoncristiani, J.-F.: Out-of-phase Late Pleistocene glacial maxima in the Western Alps reflect past changes in North Atlantic atmospheric circulation, *Geology*, 49, 1096–1101, <https://doi.org/10.1130/G48688.1>, 2021.
- Haeuselmann, P., Granger, D. E., Jeannin, P.-Y., and Lauritzen, S.-E.: Abrupt glacial valley incision at 0.8 Ma dated from cave deposits in Switzerland, *Geology*, 35, 143–146, <https://doi.org/10.1130/G23094A>, 2007.
- Hofmann, F.: Erläuterungen zu: Geologischer Atlas der Schweiz – 1052 Andelfingen (Atlasblatt 52), Schweiz. Geol. Komm., 1967.
- Hofmann, F. and Hantke, R.: Erläuterungen zu Blatt 1032 Diessenhofen des geologischen Atlas der Schweiz, Schweiz. Geol. Komm., 1964.
- Ivy-Ochs, S., Kerschner, H., Reuther, A., Preusser, F., Heine, K., Maisch, M., Kubik, P. W., and Schlüchter, C.: Chronology of the last glacial cycle in the European Alps, *J. Quaternary Sci.*, 23, 559–573, <https://doi.org/10.1002/jqs.1202>, 2008.
- Keller, O. and Krayss, E.: The rhine-linth glacier in the upper wurm: A model of the last alpine glaciation, *Quatern. Int.*, 18, 15–27, [https://doi.org/10.1016/1040-6182\(93\)90049-L](https://doi.org/10.1016/1040-6182(93)90049-L), 1993.
- Leemann, A. and Niessen, F.: Holocene glacial activity and climatic variations in the Swiss Alps: reconstructing a continuous record from proglacial lake sediments, *Holocene*, 4, 259–268, <https://doi.org/10.1177/095968369400400305>, 1994.
- Li, S., Li, S., Shan, X., Gong, C., and Yu, X.: Classification, formation, and transport mechanisms of mud clasts, *Int. Geol. Rev.*, 59, 1609–1620, <https://doi.org/10.1080/00206814.2017.1287014>, 2017.
- Lisiecki, L. E. and Raymo, M. E.: Pliocene-Pleistocene stack of globally distributed benthic stable oxygen isotope records, *PANGAEA* [data set], <https://doi.org/10.1594/PANGAEA.704257>, 2005.
- Lønne, I.: Sedimentary facies and depositional architecture of ice-contact glaciomarine systems, *Sediment. Geol.*, 98, 13–43, [https://doi.org/10.1016/0037-0738\(95\)00025-4](https://doi.org/10.1016/0037-0738(95)00025-4), 1995.
- Meyers, P. A. and Teranes, J. L.: Sediment Organic Matter, in: *Tracking Environmental Change Using Lake Sediments: Physical and Geochemical Methods*, edited by: Last, W. M. and Smol, J. P., Springer Netherlands, Dordrecht, 239–269, [https://doi.org/10.1007/0-306-47670-3\\_9](https://doi.org/10.1007/0-306-47670-3_9), 2001.
- Mulder, T. and Alexander, J.: The physical character of subaqueous sedimentary density flows and their deposits, *Sedimentology*, 48, 269–299, <https://doi.org/10.1046/j.1365-3091.2001.00360.x>, 2001.
- Müller, E. R.: Mittelpleistozäne Schottervorkommen zwischen dem Thurtal und Schaffhausen, *Swiss Bulletin für angewandte Geologie*, 18/1, 3–27, ETH Zürich, <https://doi.org/10.5169/SEALS-391135>, 2013.
- Penck, A. and Brückner, E.: *Die Alpen im Eiszeitalter*, Tauchnitz, Leipzig, 1909.
- Pietsch, J. and Jordan, P.: Digitales Höhenmodell Basis Quartär der Nordschweiz – Version 2014 und ausgewählte Auswertungen, *Nagra Arbeitsber. NAB 14-02*, 2014.



- Pomper, J., Salcher, B. C., Eichkitz, C., Prasicek, G., Lang, A., Lindner, M., and Götz, J.: The glacially overdeepened trough of the Salzach Valley, Austria: Bedrock geometry and sedimentary fill of a major Alpine subglacial basin, *Geomorphology*, 295, 147–158, <https://doi.org/10.1016/j.geomorph.2017.07.009>, 2017.
- Preusser, F., Reitner, J. M., and Schlüchter, C.: Distribution, geometry, age and origin of overdeepened valleys and basins in the Alps and their foreland, *Swiss J. Geosci.*, 103, 407–426, <https://doi.org/10.1007/s00015-010-0044-y>, 2010.
- Preusser, F., Graf, H. R., Keller, O., Krayss, E., and Schlüchter, C.: Quaternary glaciation history of northern Switzerland, *E&G Quaternary Sci. J.*, 60, 21, <https://doi.org/10.3285/eg.60.2-3.06>, 2011.
- Reber, R. and Schlunegger, F.: Unravelling the moisture sources of the Alpine glaciers using tunnel valleys as constraints, *Terra Nova*, 28, 202–211, <https://doi.org/10.1111/ter.12211>, 2016.
- Ruddiman, W. F., Raymo, M., and McIntyre, A.: Matuyama 41 000-year cycles: North Atlantic Ocean and northern hemisphere ice sheets, *Earth Planet. Sci. Lett.*, 80, 117–129, [https://doi.org/10.1016/0012-821X\(86\)90024-5](https://doi.org/10.1016/0012-821X(86)90024-5), 1986.
- Schaller, S., Böttcher, M. E., Buechi, M. W., Epp, L. S., Fabbri, S. C., Gribenski, N., Harms, U., Krastel, S., Liebezeit, A., Lindhorst, K., Marxen, H., Raschke, U., Schleheck, D., Schmiedinger, I., Schwalb, A., Vogel, H., Wessels, M., and Anselmetti, F. S.: Postglacial evolution of Lake Constance: sedimentological and geochemical evidence from a deep-basin sediment core, *Swiss J. Geosci.*, 115, 7, <https://doi.org/10.1186/s00015-022-00412-1>, 2022.
- Schlüchter, C.: The Swiss glacial record – a schematic summary, in: *Developments in Quaternary Sciences*, Elsevier, vol. 2, 413–418, [https://doi.org/10.1016/S1571-0866\(04\)80092-7](https://doi.org/10.1016/S1571-0866(04)80092-7), 2004.
- Schwenk, M. A., Schläfli, P., Bandou, D., Gribenski, N., Douillet, G. A., and Schlunegger, F.: From glacial erosion to basin overfill: a 240 m-thick overdeepening–fill sequence in Bern, Switzerland, *Sci. Dril.*, 30, 17–42, <https://doi.org/10.5194/sd-30-17-2022>, 2022.
- Spötl, C., Koltai, G., Jarosch, A. H., and Cheng, H.: Increased autumn and winter precipitation during the Last Glacial Maximum in the European Alps, *Nat. Commun.*, 12, 1839, <https://doi.org/10.1038/s41467-021-22090-7>, 2021.
- Valla, P. G., Shuster, D. L., and van der Beek, P. A.: Significant increase in relief of the European Alps during mid-Pleistocene glaciations, *Nat. Geosci.*, 4, 688–692, <https://doi.org/10.1038/ngeo1242>, 2011.



## Coring tools have an effect on lithification and physical properties of marine carbonate sediments

David De Vleeschouwer<sup>1</sup>, Theresa Nohl<sup>1,2</sup>, Christian Schulbert<sup>3</sup>, Or M. Bialik<sup>1</sup>, and Gerald Auer<sup>4</sup>

<sup>1</sup>Institute of Geology and Paleontology, University of Münster, Corrensstr. 24, 48149 Münster, Germany

<sup>2</sup>Institute of Palaeontology, University of Vienna, Josef-Holaubek-Platz 2 (UZA II), 1090 Vienna, Austria

<sup>3</sup>Geozentrum Nordbayern, Section Palaeontology, Friedrich-Alexander University Erlangen–Nürnberg (FAU),  
Loewenichstr. 28, 91054 Erlangen, Germany

<sup>4</sup>University of Graz, Department of Earth Sciences, NAWI Graz Geocenter,  
Heinrichstraße 26, 8010 Graz, Austria

**Correspondence:** David De Vleeschouwer (ddevlees@uni-muenster.de)

Received: 20 June 2023 – Revised: 9 August 2023 – Accepted: 11 August 2023 – Published: 26 October 2023

**Abstract.** The International Ocean Discovery Program (IODP) *JOIDES Resolution* Science Operator typically uses an advanced piston corer (APC) in soft ooze and sediments and an extended core barrel (XCB) in firm sediments. The coring tool exchange typically occurs around the same depth in adjacent holes of the same site. However, during IODP Expedition 356, the coring tool switch occurred at different depths: IODP Sites U1463 and U1464 are marked by a stratigraphic interval (> 25 m thick) that was XCB cored in one hole and APC cored in other holes. Shipboard scientists remarked that APC-cored sediments were unlithified or partially lithified, while XCB-cored sediments were fully lithified. This difference in sedimentological description of the same formation seems to be an effect of coring technique. To provide further insight, we assessed the physical properties (bulk density, porosity, and P-wave velocity), downhole wireline logging data, scanning electron microscope (SEM) images, and micro-computed tomography ( $\mu$ CT) scans of those intervals.

We find systematic differences between the different coring techniques. XCB cores are characterized by systematically lower bulk density, higher porosity, and higher P-wave velocity than APC cores. Downhole logging data suggest that the original P-wave velocity of the formation is better preserved in XCB cores, despite the typical “biscuit-and-gravy” core disturbance (i.e. well-preserved core fragments surrounded by squelched core material). In conjunction with SEM and  $\mu$ CT images, we conclude that the APC tool destroyed early lithification by breaking cements between individual grains. Moreover,  $\mu$ CT images reveal denser packing and smaller pore volumes in the APC cores. These sedimentary changes likely occur when the APC pressure wave passes through the sediment. The destruction of grain-to-grain cements provides an explanation for the significantly lower P-wave velocities in APC cores. Interestingly, the gravy sections in XCB drilled cores mimic the destruction of early lithification and reduction of pore volume. We conclude that APC remains the tool of choice for recovering soft sediments, especially for paleoclimate purposes. However, for the study of lithification, XCB biscuits provide a more representative image of the formation. For the study of early diagenesis, further studies are required to ascertain the preservation of key sedimentary features using existing and new drilling tools.

## 1 Introduction

Lithification is the process by which loose sediment is transformed into solid rock. This transformation can involve biochemical, physicochemical, and mechanical processes at different stages of burial, from cementation and dissolution-precipitation at the seafloor to pressure-/temperature-induced alteration in several hundreds of metres of depth (Shinn, 1969; Garrison and Kennedy, 1977; Herbert, 1993; Buryakovskiy et al., 2012; Sample et al., 2017; Ge et al., 2020; Sulpis et al., 2022).

In the case of carbonate sediment, the main lithification pathway is cementation, in which minerals such as calcite, aragonite, or dolomite precipitate from interstitial water and fill the spaces between carbonate and detrital grains. Thereby, a solid matrix originates, which binds together the grains. Cementation can manifest in different forms: (1) the presence of cements that provide insights into the depositional or diagenetic environment (Friedman, 1964; Bathurst, 1972, 1974, 1980; Flügel, 1982); (2) the transformation of mud into micrite during early diagenesis, a process known as micritization (Folk et al., 1965; Munnecke, 1997; Munnecke et al., 2023); (3) late diagenetic transformations such as pressure dissolution (Moore and Wade, 2013); (4) dolomitization, during which dolomite replaces the original mineral composition (Budd, 1997; McKenzie and Vasconcelos, 2009; Mavromatis et al., 2014; Reuning et al., 2022); and (5) the diagenetic transformation of any of the four cases mentioned (Harris et al., 1985). Lithification and cementation modify the physical properties of the sediment, including porosity, density, and P-wave velocity (Fabricius, 2003). However, the precise mechanisms behind these transformations remain a topic of ongoing debate. However, it is clear that, when sediments undergo the process of cementation and mineral grains bind together, and when compaction is caused by the pressure of overlying sediments, loose sediments gradually transform into a resilient and lithified carbonate rock.

Identifying and separating the processes that drive lithification is crucial to infer original paleo-environmental information. Doing so becomes exceedingly complicated as several aspects of lithifying carbonate sediments are still not understood. Especially the early diagenetic transformation of soft sediments into solid rock remains enigmatic (Reid et al., 2000; Nohl et al., 2021; Tagliavento et al., 2021; Reuning et al., 2022; Munnecke et al., 2023). What can be inferred is that the microbial decay of organic matter causes variable geochemical gradients impacting porewater alkalinity and pH, which leads to the dissolution of aragonite and a reprecipitation of  $\text{CaCO}_3$  as calcite cement (Froelich et al., 1979; Berner, 1980; Munnecke and Samtleben, 1996; Soetaert et al., 2007; Wurgalt et al., 2019; Reuning et al., 2022). However, the exact processes leading to dissolution and precipitation of  $\text{CaCO}_3$ , the exact depth within the sediment column, and the source of both calcium and carbonate in interstitial waters, remain largely unconstrained and thus under

debate. The existence of this knowledge gap holds significant implications, as the dissolution of substantial portions of carbonate sediment, such as aragonite in modern sediments, has the potential to be transported back into the seawater. Furthermore, lithological alternations, such as between limestone and marl, are often used for cyclostratigraphic purposes, introducing interpretations in terms of past climate change and new chronostratigraphic information (Sinnesael et al., 2019). However, the robust identification of lithological cyclicity and its attribution to Milankovic forcing requires insights into the lithification process and the early diagenetic history of sediments in different depositional environments. Such insights start with correctly observing and pinpointing the transition of unlithified into lithified sediment in modern systems. Moreover, the degree to which sediment is lithified has further implications for reconstructing faunal composition and abundance. Indeed, several processes involved in lithification act as a taphonomic filter (Hendy, 2011; Nawrot, 2012; Nohl et al., 2019).

Scientific drilling within the International Ocean Discovery Program (IODP) framework provides an opportunity to identify and analyse the transition from unconsolidated to lithified sediments beneath the current seafloor. Curiously though, IODP Expedition 356 shipboard scientists noted that the lithification description of a particular formation was dependent on the coring technique employed (Gallagher et al., 2017a). On this expedition, the RV *JOIDES Resolution* deployed the four standard wireline coring tools: the advanced piston corer (APC), the half-length advanced piston corer (HLAPC), the extended core barrel (XCB), and the rotary core barrel (RCB). In sedimentary layers of alternating hardness, like on Expedition 356, a typical coring strategy is to change back and forth between the use of the APC, the HLAPC, and the XCB to best capture the full stratigraphy. This coring strategy had the consequence that at multiple sites, the same formation was cored by the XCB in one hole and by the (HL)APC in other holes. Thereby, the same stratigraphic interval, cored by different coring techniques, yielded differently lithified sediments. Typically, the APC-cored sediments in one hole were described as unlithified or partially lithified, while XCB-cored sediments in the other hole were assessed to be fully lithified. In this paper, we evaluate the effect of coring tools on lithification and physical properties of marine sediments in order to obtain new insights into the transition from soft sediment to lithified rock in an IODP context, as well as to report a potential bias introduced by the choice of coring tool.



## 2 Materials and methods

### 2.1 IODP sites at which the same formation was recovered using different coring tools

#### 2.1.1 Site U1463

Site U1463 (141 m water depth; Fig. 1) is situated on a flat outer ramp, with a seabed that consists of poorly sorted carbonate-rich sediment (bioclastic gravel, sand, and mud). Site U1463 is subdivided into five lithostratigraphic units: from top to bottom, Site U1463 consists of unlithified wackestone and mudstone with abundant peloids (Unit I); alternating unlithified wackestone, packstone, and mudstone intervals (Unit II); well-sorted homogeneous mudstone containing fine sand-sized grains (Unit III, both described as lithified and unlithified); lithified grainstone with abundant macrofossils (Unit IV); and lithified dolostone with sand-sized pyrite and glauconite grains (Unit V). Unit III contains the stratigraphic layers that were cored with different coring tools: this interval of interest extends between 280–400 m core depth below sea floor (CSF-A). It was cored with the XCB in Hole U1463B (U1463B 34X–46X), with the HLAPC in Hole U1463C (U1463C 33F–61F) and with both the APC and the HLAPC in Hole U1463D (U1463D 32H–47F). The different holes of a single site can be considered as sampling the same stratigraphic interval, as the research vessel was only offset by 20 m between the different holes. Potential differences in lithification and physical properties of the same formation between the different holes can therefore only be explained by the coring tools used.

#### 2.1.2 Site U1464

Site U1464 is also situated within an outer ramp setting (270 m water depth), about 100 km northeast of Site U1463 and 50 km southeast of the Rowley Shoals. The site is located adjacent and shoreward to a drowned “fossil” reef/shoal (~ 5 km; Ryan et al., 2009). Site U1464 is divided into five lithostratigraphic units: from top to bottom, Site U1464 consists of unlithified sediments with peloids in varying abundances (Unit I), unlithified homogeneous wackestone including a packstone interval (Unit II), unlithified homogeneous mudstone (Unit III), dolomitic limestone and dolostone (Unit IV, described as lithified and unlithified, and V, described as lithified). The stratigraphic layers that were cored with different coring tools belong to the bottom of Unit III and the topmost part of Unit IV: the interval of interest extends between 285–315 m CSF-A. It was cored with the APC and the HLAPC in Hole U1464B (U1464B 33H–35F), with the RCB in Hole U1464C (U1464C 2R–3R) and with the XCB in Hole U1464D (U1464D 33X–34X). Similar to Site U1463, the vessel was offset by 20 m for coring the different holes of Site U1464.

#### 2.1.3 Site U1482

Site U1482 (IODP Expedition 363) is a further site offshore northwest Australia that has a significant stratigraphic interval cored by several coring tools. Between 340 and 380 m CSF-A, Hole U1482A and U1482B were cored with the HLAPC (U1482A 38F–45F and U1482B 41F–45F), while U1482C was cored with the XCB (U1482C 39X–42X). Nevertheless, this site is not discussed further in this paper because discrete bulk density, porosity, and P-wave velocity measurements of these sediments were only measured in U1482A in the interval of interest, and the shipboard sedimentologists did not explicitly report the degree of lithification. These two factors result in the available shipboard data not allowing for a detailed comparison of sediment properties between different coring tools. The physical property data obtained with the whole-round multisensor logger (WRMSL) do not provide a suitable alternative because of the difference in diameter between the APC and XCB cores. The Expedition 363 shipboard scientists attempted to correct for this effect by applying an XCB correction factor, but their attempt was unsatisfactory as it introduced significant offsets between whole-round and discrete measurements further downcore (Rosenthal et al., 2018).

### 2.2 Shipboard discrete moisture and density and P-wave velocity measurements

We only consider shipboard physical property measurements carried out on discrete samples (bulk density and porosity) and directly on the split-core surface (P-wave). Hence, we do not consider physical property measurements carried out on whole-round sections because their results are strongly affected by the extent to which the core liner is filled with sediment.

Discrete samples were collected shipboard from the working halves to determine wet and dry bulk density, grain density, water content, and porosity. A detailed description of the analytic procedure can be found in Gallagher et al. (2017b), who followed the guidelines provided in Blum (1997). Here, we provide a short summary of the applied methods. Sediment samples were placed in Wheaton glass or plastic vials before wet and dry sediment weighing. The weights of wet and dry sample masses ( $M_{\text{wet}}$  and  $M_{\text{dry}}$ ) were determined to a precision of 0.005 g using two Mettler Toledo electronic balances, with one acting as a reference. A standard weight of similar value to the sample was placed on the reference balance to increase accuracy. A computer averaging system was used to compensate for the ship’s motion. The default setting of the balances is 300 measurements (taking ~ 1.5 min). Dry sample volume ( $V_{\text{dry}}$ ) was determined using a hexapycnometer system of a six-celled custom-configured Micromeritics AccuPyc 1330TC helium-displacement pycnometer. The precision of each cell is 1 % of the full-scale volume. Volume measurement was preceded by three purges of the sample

chamber with helium warmed to  $\sim 28^\circ\text{C}$ . Three measurement cycles were run for each sample. A reference volume (set of two calibration spheres) was placed sequentially in one of the chambers to check for instrument drift and systematic error. The volumes occupied by the numbered vials were calculated before the cruise by multiplying each vial's weight by the average density of the vial glass. Dry mass and volume were measured after samples were heated in an oven at  $105^\circ\text{C} \pm 5^\circ\text{C}$  for 24 h and allowed to cool in a desiccator. The mass of the evaporated water ( $M_{\text{water}}$ ) and salt ( $M_{\text{salt}}$ ) in the sample are given by

$$M_{\text{water}} = M_{\text{wet}} - M_{\text{dry}}$$

$$M_{\text{salt}} = M_{\text{water}} \left[ \frac{s}{1-s} \right],$$

where  $s$  is the assumed saltwater salinity (0.035) corresponding to the pore water density ( $\rho_{\text{pw}}$ ) of  $1.024 \text{ g cm}^{-3}$  and a salt density ( $\rho_{\text{salt}}$ ) of  $2.22 \text{ g cm}^{-3}$ . The corrected mass of pore water excluding salt ( $M_{\text{pw}}$ ), the volume of pore water ( $V_{\text{pw}}$ ), the volume of salt ( $V_{\text{salt}}$ ), and wet volume ( $V_{\text{wet}}$ ) are

$$M_{\text{pw}} = \frac{M_{\text{water}}}{1-s}$$

$$V_{\text{pw}} = \frac{M_{\text{pw}}}{\rho_{\text{pw}}}$$

$$V_{\text{salt}} = \frac{M_{\text{salt}}}{\rho_{\text{salt}}}$$

$$V_{\text{wet}} = V_{\text{dry}} - V_{\text{salt}} + V_{\text{pw}}.$$

Wet bulk density ( $\rho_{\text{wet}}$ ) and porosity ( $\phi$ ) are calculated as

$$\rho_{\text{wet}} = \frac{M_{\text{wet}}}{V_{\text{wet}}}$$

$$\phi = \frac{V_{\text{pw}}}{V_{\text{wet}}}.$$

Moisture and density measurements during Expedition 356 were calculated with the MADMax shipboard programme, set with the “Method C” calculation process.

### 2.3 Downhole logging

At Site U1463, downhole measurements were conducted in Hole U1463B. The porosity and bulk density of the formations were measured with the Accelerator Porosity Sonde (APS) and the Hostile Environment Litho-Density Sonde (HLDS), respectively. Both tools were part of the triple combo tool string that was run between 452 m wireline log-matched depth below seafloor (WMSF) and the seafloor. The results were judged to be of very good quality, based on the systematic variation in the logs, the standoff distance between the tool and the borehole wall, and the consistency with the discrete moisture and density measurements on

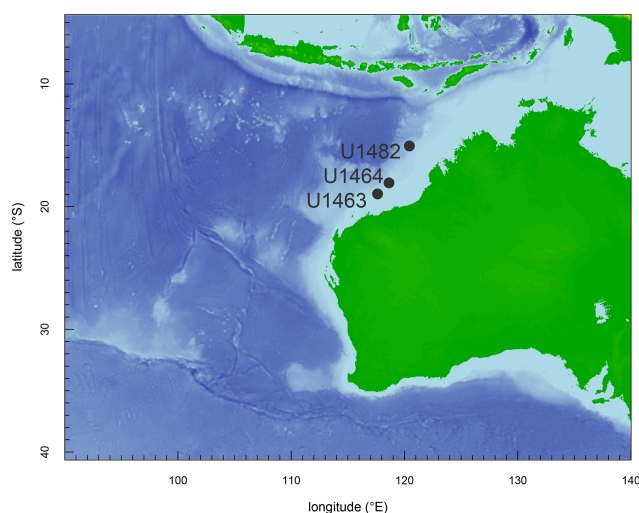


**Figure 1.** Map of the studied sites on the North West Shelf of Australia.

cores (Gallagher et al., 2017c). Sonic P-wave velocities along the borehole wall were determined by the dipole sonic imager (DSI) mounted on the Formation Micro Scanner (FMS)-sonic tool string. At Site U1463, the FMS-sonic string was deployed between 444–122 m WMSF. The downhole sonic velocities are considered to be of good quality because the FMS made full contact with the borehole wall, and the FMS resistivity images are generally of good quality (Gallagher et al., 2017c). At Site U1464, the wireline tool became stuck in the hole below the interval of interest on the first pass up with the triple combo tool string. Unfortunately, the HLDS and APS were turned off during the down pass, and downhole logging with the FMS-sonic was not attempted following the recovery of the triple combo. These circumstances imply that Site U1464 does not have wireline logging data that can be used to groundtruth bulk density, porosity, and P-wave velocity data from cores.

The HLDS contains a radioactive  $^{137}\text{Cs}$  gamma ray source (622 keV) and far and near gamma ray detectors mounted on a shielded skid, which is pressed against the borehole wall by a hydraulically activated decentralizing arm. Gamma rays emitted by the source undergo Compton scattering, in which gamma rays are scattered by electrons in the formation. The number of scattered gamma rays that reach the detectors is proportional to the density of electrons in the formation, which is, in turn, related to bulk density.

The APS includes a Minitron neutron generator that produces fast (14.4 MeV) neutrons and five detectors positioned at different distances from the Minitron. The tool counts neutrons that arrive at the detectors after being scattered and slowed by collisions with atomic nuclei in the formation. The highest energy loss occurs when neutrons collide with hydrogen nuclei, which have practically the same mass as the neutron (the neutrons bounce off of heavier elements without

losing much energy). In low-porosity formations, neutrons can travel farther before being captured, and the count rates increase at the detector. However, because hydrogen bound in minerals such as clays or hydrocarbons also contributes to the measurement, the raw porosity value is often overestimated.

The DSI measures the transit times between sonic transmitters and an array of eight receivers. It combines replicate measurements, thus providing a direct measurement of sound velocity through formations. Along with the monopole transmitters found on most sonic tools, the DSI also has two crossed-dipole transmitters that allow the measurement of shear wave velocity in addition to compressional wave velocity. Dipole measurements are necessary to measure shear velocities in slow formations, with shear velocity less than the velocity of sound in the borehole fluid. Such slow formations are typically encountered in deep-ocean drilling.

## 2.4 Micro-computed tomography (CT) scans

Six micro-CT scans were performed with the General Electric Phoenix V|tome|  $\times$  S240 of the Palaeontology section of the Geozentrum Nordbayern at the University of Erlangen–Nürnberg, Germany. The micro-CT was equipped with the Phoenix 180NF x-ray source with a high-energy target (tungsten on diamond window) and the Phoenix DXR 250RT detector at 200  $\mu$ m pixel size and 1.000  $\times$  1.000 pixels. Scanning was done with 100 kV and 100  $\mu$ A at a resolution of 10  $\mu$ m in a collimated cone beam and a 0.1 mm copper filter. Raw data were reconstructed with Phoenix Datos|  $\times$  software using a GPU-supported Feldkamp algorithm based on filtered backprojection. CT data post-processing was performed with the ORS Dragonfly software version 2023.2 on a Windows 10 workstation. For noise reduction of the reconstructed data sets within Dragonfly, a Gaussian filter (3-D mode, kernel-size 3) was used. From all data sets, a central cube-shaped volume of 4 mm edge length was selected as a sample volume for the pore analysis. To detect the pores from the material of the samples, a threshold was defined to distinguish pore volume from material volume. To eliminate noise and artefacts, all pores smaller than 27 voxels were excluded from the analysis. For visualization, the pore spaces were rendered in 3-D with a colour scheme according to the respective volume (number of voxels) of the pores.

## 2.5 Scanning electron microscope (SEM)

Six samples were imaged using a Zeiss Gemini DSM982 field-emission scanning electron microscope at the University of Graz, Department of Earth Sciences. For each sample, several fracture pieces were mounted on a standard SEM stub using conductive graphite tape before being coated with a carbon/platinum coating using a Leica EM ACE600 sputter coater. We applied a combination of external and in-lens secondary electron (SE) detectors for high-resolution imaging

(up to 100 000 $\times$ ). External and in-lens SE signals were combined using the DISS5 imaging software (point electronic GmbH) and dynamically adapted to maximize image contrast for individual grains and early diagenetic features for each image.

## 3 Results

This paper is motivated by the first remarkable observation that the degree of lithification reported for exactly the same stratigraphic interval by the shipboard sedimentologists varies depending on the coring technique used (as shown for U1463 and U1464 in Figs. 2 and 3, respectively). At Hole U1463B, the sediment became increasingly stiff at  $\sim$ 285 m CSF-A, which is where the drillers switched from HLAPC to XCB coring. In the next hole, Hole U1463C, the strategy was to use HLAPC cores until refusal, which happened at  $\sim$ 292 m CSF-A. The XCB-obtained U1463B interval displays a type of core disturbance referred to as “biscuits and gravy”. The XCB coring tool is designed such that the inner core liner does not rotate together with the drilling bit. Thereby the transfer of rotary torque from the cutting shoe to the cored formation is reduced yet not entirely eliminated (JOIDES Resolution Science Operator, 2014). This torque-transfer phenomenon entails the fragmentation of the cored material into distinct chunks, known as “biscuits”. The rotary motion of the core barrel in XCB drilling causes the biscuit fragments to rub against each other, resulting in the formation of ground sediment. The slurry created by mixing the ground sediment with drilling fluid and seawater is what generates the “gravy”. Gravy is typically observed in the core around and between the biscuits. Since biscuits provide a more accurate representation of the cored lithology, they are chosen for shipboard discrete physical property measurements (as shown in Figs. 2 and 3) and used for the sedimentological core description. Thereby, it is remarkable that the U1463B XCB biscuits between 330–400 m CSF-A are described as “lithified”, whereas the HLAPC cores from exactly the same stratigraphic interval in U1463C were reported to be only partially lithified (Fig. 2). The same contrasting pattern can be observed at Site U1464. There, XCB cores in Hole U1464D between 307–317 m CSF-A are described as lithified, contrary to the (HL)APC cores in the same stratigraphic interval, which were unlithified (Fig. 3). This significant variation in sediment description is not due to changes between night and day shifts but rather reflects a systematic difference in the external appearance of sediment cores from the same stratigraphic interval, depending on the coring tool used.

### 3.1 Physical properties

At Site U1463, the physical properties (bulk density, porosity, P-wave velocity) from discrete measurements show systematic differences between holes. The XCB cores from Hole



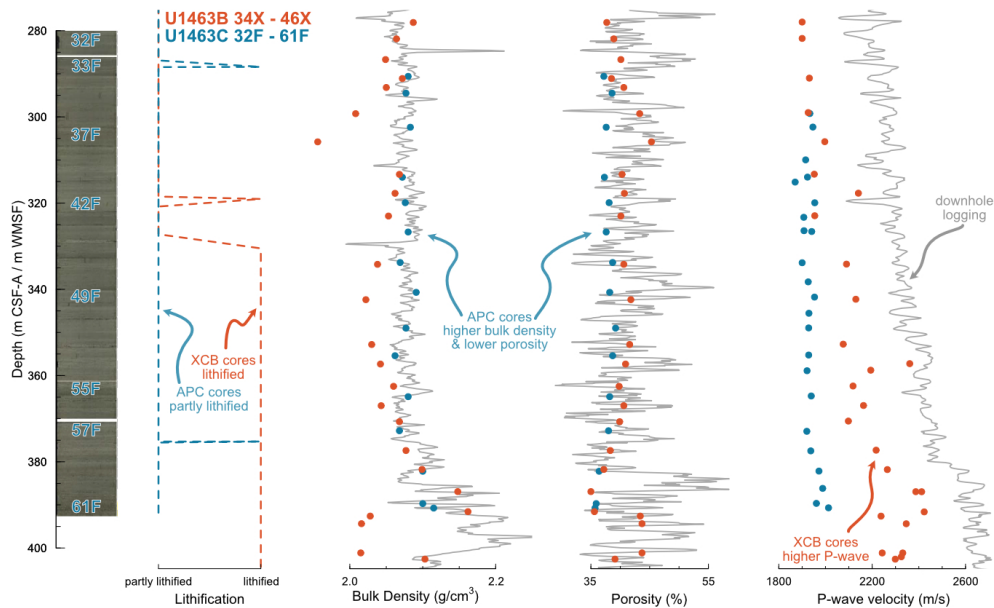


**Figure 2.** Lithification, bulk density, porosity, and P-wave velocity data measured at Site U1463. Orange data originate from XCB cores (Hole U1463B), blue data refer to HLAPC cores (Hole U1463C), and grey data reflect wireline logging data. Note that biscuits were selected for discrete physical property measurements on XCB cores.

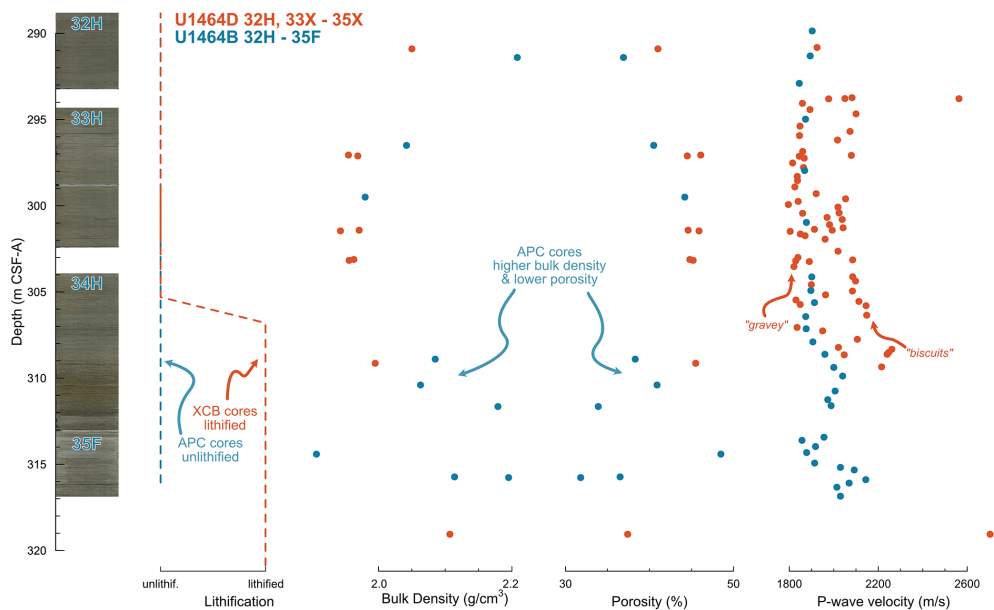


**Figure 3.** Lithification, bulk density, porosity, and P-wave velocity data measured at Site U1464. Orange data originate from XCB cores (Hole U1463D), blue data refers to (HL)APC cores (Hole U1464B). Note that biscuits were selected for discrete physical property measurements on XCB cores. Discrete P-wave velocity measurements constitute an exception as both biscuits and gravity were measured from XCB cores, with a bimodal distribution in the obtained velocities.

U1463B are characterized by systematically lower bulk density, higher porosity, and higher P-wave velocities (orange data in Fig. 2) compared to the HLAPC cores from Hole U1463C (blue data in Fig. 2). When compared to the in situ downhole logging wireline data, it seems that the bulk density data from the HLAPC cores are in closer agreement with

the wireline data. However, the offset in bulk density between HLAPC and XCB cores is often smaller than  $0.05 \text{ g cm}^{-3}$ , which is of the same order as the variability in the wireline data. For porosity, the offset between coring techniques is only a few percent. The HLAPC-XCB porosity offset is thus dwarfed by the large variability that marks the wire-

line porosity data. We note that the wireline porosity data often reflect an overestimate of the true porosity of the formation (see “Materials and methods”). This is especially the case for clay-rich formations like the studied interval. However, despite this consideration, it is not possible to determine whether HLAPC or XCB porosity data align more closely with the downhole logging data. On the other hand, the P-wave velocity data show a very clear picture, with the XCB cores approaching the downhole logging data more closely than the HLAPC data. This observation is independent of a possible mismatch between depth scales. In this respect, we note that core-based measurements are reported along the CSF-A depth scale, whereas the wireline data use the WMSF depth scale. The relation between both depth scales was determined by the correlation of distinctive features in core-based and wireline NGR (natural gamma radiation; Christensen et al., 2017; Gallagher et al., 2017c) and amounts between 3 and 6 m in the studied interval.

At Site U1464, downhole wireline logging attempts with the HLDS, APS, and DSI were unsuccessful at Site U1464, preventing any core–log comparisons. Nevertheless, one can observe similar patterns in terms of physical properties at Site U1464 compared to Site U1463. The XCB cores from Hole U1464D generally display lower bulk density and higher porosity (orange data in Fig. 3) compared to the (HL)APC cores from Hole U1464B (blue data in Fig. 3). Furthermore, and again similar to Site U1463, the highest P-wave velocities at U1464 come from XCB cores. However, the pattern becomes more nuanced, with P-wave velocities obtained from XCB cores from Hole U1464D falling into two distinct velocity end members. Low XCB P-wave velocities correspond to fine-grained pseudo-laminar material (gravy) that is considered to be drilling slurry, whereas the higher velocities are from hard, coarser-grained semi-lithified and less disturbed portions of the core (biscuits). The low-velocity end member of the XCB cores neatly corresponds to the velocities observed in APC cores from Hole U1464B. The high-velocity end member of the XCB cores is offset by  $\sim 150 \text{ m s}^{-1}$ .

The effect of the biscuit-and-gravy core disturbance is not limited to P-wave velocity. Bulk density data obtained by the whole-round logger for XCB-Core U1461B 86X clearly show that gravy is characterized by higher bulk density compared to biscuits (Fig. 4).

### 3.2 Micro-computed tomography (CT) scans

Micro-computed tomography ( $\mu$ CT) images were captured of small cubes of sediment from three adjacent sections from Hole U1463B, spanning the switch in coring technique from HLAPC to XCB. Samples come from sections U1463B 33F2 and 33F3 (281.20–284.16 m CSF-A) and section U1463B 34X1 (284.40–285.90 m CSF-A), all belonging to the same lithostratigraphic subunit. The samples were deliberately chosen to be closely spaced stratigraphically on ei-

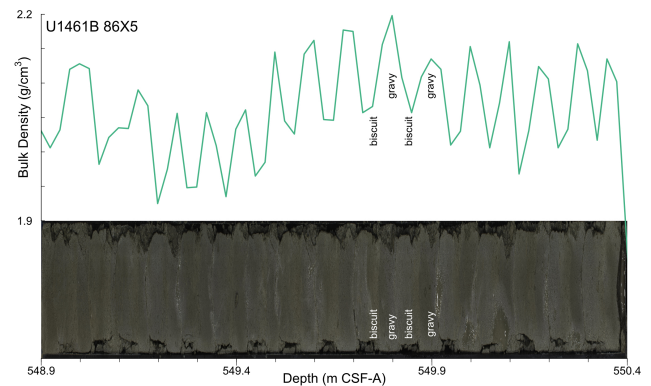


**Figure 4.** The effect of the biscuit-and-gravy core disturbance on bulk density in XCB cores. Gravy is characterized by a higher bulk density compared to biscuits.

ther side of the HLAPC-XCB switch. This sampling allows for an assessment of the impact of drilling technique while at the same time limiting stratigraphic variability along the depth axis. The only core disturbance recorded by the ship-board sedimentologists in this interval is moderate gravy and biscuits in section U1463B 34X1. However, we note that core pictures of section U1463 33F3 reveal a slight deformation of the sediment, with uparching bed contacts and indications of vertical flowage of sediment along the core liner (Jutzeler et al., 2014).

The smallest micro-pores, which measure  $< 0.002 \text{ mm}^3$ , appear as dark purple volumes in the images, while foraminifera are shown in yellow, typically measuring  $0.003\text{--}0.005 \text{ mm}^3$  (Fig. 5a–f). The comparison of  $\mu$ CT images according to drilling technique seems to suggest that XCB samples are characterized by a greater abundance of micro-pores in comparison to APC cores. The quantification of Feret diameters of identified pores in the CT images supports this visual observation. The distribution of Feret diameters is more right-skewed, with a higher mode for pores with a  $\sim 0.1 \text{ mm}$  diameter. The XCB cores thus appear to exhibit a higher abundance of micro-pores ( $< 0.002 \text{ mm}^3$ ) compared to the APC cores.

### 3.3 SEM imaging of pore space and cements

SEM analysis allowed the state of pore space and cements to be observed in great detail (Fig. 6a, b). The XCB-derived samples exhibit calcite cements well attached to primary sediment grains (Fig. 6c) and build a cemented structure within the sediment, indicative of early lithification. The HLAPC-derived samples, on the other hand, also contain calcite cement crystals (Fig. 6b, d), though the cements are unattached to sediment grains, and the pore volume seems reduced (Fig. 6d). This detachment can also be observed for sediment grains such as foraminifera, which are separated by a thin gap from the formerly attached matrix (Fig. 6f).

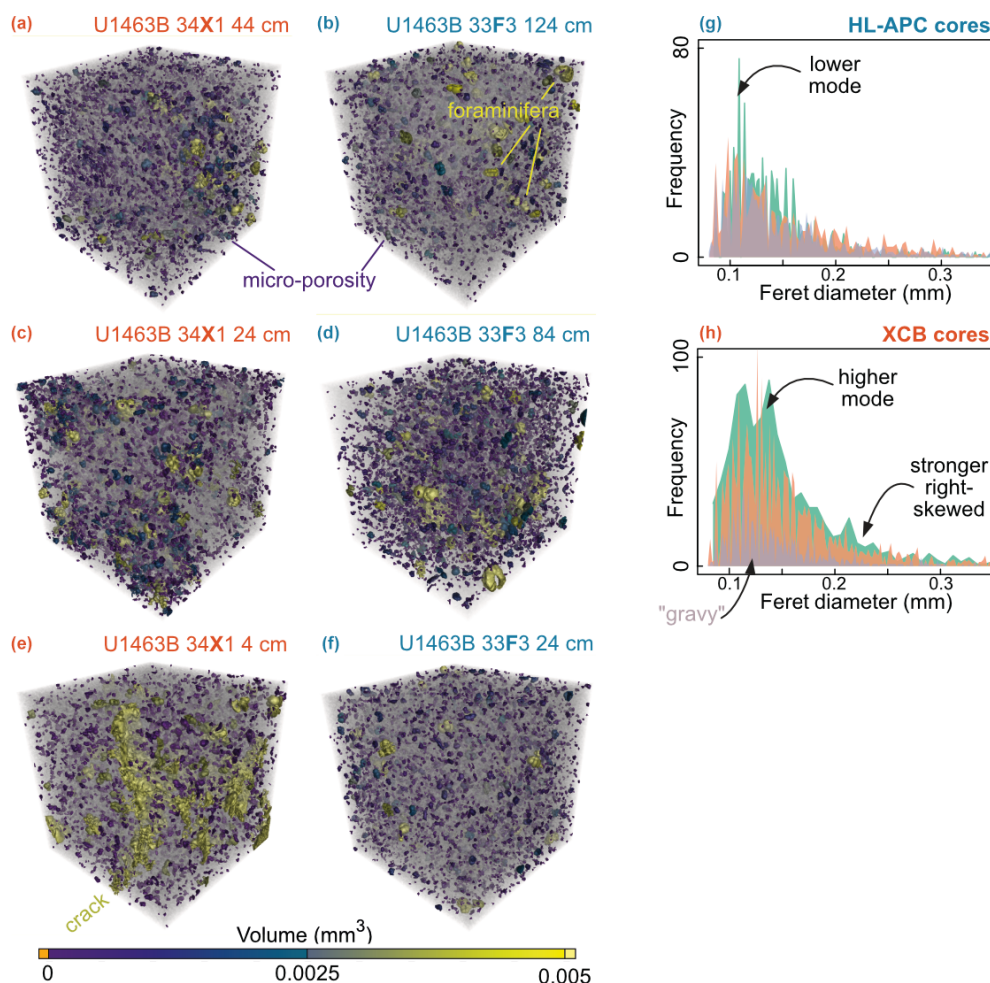


**Figure 5.** Micro-porosity as captured by  $\mu$ CT images of adjacent HL-APC and XCB cores at Hole U1463B. (a–f) XCB samples exhibit slightly more abundant and slightly larger micro-pores ( $< 0.002 \text{ mm}^3$ , purple) than APC cores. However, we acknowledge that the difference is hard to discern visually. Foraminifera and cracks within the samples are depicted in yellow. (g–h) The distribution of Feret diameters helps to visualize the difference in micro-porosity, with a more right-skewed distribution and a higher mode for XCB cores compared to HL-APC samples. Note that the samples are all from the same hole, closely spaced ( $\pm 1 \text{ m}$ ) on either side of the HL-APC–XCB switch in Hole U1463B.

#### 4 Discussion

The data presented from Sites U1463 and U1464 indicate that the (HL)APC technique utilized by IODP potentially leads to the partial loss of lithification and a reduction in P-wave velocity. Additionally, micro-porosity in APC cores seems lower than equivalent XCB cores, resulting in noticeable effects on bulk density and porosity. We suspect that the hydraulic force exerted by the inner core barrel of an APC core as it penetrates the sediment is the most probable explanation for this observation.

The APC coring technique is known to produce high-quality and high-resolution sedimentary records for paleoclimate purposes, preserving original sedimentary structures as well as soft-sediment deformations. However, the pressure wave that is sent through the sedimentary formation exerts a dynamic stress on the individual grains. The piston force of

(HL-)APC coring can amount up to 125 kN (JOIDES Resolution Science Operator, 2014). This stress can lead to a temporary rearrangement of the grains. Essentially, the wave creates a temporary increase in pressure that pushes the grains closer together, resulting in a more tightly packed arrangement, i.e. condensation. The effect is often referred to as “acoustic compaction” and could explain the changes in the physical properties of the sediment, such as increased density and reduced porosity (Figs. 2, 3) and fewer micro-pores (Fig. 5). Here, we illustrate this effect by means of SEM images, showing a much denser packing of carbonate grains and clay minerals in the APC core (Fig. 6b) compared to the adjacent XCB core (Fig. 6a).

Another potential effect of the APC-generated pressure wave is the breaking of early cements in a carbonate sediment. The XCB-core SEM images in Fig. 6c exhibit continuous, uninterrupted sparitic cements, connecting different



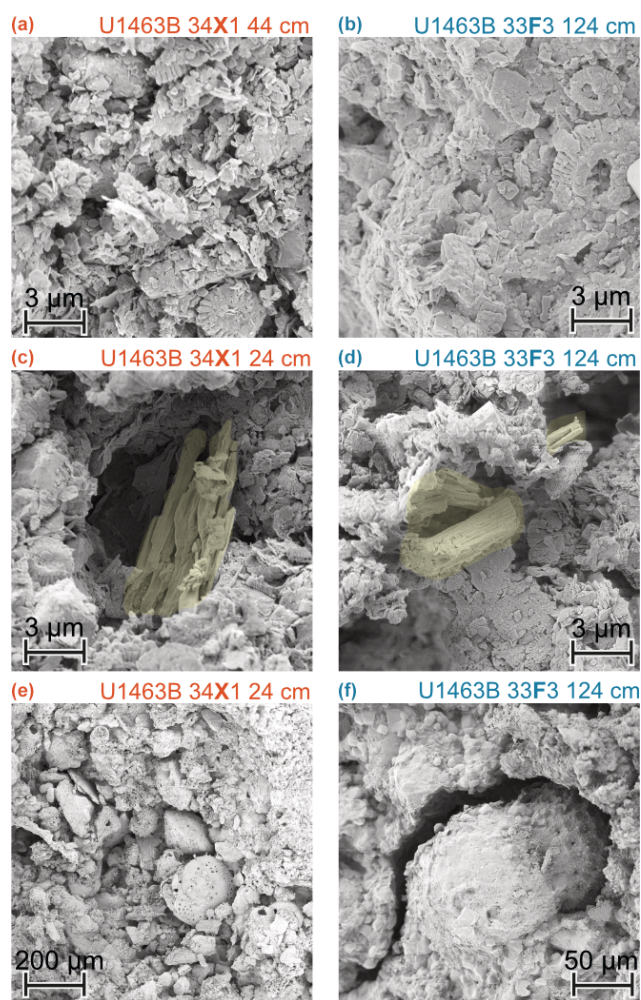


**Figure 6.** Scanning electron microscope (SEM) pictures of adjacent HLAPC and XCB cores at Hole U1463B. (a) Loosely packed matrix consisting of clay minerals and nanofossils, allowing for a high abundance of micro-pores. (b) Densely packed matrix consisting of clay minerals and nanofossils. (c) Sparitic cement (highlighted in yellow) growing in a loosely packed matrix of clay minerals and nanofossils. (d) Disaggregated, broken sparitic crystal (highlighted in yellow) in a matrix of clay minerals and nanofossils. (e) Overview image showing a benthic foraminifer in a loosely packed matrix. (f) Planktic foraminifer that is fully separated from its densely packed matrix by a micro-crack. Note that the samples are all from the same hole, closely spaced ( $\pm 1$  m) on either side of the HLAPC-XCB switch in Hole U1463B.

components of the carbonate mudstone and often overgrowing the clay matrix. However, similar sparitic cements appear broken and disrupted in Fig. 6d, which is from an adjacent APC core. These images suggest that the APC-generated pressure wave may have caused the cements to break apart and become discontinuous. This effect likely constitutes the underlying reason for the observed differences in lithification of the sediment between XCB and APC cores. Moreover, the disruption of early cements could also explain the

large offset in P-wave velocity measured between the APC and XCB cores. A P-wave travels through the sedimentary formation faster when it can use early cements as a pathway between different components of the sediment. However, when these cements are discontinued, as in the case of the APC cores (Fig. 6d), the P-wave needs to travel around, leading to a lower velocity. It seems likely that the APC-core sediments and XCB-core gravity exhibit similar P-wave velocities because both lack the connectivity of early cements. For the first, inter-grain early cements, as well as possibly inter-grain pressure-solution bindings, are destroyed by the APC-generated pressure wave, whereas for the latter, the sediment grinding by rotary drilling is responsible for the loss of sedimentary strength and gravity production.

In addition to the breaking of early cements, another factor that might have contributed to the lower P-wave velocities in APC cores is the detaching of components like foraminifera and other bioclasts from the surrounding matrix. For instance, the SEM image in Fig. 6f illustrates a planktonic foraminifer that appears disconnected from its densely packed micritic matrix. We suspect that this detachment could have been the result of the hydraulic pressure wave travelling through the sediment upon APC coring. In contrast, we juxtapose this image with an image of a benthic foraminifer in an XCB core that occurs in a loosely packed matrix (Fig. 6e). The detachment and possible fracturing of carbonate components might have contributed to a reduction in inter-grain contacts and, as a consequence, a lower P-wave velocity in APC cores.

The impact of coring technique on the physical appearance of carbonate sediments poses a challenge to sedimentologists studying early diagenesis and lithification. APC coring destroys early cements and causes an artificially increased packing of sedimentary grains. Conversely, XCB cores destroy large parts of the original sedimentary fabrics and textures by producing gravity, leaving only biscuits as snapshots of the original sedimentary formation. The results of this study thus highlight the necessity to keep developing new scientific drilling techniques that are better aligned with the scientific needs of sedimentological research towards lithification and early diagenesis. The extended nose sampler could be such an option, whereby the core barrel is not fired into the formation. Instead, the core barrel is pushed into the formation, increasing the push force when hard formations are encountered, and vice versa.

## 5 Conclusions

The results of this study demonstrate that there are significant differences between the lithology and physical properties of sediments recovered by APC and XCB techniques in carbonate sediments. While APC coring remains the gold standard for paleoceanography research due to its ability to provide continuous, high-quality cores over long intervals, the data

presented here suggest that XCB cores may give a more accurate representation of the micro-porosity, inter-grain connections, and P-wave velocity of the cored sedimentary formation. Indeed, the hydraulic pressure wave generated during the deployment of the APC-core barrel can cause acoustic compaction and can cause early sparitic cements to disaggregate, thereby destroying early lithification and the accompanying sedimentary features.

For that reason, we make researchers interested in studying early diagenetic pathways in carbonate sediments from IODP cores aware of this phenomenon and recommend the use of XCB biscuits cores instead of APC cores in overlapping intervals in carbonate sediments. Indeed, XCB biscuits may provide more valuable insights into the microstructure and lithification of the sedimentary formation in such cases. Ideally, a combination of APC and XCB coring should be applied to provide a complete picture of lithification and sediment composition when studying early diagenetic pathways. To do so, it would be interesting to also experiment with alternative coring tools, like the extended nose corer (JOIDES Resolution Science Operator, 2014; Talalay, 2022). This coring tool potentially offers an intermediate solution between APC and XCB, whereby a core liner is pushed into the sediment without the immense hydraulic pressure. To date, it also remains unclear as to what extent this issue extends into other, more cohesive lithologies. Nevertheless, this study highlights the importance of carefully considering the choice of coring technique when planning sediment coring programmes and when interpreting subsequent analyses.

**Data availability.** The physical property data, core pictures, and downhole logging data presented in Figs. 2 and 3 are available from the IODP LIMS database (<https://web.iodp.tamu.edu/LORE/>, JOIDES Resolution Science Operator, 2023) and the IODP logging database (<https://mlp.ldeo.columbia.edu/logdb/>, Columbia University, 2023). Raw data of micro-CT scans and SEM images are available from De Vleeschouwer et al. (2023).

**Author contributions.** DDV, TN, and GA conceptualized the research. GA carried out the SEM images. CS carried out the micro-CT analyses. All authors contributed to the interpretation of the results. DDV wrote the paper with input of all co-authors.

**Competing interests.** The contact author has declared that none of the authors has any competing interests.

**Disclaimer.** Publisher's note: Copernicus Publications remains neutral with regard to jurisdictional claims in published maps and institutional affiliations.

**Acknowledgements.** This research used samples and data provided by the International Ocean Discovery Program (IODP). We thank all IODP Expedition 356 scientific participants and crew for making this study possible. Special thanks go to Michelle Kominz (Western Michigan University) for pointing out the remarkable difference in lithification during the expedition. We are also grateful to the European Consortium for Ocean Research and Drilling (ECORD) for funding the MagellanPlus Workshop “TIMOR – Tracing Monsoon, Ocean currents and diagenetic carbon redistribution) on 19–22 May 2022 in Vienna, Austria. We thank Christian Vollmer (University of Münster) for technical assistance. We thank David McInroy and Robert McKay for their constructive and thoughtful reviews.

**Review statement.** This paper was edited by Ulrich Harms and reviewed by David McInroy and Robert McKay.

## References

- Bathurst, R. G. C.: Carbonate sediments and their diagenesis, Developments in sedimentology, Elsevier, 658 pp., ISBN 978-0-444-40891-4, 1972.
- Bathurst, R. G. C.: Marine diagenesis of shallow water calcium carbonate sediments, *Annu. Rev. Earth Pl. Sci.*, 2, 257–274, 1974.
- Bathurst, R. G. C.: Lithification of carbonate sediments, *Sci. Prog.*, 66, 451–471, 1980.
- Berner, R. A.: Early diagenesis: A theoretical approach, 1, Princeton University Press, ISBN 9780691082608, 256 pp., 1980.
- Blum, P.: Physical properties handbook: A guide to the shipboard measurement of physical properties of deep-sea cores, ODP Tech. Note, 26, 113 pp., <https://doi.org/10.2973/odp.tn.26.1997>, 1997.
- Budd, D. A.: Cenozoic dolomites of carbonate islands: Their attributes and origin, *Earth-Sci. Rev.*, 42, 1–47, [https://doi.org/10.1016/S0012-8252\(96\)00051-7](https://doi.org/10.1016/S0012-8252(96)00051-7), 1997.
- Buryakovsky, L., Chilingar, G. V., Rieke, H. H., and Shin, S.: Fundamentals of the petrophysics of oil and gas reservoirs, John Wiley & Sons, ISBN 978-1-118-34447-7, 400 pp., 2012.
- Christensen, B. A., Renema, W., Henderiks, J., De Vleeschouwer, D., Groeneveld, J., Castañeda, I. S., Reuning, L., Bogus, K., Auer, G., Ishiwa, T., McHugh, C. M., Gallagher, S. J., Fulthorpe, C. S., and Scientists, I. E.: Indonesian throughflow drove australian climate from humid pliocene to arid pleistocene, *Geophys. Res. Lett.*, 44, 6914–6925, <https://doi.org/10.1002/2017GL072977>, 2017.
- De Vleeschouwer, D., Nohl, T., Schulbert, C., Bialik, O. M., and Auer, G.: Coring tools have an effect on lithification and physical properties of marine carbonate sediments, Zenodo [data set], <https://doi.org/10.5281/zenodo.8319206>, 2023.
- Columbia University: Division of Marine and Large Programs, Search Logging Data, Columbia University [data set], <https://mlp.ldeo.columbia.edu/logdb/> (last access: 10 September 2023), 2023.
- Fabricius, I. L.: How burial diagenesis of chalk sediments controls sonic velocity and porosity, *AAPG Bull.*, 87, 1755–1778, <https://doi.org/10.1306/06230301113>, 2003.

- Flügel, E.: Microfacies analysis of limestones, Springer Berlin, Heidelberg, 634 pp., <https://doi.org/10.1007/978-3-642-68423-4>, 1982.
- Folk, R. L., Pray, L. C., and Murray, R. C.: Some aspects of recrystallization in ancient limestones, in: Dolomitization and limestone diagenesis, SEPM Society for Sedimentary Geology, 13, 14–48, <https://doi.org/10.2110/pec.65.07.0014>, 1965.
- Friedman, G. M.: Early diagenesis and lithification in carbonate sediments, *J. Sediment Res.*, 34, 777–813, <https://doi.org/10.1306/74d71195-2b21-11d7-8648000102c1865d>, 1964.
- Froelich, P. N., Klinkhammer, G. P., Bender, M. L., Luedtke, N. A., Heath, G. R., Cullen, D., Dauphin, P., Hammond, D., Hartman, B., and Maynard, V.: Early oxidation of organic matter in pelagic sediments of the eastern equatorial atlantic: Suboxic diagenesis, *Geochim. Cosmochim. Ac.*, 43, 1075–1090, [https://doi.org/10.1016/0016-7037\(79\)90095-4](https://doi.org/10.1016/0016-7037(79)90095-4), 1979.
- Gallagher, S., Fulthorpe, C., Bogus, K., Auer, G., Baranwal, S., Castañeda, I., Christensen, B., Vleeschouwer, D. D., Franco, D., and Groeneveld, J.: Expedition 356 summary, 43 pp., <https://doi.org/10.14379/iodp.proc.356.101.2017>, 2017a.
- Gallagher, S. J., Fulthorpe, C. S., Bogus, K., Auer, G., Baranwal, S., Castañeda, I. S., Christensen, B. A., De Vleeschouwer, D., Franco, D. R., Groeneveld, J., Gurnis, M., Haller, C., He, Y., Henderiks, J., Himmler, T., Ishiwa, T., Iwatani, H., Jatinigrum, R. S., Kominz, M. A., Korpanty, C. A., Lee, E. Y., Levin, E., Mamo, B. L., McGregor, H. V., McHugh, C. M., Petrick, B. F., Potts, D. C., Rastegar Lari, A., Renema, W., Reuning, L., Takayanagi, H., and Zhang, W.: Expedition 356 methods, in: Indonesian throughflow, edited by: Gallagher, S. J., Fulthorpe, C. S., Bogus, K., and the Expedition 356 Scientists, Proceedings of the International Ocean Discovery Program, College Station, TX, <https://doi.org/10.14379/iodp.proc.356.102.2017>, 2017b.
- Gallagher, S. J., Fulthorpe, C. S., Bogus, K., Auer, G., Baranwal, S., Castañeda, I. S., Christensen, B. A., De Vleeschouwer, D., Franco, D. R., Groeneveld, J., Gurnis, M., Haller, C., He, Y., Henderiks, J., Himmler, T., Ishiwa, T., Iwatani, H., Jatinigrum, R. S., Kominz, M. A., Korpanty, C. A., Lee, E. Y., Levin, E., Mamo, B. L., McGregor, H. V., McHugh, C. M., Petrick, B. F., Potts, D. C., Rastegar Lari, A., Renema, W., Reuning, L., Takayanagi, H., and Zhang, W.: Site u1463, in: Indonesian throughflow, edited by: Gallagher, S. J., Fulthorpe, C. S., Bogus, K., and the Expedition 356 Scientists, Proceedings of the International Ocean Discovery Program, College Station, TX, <https://doi.org/10.14379/iodp.proc.356.108.2017>, 2017c.
- Garrison, R. E. and Kennedy, W. J.: Origin of solution seams and flaser structure in upper cretaceous chalks of southern england, *Sediment Geol.*, 19, 107–137, [https://doi.org/10.1016/0037-0738\(77\)90027-6](https://doi.org/10.1016/0037-0738(77)90027-6), 1977.
- Ge, Y., Pederson, C. L., Lokier, S. W., Traas, J. P., Nehrke, G., Neuser, R. D., Goetschl, K. E., and Immenhauser, A.: Late holocene to recent aragonite-cemented transgressive lag deposits in the abu dhabi lagoon and intertidal sabkha, *Sedimentology*, 67, 2426–2454, <https://doi.org/10.1111/sed.12707>, 2020.
- Harris, P. M., Kendall, C. G. S. C., Lerche, I., Schneidermann, N., and Harris, P. M.: Carbonate cementation – a brief review, in: Carbonate cements: Based on a symposium sponsored by the society of economic paleontologists and mineralogists, SEPM Society for Sedimentary Geology, 36, 79–96, <https://doi.org/10.2110/pec.85.36.0079>, 1985.
- Hendy, A. J.: Taphonomic overprints on phanerozoic trends in biodiversity: Lithification and other secular megabiases, in: Taphonomy. Aims & scope topics in geobiology book series, edited by: Allison, P. A. and Bottjer, D. J., Springer, Dordrecht, 19–77, [https://doi.org/10.1007/978-90-481-8643-3\\_2](https://doi.org/10.1007/978-90-481-8643-3_2), 2011.
- Herbert, T. D.: Differential compaction in lithified deep-sea sediments is not evidence for “diagenetic unmixing”, *Sediment Geol.*, 84, 115–122, [https://doi.org/10.1016/0037-0738\(93\)90049-B](https://doi.org/10.1016/0037-0738(93)90049-B), 1993.
- JOIDES Resolution Science Operator: Coring tools and technology: <https://iodp.tamu.edu/tools/index.html> (last access: 8 August 2023), 2014.
- JOIDES Resolution Science Operator: IODP LIMS database, <https://web.iodp.tamu.edu/LORE/> (last access: 10 September 2023), 2023.
- Jutzeler, M., White, J. D. L., Talling, P. J., McCanta, M., Morgan, S., Le Friant, A., and Ishizuka, O.: Coring disturbances in iodp piston cores with implications for offshore record of volcanic events and the missoula megafloods, *Geochem. Geophys. Geosy.*, 15, 3572–3590, <https://doi.org/10.1002/2014GC005447>, 2014.
- Mavromatis, V., Meister, P., and Oelkers, E. H.: Using stable mg isotopes to distinguish dolomite formation mechanisms: A case study from the peru margin, *Chem. Geol.*, 385, 84–91, <https://doi.org/10.1016/j.chemgeo.2014.07.019>, 2014.
- McKenzie, J. A. and Vasconcelos, C.: Dolomite mountains and the origin of the dolomite rock of which they mainly consist: Historical developments and new perspectives, *Sedimentology*, 56, 205–219, <https://doi.org/10.1111/j.1365-3091.2008.01027.x>, 2009.
- Moore, C. H. and Wade, W. J.: Chapter 5 – carbonate diagenesis: Introduction and tools, in: Developments in sedimentology, edited by: Moore, C. H., and Wade, W. J., Elsevier, 67–89, <https://doi.org/10.1016/B978-0-444-53831-4.00005-7>, 2013.
- Munnecke, A.: Bildung mikritischer kalke im silur auf gotland, *Cour Forsch Senck*, 198, 1–131, 1997.
- Munnecke, A. and Samtleben, C.: The formation of micritic limestones and the development of limestone-marl alternations in the silurian of gotland, sweden, *Facies*, 34, 159–176, <https://doi.org/10.1007/BF02546162>, 1996.
- Munnecke, A., Wright, V. P., and Nohl, T.: The origins and transformation of carbonate mud during early marine burial diagenesis and the fate of aragonite: A stratigraphic sedimentological perspective, *Earth-Sci. Rev.*, 239, 104366, <https://doi.org/10.1016/j.earscirev.2023.104366>, 2023.
- Nawrot, R.: Decomposing lithification bias: Preservation of local diversity structure in recently cemented storm-beach carbonate sands, san salvador island, bahamas, *Palaaios*, 27, 190–205, <https://doi.org/10.2110/palo.2011.p11-028r>, 2012.
- Nohl, T., Jarochowska, E., and Munnecke, A.: Revealing the genesis of limestone-marl alternations: A taphonomic approach, *Palaaios*, 34, 15–31, <https://doi.org/10.2110/palo.2018.062>, 2019.
- Nohl, T., Steinbauer, M. J., Sinnesael, M., and Jarochowska, E.: Detecting initial aragonite and calcite variations in limestone-marl alternations, *Sedimentology*, 68, 3102–3115, <https://doi.org/10.1111/sed.12885>, 2021.
- Reid, R. P., Visscher, P. T., Decho, A. W., Stolz, J. F., Bebout, B. M., Dupraz, C., Macintyre, I. G., Paerl, H. W., Pinckney, J. L., Prufert-Bebout, L., Steppe, T. F., and DesMarais, D. J.:



- The role of microbes in accretion, lamination and early lithification of modern marine stromatolites, *Nature*, 406, 989–992, <https://doi.org/10.1038/35023158>, 2000.
- Reuning, L., Deik, H., Petrick, B., Auer, G., Takayanagi, H., Iryu, Y., Courtillot, M., and Bassetti, M.-A.: Contrasting intensity of aragonite dissolution and dolomite cementation in glacial versus interglacial intervals of a subtropical carbonate succession, *Sedimentology*, 69, 2131–2150, <https://doi.org/10.1111/sed.12985>, 2022.
- Rosenthal, Y., Holbourn, A. E., Kulhanek, D. K., Aiello, I. W., Babila, T. L., Bayon, G., Beaufort, L., Bova, S. C., Chun, J.-H., Dang, H., Drury, A. J., Dunkley Jones, T., Eichler, P. P. B., Fernando, A. G. S., Gibson, K. A., Hatfield, R. G., Johnson, D. L., Kumagai, Y., Li, T., Linsley, B. K., Meinicke, N., Mountain, G. S., Opdyke, B. N., Pearson, P. N., Poole, C. R., Ravelo, A. C., Sagawa, T., Schmitt, A., Wurtzel, J. B., Xu, J., Yamamoto, M., and Zhang, Y. G.: U1482, in: *Western pacific warm pool*, edited by: Rosenthal, Y., Holbourn, A. E., Kulhanek, D. K., and the Expedition 363 Scientists, International Ocean Discovery Program, College Station, TX, <https://doi.org/10.14379/iodp.proc.363.103.2018>, 2018.
- Ryan, G., Bernardel, G., Kennard, J., Jones, A. T., Logan, G., and Rollet, N.: A pre-cursor extensive miocene reef system to the rowley shoals reefs, western australia: Evidence for structural control of reef growth or natural hydrocarbon seepage?, *The APPEA Journal*, 49, 337–364, <https://doi.org/10.1071/AJ08021>, 2009.
- Sample, J. C., Torres, M. E., Fisher, A., Hong, W.-L., Desgrigneville, C., Defliese, W. F., and Tripathi, A. E.: Geochemical constraints on the temperature and timing of carbonate formation and lithification in the nankai trough, nantrioseize transect, *Geochim. Cosmochim. Ac.*, 198, 92–114, <https://doi.org/10.1016/j.gca.2016.10.013>, 2017.
- Shinn, E. A.: Submarine lithification of holocene carbonate sediments in the persian gulf, *Sedimentology*, 12, 109–144, <https://doi.org/10.1111/j.1365-3091.1969.tb00166.x>, 1969.
- Sinnesael, M., De Vleeschouwer, D., Zeeden, C., Batenburg, S. J., Da Silva, A.-C., de Winter, N. J., Dinarès-Turell, J., Drury, A. J., Gambacorta, G., Hilgen, F. J., Hinnov, L. A., Hudson, A. J. L., Kemp, D. B., Lantink, M. L., Laurin, J., Li, M., Liebrand, D., Ma, C., Meyers, S. R., Monkenbusch, J., Montanari, A., Nohl, T., Pälke, H., Pas, D., Ruhl, M., Thibault, N., Vahlenkamp, M., Valero, L., Wouters, S., Wu, H., and Claeys, P.: The cyclostratigraphy intercomparison project (cip): Consistency, merits and pitfalls, *Earth-Sci. Rev.*, 199, 102965, <https://doi.org/10.1016/j.earscirev.2019.102965>, 2019.
- Soetaert, K., Hofmann, A. F., Middelburg, J. J., Meysman, F. J. R., and Greenwood, J.: Reprint of “the effect of biogeochemical processes on ph”, *Mar. Chem.*, 106, 380–401, <https://doi.org/10.1016/j.marchem.2007.06.008>, 2007.
- Sulpis, O., Agrawal, P., Wolthers, M., Munhoven, G., Walker, M., and Middelburg, J. J.: Aragonite dissolution protects calcite at the seafloor, *Nat. Commun.*, 13, 1104, <https://doi.org/10.1038/s41467-022-28711-z>, 2022.
- Tagliavento, M., John, C. M., Anderskouv, K., and Stemmerik, L.: Towards a new understanding of the genesis of chalk: Diagenetic origin of micarbs confirmed by clumped isotope analysis, *Sedimentology*, 68, 513–530, <https://doi.org/10.1111/sed.12802>, 2021.
- Talalay, P. G.: Geological and scientific offshore drilling and core sampling in ice-covered waters, in: *Geotechnical and exploration drilling in the polar regions*, edited by: Talalay, P. G., Springer International Publishing, Cham, 339–383, [https://doi.org/10.1007/978-3-031-07269-7\\_11](https://doi.org/10.1007/978-3-031-07269-7_11), 2022.
- Wurgaft, E., Findlay, A. J., Vigderovich, H., Herut, B., and Sivan, O.: Sulfate reduction rates in the sediments of the mediterranean continental shelf inferred from combined dissolved inorganic carbon and total alkalinity profiles, *Mar. Chem.*, 211, 64–74, <https://doi.org/10.1016/j.marchem.2019.03.004>, 2019.



# Poor Man's Line Scan – a simple tool for the acquisition of high-resolution, undistorted drill core photos

Lukas Gegg<sup>1</sup> and Johann Gegg<sup>2</sup>

<sup>1</sup>Institute of Earth and Environmental Sciences, University of Freiburg,  
Albertstraße 23b, 79104 Freiburg, Germany

<sup>2</sup>independent engineer: 85132 Schernfeld, Germany

**Correspondence:** Lukas Gegg (lukas.egg@geologie.uni-freiburg.de)

Received: 13 June 2023 – Revised: 11 August 2023 – Accepted: 21 August 2023 – Published: 26 October 2023

**Abstract.** The analysis and presentation of drill cores, an essential part of geoscientific research, requires the acquisition of high-quality core photos. Typically, core photos are either taken by hand, which often results in poor and inconsistent image quality and perspective distortions, or with large, heavy, and thus inflexible as well as expensive line scan setups. We present a simple, portable “Poor Man's Line Scan” setup that turns a customary smartphone into a semi-automatic core scanner utilising its panoramic photo function while guided on a rail in order to record undistorted core photographs at high resolution. The resulting images, although affected by some minor artefacts, are clearly superior in quality and resolution to single photos taken by hand and are comparable to images taken with commercial line scan cameras. The low cost (~EUR 100) and high flexibility, including the potential for modifications, of our tool make it an interesting alternative to the classical line scan setup.

## 1 Introduction

Drill cores recovered from commercial or scientific boreholes are one of the most important tools in geoscientific research but also in applied fields of work such as ground investigation. For the detailed description, presentation, and interpretation of drill cores, high-quality core photos are essential (Ettensohn, 1994; Dolgiy et al., 2015). In addition, employing state-of-the-art techniques, core photos can allow further analyses such as automated grain size (Tran et al., 2022) or lithological classification (Fu et al., 2022). However, the dimensions of drill cores, which are typically 5–20 cm in diameter and 1 or several metres long, make the acquisition of suitable images challenging.

Whole-core photographs taken from a distance with a handheld camera often lack detail and are affected by perspective distortions but can be improved by sophisticated imaging setups (e.g. USBR, 1998). The best results are achieved by line scan imaging, where an electric motor moves a drill core past a fixed camera acquiring sequential images that are subsequently automatically stitched together, resulting in a full core photo (e.g. Geotek Limited, 2017).

However, such setups are not only expensive but also large, heavy, and thus stationary.

Fortunately, current smartphones equipped with a panoramic photo mode are capable of the same image-stitching process that is used in classical line scan imaging (Altaratz and Frosh, 2021). We present a simple and inexpensive (~EUR 100, excluding phone) setup we refer to as “Poor Man's Line Scan” (PML) that turns a customary smartphone into a semi-automatic core scanner capable of acquiring high-resolution, undistorted, top-down, i.e. non-unrolled, bisected and whole-round drill core images. Moreover, being portable, the PML can readily be taken into the field, to construction sites, or to core repositories.

## 2 Setup and procedure

The PML setup consists of a 1 m long track, over which a smartphone, in our case an Apple® iPhone SE 2020, is guided along a drill core at a fixed distance of ~15 cm in order to acquire a scan image in panoramic picture mode, with a width / height ratio of > 4 and with the drill core in question being recorded in great detail. As the track, we selected

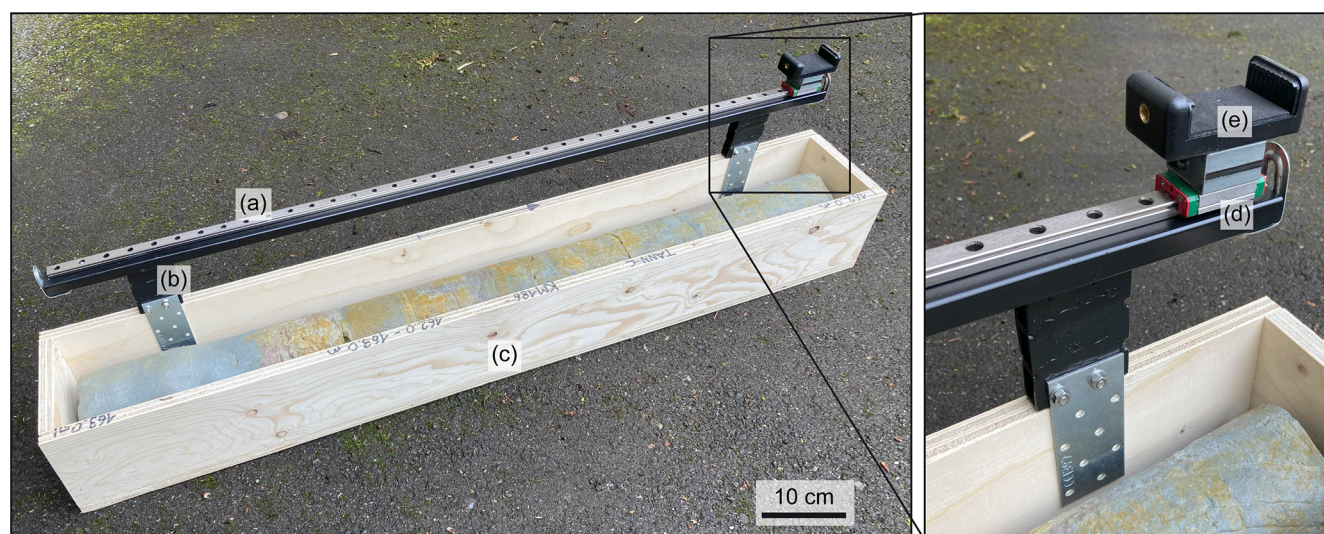


**Figure 1.** The “Poor Man’s Line Scan” setup for core photo acquisition. It consists of a guide rail (a) bolted to a steel frame (b) that can be attached to a wooden core box (c). A ball-bearing-mounted slide block (d) moves a smartphone attached with a phone clamp (e) along the rail in order to acquire a continuous image in panoramic picture mode.

an MGN12H (12 mm wide) linear guide rail that is commonly used, for example, in 3D printing (Fig. 1). This rail is bolted to a square steel frame with a U-shaped seating that allows placing it on the sidewall of a typical wooden drill core box, to which a tape measure is attached for scale. A spring-loaded phone clamp is fitted to a ball-bearing-mounted block that slides over the rail with minimal play. With the smartphone clamped to the slide block and auto-focused on one of the core ends, the panoramic photo acquisition is started, and the phone is guided along the core by hand in order to acquire a coherent scan image. Inconsistencies in acquisition speed are accounted and corrected for by the phone software, and a warning message notifies users if the scanning is done too rapidly. For ideal results, we recommend photographing in naturally or artificially well-lit surroundings but without direct light on the drill core in order to avoid hard cast shadows. Shadows from the core box can be avoided by propping a bisected core up on its other half, so that the surface to be imaged is level with the box edge. To ensure the comparability of different images, we further recommend attaching a colour correction card to the drill core or core box, allowing for appropriate image editing afterwards.

The photos presented in the following were taken from selected cores of the International Continental Scientific Drilling Program (ICDP) borehole 5068\_1\_C in Tannwald, southern Germany (Anselmetti et al., 2022). Line scan photos were recorded with a Geotek Core Imaging System (Geotek Limited, 2017) in the laboratory of the University of Bern. Further images were taken in daylight with the iPhone SE 2020 and the PML setup as shown in Fig. 1 and, for comparison, with the same smartphone camera held by hand from a distance. The length of the PML scan image is restricted by

the capabilities of the smartphone available (i.e. the maximum width of a panoramic picture). Here, 1 m core sections had to be imaged on two separate photos and later stitched together manually using the freeware GIMP (GNU Image Manipulation Program). Apart from that, the smartphone photos were not edited (e.g. contrast enhancement or colour correction).

### 3 Results

The aspect ratios of a photographed core are identical for all three imaging approaches (Fig. 2a–c: width/length = 1/9.5). However, while core photos taken with a handheld camera suffer from major perspective distortions, especially near the core ends, those acquired with the PML are significantly truer to the original (Fig. 3). With the presented setup, we acquired scan images with a resolution of  $\sim 250$  px per core centimetre, which is comparable to classical line scan images, and enable users to zoom in on small-scale details such as individual clasts (Fig. 4). The manual stitching-together of individual images – here two per 1 m core section – takes a few minutes at a time and on some occasions resulted in a minor artefact in the image centre. Other minor artefacts may result from vibrations during photo acquisition (Fig. 5).

### 4 Assessment and conclusion

The comparison of different imaging techniques reveals that core photos taken individually with a handheld smartphone camera from a distance are suitable for low-resolution illustrative purposes where small-scale details are not relevant



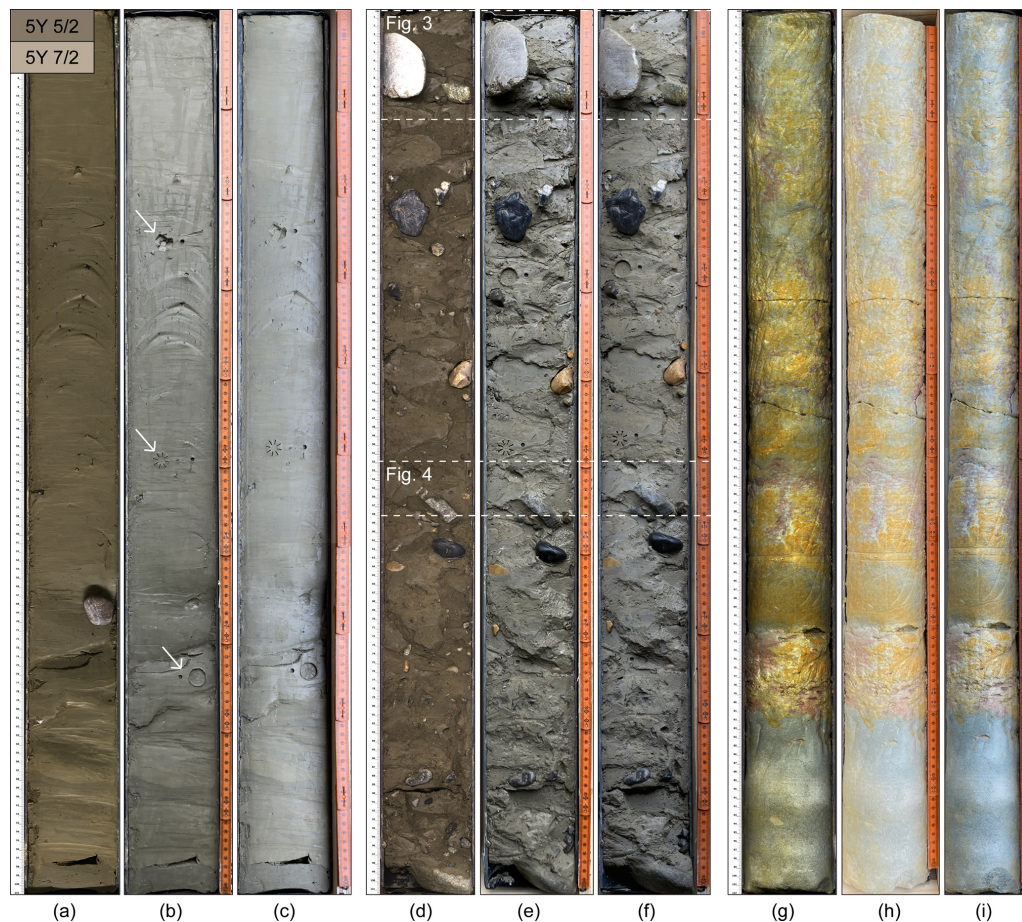


**Figure 2.** Comparison of photos of different drill cores (10 cm diameter, 1 m length) from ICDP borehole 5068\_1\_C (Anselmetti et al., 2022), taken with different imaging setups. **(a–c)** Pleistocene glaciolacustrine fines; bisected drill core with a mostly smooth surface. **(d–f)** Pleistocene glacial diamicts; bisected core with a very irregular surface. **(g–i)** Oligocene to Miocene siltstone and sandstone; whole-round core. Panels **(a)**, **(d)**, and **(g)** were taken with a classic Geotek line scan camera setup and artificial lighting in the laboratory in December 2022 (© Bennet Schuster, University of Freiburg and University of Bern); panels **(b)**, **(e)**, and **(h)** with a customary smartphone camera (Apple® iPhone SE 2020) from a distance; and panels **(c)**, **(f)**, and **(i)** with the same phone camera using the PML setup, the latter both in daylight in May 2023. Differences in colour appearance are mainly attributed to artificial vs. natural lighting, and some colour change may have also occurred during storage after bisecting. For reference, the Pleistocene deposits were, in comparison to a Munsell colour chart, classified as mainly yellowish grey (5Y 7/2) to light olive grey (5Y 5/2) directly after opening. The corresponding RGB colours after Centore (2013) are provided in the top left corner. Note: cores in panels **(b)** and **(c)** and in **(e)** and **(f)** have surficial marks from in situ geotechnical testing; see arrows in **(b)**.

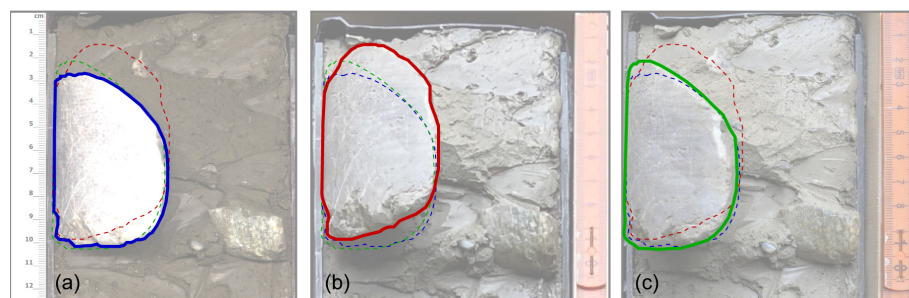


**Figure 3.** Comparison of the depiction of the large quartzite clast at the top of Fig. 2d–f, which sticks out several centimetres from the bisected core surface and therefore appears differently when photographed with different focal lengths. The Geotek line scan **(a)**, © Bennet Schuster, University of Freiburg and University of Bern) as well as the PML **(c)** reproduce the clast shape true to the original, whereas it is visibly distorted in the photograph taken of the full core from a distance **(b)**.



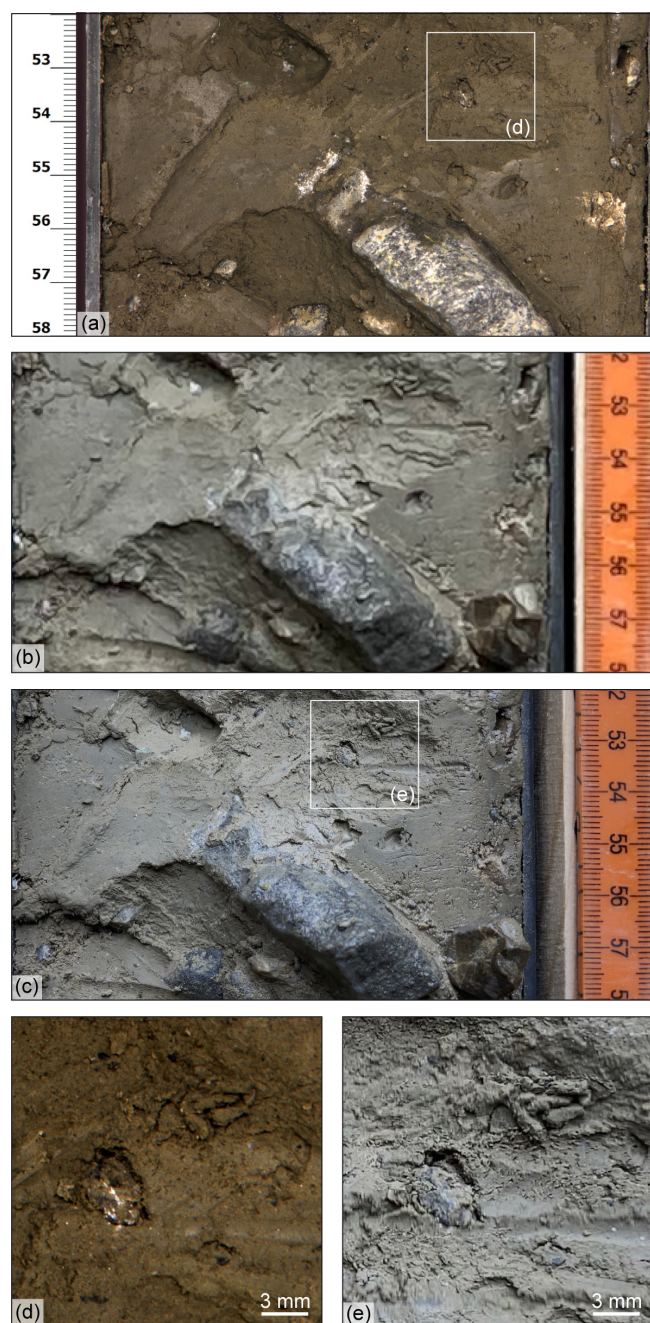


**Figure 4.** Detailed comparison of a selected interval from one of the drill cores presented in Fig. 2. Shown is a bisected core with an irregular surface resulting in high-contrast core photos. The same interval has been imaged with different setups: (a) line scan (© Bennet Schuster, University of Freiburg and University of Bern), (b) handheld phone camera from a distance, and (c) phone camera with the PML. Panels (d) and (e) show zoom-ins of (a) and (c), respectively.

if the photos are taken meticulously to avoid distortions as much as possible (Fig. 2). For detailed imaging of entire drill cores, in order to archive or further analyse the sec-

tions, this is not adequate as the limited image resolution does not allow for sufficient magnification. Here, line scan images are clearly superior due to their high resolution and image fidelity (i.e. absence of perspective distortions). However, the comparison shows that scan images taken with our PML setup and a smartphone allow a similarly high degree of detail as well as image fidelity (Figs. 3, 4). The resolution of  $\sim 250$  px per core centimetre, corresponding to a pixel size of  $\sim 40 \mu\text{m}$ , is in the same range as the Geotek Core Imaging System considered for comparison (Geotek Limited, 2017).

Thus, the results achieved with the presented core photography setup are compelling. The image quality achieved with our setup comes close to proper line scan images but at a fraction of the cost ( $\sim \text{EUR } 100$  excluding phone) and, as a second major advantage, with the benefit of the flexibility of a portable setup. Therefore, it does not have to be set up stationarily in a core laboratory but can be easily transported and utilised for example at a drill site or a core repository. Furthermore, it is straightforward to use and requires only minimal training for the operator. Disadvantages of the PML include minor image artefacts that could not be entirely avoided (Fig. 5) as well as the inconvenience of transferring the acquired photos from the smartphone to the computer and of cropping and, if necessary, stitching individual photos together. In addition, the present setup depends on suitably well-lit surroundings and, especially if light conditions change over time, may require later manual image editing (e.g. contrast enhancement or colour correction; note: PML pictures are unedited in all figures). Like the Geotek line scan it is suitable only for top-down and not for unrolled core photos; however the out-of-the-box image-stitching capabilities of a smartphone might also be a suitable basis for an unrolled core imaging setup.

As presented here, the PML is a very simple tool, and further modifications can be made as desired. For instance, it might be more convenient to mount the guard rail on a tabletop rack instead of a core box. We suggest further that image quality can most likely be further enhanced by using a newer smartphone with a more sophisticated camera. Also, a multidirectional LED setup could be attached to the sliding block allowing for more consistent and, where appropriate, brighter lighting of the drill core. For wet or otherwise highly reflective core surfaces, an additional polarising filter might be helpful to reduce glare.

In summary, we argue that the PML tool may be an interesting alternative to an inflexible and costly conventional line scan setup, especially for working groups that only occasionally deal with drill cores. While it is introduced here in the context of drill core photography, it could of course also be applied in other fields of work that are concerned with objects of comparable length / width ratios.

**Code and data availability.** No code or data sets were used in this article.

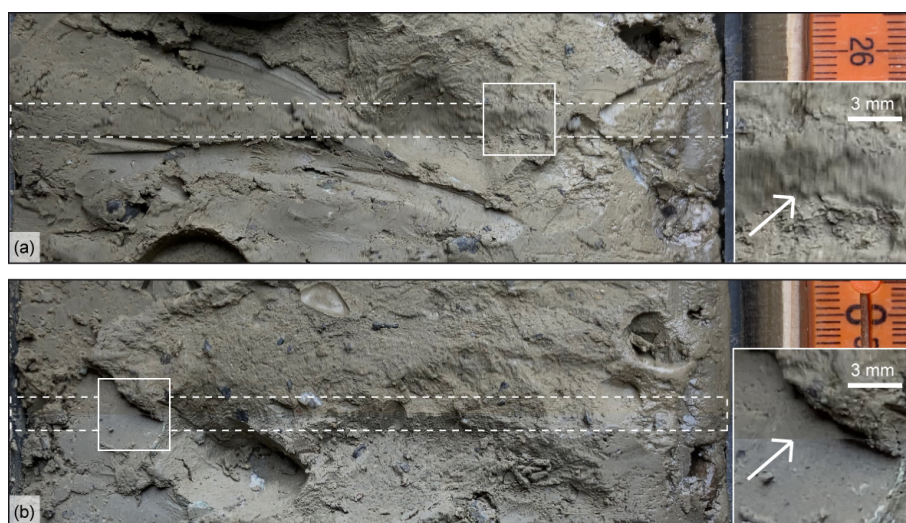


**Figure 5.** Potential artefacts of core photos taken with the PML setup include (a) blurred bands as a result of vibrations during the panoramic picture acquisition (highlighted by dashed lines and zoomed inset) and (b) minor misfits and/or colour changes where two separate images are manually stitched together. Note: the latter could be improved if lens aperture and white balance of the phone camera could be adjusted manually.

**Author contributions.** LG developed the concept and initial design of the PML, which was improved on by both authors before JG built the prototype. The paper and figures were drafted by LG and finalised by both authors.

**Competing interests.** The contact author has declared that none of the authors has any competing interests.

**Disclaimer.** Publisher's note: Copernicus Publications remains neutral with regard to jurisdictional claims in published maps and institutional affiliations.

**Acknowledgements.** We thank Bennet Schuster (University of Freiburg and University of Bern) for providing access to and line scan images of the drill cores from Tannwald (ICDP 5068\_1\_C). We further thank Thomas Wiersberg for editorial handling, and Kristina Brady Shannon (University of Minnesota) and Henning Lorenz (University of Uppsala) for their constructive and thorough review of our manuscript.

**Review statement.** This paper was edited by Thomas Wiersberg and reviewed by Henning Lorenz and Kristina Brady Shannon.

## References

Altartatz, D. and Frosh, P.: Sentient Photography: Image-Production and the Smartphone Camera, *Photograph.*, 14, 243–264, <https://doi.org/10.1080/17540763.2021.1877788>, 2021.

- Anselmetti, F. S., Bavec, M., Crouzet, C., Fiebig, M., Gabriel, G., Preusser, F., Ravazzi, C., and DOVE scientific team: Drilling Overdeepened Alpine Valleys (ICDP-DOVE): quantifying the age, extent, and environmental impact of Alpine glaciations, *Sci. Drill.*, 31, 51–70, <https://doi.org/10.5194/sd-31-51-2022>, 2022.
- Centore, P.: Conversions between the Munsell and sRGB colour systems, <https://www.munsellcolourscienceforpainters.com/ConversionsBetweenMunsellAndRGBsystems.pdf> (last access: 9 August 2023), 2013.
- Dolgiy, K., Belashev, B., and Gorkovets, V.: Automated drill core scanning, *Int. J. Innov. Res. Eng. Managem.*, 2, 85–90, 2015.
- Ettensohn, F. R.: Development and Potential of Core-Logging Manuals, *Geotech. Test. J.*, 17, 393–398, <https://doi.org/10.1520/GTJ10114J>, 1994.
- Fu, D., Su, C., Wang, W., and Yuan, R.: Deep learning based lithology classification of drill core images, *Plos One*, 17, e0270826, <https://doi.org/10.1371/journal.pone.0270826>, 2022.
- Geotek Limited: Geotek Core Imaging System (CIS): High resolution linescan photographs for immediate and archival core record applications, Geotek Limited, <http://www.geotek.co.uk/wp-content/uploads/2017/06/MSCL-CIS.pdf> (last access: 17 May 2023), 2017.
- Tran, T. T., Payenberg, T. H., Jian, F. X., Cole, S., and Barranco, I.: Deep convolutional neural networks for generating grain-size logs from core photographs, *AAPG Bull.*, 106, 2259–2274, <https://doi.org/10.1306/100212121019>, 2022.
- USBR: Guidelines for Core Logging, USBR Engineering Geology Field Manual, 2nd edn., vol. I, United States Department of the Interior Bureau of Reclamation, 432 pp., 294–312, 1998.





## Workshop report: PlioWest – drilling Pliocene lakes in western North America

Alison J. Smith<sup>1</sup>, Emi Ito<sup>2</sup>, Natalie Burls<sup>3</sup>, Leon Clarke<sup>4</sup>, Timme Donders<sup>5</sup>, Robert Hatfield<sup>6</sup>,  
Stephen Kuehn<sup>7</sup>, Andreas Koutsodendris<sup>8</sup>, Tim Lowenstein<sup>9</sup>, David McGee<sup>10</sup>, Peter Molnar<sup>11,†</sup>,  
Alexander Prokopenko<sup>12</sup>, Katie Snell<sup>13</sup>, Blas Valero Garcés<sup>14</sup>, Josef Werne<sup>15</sup>, Christian Zeeden<sup>16</sup>, and  
the PlioWest Working Consortium<sup>+</sup>

<sup>1</sup>Department of Earth Sciences, Kent State University, Kent, OH 44242, USA

<sup>2</sup>Department of Earth and Environmental Sciences, University of Minnesota, Minneapolis, MN 55455, USA

<sup>3</sup>Department of Atmospheric, Ocean & Earth Sciences, George Mason University, Fairfax, VA 22030, USA

<sup>4</sup>Department of Environmental Sciences, Manchester Metropolitan University, Manchester, M15 6BH, UK

<sup>5</sup>Department of Physical Geography, Utrecht University, Utrecht, 3584 CB, the Netherlands

<sup>6</sup>Department of Geological Sciences, University of Florida, Gainesville, FL 32611, USA

<sup>7</sup>Department of Physical and Environmental Sciences, Concord University, Athens, WV 24712, USA

<sup>8</sup>Institute of Earth Sciences, Heidelberg University, 69120 Heidelberg, Germany

<sup>9</sup>Department of Geological Sciences and Environmental Studies,  
Binghamton University, Binghamton, NY 13902, USA

<sup>10</sup>Department of Earth, Atmospheric and Planetary Sciences, Massachusetts Institute of Technology,  
Cambridge, MA 02139, USA

<sup>11</sup>Department of Geological Sciences, CIRES, University of Colorado Boulder, Boulder, CO 80309, USA

<sup>12</sup>Department of Geological Sciences, University of South Carolina, Columbia, SC 29208, USA

<sup>13</sup>Department of Geological Sciences, University of Colorado Boulder, Boulder, CO 80309, USA

<sup>14</sup>Pyrenean Institute of Ecology (IPE), CSIC, Zaragoza 50080, Spain

<sup>15</sup>Department of Geology & Environmental Science, University of Pittsburgh, Pittsburgh, PA 15260, USA

<sup>16</sup>Department of Rock Physics & Borehole Geophysics, Leibniz Institute for Applied Geophysics,  
30655 Hanover, Germany

<sup>†</sup>deceased

<sup>+</sup>A full list of authors appears at the end of the paper.

**Correspondence:** Alison J. Smith (alisonjs@kent.edu) and Emi Ito (eito@umn.edu)

Received: 14 May 2022 – Revised: 12 October 2022 – Accepted: 11 November 2022 – Published: 26 October 2023

**Abstract.** The Pliocene Epoch is a focus of scientific interest as a period of sustained global warmth, with reconstructed CO<sub>2</sub> concentrations and a continent configuration similar to modern. Numerous studies suggest that the Pliocene was warmer and largely wetter than today, at least in the subtropics, which contrasts with the long-term hydroclimatic response of drying conditions predicted by most climate model simulations. Two key features of Pliocene warmth established from sea surface temperature reconstructions could affect dynamic changes that influence the hydrologic cycle: (1) a weaker Pliocene zonal gradient in sea surface temperature (SST) between the western and eastern equatorial Pacific resembling El Niño-like conditions and (2) polar-amplified Pliocene warmth, supporting a weaker Equator-to-pole temperature gradient. The distribution of wet conditions in western North America and the timing of late Pliocene–Quaternary aridification offer the potential to evaluate the relative roles of these two external forcings of the climate in western North America, with broader global implications for Mediterranean-type climate (MTC) regions. We convened a virtual ICDP workshop that spanned a 2-week period in September 2021, to choose optimal drill sites and legacy cores to address the overall scientific goals, flesh out research questions, and discuss how best to answer them. A total of 56 participants

from 12 countries (17 time zones), representing a wide range of disciplines, came together virtually for a series of plenary and working group sessions. We have chosen to study five basins (Butte Valley, Tule Lake, Lake Idaho, Searles Lake, and Verde Valley) that span  $7^\circ$  of latitude to test our hypotheses and to reconstruct the evolution of western North American hydroclimate with special focus on the time ranges of 4.5–3.5 and 3–2.5 Myr. Although individual Pliocene lake records occur in many areas of the world, the western North American basins are unique and globally significant as deep perennial freshwater Pliocene lakes latitudinally arrayed in a MTC region and are able to capture a response to Pacific forcing. We propose new drill cores from three of these basins. During the workshop, we discussed the stratigraphy and subsurface structure of each basin and revised the chronological frameworks and the basin-to-basin correlations. We also identified the best-suited proxies for hydroclimate reconstructions for each particular basin and put forward a multi-technique strategy for depth–age modeling. Reconstructions based on data from these sites will complement the SST reconstructions from global sites spanning the last 4.5 Ma and elucidate the large-scale hydrological cycle controls associated with both global warming and cooling.

## 1 Introduction

The Pliocene Epoch has become the focus of scientific interest as a period of sustained global warmth. With reconstructed  $\text{CO}_2$  concentrations in the range of 350–450 ppm and a continent configuration similar to modern, the Pliocene is an appropriate analogue for testing the capabilities of numerical models used to predict climate and ecological change over the coming century. An array of geologic studies now suggests that the Pliocene was warmer and largely wetter, at least in the subtropics, than today, which contrasts with the long-term hydroclimatic response seen in most climate models in response to elevated  $\text{CO}_2$  (Molnar and Cane, 2007; Ibarra et al., 2018; Lepar and Firk, 2015; Lukens et al., 2019). But what caused wetter conditions in subtropical Mediterranean-type climate (MTC) regions (Rundel et al., 2016) in the Pliocene, when theory and model simulations indicate that these regions become drier with global warming? Where were those sources of precipitation in these MTC regions (Rundel et al., 2016; Fu et al., 2022), and how did the hydroclimatic regime change with the onset of Pleistocene glacial–interglacial cycles? Answering these and related questions requires a spatial gradient of high-resolution multiproxy terrestrial paleoclimate records that are central to ICDP’s Research Plan for 2020–2030 in the focus area of environmental change and water resources.

Understanding the Pliocene hydrological cycle is a target of the PlioWest project, as our ability to predict future hydroclimatic conditions may be limited by how well we replicate these conditions during Pliocene peak warmth. We convened a virtual ICDP workshop that spanned a 2-week period in September 2021, to choose optimal drill sites and legacy cores to address the overall scientific goals, flesh out research questions, and discuss how best to answer them. The overarching plan of this workshop, to bring together an international group of scientists to work collaboratively on how best to approach the question of causal mechanisms of wetter conditions in the Pliocene in MTC regions, was success-

fully achieved despite the less-than-optimal, virtual meeting format.

## 2 Workshop structure

The 2020–2021 global pandemic blocked our abilities to offer an in-person international workshop in September 2020. After a year’s postponement, we had hoped to offer a hybrid workshop, with online sessions and an in-person component to take place in Minneapolis, Minnesota, at the CSD Core Lab facility. That model was also necessarily abandoned as the pandemic persisted, and we embarked on an entirely virtual workshop for 56 registrants from 12 countries, following advertisement of the workshop with AGU and ICDP (Fig. 1). The workshop took place as a series of meetings using Zoom and was completed over the month of September 2021 in 90 min sessions, co-chaired by Alison J. Smith (Kent State University) and Emi Ito (University of Minnesota). The workshop consisted of three plenary sessions, with the first two plenaries each separated by 10 discussion group sessions of 60–90 min length. These discussion groups were separately scheduled events, with no more than six discussants in any session. Plenary sessions included a few invited presentations followed by verbal summaries. All notes, presentations, site data, and other relevant material were accessible to the registrants through a web-based communication site. In the final plenary session, consensus was reached on the overall strategy and drill sites to be studied, and a development timeline and action items were summarized about the next steps towards completion of a compelling full ICDP proposal. Focus groups were then identified to continue specific work via Zoom meetings towards the completion of a drilling proposal for submission to the ICDP. Because a seismic survey for one of the basins needs to be done, we are working toward the January 2024 drilling proposal deadline.

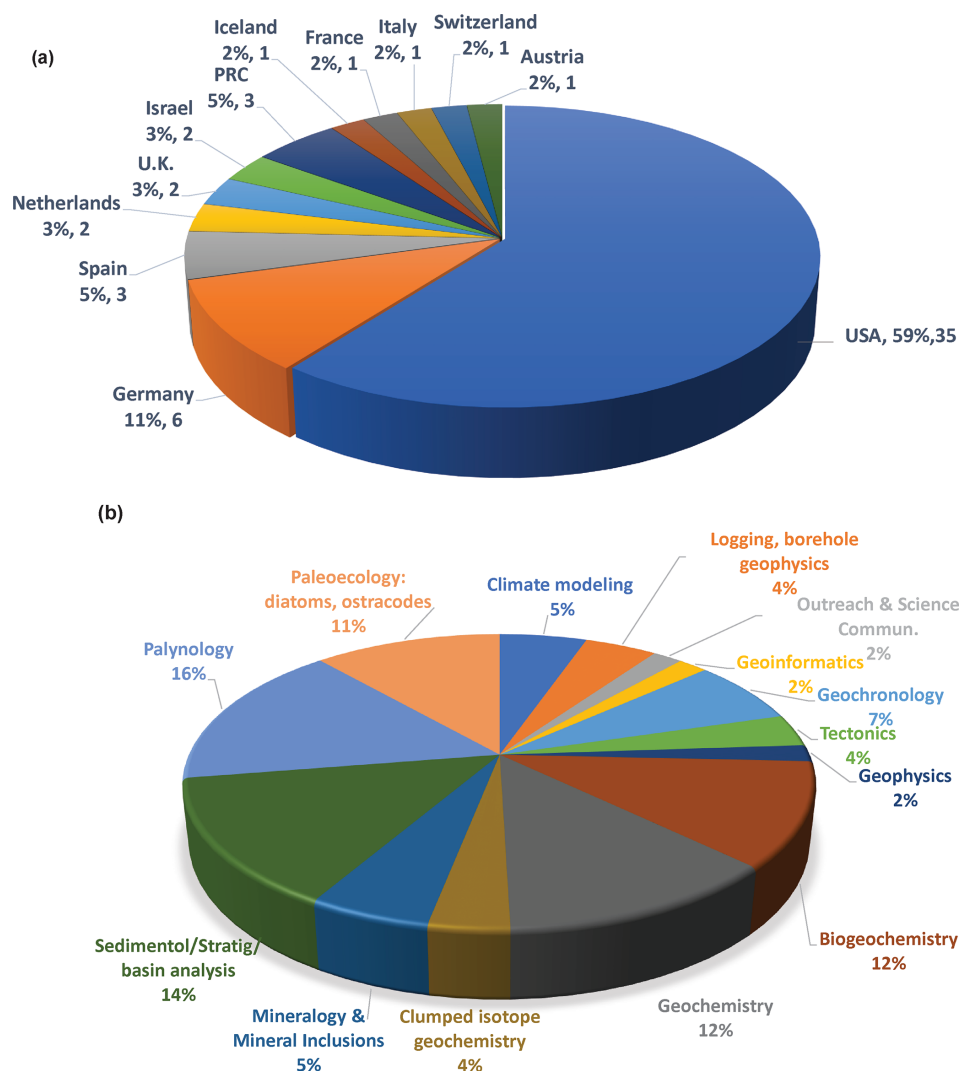


**Figure 1.** Statistics of the PlioWest workshop participants showing (a) locations of participants (shown as percentage and as actual number) and (b) the distribution of expertise by percentage. The total number of registered participants was 56 from 12 nations.

### 3 Hypotheses regarding a wet Pliocene

Why the Pliocene was warmer and, in some regions, wetter than conditions predicted for the end of this century is a challenging question with many societal implications. The primary mechanism leading to future projected drying in Southern California, and other MTC regions, is a thermodynamically driven increase in the moisture transport divergence from these regions (Seager et al., 2010; Seager and Vecchi, 2010). This mechanism follows a simple thermodynamic argument for how the hydrological cycle might respond to increases in global temperature given the Clausius–Clapeyron relation, whereby warm air can hold more moisture than cold air (Held and Soden, 2006) (Fig. 2a). While limitations exist in this first-order argument over land (Byrne and O’Gorman, 2015), climate model projections (Seager et al., 2010; Seager and Vecchi, 2010), and near-equilibrium simulations in

which CO<sub>2</sub> is abruptly increased (Fig. 2a, c, e), do indeed simulate the general drying of Mediterranean climate zones.

Substantial changes in atmospheric circulation (Burls and Federov, 2017; Fu et al., 2021; Menemenlis et al., 2022), which this simple thermodynamic expectation neglects, could however act to counter subtropical drying and lead to the *opposite* response – wetter subtropical conditions (Fig. 2b, d, f). A paired latitudinal and longitudinal transect of records as proposed here is the only research strategy able to test these atmospheric circulation hypotheses by capturing the north–south and east–west hydroclimatic gradients and the temporal and spatial extent of these changes in moisture delivery.

Pliocene surface temperature reconstructions show two key features that climate models struggle to reproduce. These have the potential to bring about atmospheric circulation



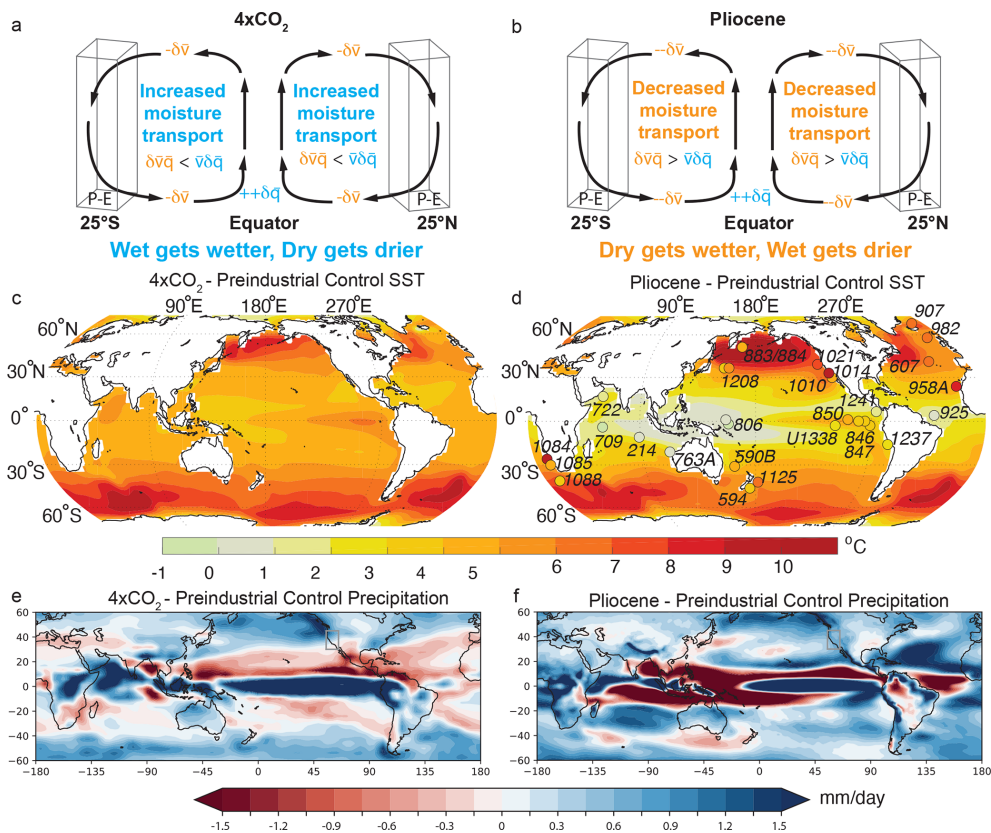


**Figure 2.** An illustration of the competition between thermodynamically forced subtropical drying due to a global mean temperature increase and the dynamically forced subtropical wetting due to weakening surface temperature gradients and hence atmospheric circulation, most notably the Hadley atmospheric overturning circulation, schematically shown in (a) and (b). While there is some weakening of gradients, under  $4 \times \text{CO}_2$  ( $4 \times 280 \text{ ppm}$ ) (c, e), the global mean temperature change dominates (relatively speaking), leading to either reduced or nearly unchanged annual mean precipitation in MTC regions. A strong reduction in gradients during the Pliocene leads to wetter conditions in most MTC regions (d, f) despite global warming. The superimposed circles in panel (d) indicate Early Pliocene sea surface temperature reconstructions, portrayed on a surface consistent with Early Pliocene proxy data. Adapted by Natalie Burls from Burls and Fedorov (2017, Figs. 1 and 4).

changes that could have supported wetter conditions in western and other MTC regions across the globe.

One such feature is a Pliocene zonal gradient in sea surface temperature (SST) between the western and eastern equatorial Pacific that is weaker than the present day, resembling El Niño-like conditions (e.g., Chaisson and Ravelo, 2000; Wara et al., 2005; Groeneveld et al., 2006; Lawrence et al., 2006; Ravelo et al., 2006; Dekens et al., 2007; Herbert et al., 2016). The atmospheric response to modern El Niño events leads to an equatorward shift and eastward extension of the subtropical jet, a strengthened Aleutian Low, and heavier winter rainfall over the southwestern but not the northwestern USA (e.g., Schonher and Nicholson, 1989; Trenberth et al., 1998; Seager et al., 2010), with a somewhat similar response projected for the future in models that include a more El Niño-like mean state (Allen and Luptowitz, 2017). It follows that lakes, at least in part of the southwestern USA, might have resulted from atmospheric circulation patterns associated with a permanently warm eastern tropical Pacific during

the Pliocene. Following the modern association, one might predict that a permanent El Niño-like Pliocene SST distribution supported an enhancement of today's winter rainfall patterns (Molnar and Cane, 2002, 2007; Winnick et al., 2013; Ibarra et al., 2018) but with more weighting towards central-southern California and less over the Pacific Northwest, following the dipole nature of the modern climate teleconnection.

A second feature is polar-amplified Pliocene warmth, supporting a weaker Equator-to-pole (meridional) temperature gradient (Dowsett et al., 2012), specifically between the tropics and the midlatitudes (e.g., Brierley et al., 2009; Fedorov et al., 2015), as this scales with Hadley strength. The reduced meridional temperature gradient during the Pliocene offers a mechanism for creating wetter subtropics globally (Burls and Fedorov, 2017); by supporting a weaker Hadley circulation, it allows for a reduction in the divergence of moisture from the arid subtropics that overcomes the thermodynamic enhancement that occurs with global warming, giving rise

to dry-gets-wetter conditions in the subtropics (Fig. 2b, d). For the western USA, climate simulations with a strongly reduced Equator-to-pole (and equatorial zonal) gradient support wetter conditions in Southern California through more summer rainfall, as well as to the north through increased winter rainfall (Fig. 2f, Burls and Fedorov, 2017). Thus this mechanism might predict wetter conditions for both the northern and southern sites in this proposed study.

Reconstructing the distribution and seasonality of wet conditions in western North America and the timing of late Pliocene–Pleistocene aridification offers the potential to evaluate the role of these two mechanisms. Evidence suggests that they were likely linked (Fedorov et al., 2015) and therefore working in tandem. *Our working hypothesis is that the hydroclimate of western North America was, in addition to global warmth, dictated by changes in the strength of Pacific zonal and meridional surface temperature gradients.* We plan to drill cores from three of these basins (see Sect. 4, “Proposed drilling sites”) in order to reconstruct the evolution of the western North American hydroclimate, with special focus on the time ranges from 4.5–3.5 and 3–2.5 Ma. Focus on these time ranges will bring attention to the Early Pliocene hydroclimatic conditions and also to the later onset of the glacial–interglacial cycle and intensification of Northern Hemisphere glaciation.

We have created a synthetic time series of precipitation estimates for the northern Butte Valley region (Fig. 3a) and southern Searles Lake and Verde Valley region (Fig. 3b) to explore how our working hypotheses can be tested. This initial analysis suggests that the precipitation history should have varied to differing extents in the subtropical vs mid-latitude portions of the study region and could be compared with the multiproxy records from the proposed array of lake coring sites.

Additional hypotheses to be tested include the following:

- Pliocene warmth led to systematic changes in precipitation seasonality and extremes.
- Establishment and later disappearance of large freshwater ecosystems profoundly affected the establishment of and subsequent dispersal, extirpation, or extinction of fauna and flora.
- Marine Isotope Stages (MIS) M2 and KM2 events were of sufficient magnitude and duration to be recorded in these MTC lake sediments.

#### 4 Proposed drilling sites

Although Pliocene lake basins occur in several subtropical and MTC regions worldwide (Mediterranean Basin, Southwestern Australia, Chile, California, China, and others), western North America contains the only set of deep, permanent lake basins that span several degrees of latitude and that existed during most of the Pliocene Epoch. Western

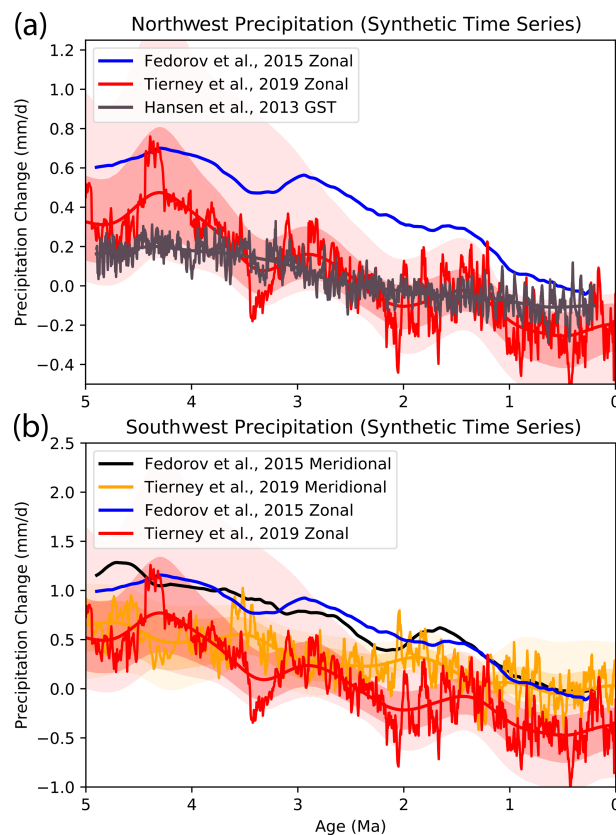


**Figure 3.** Synthetic time series of (a) northwest (41–45° N, 122–115° W) and (b) southwest (31–35° N, 118–114° W) annual mean precipitation change relative to preindustrial (or 0–0.5 Ma) (in mm per day) derived as a function of the zonal and meridional SST gradient reconstructions presented in Fedorov et al. (2015) and Tierney et al. (2019) (the light shading represents the full range and the darker shading the 95 % uncertainty range provided for the gradient estimates of Tierney et al., 2019), as well as the global mean surface temperature reconstruction of Hansen et al. (2013). Synthetic time series were generated using the relationships (statistically significant at the 95 % confidence interval) between regional precipitation and the zonal and meridional SST gradients, respectively, as well as global mean temperature, across the 30, fully coupled, global climate model experiments (Burls and Fedorov, 2017). These results suggest the southern drill sites should exhibit more Pliocene “wetting” relative to pre-industrial than the northern sites (proposed drill site and legacy cores included), as well as be more sensitive to both zonal and meridional SST gradient changes (more dynamically driven), as opposed to the northern site, which should display more sensitivity to global mean temperature (more thermodynamically driven). Figure created by Natalie Burls.

North America contains accessible and under-recognized paleolacustrine records that hold the keys to understanding the drivers of wetter conditions in Pliocene subtropical drylands worldwide.

Going into the workshop, we had an array of possible drilling sites, identified during a smaller previous EarthRates-funded workshop. These included Summer Lake,

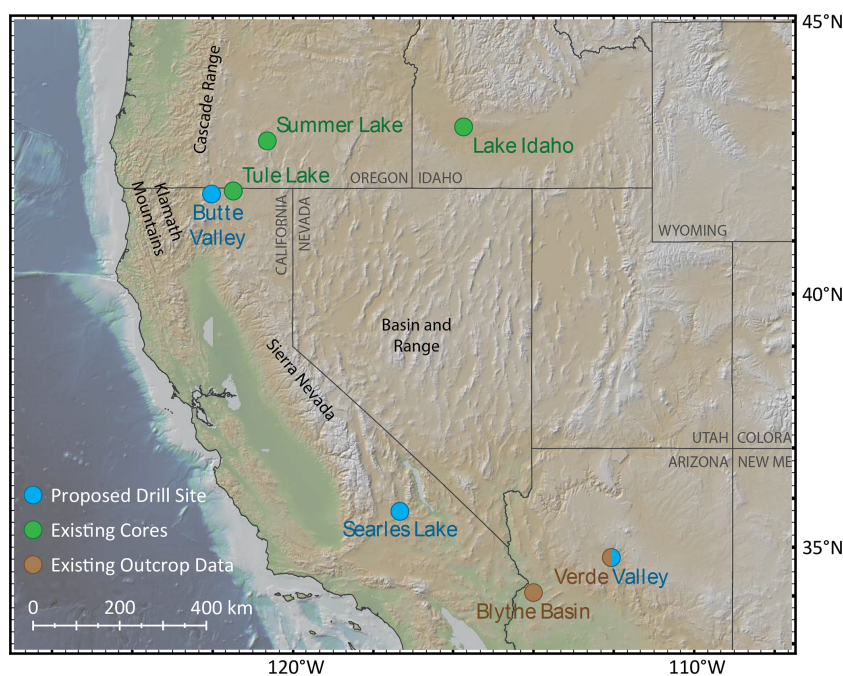


**Figure 4.** Location map of proposed drill sites and sites with existing sediment core and outcrop material available for study from previous drilling campaigns. Existing material from Blythe Basin and Verde Valley is from outcrop studies only. The Summer Lake records are short cores. Searles Lake and Butte Valley each have a Plio-Pleistocene core (see Fig. 5). All sites were discussed and evaluated during the workshop. The Cascade Range, Klamath Mountains, Sierra Nevada, and the Basin and Range are also shown. Figure created by Robert Hatfield, made with GeoMapApp (<http://www.geomapapp.org>, last access: 29 December 2021)/CC BY (Ryan et al., 2009).

Oregon; Lake Idaho, Idaho; Butte Valley, California; Tule Lake, California; Searles Lake, California; and Blythe Basin, Arizona (Fig. 4). Discussion focused on the previous work at these sites, the likelihood of recovering continuous sediments reaching to at least 4.5 Ma, the presence/absence of carbonates and organic biomarkers, site access, available subsurface data for robust site characterizations, and the likelihood of developing depth–age models and robust correlation models across the study region. We learned that Blythe Basin was likely to capture only the Lower Pliocene, which led to a discussion of possible replacement sites, leading us to discuss Verde Valley, Arizona, a site in central Arizona that had no drilling history but a record of outcrop studies. We reached consensus towards the end of the workshop to drill four sites which showed great promise: Lake Idaho, Butte Valley, Searles Lake, and Verde Valley. This plan was later altered to three drill sites, based on new dating information from Lake Idaho, which indicated the paleolacustrine record at Mountain Home drill site was no older than about 3.1 Ma (Alexander Prokopenko, personal communication, December 2021). The older sediments of Lake Idaho are likely to be found farther west and lie beneath thick layers of basalt making site survey uninformative and costly. The final list of drill sites for the project included Butte Valley and Searles Lake, California, and Verde Valley, Arizona (Figs. 4 and 5). We also intend to study the existing USGS legacy cores

from Butte Valley, Tule Lake, Lake Idaho (USGS–Bruneau Core), and Searles Lake and to collaborate with the ICDP HOTSPOT team that recovered the Plio-Pleistocene paleolacustrine record from Mountain Home, Idaho (Figs. 4 and 5). Combined, our sites comprise a north–south transect covering about 7° in latitude (1380 km), to capture the changing hydroclimatic gradients over time. Both northern and southern sites consist of lake records with ~ 600 km E–W distance between them, enabling us to examine the extent and duration of westerly moisture transport across this north–south transect.

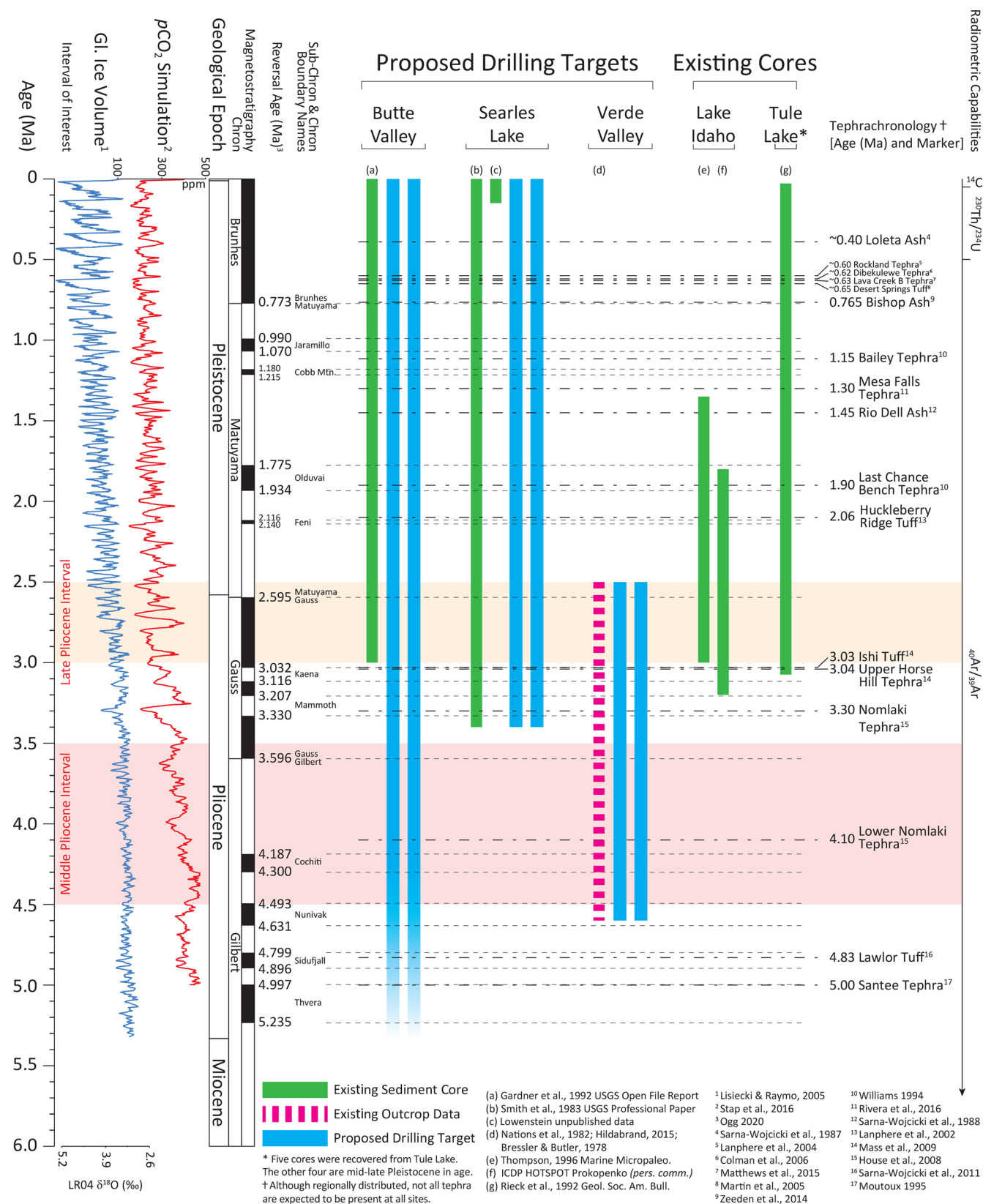
## 5 Analytical strategy

Our science team will use an integrated strategy in analyzing the complex story of paleoclimate and paleoecology in these Pliocene and Plio-Pleistocene lake sediment records of western North America. The strategies are described in brief here. The range of scientific expertise represented by our project team is shown in Fig. 1b.

### 5.1 Chronology

We will combine multiple dating techniques to maximize temporal precision and coverage, as well as robust correlations between paleolakes. The underlying framework for this chronology will be improved accuracy of depth and





stratigraphic information. Core depths will be tied to logging depth through common gamma ray data obtained during downhole logging and from core-scanning measurements. Where available, overlapping cores from multiple holes at the same site will be correlated to generate a composite depth scale and continuous stratigraphic section (e.g. Hatfield et al., 2020). Using this foundation, depth will be mapped to time using a suite of methods, primarily through paleomagnetic polarity stratigraphy and tephrostratigraphy supported by biostratigraphy (pollen and spores), radiometric dating (uranium–thorium, argon–argon, beryllium-10), and, where available, orbital and/or climatic tuning. The multiproxy integrated age–depth model will be generated using Bayesian approaches (e.g. Loughheed and Obrochta, 2019) that allow for realistic estimates of uncertainty.

## 5.2 Climate and environmental proxies

Paleobiological analyses, augmented by organic and inorganic geochemical proxies, are key components of the planned overarching post-coring scientific measurements. We aim to reconstruct both the (i) paleoclimatic evolution and (ii) biotic response to climatic and geological forcing. Biological proxies include pollen, diatoms and ostracodes, and geochemical/biochemical proxies include leaf-wax hydrogen isotopes, algal lipid  $\delta^2\text{H}$ , and  $\delta^{13}\text{C}$  and  $\delta^{18}\text{O}$  from inorganic and biogenic carbonates. Wildfire, an important part of terrestrial ecosystems in the study region, will be studied through analysis of such proxies as charcoal, PAHs (polycyclic aromatic hydrocarbons),  $\delta^{13}\text{C}$  in leaf waxes, and phytoliths. Analyses will be carried out at different temporal resolutions in order to identify both tectonic to orbital timescale trends and suborbital to sub-millennial timescale variability to produce datasets that are most relevant to present-day anthropogenic climate and ecosystem change.

## 6 Societal relevance

PlioWest has clear links to water security and landscape change, which are ongoing topics of increasing interest to all stakeholders in western North America, including Native American tribal communities, watershed managers, and agricultural planners. Development of educational outreach opportunities involving these topics will be an important aspect of the NSF and other funding agency proposals. Although the proposed drill sites are all situated on federal land (with the exception of Searles Lake, on privately owned land), these lands and the environments they represent are part of Native American cultural heritage. We will involve key stakeholders (local schools, colleges, public libraries, state and national parks, museums, businesses, and tribal representatives) at the early stages of project planning to learn what information we can gather that is important for them and their communities. This method, known as community-driven research (CDR; Pandya, 2014, and the mission of AGU's Thriving Earth Ex-

change), has been shown to increase community buy-in and trust in the results of the research. We will further develop these plans in consultation with the CSD Facility and with the Geoscience Alliance, an NSF-funded organization whose goal is to broaden participation of Native Americans in geosciences. This approach dovetails with a growing area of co-production of research (Zurba et al., 2022), and we look forward to opportunities to work collaboratively in this way with tribal communities.

Additionally, by working with the public access community database Neotoma (<https://www.neotomadb.org/>, last access: 28 November 2022), data and educational tools will become available to the public for use in educational settings at many levels, from secondary education through university level. Finally, we plan to create openly available educational videos throughout the project, following in the path of impactful examples such as the AN-DRILL project (<https://www.wgtn.ac.nz/antarctic/research/past-research-prog/andrill>, last access: 28 November 2022), which can serve secondary school and university students, as well as the public.

## 7 Conclusion

By recovering continuous core records from the targeted paleolake sites, we expect to gain insights into those step changes that occurred during the Early Pliocene warm period and subsequent Pleistocene cooling that accompanied the hydroclimatic changes in this MTC region. The mechanisms involved may have led to systematic changes in rainfall seasonality and extremes and may have changed the ecology of the entire region. Gaining new knowledge about these interlinked changes will certainly impact those working in the areas of climate change, water and food security, and ecological and environmental sciences. Climate extremes, beyond those of present-day climate, offer opportunities to test climate models used to predict future climate scenarios. The possible mismatch of predictions of a drier future climate for MTC regions, including the western USA, epitomizes how understanding the wet Pliocene can show how paleoclimate can be used to test and improve models and thus understanding of the global system that has direct societal relevance. The outcome of this study will benefit climate modelers, policy makers, and the many communities that make use of those models.

We also note that the virtual ICDP workshop format is doable and can achieve completion of a full ICDP proposal but is not the most desirable means of conducting a scientific workshop. The weak point in this format is the difficulty of generating an environment that produces spontaneous scientific discussions and a spirit of camaraderie, as well as the logistical challenges of drawing multiple individuals together when subject to their individual commitments. We were able to achieve our goals over a more expanded time frame (mul-

tiple meetings over a 2-week period) and with meticulous planning and constant adjustments to those plans by the two convenors of the workshop (Alison J. Smith and Emi Ito). Of course, the key benefit of a virtual workshop was much reduced cost as we had no travel and accommodation costs, but in the end, we found there is no substitute for in-person scientific workshops, and we look forward to the imminent return of such events.

**Data availability.** No datasets were used in this article.

**Team list.** PlioWest Working Consortium list: David Adam (retired, Clear Lake Environmental Research Center, Clear Lake, USA), Scott Anderson (School of Earth and Sustainability, Northern Arizona University, Flagstaff, USA), Tripti Bhattacharya (Department of Earth and Environmental Sciences, Syracuse University, Syracuse, USA), Christopher Brierley (Department of Geography, University College London, London, UK), Jordon Bright (School of Earth and Sustainability, Northern Arizona University, Flagstaff, USA), Erik Brown (Department of Earth and Environmental Sciences, University of Minnesota, Duluth, USA), Natalie Burls (Department of Atmospheric, Ocean and Earth Sciences, George Mason University, Fairfax, USA), Kat Cantner (Continental Scientific Drilling Facility, Department of Earth and Environmental Sciences, University of Minnesota, Minneapolis, USA), Leon Clarke (Department of Natural Sciences, Manchester Metropolitan University, Manchester, UK), Timme Donders (Department of Physical Geography, Utrecht University, Utrecht, the Netherlands), Peter Fawcett (Department of Earth and Planetary Sciences, University of New Mexico, Albuquerque, USA), Sarah Feakins (Department of Earth Sciences, University of Southern California, Los Angeles, USA), Troy Ferland (Lamont-Doherty Earth Observatory, Columbia University, Palisades, USA), Sherilyn Fritz (Department of Earth and Atmospheric Sciences and School of Biological Sciences, University of Nebraska, Lincoln, USA), Minmin Fu (Department of Earth and Planetary Sciences, Harvard University, Cambridge, USA), Thomas Giesecke (Department of Physical Geography, Utrecht University, Utrecht, the Netherlands), Pénélope González-Sampériz (Pyrenean Institute of Ecology (IPE), CSIC, Zaragoza, Spain), Emmanuel Guillermin (Charney School of Marine Sciences, University of Haifa, Haifa, Israel), Matthias Halisch (Petrophysics & Borehole Geophysics Department, Leibniz Institute of Applied Geophysics, Hannover, Germany), Robert Hatfield (Department of Geological Sciences, University of Florida, Gainesville, USA), Timothy Herbert (Department of Earth, Environmental, and Planetary Sciences, Brown University, Providence, USA), Daniel Ibarra (Department of Earth, Environmental, and Planetary Sciences, Brown University, Providence, USA), Emi Ito (Department of Earth and Environmental Sciences, University of Minnesota, Minneapolis, USA), Joseph Janick (independent researcher, Binghamton, New York, USA), Gonzalo Jiménez-Moreno (Department of Stratigraphy and Paleontology, University of Granada, Granada, Spain), Andreas Koutsodendris (Institute of Earth Sciences, Heidelberg University, Heidelberg, Germany), Stephen Kuehn (Department of Physical and Environmental Sciences, Concord University, Athens, USA), Anthony Layzell

(Kansas Geological Survey, University of Kansas, Lawrence, USA), Tim Lowenstein (Department of Geological Sciences and Environmental Studies, Binghamton University, Binghamton, USA), Maria Beatrice Magnani (Roy M. Huffington Department of Earth Sciences, Southern Methodist University, Dallas, USA), Miguel Marazuela Calvo (Department of Environmental Geosciences, University of Vienna, Vienna, Austria), David McGee (Department of Earth, Atmospheric, and Planetary Sciences, Massachusetts Institute of Technology, Cambridge, USA), Maud Meijers (Senckenberg Biodiversity and Climate Research Center, Frankfurt, Germany), Steffen Mischke (School of Engineering and Natural Sciences, University of Iceland, Reykjavik, Iceland), Peter Molnar (deceased, Department of Geological Sciences, University of Colorado Boulder, Boulder, USA), Andreas Mulch (Senckenberg–Leibniz Institution for Biodiversity and Earth System Research (SGN), Frankfurt, Germany), Sebastien Nomade (CEA Paris-Saclay and Paris-Saclay University, Gif sur Yvette, France), Anders Noren (Continental Scientific Drilling Facility, Department of Earth and Environmental Sciences, University of Minnesota, Minneapolis, USA), Richard Owen (Department of Geography, Hong Kong Baptist University, Kowloon, Hong Kong), Roberta Pini (Institute of Environmental Geology and Geoengineering, Italian National Research Council, Milano, Italy), Alexander Prokopenko (School of Earth, Ocean & Environment, University of South Carolina, Columbia, USA), Julian Sachs (School of Oceanography, University of Washington, Seattle, USA), James Sample (School of Earth and Sustainability, Northern Arizona University, Flagstaff, USA), Katie Snell (Department of Geological Sciences, University of Colorado Boulder, Boulder, USA), Scott Starratt (United States Geological Survey – Menlo Park, USA), Alison J. Smith (Department of Earth Sciences, Kent State University, Kent, USA), Vania Stefanova (Department of Earth and Environmental Sciences, University of Minnesota, Minneapolis, USA), Camille Thomas (Department of Earth Sciences, University of Geneva, Geneva, Switzerland), Aradhna Tripaati (Department of Atmospheric and Oceanic Sciences and Department of Earth, Planetary, and Space Sciences, University of California, Los Angeles, USA), Blas Valero Garcés (Pyrenean Institute of Ecology (IPE), CSIC, Zaragoza, Spain), Nicholas Waldmann (Dr. Moses Strauss Department of Marine Geosciences, University of Haifa, Haifa, Israel), Jiuyi Wang (Institute of Mineral Resources, Chinese Academy of Geological Sciences, Beijing, PRC), Josef Werne (Department of Geology and Environmental Science, University of Pittsburgh, Pittsburgh, USA), Sarah White (deceased, Department of Geography, University of California, Berkeley, USA), Jack Williams (Department of Geography, University of Wisconsin, Madison, USA), Thomas Wonik (Department of Rock Physics & Borehole Geophysics, Leibniz Institute of Applied Geophysics, Hannover, Germany), Christian Zee-den (Department of Rock Physics & Borehole Geophysics, Leibniz Institute of Applied Geophysics, Hannover, Germany), Yan Zhao (Institute of Geographic Sciences and Natural Resources Research, Chinese Academy of Sciences, Beijing, PRC).

**Author contributions.** All co-authors contributed to the text and figures that resulted in the submission of a full ICDP proposal and this workshop report. AJS and EI co-chaired the workshop and co-wrote the workshop report with involvement from all co-authors as follows: AJS provided Fig. 1. NB provided Figs. 2 and 3. RH



provided Figs. 4 and 5. LC, TD, PM, AK, and BVG revised and edited the final version of the paper. SK, CZ, DM, AP, BVG, and RH provided chronological and stratigraphic input. LC, KS, TL, BVG, and JW provided multi-proxy input. Workshop participants contributed intellectual input.

**Competing interests.** The contact author has declared that none of the authors has any competing interests.

**Disclaimer.** Publisher's note: Copernicus Publications remains neutral with regard to jurisdictional claims in published maps and institutional affiliations.

**Acknowledgements.** Presentations by Jordan Bright, Natalie Burls, Minmin Fu, Dan Ibarra, Stephen Kuehn, Tim Lowenstein, David McGee, Peter Molnar, Alexander Prokopenko, and Alison J. Smith set the stage for various discussions. Working group verbal summaries were given by Kat Cantner, Timme Donders, Tim Herbert, Tim Lowenstein, Peter Molnar, Anders Noren, Katie Snell, Scott Starratt, Blas Valero Garcés, and Christian Zeeden. We thank Carola Kogler of the ICDP, for logistical help with all three virtual plenary sessions. We report with sadness that two members of the PlioWest Consortium, Peter Molnar and Sarah White, passed away this summer after this paper had been submitted.

**Financial support.** This workshop was supported by the International Continental Drilling Program.

**Review statement.** This paper was edited by Thomas Wiersberg and reviewed by Julie Brigham-Grette and one anonymous referee.

## References

- Allen, R. J. and Luptowitz, R.: El Niño-like teleconnection increases California precipitation in response to warming, *Nat. Commun.*, 8, 1–15, 2017.
- Bressler, S. and Butler, R.: Magnetostratigraphy of the Late Tertiary Verde Formation, central Arizona, *Earth Planet. Sci. Lett.*, 38, 319–330, 1978.
- Brierley, C. M., Fedorov, A. V., Liu, Z., Herbert, T. D., Lawrence, K. T., and LaRiviere, J. P.: Greatly Expanded Tropical Warm Pool and Weakened Hadley Circulation in the Early Pliocene, *Science*, 323, 1714–1718, <https://doi.org/10.1126/science.1167625>, 2009.
- Burls, N. J. and Fedorov, A. V.: Wetter subtropics in a warmer world: contrasting past and future hydrological cycles, *P. Natl. Acad. Sci. USA*, 114, 12888–12893, 2017.
- Byrne, M. P. and O’Gorman, P. A.: The response of precipitation minus evapotranspiration to climate warming: Why the “wet-get-wetter, dry-get-drier” scaling does not hold over land, *J. Climate*, 28, 8078–8092, <https://doi.org/10.1175/JCLI-D-15-0369.1>, 2015.
- Chaisson, W. P. and Ravelo, A. C.: Pliocene development of the east-west hydrographic gradient in the tropical Pacific, *Paleoceanography*, 15, 497–505, 2000.
- Colman, S. M., Kaufman, D. S., Bright, J., Heil, C., King, J. W., Dean, W. E., Rosenbaum, J. G., Forester, R. M., Bischoff, J. L., Perkins, M., and McGeehin, J. P.: Age model for a continuous, ca. 250-ka Quaternary lacustrine record from Bear Lake, Utah–Idaho, *Quat. Sci. Rev.*, 25, 2271–2282, 2006.
- Dekens, P. S., Ravelo, A. C., and McCarthy, M. D.: Warm upwelling regions in the Pliocene warm period, *Paleoceanography*, 22, PA3211, <https://doi.org/10.1029/2006PA001394>, 2007.
- Dowsett, H. J., Robinson, M. M., Haywood, A. M., Hill, D. J., Dolan, A. M., Stoll, D. K., Chan, W. L., Abe-Ouchi, A., Chandler, M. A., Rosenbloom, N. A., and Otto-Bliesner, B. L.: Assessing confidence in Pliocene sea surface temperatures to evaluate predictive models, *Nat. Clim. Change*, 2, 365–371, <https://doi.org/10.1038/nclimate1455>, 2012.
- Fedorov, A. V., Burls, N. J., Lawrence, K. T., and Peterson, L. C.: Tightly linked zonal and meridional sea surface temperature gradients over the past five million years, *Nat. Geosci.*, 8, 975–980, 2015.
- Fu, M., Cane, M. A., Molnar, P., and Tziperman, E.: Wetter subtropics lead to reduced Pliocene coastal upwelling, *Paleoceanography and Paleoclimatology*, 36, e2021PA004243, <https://doi.org/10.1029/2021PA004243>, 2021.
- Fu, M., Cane, M. A., Molnar, P., and Tziperman, E.: Warmer Pliocene upwelling site SST leads to wetter subtropical coastal areas: A positive feedback on SST, *Paleoceanography and Paleoclimatology*, 37, PA4357, <https://doi.org/10.1029/2021PA004357>, 2022.
- Gardner, J. V., Bradbury, J. P., Dean, W. E., Adam, D. P., and Sarna-Wojcicki, A. M.: Report of Workshop 92 on the correlation of marine and terrestrial records of climate changes in the western United States, 7–10 April 1992, Watsonville, California, USA, US Geological Survey Open-File Report, 92–402, <https://pubs.usgs.gov/of/1992/0402/report.pdf> (last access: 7 December 2022), 1992.
- Groeneveld, J., Steph, S., Tiedemann, R., Garbe-Schonberg, D., Nürnberg, D., and Sturm, A.: Pliocene mixed-layer oceanography for Site 1241, using combined Mg / Ca and  $\delta^{18}\text{O}$  analyses of *Globigerinoides sacculifer*, in: Proc. ODP, Sci. Results, 202, edited by: Tiedemann, R., Mix, A. C., Richter, C., and Ruddiman, W. F., College Station, Texas (Ocean Drilling Program), 1–27, <https://doi.org/10.2973/odp.proc.sr.202.209.2006>, 2006.
- Hansen, J., Sato, M., Russell, G., and Kharecha, P.: Climate sensitivity, sea level and atmospheric carbon dioxide, *Philos. T. Roy. Soc. A*, 371, 20120294, <https://doi.org/10.1098/rsta.2012.0294>, 2013.
- Hatfield, R. G., Woods, A., Lehmann, S. B., Weidhaas IV, N., Chen, C. Y., Abbott, M. B., and Rodbell, D. T.: Stratigraphic correlation and splice generation for sediments recovered from a large lake drilling project: an example from Lake Junín, Peru, *J. Paleolimnol.*, 63, 83–100, <https://doi.org/10.1007/s10933-019-00098-w>, 2020.
- Held, I. M. and Soden, B. J.: Robust responses of the hydrological cycle to global warming, *J. Climate*, 19, 5686–5699, <https://doi.org/10.1175/JCLI3990.1>, 2006.
- Herbert, T. D., Lawrence, K. T., Tzanova, A., Peterson, L. C., Caballero-Gill, R., and Kelly, C. S.: Late Miocene global cool-

- ing and the rise of modern ecosystems, *Nat. Geosci.*, 9, 843–847, <https://doi.org/10.1038/ngeo2813>, 2016.
- Hildabrand, T. C.: Lithofacies characterization and chemostratigraphy of the Pliocene Verde Formation, northern Verde Valley, Central Arizona, MS Thesis, Northern Arizona University, ProQuest Dissertations & Theses A&I, ProQuest Dissertations & Theses Global, 1710514347, 157 pp., 2015.
- House, P. K., Pearthree, P. A., and Perkins, M. E.: Stratigraphic evidence for the role of lake spillover in the inception of the lower Colorado River in southern Nevada and western Arizona, in: *Late Cenozoic Drainage History of the Southwestern Great Basin and Lower Colorado River Region: Geologic and Biotic Perspectives*, edited by: Reheis, M. C., Hershler, R., and Miller, D. M., *Geol. S. Am. S.*, 439, 335–353, [https://doi.org/10.1130/2008.2439\(15\)](https://doi.org/10.1130/2008.2439(15)), 2008.
- Ibarra, D. E., Oster, J. L., Winnick, M. J., Rugenstein, J. K. C., Byrne, M. P., and Chamberlain, C. P.: Warm and cold wet states in the western United States during the Pliocene-Pleistocene, *Geology*, 46, 355–358, 2018.
- Lanphere, M. A., Champion, D., Christiansen, R. L., and Obradovich, J. D.: Revised ages for tuffs of the Yellowstone Plateau volcanic field: Assignment of the Huckleberry Ridge Tuff to a new geomagnetic polarity event, *Geol. Soc. Am. Bull.*, 114, 559–568, [https://doi.org/10.1130/0016-7606\(2002\)114<0559:RAFTOT>2.0.CO;2](https://doi.org/10.1130/0016-7606(2002)114<0559:RAFTOT>2.0.CO;2), 2002.
- Lanphere, M. A., Champion, D., Clynne, M. A., Lowenstern, J. B., Sarna-Wojcicki, A. M., and Wooden, J. L.: Age of the Rockland tephra, western USA, *Quat. Res.*, 62, 94–10, <https://doi.org/10.1016/j.yqres.2004.03.001>, 2004.
- Lawrence, K. T., Liu, Z.-H., and Herbert, T. D.: Evolution of the eastern tropical Pacific through Plio-Pleistocene glaciation, *Science*, 312, 79–83, 2006.
- Lepar, M. and Ferk, M.: Karst pocket valleys and their implications on Pliocene – Quaternary hydrology and climate: Examples from the Nullarbor Plain, southern Australia, *Earth Sci. Rev.*, 150, 1–13, 2015.
- Lisiecki, L. and Raymo, M.: A Pliocene-Pleistocene stack of 57 globally distributed benthic  $\delta^{18}\text{O}$  records, *Paleoceanography and Paleoclimatology*, 20, PA1003, <https://doi.org/10.1029/2004PA001071>, 2005.
- Lougheed, B. C. and Obrochta, S. P.: A rapid, deterministic age-depth modeling routine for geological sequences with inherent depth uncertainty. *Paleoceanography and Paleoclimatology*, 34, 122–133, <https://doi.org/10.1029/2018PA003457>, 2019.
- Lukens, W., Fox, D., Snell, K., Wiest, L., Layzell, A., Uno, K., Polissar, P., Martin, R., Fox-Dobbs, K., and Peláez-Campomanes, P.: Pliocene paleoenvironments in the Meade Basin, southwest Kansas, USA, *J. Sed. Res.*, 89, 416–439, 2019.
- Martin, J. E., Patrick, D., Kihm, A. J., Foit Jr., F. F., and Grandstaff, D. E.: Lithostratigraphy, tephrochronology, and Rare Earth Element geochemistry of fossils at the classical Pleistocene Fossil Lake area, South Central Oregon, *J. Geol.*, 113, 139–155, 2005.
- Mass, K. B., Cashman, P. H., and Trexler Jr., J. H.: Stratigraphy and structure of the Neogene Boca basin, northeastern California: Implications for late Cenozoic tectonic evolution of the northern Sierra Nevada, in: *Late Cenozoic Structure and Evolution of the Great Basin-Sierra Nevada Transition*, edited by: Oldow, J. S. and Cashman, P. H., *Geol. S. Am. S.*, 447, 147–170, [https://doi.org/10.1130/2009.2447\(09\)](https://doi.org/10.1130/2009.2447(09)), 2009.
- Matthews, N. E., Vazquez, J. A., and Calvert, A. T.: Age of the Lava Creek supereruption and magma chamber assembly at Yellowstone based on  $^{40}\text{Ar}/^{39}\text{Ar}$  and U-Pb dating of sanidine and zircon crystals, *Geochem. Geophys. Geosy.*, 16, 2508–2528, <https://doi.org/10.1002/2015GC005881>, 2015.
- Menemenlis, S., White, S. M., Ibarra, D. E., and Lora, J. M.: A proxy-model comparison for mid-Pliocene warm period hydroclimate in the Southwestern US, *Earth Planet. Sci. Lett.*, 596, 117803, <https://doi.org/10.1016/j.epsl.2022.117803>, 2022.
- Molnar, P. and Cane, M. A.: El Niño's tropical climate and teleconnections as a blueprint for pre-Ice Age climates, *Paleoceanography*, 17, 11–1–11–13, <https://doi.org/10.1029/2001PA000663>, 2002.
- Molnar, P. and Cane, M. A.: Early Pliocene (pre-Ice Age) El Niño-like global climate: Which El Niño?, *Geosphere*, 3, 337–365, 2007.
- Moutoux, T. E.: Palynological and tephra correlations among deep wells in the modern Great Salt Lake, Utah, USA: implications for a Neogene through Pleistocene climatic reconstruction, MS Thesis, University of Arizona, 87 pp., <https://repository.arizona.edu/handle/10150/191347> (last access: 6 December 2022), 1995.
- Nations, J. D., Landye, J. J., and Hevly, R. H.: Location and chronology of Tertiary sedimentary deposits in Arizona: a review, in: *Cenozoic Nonmarine Deposits of California and Arizona, Pacific Section*, edited by: Ingersoll, R. V. and Woodburne, M. O., *SEPM*, 107–122, [https://archives.datapages.com/data/pac\\_sepm/037/037001/pdfs/107.htm](https://archives.datapages.com/data/pac_sepm/037/037001/pdfs/107.htm) (last access: 7 December 2022), 1982.
- Ogg, J. G.: Geomagnetic polarity time scale, *Geologic Time Scale*, 1, 159–192, 2020.
- Pandya, R. E.: Community driven research in the Anthropocene, in: *Future Earth-Advancing Civic Understanding of the Anthropocene*, edited by: Dalbotten, D., Roehrig, G., and Hamilton, P., *Geophys. Monogr.*, 203, American Geophysical Union, Washington, D.C., 203, 53–66, ISBN 978-1-118-85430-3, 2014.
- Ravelo, A. C., Dekens, P. S., and McCarthy, M.: Evidence for El Niño-like conditions during the Pliocene, *GSA Today*, 16, 4–11, 2006.
- Rieck, H. J., Sarna-Wojcicki, A. M., Meyer, C. E., and Adam, D. P.: Magnetostratigraphy and tephrochronology of an upper Pliocene to Holocene record in lake sediments at Tulelake, northern California, *Geol. Soc. Am. Bull.*, 104, 409–428, 1992.
- Rivera, T. A., Mark, D., Schmitz, M. D., Jicha, B. R., and Crowley, J. L.: Zircon petrochronology and  $^{40}\text{Ar}/^{39}\text{Ar}$  sanidine dates for the Mesa Falls Tuff: crystal-scale records of magmatic evolution and the short lifespan of a large Yellowstone magma chamber, *J. Petrol.*, 57, 1677–1704, <https://doi.org/10.1093/petrology/egw053>, 2016.
- Rundel, P. W., Arroyo, M. T., Cowling, R. M., Keeley, J. E., Lamont, B. B., and Vargas, P.: Mediterranean biomes: evolution of their vegetation, floras, and climate, *Annu. Rev. Ecol. Evol. S.*, 47, 383–407, 2016.
- Ryan, W. B. F., Carbotte, S. M., Coplan, J., O'Hara, S., Melkonian, A., Arko, R., Weissel, R. A., Ferrini, V., Goodwillie, A., Nitsche, F., Bonczkowski, J., and Zemsky, R.: 2009, Global Multi-Resolution Topography (GMRT) synthesis data set, *Geochem. Geophys. Geosy.*, 10, Q03014, <https://doi.org/10.1029/2008GC002332>, 2009.

- Sarna-Wojcicki, A. M., Morrison, S. D., Meyer, C. E., and Hillhouse, J. W.: Correlation of upper Cenozoic tephra layers between sediments of the western United States and eastern Pacific Ocean and comparison with biostratigraphic and magnetostratigraphic age data, *Geol. Soc. Am. Bull.*, 98, 207–223, 1987.
- Sarna-Wojcicki, A. M., Meyer, C. E., Adam, D. P., and Sims, J. D.: Correlations and age estimates of ash beds in late Quaternary sediments of Clear Lake, California, in: *Late Quaternary Climate, Tectonism and Sedimentation in Clear Lake, Northern California Coast Ranges*, edited by: Sims, J. D., *Geol. Soc. Am. S.*, 214, 141–150, 1988.
- Sarna-Wojcicki, A. M., Deino, A. L., Fleck, R. J., McLaughlin, R. J., Wagner, D., Wan, E., Wahl, D., Hillhouse, J. W., and Perkins, M.: Age, composition, and areal distribution of the Pliocene Lawlor Tuff, and three younger Pliocene tuffs, California and Nevada, *Geosphere*, 7, 599–628, <https://doi.org/10.1130/GES00609.1>, 2011.
- Schonher, T. and Nicholson, S. E.: The Relationship between California Rainfall and ENSO Events, *J. Climate*, 2, 1258–1269, 1989.
- Seager, R. and Vecchi, G. A.: Greenhouse warming and the 21st century hydroclimate of southwestern North America, *P. Natl. Acad. Sci. USA*, 107, 21277–21282, <https://doi.org/10.1073/pnas.0910856107>, 2010.
- Seager, R., Naik, N., Ting, M., Cane, M. A., Harnik, N., and Kushnir, Y.: Adjustment of the atmospheric circulation to tropical Pacific SST anomalies: Variability of transient eddy propagation in the Pacific-North America sector, *Q. J. Roy. Meteor. Soc.*, 136, 277–296, 2010.
- Smith, G. I., Barczak, V. J., Moulton, G., and Liddicoat, J. C.: Core KM-3, a surface-to-bedrock record of late Cenozoic sedimentation in Searles Valley, California. US Geol Surv Prof P, 1256, U.S. Government Printing Office, Washington, D.C., 1–24, <https://doi.org/10.3133/pp1256>, 1983.
- Stap, L. B., de Boer, B., Ziegler, M., Bintanja, R., Lourens, L. J., and van de Wal, R. S. W.: CO<sub>2</sub> over the past 5 million years: Continuous simulation and new  $\delta^{11}\text{B}$ -based proxy data, *Earth Planet. Sci. Lett.*, 439, 1–10, 2016.
- Thompson, R. S.: Pliocene and early Pleistocene environments and climates of the western Snake River Plain, Idaho, *Mar. Micropaleontol.*, 27, 141–156, 1996.
- Tierney, J. E., Haywood, A. M., Feng, R., Bhattacharya, T., and Otto-Bliesner, B. L.: Pliocene warmth consistent with greenhouse gas forcing, *Geophys. Res. Lett.*, 46, 9136–9144, 2019.
- Trenberth, K. E., Branstator, G. W., Karoly, D., Kumar, A., Lau, N.-C., and Ropelewski, C.: Progress during TOGA in understanding and modeling global teleconnections associated with tropical sea surface temperatures, *J. Geophys. Res.-Atmos.*, 103, 14291–14324, 1998.
- Wara, M. W., Ravelo, A. C., and Delaney, M. L.: Permanent El Niño-like conditions during the Pliocene Warm Period, *Science*, 309, 758–761, <https://doi.org/10.1126/science.1112596>, 2005.
- Williams, S. K.: Late Cenozoic tephrostratigraphy of deep sediment cores from the Bonneville Basin, northwest Utah, *Geol. Soc. Am. Bull.*, 106, 1517–1530, 1994.
- Winnick, M. J., Welker, J. M., and Chamberlain, C. P.: Stable isotopic evidence of El Niño-like atmospheric circulation in the Pliocene western United States, *Clim. Past*, 9, 903–912, <https://doi.org/10.5194/cp-9-903-2013>, 2013.
- Zeeden, C., Rivera, T. A., and Storey, M.: An astronomical age for the Bishop Tuff and concordance with radioisotopic dates, *Geophys. Res. Lett.*, 41, 3478–3484, <https://doi.org/10.1002/2014GL059899>, 2014.
- Zurba, M., Petriello, M. A., Madge, C., McCarney, P., Bishop, B., McBeth, S., Denniston, M., Bodwitch, H., and Bailey, M.: Learning from knowledge co-production research and practice in the twenty-first century: global lessons and what they mean for collaborative research in Nunatsiavut, *Sustain. Sci.*, 17, 449–467, <https://doi.org/10.1007/s11625-021-00996-x>, 2022.





## Workshop on drilling the Nicaraguan lakes: bridging continents and oceans (NICA-BRIDGE)

Steffen Kutterolf<sup>1</sup>, Mark Brenner<sup>2</sup>, Robert A. Dull<sup>3</sup>, Armin Freundt<sup>1</sup>, Jens Kallmeyer<sup>4</sup>,  
Sebastian Krastel<sup>5</sup>, Sergei Katsev<sup>6</sup>, Elodie Lebas<sup>5,a</sup>, Axel Meyer<sup>7</sup>, Liseth Pérez<sup>8</sup>, Juanita Rausch<sup>9</sup>,  
Armando Saballos<sup>10</sup>, Antje Schwalb<sup>8</sup>, and Wilfried Strauch<sup>10</sup>

<sup>1</sup>Dynamics of the ocean floor, GEOMAR Helmholtz Centre for Ocean Research Kiel, Kiel, Germany

<sup>2</sup>Department of Geological Sciences and Land Use and Environmental Change Institute (LUECI),  
University of Florida, Gainesville, USA

<sup>3</sup>Department of Earth and Environmental Sciences, California Lutheran University, Thousand Oaks, USA

<sup>4</sup>Helmholtz Centre Potsdam, GFZ German Research Centre for Geosciences, Potsdam, Germany

<sup>5</sup>Institute of Geosciences, Christian-Albrechts-Universität zu Kiel, Kiel, Germany

<sup>6</sup>Large Lakes Observatory and Department of Physics and Astronomy,  
University of Minnesota Duluth, Duluth, USA

<sup>7</sup>Institute of Zoology and Evolutionary Biology, University of Konstanz, Konstanz, Germany

<sup>8</sup>Institute of Geosystems and Bioindication (IGeo), Technische Universität Braunschweig,  
Braunschweig, Germany

<sup>9</sup>Particle Vision, Passage du Cardinal 13B, Fribourg, Switzerland

<sup>10</sup>Instituto Nicaragüense de Estudios Territoriales (INETER),  
Dirección General de Geología y Geofísica, Managua, Nicaragua

<sup>a</sup>now at: Géosciences Marines, Institut de Physique du Globe de Paris, Paris, France

**Correspondence:** Steffen Kutterolf (skutterolf@geomar.de)

Received: 6 August 2022 – Revised: 18 January 2023 – Accepted: 19 January 2023 – Published: 26 October 2023

**Abstract.** An international, multidisciplinary research group is proposing the “NICA-BRIDGE” drilling project, within the framework of the International Continental Scientific Drilling Program (ICDP). The project goal is to conduct scientific drilling in Lake Nicaragua and Lake Managua (Nicaragua, Central America) to obtain long lacustrine sediment records to (a) extend the neotropical paleoclimate record back to the Pliocene, making it one of the longest continental tropical climate archives in the world, and to (b) provide geological data on the long-term complex interplay among tectonics, volcanism, sea-level dynamics, climate change, and biosphere.

The lakes are the two largest in Central America, and they are located in a trench-parallel half graben that hosts the volcanic front, which developed during or prior to the Pliocene, as a consequence of subduction-related tectonic activity. The lakes are uniquely suited for multidisciplinary scientific investigation as their long, continuous sediment records (several Myr) will facilitate the study of (1) terrestrial and marine basin development at the southern Central American margin, (2) alternating lacustrine and marine environments in response to tectonic and climatic changes, (3) the longest record of tropical climate proxies, (4) the evolution of (and transition between) the Miocene to Pliocene/Pleistocene and Pleistocene to present volcanic arcs, which were separated by slab rollback, (5) the significance of the lakes as hot spots for endemism, and (6) the Great American Biotic Interchange at this strategic location, i.e., the N–S and reverse migration of fauna after the land bridge between the Americas was established.

The planned ICDP project offers an opportunity to explore these topics through continent-based seismological, volcanological, paleoclimatological, paleoecological, and paleoenvironmental studies, combined with an International Ocean Discovery Program (IODP) drill project to explore its oceanic continuation.

In preparation of this drilling project, an ICDP workshop was held in Montelimar, Nicaragua, on 2–5 March 2020 to develop drilling strategies and refine scientific questions, objectives, and hypotheses. The workshop was organized and hosted by the principal investigators and the Instituto Nicaragüense de Estudios Territoriales (INETER), with funding from the ICDP. Forty-five researchers from 12 countries participated in the workshop, including representatives from ICDP. During the workshop, previous research data on the study lakes, including new recent surveys, were reviewed, and a three-phase strategy for the proposed research was developed. The aim of Phase 0 is to complement the pre-site surveys where we identified the need for further data. In Phase I, with ICDP support, we will obtain sediment cores  $\sim 100$  m long, which will allow us to investigate many of the scientific questions. Based on the data from those drill cores, coring locations will be identified for a future Phase II, which we envisage as a combined ICDP/IODP project to collect deep drill cores in the lakes and the offshore Sandino Basin in order to extend Phase I results to much deeper time. The Sandino Basin is the oceanic continuation of the depression in which the studied lakes are located, and complementary marine drilling will improve the understanding of the evolution of this complex margin.

## 1 Introduction and study area

The two largest lakes in Central America, Lake Nicaragua (Cocibolca) and Lake Managua (Xolotlán), are situated in south-central Nicaragua and represent the largest sources of freshwater in the region (Fig. 1). They are located in the central part of the Mesoamerican Biological Corridor and host numerous endemic species such as cichlid fishes (Kautt et al., 2012). Given their proximity to the Isthmus of Panama, their sediments probably record its closure, which is one of the most important events in the diversification and extinction of late Cenozoic and modern species in North America, South America, and the Caribbean region (Montes et al., 2015). The origin of the lakes, as well as the tectonic depression hosting them, dates to at least the Pliocene, but the origin of the tectonically related marine Sandino Basin can probably be traced back even further to the Late Miocene (Funk et al., 2009). The lakes cover a combined surface area of  $\sim 9000$  km<sup>2</sup> in the tectonically active Nicaraguan Depression, which hosts the Central American volcanic front (Funk et al., 2009). The prominent 40 to 70 km wide depression extends for  $\sim 1000$  km, from the Caribbean side of Costa Rica in the southeast to the northern Gulf of Fonseca in El Salvador (Case and Holcombe, 1980; Funk et al., 2009; Mann et al., 1990). Funk et al. (2009) and Ranero et al. (2000) claimed that the two lakes possess at least 500 m of Quaternary sediment and an additional 2000 m of Pliocene sediment fill. Early reports on the geology and structure, based on K/Ar-dated volcanogenic sediments at lakeshore outcrops (McBirney and Williams, 1965; Weinberg, 1992), suggested three major tectonic phases during the basin evolution: (1) Miocene convergence, (2) Pliocene extension, and (3) Pleistocene-to-present transtensional deformation. During that long time period, the position of the volcanic front shifted in response to slab rollback, from a Miocene arc along the eastern border of the Nicaragua Depression to the Pleistocene-to-recent front that cuts through the lakes, making the depression an intra-arc basin (Taylor, 1995).

## 2 Scientific rationale

The following scientific motivations to initiate this project were subjected to challenging discussions during the workshop.

### 2.1 Tectonics and volcanism

Geographic separation of areas of different ages in the Central American volcanic arc (Fig. 1, Coyol and recent arc), together with the expected approximately continuous sedimentation in the long-lived, coexisting tectonic basins, is a situation unique to Nicaragua. Therefore, in addition to providing a very long paleoenvironmental record, sediment cores from the basin will yield important data on the tectonic and volcanic evolution of the arcs, particularly during the period of shift (how long, existence of volcanic hiatus), from the eastern Tertiary Coyol arc to the western Upper Pleistocene arc (Funk et al., 2009), and provide information that can be used to evaluate the three existing regional tectonic models for the origin of the Nicaragua depression and therefore the depositional area of the lakes: (1) transform fault model, (2) pull-apart model, and (3) bookshelf faulting model (Funk et al., 2009). Abundant volcanic deposits in sediment successions on land and in the Pacific Ocean prove the existence of radiometrically datable time markers from recent to Miocene (Kutterolf et al., 2007, 2008; Jordan et al., 2007; Schindlbeck et al., 2016; Ehrenborg 1996). Dating methods for tephra include <sup>14</sup>C (< 50 ka), <sup>238</sup>U–<sup>230</sup>Th and (U–Th) / He dating of zircon crystals (evolved tephra), and <sup>40</sup>Ar / <sup>39</sup>Ar single-crystal dating (K-rich minerals), which cover the expected age range. Fauna-bearing sediments provide additional age constraints through stable-isotope and micropaleontological analyses.

The geographic position of the Nicaraguan lakes makes them ideal for a “paleo-study” as they are upwind from the modern,  $\sim 1$  Ma, volcanic arc system and far downwind (50–100 km) from the ancient,  $> 1.5$  Ma, Tertiary volcanic arc

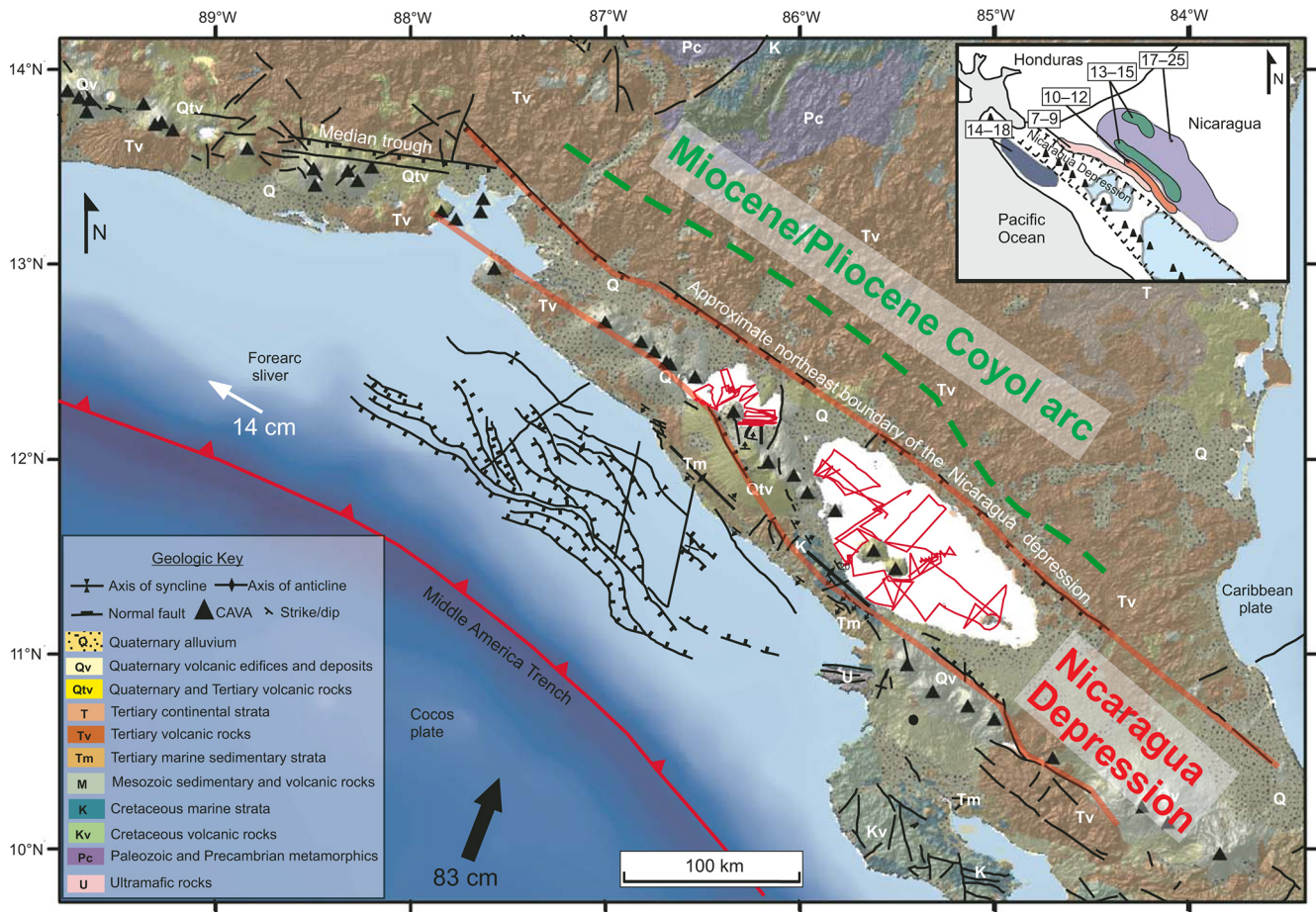


**Figure 1.** Overview map of the Central American subduction zone at Nicaragua, modified after Funk et al. (2009). Red lines outline the Nicaraguan Depression that hosts Lake Nicaragua (LN) and Lake Managua (LM) in which red lines show seismic profiles from pre-site survey. Triangles mark the Pleistocene-to-recent volcanic arc (CAVA), whereas purple and green areas outline the older Coyoil arc. White labeling inside the geological maps assists identification of units shown in the legend to the lower left. Fault lines on the submarine forearc outline the Sandino Basin. Inset shows presumed ages of volcanic rocks since the Miocene.

system (Schindlbeck et al., 2016), thus potentially providing a continuous record of tephra from both arcs but without the risk of thick, impenetrable volcanic deposits. The long tephra records will help decipher the frequency of explosive eruption at the Coyoil arc compared to the modern volcanic front, the duration of the arc shift, the occurrence or not of a volcanic hiatus during the shift, and associated changes in magmatic compositions (which, in turn, reflect crustal storage and mantle melting conditions). Accumulation rates of sediment bracketed by dated primary volcanic deposits, combined with sedimentological and geochemical analyses, can yield time series of tectonic activity/subsidence and climate changes, together with rates of volcanic activity, enabling us to investigate possible cross-correlations.

## 2.2 Paleoclimate

The availability of abundant radiometrically datable volcanic deposits in the sediment cores is an important advantage for

obtaining a long, continuous paleoclimate record that will extend much farther back in time than those retrieved from Lake Petén Itzá, Guatemala (~410 ka; Mueller et al., 2010; Correa-Metrio et al., 2012; Kutterolf et al., 2016), and Lake Chalco, central Mexico (~400 ka; Brown et al., 2019). Sediment cores from the Nicaraguan lakes and the analysis of different proxies (stable isotopes, biomarkers, pollen, sediment geochemistry) have the potential to extend the neotropical paleoclimate record back to at least the Pliocene, which would place them among the oldest archives of continental tropical paleoclimate in the world. They will be unparalleled for study of the long history of Intertropical Convergence Zone (ITCZ) oscillations and related changes in precipitation. The large Nicaraguan lakes, at ~12° N latitude, are ideally located in the heart of the northeast trade wind belt to record past variations in climate, driven by changes in the El Niño–Southern Oscillation (ENSO), i.e., fluctuations in near-equatorial sea surface temperature and air pressure



that affect precipitation on land, with consequences such as floods, droughts, and wildfires (e.g., Cai et al., 2020). The ENSO record of the cores may also serve as a record of environmental impacts, which may have been modified by different land–sea relationships in the past.

### 2.3 Paleoeecology and biosphere

The two study lakes offer an opportunity to relate their paleobiological inventory to salinity changes through time and to distinguish between ITCZ-controlled shifts in evaporation/precipitation ratio and salinity changes caused by tectonically controlled marine transgressions/regressions over the last several million years. The combination of micropaleontological, stable isotope, and sedimentological data from a suite of cores will help distinguish between tectonic and climate controls on biotic shifts. The biological proxies we have identified as most important include diatoms, ostracodes, foraminifers, and microbes. Diatoms, ostracodes, and foraminifers are sensitive to changes in water level, salinity, and ionic dominance, whereas a change in the abundance and structure of the microbial communities might serve as evidence of abrupt environmental and climate change (Moguel et al., 2021). We expect that the dramatic environmental changes in the lake region also affected proxy preservation, and we will therefore use a multi-proxy approach (diverse microfossils, biomarkers, and DNA) to provide a full record of paleoenvironmental conditions. We will investigate the hypothesis that there were repeated saltwater–freshwater interactions that arose from marine transgressions and regressions over the poorly known period when the ocean gateway closed. Repeated past connections with the marine environment presumably had substantial influence on lacustrine ecosystem biodiversity. This can be investigated, for example, by using taxa and selected genomic signatures preserved in the sediments (e.g., fishes; Kautt et al., 2012) to infer which taxa were present and how they responded and adapted to environmental changes through time. This will allow us to determine and compare evolution, diversification, and turnover rates in freshwater, brackish, and marine ecosystems. For example, diversification and turnover of diatoms appear to be more rapid in freshwaters (Nakov et al., 2019). Moreover, the combination of pollen and aquatic bioproxies will generate high-resolution information on regional and local biota since the Pliocene. Repeated marine–freshwater successions also provide a potential opportunity to study non-steady-state geochemistry in a sedimentary system and its effects on microbial community composition and metabolic activity.

Our climate and environmental record (Sect. 2.2 and 2.3) will be compared with other neotropical sediment records with similar temporality. For instance, in Phase I (Sect. 3) we will retrieve and study parallel pre-Holocene sediment cores (~100 m long), and multi-proxy results will be compared with those from other late Quaternary records such as Lake

Petén Itzá, Guatemala (Mueller et al., 2010); Lake Chalco, central Mexico (Brown et al., 2019); and the Cariaco Basin (Schneider et al., 2014). Deeper and older sediment records from Lake Nicaragua will be compared with evidence from ICDP (International Continental Scientific Drilling Program) sites extending much further back in time, including Izabal (Guatemala, ~10 Ma; Obrist-Farner et al., 2020) and Colônia (Brazil, ~5 Ma; Ledru et al., 2015). The previous data will allow us to (1) infer changes in the composition and structure of vegetation and aquatic communities since the Pliocene and (2) study the interplay between ENSO and the migration of the ITCZ. In addition, we will contribute to the knowledge of regional biogeography, and multi-proxy data will reveal the interactions between native terrestrial and aquatic species and colonizers, especially since the Great American Biotic Interchange and closure of the Isthmus of Panama.

### 2.4 Hazards

Detailed investigation of the Nicaraguan lake histories, far beyond the timescale previously studied in Central America (i.e., late Pleistocene), is germane to socio-economic issues of local, regional, and global significance, especially with respect to persistent threats from natural hazards in Nicaragua such as, for example, Managua's large earthquakes in 1931, 1972, and 2014 and the eruptions of the Cerro Negro (1992, 1995, 1999) and Momotombo (2015/2016) volcanoes. In addition to these hazards, there is also evidence for seismogenic and volcanogenic tsunamis in the lakes (Freundt et al., 2006, 2007) and in the near-shore Pacific region (Heesemann et al., 2009), disastrous lahars (Casita Volcano killed > 2000 persons in 1998), and massive landslides from the large, unstable volcanic edifices like Momotombo, Concepción, and Mombacho, with the last one responsible for ~400 deaths in 1570 (Vallance et al., 2001). Many of these hazardous events will have manifested themselves as identifiable layers in the lake sediments; next to the obvious tephra, possible examples include turbidites, seismites, and storm layers. Long time series for these hazards, derived from the drill cores, will shed light on the underlying processes that cause them, their magnitudes, and the frequencies at which they re-occur. Seismic monitoring by INETER and new seismological research projects (TUCAN project; Harmon et al., 2008) have documented the presence of active tectonic faults below the lakes, and hydrothermal springs atop the faults are observed on land. Downhole logging of drill holes for temperature, in combination with measurements of thermal conductivity from core samples, will provide further constraints on tectonic activity and heat flux in and around the lakes.

### 2.5 Environment

In 2009, the Sandino wastewater-treatment facility was installed on the shore of Lake Managua, with the aim of im-

proving lake water quality. This effort came after > 80 years of uncontrolled cultural eutrophication and contaminant pollution. Sediment and porewater, as well as microbial community analyses from cores taken in both lakes, will enable us to determine the penetration depth of pollutants into the lake deposits and their potential for being released back into the water column. Such information will be critical for evaluating how the quality of lake water and deeper groundwater would be affected by continuous pollution and by large-scale infrastructure projects in tropical lakes worldwide but in Nicaraguan lakes specifically. It will shed light on the potential impacts of the proposed construction of a canal through Lake Nicaragua that would connect the Caribbean Sea and the Pacific Ocean.

Sediment cores collected in 2006 from Lake Petén Itzá, Guatemala, revealed dramatic temperature and rainfall changes during the last 85 kyr, which had profound impacts on local terrestrial and aquatic environments, e.g., vegetation changes and lake water ion concentrations, respectively (Hodell et al., 2012; Escobar et al., 2012; Cohuo et al., 2018; Pérez et al., 2021). Much longer drill cores (and hence older deposits) from the Nicaraguan lakes will provide insights into the development of modern lake biodiversity, the impacts of climate change and abrupt natural events (e.g., volcanic eruptions, tsunamis) on aquatic biota and their possible recovery, and the environmental consequences of human activities, both past (unconstrained discharge of sewage and pollutants) and future (the planned canal through Lake Managua). Results related to these recent and ongoing environmental problems will be disseminated to the public and agency officials through suitable outreach activities (e.g., school lessons, professional training, local workshops).

In summary, long, continuous sediment cores from multiple sites in Lake Managua and Lake Nicaragua will provide some of the oldest lacustrine records of paleoclimate and paleoenvironment in the continental neotropics. The use of an array of drill sites (in Phase I, Sect. 3) is important for a continuous record, because possible gaps at one site can be filled by correlations with the other sites. The cores will thus enable us to (a) infer high-resolution neotropical paleoclimate and paleoenvironmental conditions; (b) determine the times and rates of marine transgressions and regressions, their aquatic and terrestrial ecological consequences, and their tectonic and climatic controls, also in connection with the timing, duration, and impacts of the closure of the Isthmus of Panama; (c) identify linkages between long terrestrial and marine paleoenvironmental records; (d) investigate the magnitudes and recurrence rates of natural hazards, e.g., volcanic eruptions, landslides, tsunamis, earthquakes, hurricanes; (e) constrain the timing of shifts of the volcanic arc and associated changes in magmatic compositions and volcanic activity; (f) understand the long-term basin development and the deeper structure of western Nicaragua; and (g) assess climatic, geologic, and (Holocene) anthropogenic influences on limnological variables and lake biodiversity,

e.g., past freshwater/saltwater phases initiated by tectonics and consequent effects on micro-biota and macro-biota.

### 3 The workshop

The workshop on the NICA-BRIDGE project was held in Montelimar, Nicaragua, from 2 to 5 March 2020, and it included a field trip to Lake Nicaragua and nearby volcanoes. The workshop agenda included plenary and working-group discussions that covered themes such as scientific objectives, specific drilling targets and respective challenges, and a proposal strategy to achieve the project goals. Specific topics discussed included issues related to drilling rigs to be deployed, analyses to be completed on cores, priority sections of the sediment sequences, and parallel in situ limnological monitoring, as well as logistical considerations, such as developing broad international scientific collaborations, acquiring complementary research funding, defining outreach activities, and obtaining permits. The consensus was that we will develop a multi-phase project that will involve long-term scientific engagement in the region, which will include scientific contributions for the improvement of seismic, volcanic, and tsunami monitoring and early warning by INETER.

Seismic profiles obtained in 2017 were presented at the opening of the workshop and were the basis for the discussions that followed. Twenty-seven seismic profiles were collected in Lake Nicaragua along a NW–SE transect, with several crosslines shot roughly NW–SE and ENE–WSW to the mainline (Fig. 2). The seismic lines covered a total length of  $\sim 320$  km. Unfortunately, high gas content in surface sediments often attenuated the signal, preventing the sound source from penetrating deep into the sediments. We were, however, able to collect good images from one region in the central part of the lake, which revealed a > 300 m thick sedimentary succession and provides evidence that long, continuous sediment cores can be obtained from Lake Nicaragua. The age at the base of the succession is unknown, but based on the near-surface sedimentation rate ( $0.3 \text{ m kyr}^{-1}$ ) an age of  $\sim 1$  Ma at 300 m sediment depth can be hypothesized. However, only long cores will provide data for a well-grounded age estimate.

Short sediment cores obtained by Robert A. Dull (California Lutheran University, USA) from Lake Nicaragua provide evidence for predominantly muddy lacustrine sedimentation (gyttja), intercalated with centimeter thick volcanogenic sediments in the topmost  $\sim 4$  m (Fig. 2). Sediment accumulation rates have fluctuated but display a mean of  $\sim 30 \text{ cm kyr}^{-1}$ . Preliminary geochemical and biological investigations of these cores conducted by Robert A. Dull, Sabine Wulf, Jennifer Slate, and Amy Bloom revealed variations within the last 12 kyr (Dull et al., 2023). Robert A. Dull has granted us access to the 35 short cores, which will be investigated to supplement the pre-site survey data.

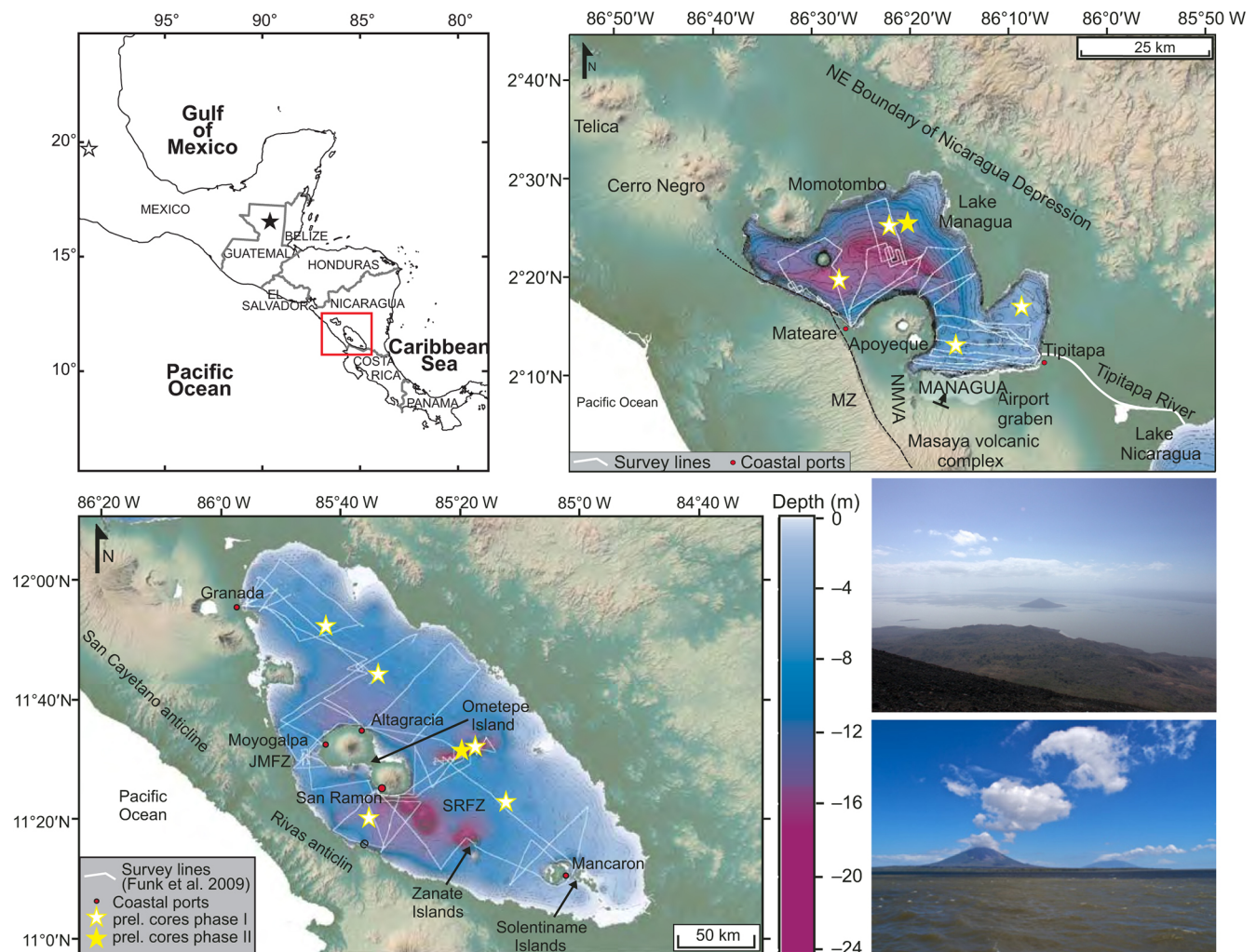


**Figure 2.** Upper left: map of southern Mexico and Central America, showing the location of the Nicaraguan study lakes. Red box indicates the area detailed in the map to the right and bottom left, and the stars are other ICDP drill sites in the region (black star represents Petén Itzá, Guatemala; white star represents Chalco, Mexico). Shuttle Radar Topography Mission imagery of Lake Managua (upper right) and Lake Nicaragua (lower left), and the Central America volcanic front in Nicaragua, modified from Funk et al. (2009). White lines show survey lines conducted by Funk et al. (2009). Bathymetric data are from the Nicaraguan hydrographic department of the Instituto Nicaragüense de Estudios Territoriales (unpublished data of INETER collected in 1979) and were supplemented by bathymetric data collected by Funk et al. (2009). Yellow stars indicate tentative locations of sites to be drilled to address scientific questions in Phases I and II of the project. Lower right: upper photo, showing Lake Managua with Momotombo Volcano, and lower photo, showing Lake Nicaragua, with Ometepe island with the Concepción and Maderas volcanoes. Photos by Steffen Kutterolf.

After presentation of seismic survey data on the first morning of the workshop (2 March), each participant introduced themselves and presented their respective expertise. This was followed by contributed talks from a number of attendees – presentations that covered multiple topics related to the NICA-BRIDGE project scientific goals, with the objective of honing old and new hypotheses, exploring drilling options, and evaluating the objectives of our study in relation to similar projects carried out previously in Central America, in adjacent areas and elsewhere. On 3 March we took a field trip to familiarize workshop participants with the landscape and the lakes. The trip involved a boat tour and a visit to the nearby

Apoyo Caldera, which is the source of the largest eruption in Nicaragua in the Late Quaternary (Fig. 3). On 4 March we divided into subgroups to focus on six overarching scientific themes: (1) paleoclimate; (2) paleoecology, biodiversity, and deep biosphere; (3) magmatic and volcanic evolution; (4) environmental impacts and physical limnology; (5) human occupation, migration, and archeology; and (6) basin history and seismogenic hazards. We used the breakout sessions to evaluate, update, modify, and consolidate the objectives listed in the workshop proposal.



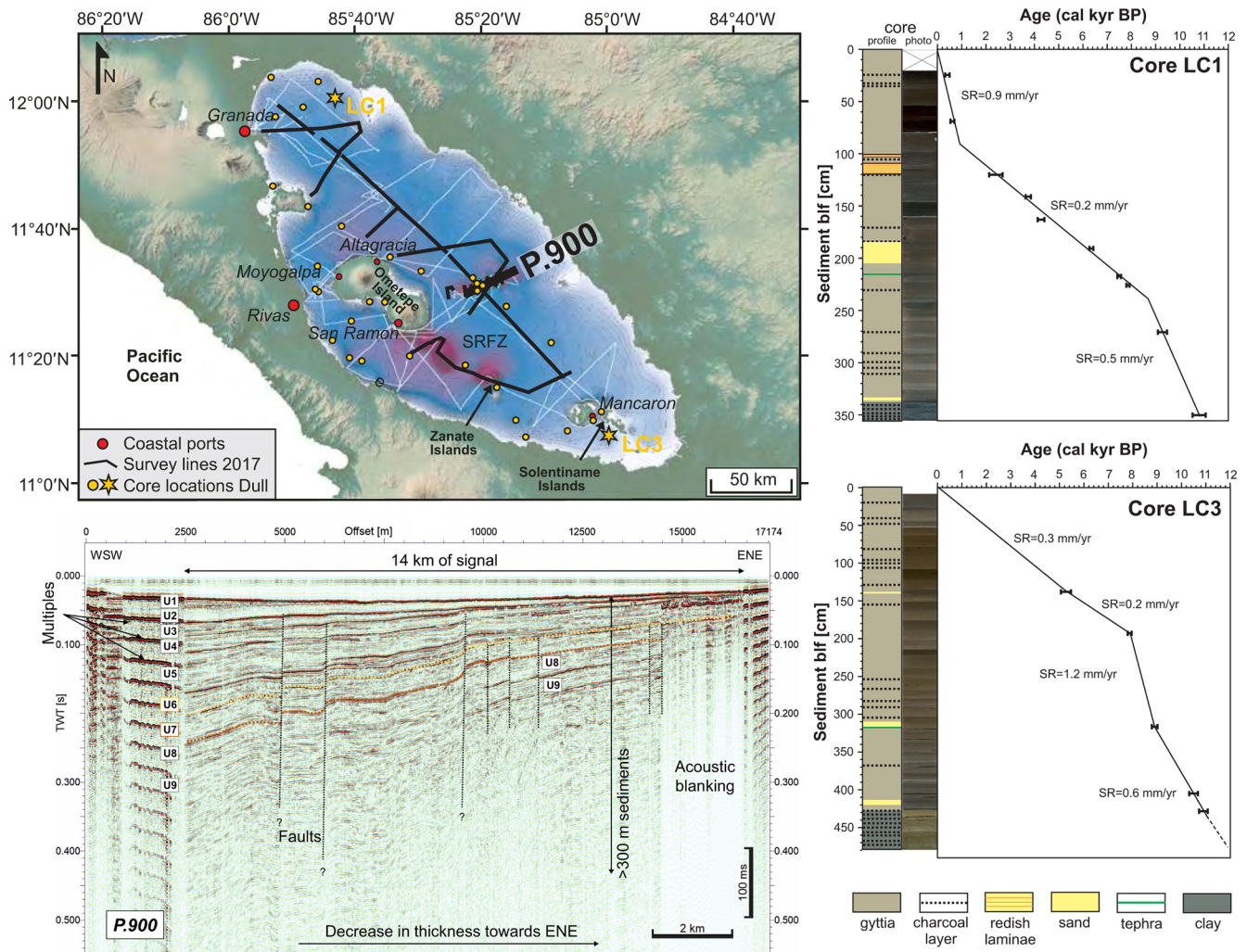


**Figure 3.** Upper left: Shuttle Radar Topography Mission imagery of Lake Nicaragua and the Central American volcanic front in southern Nicaragua, modified from Funk et al. (2009). Locations of seismic pre-site survey profiles from 2017 are shown with black lines. Seismic profile shown in the lower left is marked in bold. Light orange dots show locations of shallow cores collected by Robert A. Dull and colleagues in 2006. Sampling sites where the two cores in the right panels were collected are indicated by yellow stars on the lake map. Lower left: air gun seismic profile (P.900) east of Ometepe island, showing the upper 400 ms TWT (> 300 m, where TWT represents two-way travel time) of the sedimentary succession of the lake. Right panels: schematic profiles of two sediment cores from Lake Nicaragua (see upper left for location), showing the first ~ 4 m and respective  $^{14}\text{C}$  ages of lacustrine sedimentation. The cores are composed mainly of gyttja and intercalated tephra and sand beds, and they indicate an average sedimentation rate of  $\sim 30 \text{ cm kyr}^{-1}$  in the uppermost meters. Note that the tephra in LC1 probably correlates to the  $\sim 6 \text{ ka}$  San Antonio tephra from Masaya Caldera, Nicaragua.

### 3.1 The three-phase approach

After reconvening on Wednesday afternoon, summaries of the breakout sessions were presented and discussed by all participants. It soon became clear that we had to give greater thought to our overall scientific strategy and phasing of proposals to ICDP and IODP. We discussed the prerequisites for each stage of the project and before sunset the 45 participants agreed we would adopt a three-phase approach.

Phase 0 includes the completed pre-site surveys and will include further (and adjusted) seismic surveys, as well as collection of cores that are longer (pre-Holocene) than those

presently available. The main challenge for the seismic survey is to overcome the problem of gas-rich sediments, but it is essential for selection of optimum drilling sites. Piston cores > 10 m long will be taken with a piston corer. Such cores will establish if pre-Holocene sediments that lie below presumably harder or more clay-rich sediments in seismic unit “U2” (Fig. 2) can be drilled by piston coring and if the sediments are suitable for the proposed investigations. Funding will be obtained from national funding agencies, and submission of related proposals will start promptly to make it possible to carry out the field campaign as soon as possible.

If Phase 0 is successful, i.e., it reveals feasible target locations for drilling and yields moderately long cores, Phase I will be addressed in the first full ICDP proposal. Phase I will involve drilling of longer cores ( $\sim 100$  m) at several sites in both lakes to achieve multiple objectives, which may, however, be limited to the Late Quaternary.

Results from Phase I will be crucial for the development of Phase II, the deep-drilling phase, but will also yield “stand-alone” data that will be important to address the scientific topics listed above. Preparation of Phase I proposal for the ICDP will begin after more site survey data are in hand, but the proposal will probably not be submitted until 2024 because of pandemic-related delays. In the longer term, we anticipate that Phase II will be a combined ICDP/IODP proposal (L2S) that will involve plans to drill deep into the lakes and into the associated Sandino Basin offshore of Nicaragua’s Pacific coast. The long records obtained will ultimately enable investigation of such topics as basin and magmatic evolution along the Nicaragua depression, the debate about timing of the closure of the Isthmus of Panama, and paleoclimate extending back in time at least to the Pliocene.

With this timeline in mind, discussion went on well into the evening of 4 March, during dinner, and beyond, as each group was tasked with presenting their major scientific questions and hypotheses for each phase, along with the means to test them, by the next morning. On the morning of 5 March, we assembled to discuss the refined hypotheses presented by each group. We ultimately came up with a list of principal questions and hypotheses that would be addressed under each umbrella topic, and we decided in which phase of the project each would be addressed.

### 3.2 Specific hypotheses and objectives to be addressed

- Deep drilling in the lakes (and eventually in the ocean) will provide a unique window into the past, showing how and over what timescale slab rollback works and how it affects magmatic evolution and volcanic activity during arc shift.
- Deep drilling in lakes of the Nicaragua depression (and eventually the Sandino Basin) will reveal the basin’s development history in the context of regional tectonic evolution.
- The cores preserve a record of hazardous events that can be compared with historic volcanic, tectonic, and climate events.
- Combination of long paleoclimate records from the Nicaragua depression lakes and marine Sandino Basin will enable us to recognize and better understand possible mismatches between models and proxies (or between proxies) that are controlled by the two nearby

oceans and how they fit into modeled Northern Hemisphere or Southern Hemisphere moisture reconstructions, as well as their response to periods of stability vs. transition times (LIP, LGM, etc.).

- Coring and pre-site survey data will enable us to calibrate proxies for paleodata interpretations and to compile a ground-truth database of past impacts and possible future anthropogenic impacts as well as related societal consequences.
- Repetitive abrupt and stressful environmental changes are the main cause of high endemism in the lakes.
- Deposition of volcanoclastic event layers (e.g., ignimbrites) affected all trophic levels (microbes to fishes) in the lake ecosystem. Where the system recovered, it is different from before the ignimbrite deposition.
- Aquatic ecosystems surrounding Lake Nicaragua and Lake Managua served as refugia for freshwater species during marine intrusions in the large lakes.
- Changes in biodiversity during glacial–interglacial cycles and/or caused by regional tectonic changes (e.g., Isthmus of Panama) can be identified.
- Sediments from the lakes preserve traces of the activities of early human settlers and will clarify their settlement history.

This framework will guide us during the preparation of proposals for the different drilling phases. The workshop ended after lunch on 5 March, and the participants returned to Managua, before departing that evening or the next day.

## 4 Summary and further impact of the project

The NICA-BRIDGE workshop participants decided to propose a milestone-driven three-phase project to ICDP (Phase 0 (partially) and Phase I) and later to ICDP/IODP (Phase II). Ultimately, the project will involve short- and long-core drilling in the Nicaraguan lakes and in the Pacific Sandino Basin to collect sediment profiles and generate data to (1) infer tropical climate and environmental changes and their external controlling mechanisms over several million years, (2) assess magnitudes and recurrence times of multiple natural hazards, (3) help develop guidelines for lake management and improvement of socio-economic conditions in Nicaragua, and (4) provide “baseline” environmental data for monitoring lake conditions in light of the planned Pacific–Caribbean canal construction.

This multidisciplinary, international project will include Nicaraguan colleagues, students, and professionals from multiple disciplines who will participate in all aspects of the endeavor. The project will therefore draw enormous attention

to Nicaragua and its scientific community, and it will encourage future, socially relevant international research collaborations in the country. Drilling of the Nicaraguan lakes, under the broad umbrella of paleoclimate, paleoenvironment, and paleoecology, will have broad scientific and socio-economic impacts and contribute to three major societal themes addressed by ICDP: “Climate & Ecosystems”, “Deep Biosphere”, and “Natural Hazards”.

## Appendix A

**Table A1.** Workshop participants.

Participant	Affiliation	Country	Expertise
Guillermo Alvarado	Comisión Nacional de Prevención de Riesgos y Atención de Emergencias (CNE)	Costa Rica	Volcanology and stratigraphy
Greyving Argüello	Instituto Nicaragüense de Estudios Territoriales, Nicaragua (INETER)	Nicaragua	Geodesy and surveying, hydrogeology, volcanology
Rosario Avilés	INETER	Nicaragua	Volcanology
Thorsten Bauersachs	Christian-Albrechts-Universität zu Kiel, Kiel (CAU)	Germany	Organic geochemistry, biomarkers, paleodata, geomicrobiology
Melissa Berke	University of Notre Dame	USA	Organic geochemistry, molecular paleoclimatology
Jennifer Brandstätter	University of Graz	Austria	Structural geology, hydrogeology
Mark Brenner	University of Florida	USA	Paleolimnology, paleoclimate
Erik Brown	University of Minnesota	USA	Geochemistry, paleoclimate
Margarita Caballero Miranda	Universidad Nacional Autónoma de México (UNAM)	Mexico	Paleolimnology, paleoclimate, diatoms
Cristiano Chiessi	University of Sao Paulo	Brazil	Paleoclimate, paleoceanography
Leon Clark	Manchester Metropolitan University	UK	Paleoclimate, stable isotopes
Robert A. Dull	California Lutheran University	USA	Geoarchaeology, land use history, natural hazards, paleoecology
Paula Echeverría-Galindo	Technische Universität Braunschweig	Germany	Paleolimnology, aquatic bioindicators
Alejandro Fernández	University of Minnesota	USA	Paleoclimate, geochemistry
Ricarda Gatter	University of Bremen	Germany	Rock mechanics, volcanic and subaqueous landslide hazards
Carmen Gutiérrez	INETER	Nicaragua	Geology, landslide mapping
Torsten Haberzettl	University of Greifswald	Germany	Paleoclimate, sedimentology, paleomagnetism, environmental magnetism
Walter Hernández	formerly at Servicio Nacional de Estudios Territoriales (SNET)	El Salvador	Geology
Lisa Hlinka	Queens College, New York	USA	Volcanology, magma geochemistry, magmatic processes
Jens Kallmeyer	GFZ – German Research Centre for Geosciences, Potsdam	Germany	Biogeochemistry, geomicrobiology
Sergei Katsev	University of Minnesota	USA	Physical limnology, sediment geochemistry
Sebastian Krastel	CAU	Germany	Hydroacoustics, seismic imaging



**Table A1.** Continued.

Participant	Affiliation	Country	Expertise
Steffen Kutterolf	GEOMAR Helmholtz-Zentrum für Ozeanforschung Kiel	Germany	Volcanology, tephrostratigraphy, marine geology
Elodie Lebas	CAU	Germany	Marine geophysics, seismology
Niklas Leicher	University of Cologne	Germany	Tephrostratigraphy and tephrochronology
Marc-Antoine Longré	Queens College, New York	USA	Volcanology, igneous petrology
Amy Myrbo	University of Minnesota	USA	Outreach, sedimentology, geochemistry
Anders Noren	Continental Scientific Drilling Facility (CSD)	USA	Drilling logistics and core curation
Jonathan Obrist-Farner	Missouri University of Science and Technology	USA	Sedimentology, tectonics, paleoclimate
Beatriz Ortega	UNAM	Mexico	Paleoclimate, stratigraphy, sedimentology, environmental magnetism
Liseth Pérez	Technische Universität Braunschweig	Germany	Paleolimnology, paleoclimate, aquatic bioindicators (ostracodes)
Marino Protti	Observatorio Vulcanológico y Sismológico de Costa Rica (OVSICORI)	Costa Rica	Geology, geophysics, subduction processes
Juanita Rausch	Particle Vision GmbH, Fribourg	Switzerland	Single-particle analysis applied to environmental sciences and volcanology
Pierre Rochette	Aix-Marseille University	France	Rock magnetism, paleomagnetism, petrophysics
Armando Saballos	INETER	Nicaragua	Volcanology, remote sensing
María Sandoval	Universidad de Costa Rica	Costa Rica	Micropaleontology, biostratigraphy (radiolarians)
Ivan Savov	University of Leeds, School of Earth and Environment	UK	Volcanology
Julie Schindlbeck-Belo	GEOMAR Helmholtz-Zentrum für Ozeanforschung Kiel	Germany	Tephrostratigraphy, physical volcanology, climate–volcanism interactions
Byron Steinman	University of Minnesota	USA	Paleoclimate, model simulations
Wilfried Strauch	INETER	Nicaragua	Seismology, tsunami warning, landslides, volcano monitoring
Emilio Talavera	INETER	Nicaragua	Seismology, tsunamis
Virginia Tenorio	INETER	Nicaragua	Seismology, tsunamis
Julian Torres-Dowdall	University of Notre Dame	USA	Ecological and evolutionary biology, genetics and genomics
Kurt Wogau	UNAM	Mexico	Geochemistry, environmental magnetism
Yuzuru Yamamoto	Kobe University	Japan	Structural geology, tectonics, submarine landslides

**Data availability.** Seismic data presented in this paper (Fig. 3) were collected during different campaigns. The data were made available for the workshop to identify potential drill sites. However, all data are currently being used in ongoing projects and have not yet been copied into public databases. The data can be obtained from the authors upon reasoned request.

**Author contributions.** This paper is the report of an ICDP workshop; it is based on the outcome of the workshop and the workshop proposal and reflects this by the authors. It was designed, written, and illustrated by SKu with editorial changes made by AF, LP, AS, MB, JR, EL, SKr, JK, RAD, WS, SKa, AM, and ASa.

**Competing interests.** The contact author has declared that none of the authors has any competing interests.

**Disclaimer.** Publisher's note: Copernicus Publications remains neutral with regard to jurisdictional claims in published maps and institutional affiliations.

**Acknowledgements.** The ICDP workshop was strongly assisted in terms of organizational help and operational drilling knowledge by the International Continental Scientific Drilling Program. We gratefully acknowledge constructive ideas, suggestions, and discussions by all workshop participants listed above as well as the helpful reviewer comments that improved this report.

**Financial support.** This research has been supported by the International Continental Scientific Drilling Program (grant: workshop proposal 17-2018 NICABRIDGE).

**Review statement.** This paper was edited by Thomas Wiersberg and reviewed by Blas Valero Garcés and one anonymous referee.

## References

- Brown, E. T., Caballero, M., Cabral Cano, E., Fawcett, P. J., Lozano-García, S., Ortega, B., Pérez, L., Schwalb, A., Smith, V., Steinman, B. A., Stockhecke, M., Valero-Garcés, B., Watt, S., Wattrus, N. J., Werne, J. P., Wonik, T., Myrbo, A. E., Noren, A. J., O'Grady, R., Schnurrenberger, D., and the MexiDrill Team: Scientific drilling of Lake Chalco, Basin of Mexico (MexiDrill), *Sci. Dril.*, 26, 1–15, <https://doi.org/10.5194/sd-26-1-2019>, 2019.
- Cai, W., McPhaden, M. J., Grimm, A. M., Rodrigues, R. R., Taschetto, A. S., Garreaud, R. D., Dewitte, B., Poveda, G., Ham, Y. G., Santoso, A., Ng, B., Anderson, W., Wang, G., Geng, T., Jo, H. S., Marengo, J. A., Alves, L. M., Osman, M., Li, S., Wu, L., Karamperidou, C., Takahashi, K., and Vera, C.: Climate impacts of the El Niño–Southern Oscillation on South America, *Nature Reviews Earth and Environment*, 1, 215–231, <https://doi.org/10.1038/s43017-020-0040-3>, 2020.
- Case, J. and Holcombe, T.: *Geologic-Tectonic Map of the Caribbean Region*. U.S. Geological Survey Miscellaneous Investigations Map I-1100: scale 1:1 000 000, <https://doi.org/10.3133/i1100>, 1980.
- Cohuo, S., Macario-González, L., Pérez, L., Sylvestre, F., Paillés, C., Curtis, J., Kutterolf, S., Wojewódka, M., Zawisza, E., Szeroczynska, K., and Schwalb, A.: Ultrastructure and aquatic community response to Heinrich Stadials (HS5a–HS1) in the continental northern Neotropics, *Quaternary Sci. Rev.*, 197, 75–91, <https://doi.org/10.1016/j.quascirev.2018.07.015>, 2018.
- Correa-Metrio, A., Bush, M. B., Cabrera, K. R., Sully, S., Brenner, M., DHodell, D. A., Escobar, J. H., and Guilderson, T. J.: Rapid climate change and no-analog vegetation in lowland Central America during the last 86 000 years, *Quaternary Sci. Rev.*, 38, 63–75, <https://doi.org/10.1016/j.quascirev.2012.01.025>, 2012.
- Dull, R. A., Bowen, S. W., Slate, J. E., Bloom, A. M., Mann, P., and McIntosh, K. D.: Late Quaternary paleoenvironments of Lake Nicaragua, Central America, in review, 2023.
- Ehrenborg, J.: A new stratigraphy for the Tertiary volcanic rocks of the Nicaraguan highland, *Geol. Soc. Am. Bull.*, 108, 830–842, 1996.
- Escobar, J., Hodell, D. A., Brenner, M., Curtis, J. H., Gilli, A., Müller, A. D., Anselmetti, F. S., Ariztegui, D., Grzesik, D. A., Pérez, L., Schwalb, A., and Guilderson, T. J.: A ~43-ka record of paleoenvironmental change in the Central American lowlands inferred from lacustrine ostracod  $\delta^{18}\text{O}$ , *Quaternary Sci. Rev.*, 37, 92–104, <https://doi.org/10.1016/j.quascirev.2012.01.020>, 2012.
- Freundt, A., Kutterolf, S., Wehrmann, H., Schmincke, H.-U., and Strauch, W.: Eruption of the dacite to andesite zoned Mateare Tephra, and associated tsunamis in Lake Managua, Nicaragua, *J. Volcanol. Geotherm. Res.*, 149, 103–123, <https://doi.org/10.1016/j.jvolgeores.2005.06.001>, 2006.
- Freundt, A., Strauch, W., Kutterolf, S., and Schmincke, H.-U.: Volcanogenic tsunamis in lakes: examples from Nicaragua and general implications, *Pure Appl. Geophys.*, 164, 527–545, <https://doi.org/10.1007/s00024-006-0178-z>, 2007.
- Funk, J., Mann, P., McIntosh, K. and Stephens, J.: Cenozoic tectonics of the Nicaraguan depression, Nicaragua, and Median Trough, El Salvador, based on seismic-reflection profiling and remote-sensing data, *GSA Bulletin*, 121, 1491–1521, 2009.
- Harmon, N., Gerstoft, P., Rychert, C. A., Abers, G. A., Salas de la Cruz, M., and Fischer, K. M.: Phase velocities from seismic noise using beamforming and cross correlation in Costa Rica and Nicaragua, *Geophys. Res. Lett.*, 35, L19303, <https://doi.org/10.1029/2008GL035387>, 2008.
- Heesemann, M., Grevemeyer, I., and Villinger, H.: Thermal constraints on the frictional conditions of the nucleation and rupture area of the 1992 Nicaragua tsunami earthquake, *Geophys. J. Int.*, 179, 1265–1278, <https://doi.org/10.1111/j.1365-246X.2009.04187.x>, 2009.
- Hodell, D. A., Turchyn, A. J., Wiseman, C. V., Escobar, J., Curtis, J. H., Brenner, M., Gilli, A., Anselmetti, F. S., Ariztegui, D., Perez, L., Schwalb, A., and Brown, E.: Late glacial temperature and precipitation changes in the lowland Neotropics by tandem measurements of  $\delta^{18}\text{O}$  in biogenic carbonate and gypsum hydration water, *Geochim. Cosmochim. Acta*, 77, 352–368, <https://doi.org/10.1016/j.gca.2011.11.026>, 2012.
- Jordan, B. R., Sigurdsson, H., Carey, S. N., Rogers R., and Ehrenborg, J.: Geochemical variation along and across the Central American Miocene paleoarc in Honduras and Nicaragua, *Geochim. Cosmochim. Acta*, 71, 3581–3591, 2007.
- Kautt, A. F., Elmer, K. R., and Meyer, A.: Genomic signatures of divergent selection and speciation patterns in a “natural experiment”, the young parallel radiations of Nicaraguan crater lake cichlid fishes, *Mol. Ecol.*, 21, 4770–4786, 2012.
- Kutterolf, S., Freundt, A., Pérez, W., Wehrmann, H., and Schmincke, H. U.: Late Pleistocene to Holocene temporal succession and magnitudes of highly-explosive volcanic eruptions in west-central Nicaragua, *J. Volcanol. Geotherm. Res.*, 163, 55–82, <https://doi.org/10.1016/j.jvolgeores.2007.02.006>, 2007.
- Kutterolf, S., Freundt, A., Peréz, W., Mörz, T., Schacht, U., Wehrmann, H., and Schmincke, H. U.: Pacific offshore record of plinian arc volcanism in Central America: 1. Along-

- arc correlations, *Geochem. Geophys. Geosyst.*, 9, Q02S01, <https://doi.org/10.1029/2007GC001631>, 2008.
- Kutterolf, S., Schindlbeck, J. C., Anselmetti, F. S., Ariztegui, D., Brenner, M., Curtis, J. H., Schmidt, D., Hodell, D. A., Müller, A. D., Pérez, L., Pérez, W., Schwalb, A., Frische, M., and Wang, K.-L.: A 400-ka tephrochronological framework for Central America from Lake Petén Itzá (Guatemala) sediments, *Quaternary Sci. Rev.*, 150, 200–220, 2016.
- Ledru, M.-P., Reimold, W. U., Ariztegui, D., Bard, E., Crósta, A. P., Riccomini, C., and Sawakuchi, A. O.: Why deep drilling in the Colônia Basin (Brazil)?, *Sci. Drill.*, 20, 33–39, <https://doi.org/10.5194/sd-20-33-2015>, 2015.
- Mann, P., Schubert, C., and Burke, K.: Review of Caribbean neotectonics: The Caribbean region, in: *The Geology of North America*, edited by: Dengo, G. and Case, J. E., Geological Society of America, Boulder, Colorado, 307–338, <https://doi.org/10.1130/DNAG-GNA-H>, 1990.
- McBirney, A. R. and Williams, H.: Volcanic history of Nicaragua, *Univ. Calif. Publ. Geol. Sci.*, Berkeley and Los Angeles, 1–65, ISSN 0068-645X, 1965.
- Moguel, B., Pérez, L., Alcaraz, L., Blaz, J., Caballero, M., Muñoz-Velasco, I., Becerra, A., Laclette, J. P., Ortega-Guerrero, B., Romero-Oliva, C., Lozano, S., and Herrera-Estrella, L.: Holocene life and microbiome profiling in ancient tropical Lake Chalco, Mexico, *Sci. Rep.*, 11, 13848, <https://doi.org/10.1038/s41598-021-92981-8>, 2021.
- Montes, C., Cardona, A., Jaramillo, C., Pardo, A., Silva, J. C., Valencia, V., Ayala, C., Pérez-Angel, L. C., Rodríguez-Parra, L. A., Ramirez, V., and Niño, H.: Middle Miocene closure of the Central American Seaway, *Science*, 348, 226–229, 2015.
- Mueller, A. D., Anselmetti, F. S., Ariztegui, D., Brenner, M., Curtis, J. H., Escobar, J., Gilli, A., Grzesik, D. A., Hodell, D. A., Guilderson, T. P., Kutterolf, S., and Plötze, M. L.: Late Quaternary Palaeoenvironment of Northern Guatemala: Evidence from Deep Drill Cores and Seismic Stratigraphy of Lake Petén Itzá, *Sedimentology*, 57, 1220–1245, 2010.
- Nakov, T., Beaulieu, J. M., and Alverson, A. J.: Diatoms diversify and turn over faster in freshwater than marine environments, *Evolution*, 73, 2497–2511, 2019.
- Obrist-Farner, J., Eckert, A., Locmelis, M., Crowley, J. L., Mota-Vidaure, B., Lodolo, E., Rosenfeld, J., and Duarte, E.: The role of the Polochic Fault as part of the North American and Caribbean Plate boundary: Insights from the infill of the Lake Izabal Basin, *Basin Res.*, 32, 1347–1364, 2020.
- Pérez, L., Correa-Metrio, A., Cohuo, S., Macario González, L., Echeverría, P., Brenner, M., Curtis, J., Kutterolf, S., Stockhecke, M., Schenk, F., Bauersachs, T., and Schwalb, A.: Ecological turnover in neotropical freshwater and terrestrial communities during episodes of abrupt climate change, *Quaternary Res.*, 101, 26–36, 2021.
- Ranero, C. R., von Huene, R., and Flueh, E.: A cross section of the convergent Pacific margin of Nicaragua, *Tectonics*, 19, 335–357, 2000.
- Schindlbeck, J. C., Kutterolf, S., Freundt, A., Straub, S. M., Vannucchi, P., and Alvarado, G. E.: Late Cenozoic tephrostratigraphy offshore the southern Central American Volcanic Arc: 2. Implications for magma production rates and subduction erosion, *Geochem. Geophys. Geosyst.*, 17, 4585–4604, <https://doi.org/10.1002/2016GC006504>, 2016.
- Schneider, T., Bischoff, T., and Haug, G. H.: Migrations and dynamics of the intertropical convergence zone, *Nature*, 513, 45–53, 2014.
- Taylor, B.: *Backarc Basins*, Plenum Press, New York, <https://doi.org/10.1007/978-1-4615-1843-3>, 1995.
- Vallance, J. W., Schilling, S. P., and Devoli, G.: Lahar Hazards at Mombacho Volcano, Nicaragua, USGS open-file report 01-455, Vancouver, Washington, USA, <https://pubs.usgs.gov/of/2001/0455/> (last access: 6 February 2023), 2001.
- Weinberg, R. F.: Neotectonic development of western Nicaragua, *Tectonics*, 11, 1010–1017, 1992.





## Planning for the Lake Izabal Basin Research Endeavor (LIBRE) continental scientific drilling project in eastern Guatemala

Jonathan Obrist-Farner<sup>1</sup>, Andreas Eckert<sup>1</sup>, Peter M. J. Douglas<sup>2</sup>, Liseth Perez<sup>3</sup>, Alex Correa-Metrio<sup>4</sup>,  
Bronwen L. Konecky<sup>5</sup>, Thorsten Bauersachs<sup>6</sup>, Susan Zimmerman<sup>7</sup>, Stephanie Scheidt<sup>8</sup>, Mark Brenner<sup>9</sup>,  
Steffen Kutterolf<sup>10</sup>, Jeremy Maurer<sup>1</sup>, Omar Flores<sup>11</sup>, Caroline M. Burberry<sup>12</sup>, Anders Noren<sup>13</sup>,  
Amy Myrbo<sup>14</sup>, Matthew Lachniet<sup>15</sup>, Nigel Wattrus<sup>16</sup>, Derek Gibson<sup>1</sup>, and the LIBRE scientific team<sup>+</sup>

<sup>1</sup>Department of Geosciences and Geological and Petroleum Engineering Department, Missouri University  
of Science and Technology, Rolla, Missouri, USA

<sup>2</sup>Department of Earth and Planetary Sciences and Geotop Research Center,  
McGill University, Montreal, Quebec, Canada

<sup>3</sup>Institute of Geosystems and Bioindication, Technische Universität Braunschweig, Braunschweig, Germany

<sup>4</sup>Centro de Geociencias, Universidad Nacional Autónoma de México, Juriquilla, México

<sup>5</sup>Department of Earth and Planetary Sciences, Washington University in St. Louis, St. Louis, Missouri, USA

<sup>6</sup>Institute of Geosciences, Christian-Albrechts-Universität, Kiel, Germany

<sup>7</sup>Center for Accelerator Mass Spectrometry, Lawrence Livermore National Laboratory,  
Livermore, California, USA

<sup>8</sup>Institute of Geology and Mineralogy, University of Cologne, Cologne, Germany

<sup>9</sup>Department of Geological Sciences, University of Florida, Gainesville, Florida, USA

<sup>10</sup>GEOMAR, Helmholtz Centre for Ocean Research Kiel, Kiel, Germany

<sup>11</sup>Centro de Estudios Superiores de Energía y Minas, Universidad de San Carlos de Guatemala,  
Guatemala City, Guatemala

<sup>12</sup>Department of Earth and Atmospheric Sciences, University of Nebraska–Lincoln, Lincoln, Nebraska, USA

<sup>13</sup>Continental Scientific Drilling Facility, University of Minnesota, Minneapolis, Minnesota, USA

<sup>14</sup>Amiable Consulting, Minneapolis, Minnesota, USA

<sup>15</sup>Department of Geosciences, University of Nevada, Las Vegas, Nevada, USA

<sup>16</sup>Earth and Environmental Sciences Department, University of Minnesota Duluth, Duluth, Minnesota, USA

<sup>+</sup>A full list of authors appears at the end of the paper.

**Correspondence:** Jonathan Obrist-Farner (obristj@mst.edu)

Received: 13 January 2023 – Revised: 3 March 2023 – Accepted: 6 March 2023 – Published: 26 October 2023

**Abstract.** As Earth's atmospheric temperatures and human populations increase, more people are becoming vulnerable to natural and human-induced disasters. This is particularly true in Central America, where the growing human population is experiencing climate extremes (droughts and floods), and the region is susceptible to geological hazards, such as earthquakes and volcanic eruptions, and environmental deterioration in many forms (soil erosion, lake eutrophication, heavy metal contamination, etc.). Instrumental and historical data from the region are insufficient to understand and document past hazards, a necessary first step for mitigating future risks. Long, continuous, well-resolved geological records can, however, provide a window into past climate and environmental changes that can be used to better predict future conditions in the region. The Lake Izabal Basin (LIB), in eastern Guatemala, contains the longest known continental records of tectonics, climate, and environmental change in the northern Neotropics. The basin is a pull-apart depression that developed along the North American and Caribbean plate boundary ~ 12 Myr ago and contains > 4 km of sediment. The sedimentological archive in the LIB records the interplay among several Earth System processes. Consequently, exploration of

sediments in the basin can provide key information concerning: (1) tectonic deformation and earthquake history along the plate boundary; (2) the timing and causes of volcanism from the Central American Volcanic Arc; and (3) hydroclimatic, ecologic, and geomicrobiological responses to different climate and environmental states. To evaluate the LIB as a potential site for scientific drilling, 65 scientists from 13 countries and 33 institutions met in Antigua, Guatemala, in August 2022 under the auspices of the International Continental Scientific Drilling Program (ICDP) and the US National Science Foundation (NSF). Several working groups developed scientific questions and overarching hypotheses that could be addressed by drilling the LIB and identified optimal coring sites and instrumentation needed to achieve the project goals. The group also discussed logistical challenges and outreach opportunities. The project is not only an outstanding opportunity to improve our scientific understanding of seismotectonic, volcanic, paleoclimatic, paleoecologic, and paleobiologic processes that operate in the tropics of Central America, but it is also an opportunity to improve understanding of multiple geological hazards and communicate that knowledge to help increase the resilience of at-risk Central American communities.

## 1 Introduction

Drilling and coring in continental settings has provided answers to compelling scientific questions and has enabled us to better understand Earth and forecast how Earth Systems might behave in the future (Colman, 1996; Harms et al., 2007; NRC, 2011; Soreghan and Cohen, 2013; NASEM, 2020). Long sediment records have allowed us to infer tectonic, volcanic, climatic, environmental, and ecological processes on long temporal scales (Soreghan and Cohen, 2013). However, we still lack records from key regions around the world, including continental Central America. Despite being a relatively small region, Central America has played an outsized role in influencing several Earth System processes through geologic time (Fig. 1). For example, a major continental strike-slip fault system in Guatemala forms part of the North American–Caribbean plate boundary (Lyon-Caen et al., 2006; Authemayou et al., 2012; Ellis et al., 2019; Guzmán-Speziale and Molina, 2022) and has caused devastating earthquakes in the past (Plafker, 1976; White, 1984, 1985). The area also possesses one of the most active volcanic chains in the world along the Pacific coast (Kutterolf et al., 2008a) and hosts important biological hotspots (Graham, 2010; Correa-Metrio et al., 2011). Central American mountains influence easterly winds that affect the El Niño–Southern Oscillation and regional precipitation patterns (Baldwin et al., 2021). The closure of the Central American Isthmus that connects North and South America caused one of the most important biotic interchanges in recent geologic history (Bacon et al., 2015), modified global ocean circulation patterns (Sentman et al., 2018), and may have helped establish Northern Hemisphere glaciation (Haug et al., 2001; cf. Molnar, 2008). The many geological processes that affect the region expose a large proportion of the Central American population to multiple hazards, some of which are not well characterized and are poorly understood.

The Lake Izabal Basin (LIB) in eastern Guatemala is an active pull-apart basin along the North American and Caribbean plate boundary (Figs. 1, 2), with > 4 km of sed-

iment that likely began to accumulate during the Miocene (~ 12 Myr ago; Obrist-Farner et al., 2020). Seismic stratigraphic investigations indicate that the basin is deep and asymmetric: it is the result of a complex interplay between tectonics and sedimentation (Bartole et al., 2019). The accumulated deposits preserve potentially unrivalled continental paleoclimatic, volcanic, paleoseismic, and paleoecologic records of the region. The location of the basin along a major tectonic plate boundary, the thick and asymmetric sediment record, and frequent eruption of tephras for chronology make the LIB an ideal location for a project within the International Continental Scientific Drilling Program (ICDP). Drilling in the LIB will enable better quantification of seismic hazards and coring the basin's asymmetric infill will provide a continuous Miocene-to-recent sediment record. Recovery of such a long record will provide opportunities to investigate the following: (1) the seismo-tectonic evolution of the basin and of the North American and Caribbean plate boundary; (2) neotropical hydroclimate from the late Miocene to present, providing constraints on terrestrial hydroclimate responses to tectonic, greenhouse gas, and orbital variations; (3) biological and ecological dynamics related to the period during which the land bridge developed between North and South America and related to glacial–interglacial cycles that were established in the Quaternary; (4) the history of explosive volcanism from the northern Central American Volcanic Arc (CAVA); and (5) the diversity and abundance of life in the terrestrial deep biosphere, as well as feedback dynamics on nutrient cycles (e.g., carbon and nitrogen) through geomicrobiological processes.

## 2 The Lake Izabal Basin Research Endeavor (LIBRE) project

In August 2022, we organized and held a workshop in the city of Antigua, Guatemala, with 65 scientists from 13 countries and 33 institutions. Workshop discussions focused on the rationale for the project and drafting of scientific questions and hypotheses that can be addressed using instru-

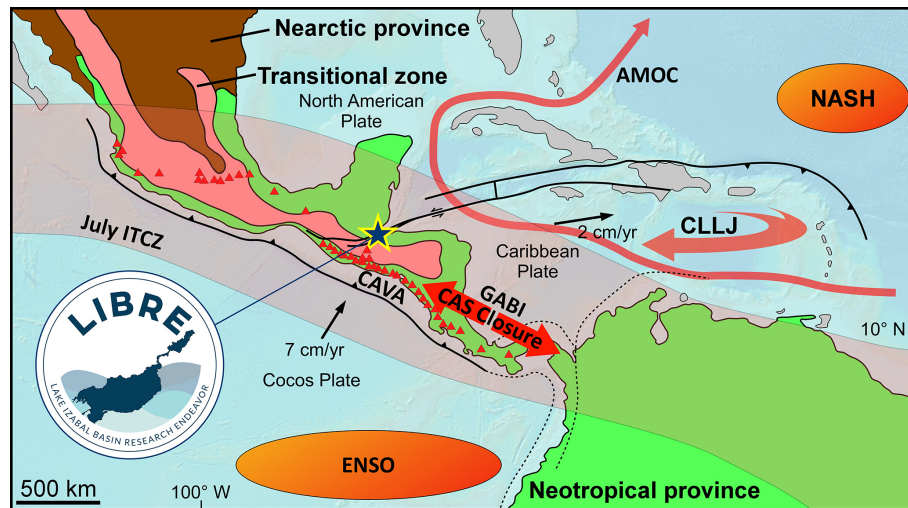


**Figure 1.** Tectonic map of Central America and northern South America (modified from Mann, 2007) showing the diverse Earth System processes that interact in the vicinity of the Lake Izabal Basin (yellow star). The basin is located at the boundary between the North American and Caribbean tectonic plates, where devastating earthquakes have occurred in the past. The basin is also located at the transitional zone between Nearctic and Neotropical provinces (Holt et al., 2013). Several ocean–atmosphere processes influence regional hydroclimate, such as the position of the Intertropical Convergence Zone (ITCZ), the El Niño–Southern Oscillation (ENSO), the North Atlantic Subtropical High (NASH), and the Caribbean Low-Level Jet (CLLJ). Closure of the Central American Seaway (CAS closure) resulted in the Great American Biotic Interchange (GABI) and in changes in the Atlantic Meridional Overturning Circulation (AMOC). Finally, the basin is located north of one of the most active volcanic chains in the world, the Central American Volcanic Arc (CAVA).

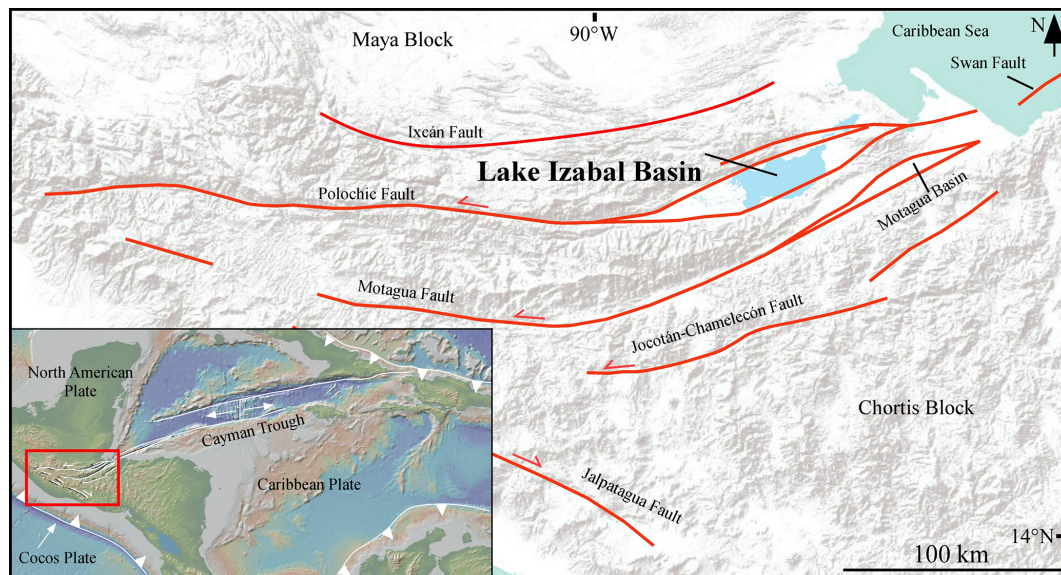


**Figure 2.** Topographic and tectonic map of southern Guatemala showing the main fault traces of the Polochic–Motagua Fault System and the location of the Lake Izabal Basin. Inset map shows the tectonic and topographic map of the Caribbean region, highlighting the location of the study area and the North American and Caribbean plate boundary. Modified from Obrist-Farner et al. (2020).

mented boreholes and drill cores from the basin, and chronological tools and outreach activities. With that in mind, the group identified drilling targets and discussed logistics associated with a drilling campaign. Key government and industry collaborators in Guatemala donated data sets that were discussed during the workshop. For instance, the Guatemalan

government provided seismic data from the LIB that was acquired by the Arco oil company in 1978 (Fig. 3), of which 332 km was acquired in Lake Izabal and 127 km in the alluvial plain to the east. The Shell Oil Company reprocessed all Arco lines in 1991 and acquired an additional 69 km of seismic lines on land and 431 km in Lake Izabal. In addition,



the Guatemalan government made available all data from the Colorado-1 well, which was drilled in 1993 on the eastern side of the LIB (Fig. 3) and provides information related to lithologies, seismic velocities, and age of the basin fill. The data sets are key to our understanding of the LIB and helped us formulate hypotheses based on the potential geological time intervals we expect to recover from the basin.

### 3 Current knowledge of the Lake Izabal Basin

During the workshop, participants discussed available data from the LIB. The LIB is 80 km long and 20 km wide (Fig. 2). The eastern side of the basin is occupied by Lake Izabal ( $15^{\circ}30' \text{ N}$ ,  $89^{\circ}10' \text{ W}$ ), whereas the western side contains a wetland of international importance, the Ramsar site Bocas del Polochic (Ramsar site no. 813). Lake Izabal is shallow ( $z_{\text{max}} = 15 \text{ m}$ ) and polymictic, with a temperature difference between surface and bottom waters of only  $\sim 2^{\circ}\text{C}$  (Brinson and Nordlie, 1975). Mean annual precipitation in the region is  $\sim 3300 \text{ mm}$  (Duarte et al., 2021), and the climate is characterized by a rainy season that extends from May through December and a dry season from January to April (Duarte et al., 2021). The basin is confined to the north by the Santa Cruz Mountain Range, to the south by the Minas Mountain Range, and to the east by the Mico Mountains (Fig. 3).

Outcrop studies, seismic stratigraphic analysis, and syntheses of industry well data provide constraints on the timing of basin formation and the basin's stratigraphic architecture. Three formations make up the Tertiary stratigraphy of the Izabal region (Fig. 4; Powers, 1918; Vinson, 1962; Mota-Vidaure, 1989; Obrist-Farner et al., 2020). The oldest formation is the Upper Oligocene to Lower Miocene Rio Dulce Formation, which rests unconformably on top of marine Permian limestones (Vinson, 1962). The Rio Dulce Formation consists of marine limestones that are light buff, tan, and cream-colored, with abundant coral and mollusk fragments (Powers, 1918; Vaughan, 1919; Vinson, 1962). The formation is overlain unconformably by the informally defined terrigenous mid-Miocene Carboneras formation (Mota-Vidaure, 1989). The lower part of the Carboneras formation is constrained to the Serravallian by zircon weighted-mean  $^{206}\text{Pb}/^{238}\text{U}$  ages of  $12.060 \pm 0.008 \text{ Ma}$  from a volcanic tuff  $\sim 30 \text{ m}$  above the Rio Dulce–Carboneras unconformity (Obrist-Farner et al., 2020). The Carboneras formation is composed of claystone, siltstone, marl, sandstone, conglomerate, and lignite beds (Mota-Vidaure, 1989; Obrist-Farner et al., 2020). The uppermost formation is the Herrería Formation, constrained to the Pliocene–Pleistocene based on freshwater gastropod shells (Powers, 1918). The formation is composed of claystone, siltstone, marl, sandstone, conglomerate, and lignite beds (Powers, 1918; Vinson, 1962). Correlation between outcrop information and seismic profiles by Obrist-Farner et al. (2020) indicates that the Carboneras for-

mation forms part of the initial infill of the LIB, constraining basin initiation to the mid-Miocene.

Seismic stratigraphic studies revealed that the basin is asymmetric in both a north–south and an east–west direction. In a north–south direction, the basin geometry resembles that of a half-graben, resulting from transform-normal extension along the Polochic Fault (Ben-Avraham and Zoback, 1992), with the thickest sedimentary package occurring parallel to the principal deformation zone (Bartole et al., 2019; Fig. 5). In an east–west direction, basin asymmetry resulted from a migrating depocenter similar in form to extant (Crowell, 2003) and young (Beeson et al., 2017) pull-apart basins along the San Andreas Fault, California (USA). The LIB depocenter has migrated  $\sim 70 \text{ km}$  during Polochic Fault displacement (Bartole et al., 2019), with a basin infill that thickens on the western side (Fig. 5). Constraints on the basin stratigraphy are based on the Colorado-1 industry well (Shell Oil Company, Exploradora y Productora de Guatemala: Informe final de exploración, unpublished report, 1993). Located on the eastern side of the basin (Fig. 3), the well was drilled through 1400 m of sediment before it was plugged and abandoned. Cuttings from the well indicate that the lowermost strata (1400–500 m) are composed of mudstone with thin sandstone beds, with the appearance of coal from 1000 to 800 m and conglomerate from 600 to 500 m. Conglomerate and sandstone content become more dominant from 500 to  $\sim 200 \text{ m}$ , with an increase in mudstone and limestone from 200 m to the surface (Obrist-Farner et al., 2020). Correlation among outcrops, seismic profiles, and the Colorado-1 well indicate that the 1400 m drilled by the well is younger than 12 Ma (Obrist-Farner et al., 2020), and preliminary palynological results support this interpretation based on Tortonian-age pollen ( $\sim 8 \text{ Ma}$ ) found in cutting samples at  $\sim 1200 \text{ m}$ .

Short sediment cores from Lake Izabal further constrain the stratigraphy of the basin and reveal climate and environmental change during the Holocene. Variations in elemental abundances in a 7.6 m radiocarbon-dated sediment core obtained from the northwest side of the basin (Loc5 in Fig. 3) suggest a hydroclimate shift from drier to wetter conditions from the early to the mid-Holocene and stable hydroclimatic conditions thereafter until  $\sim 1000$  years ago when drier conditions returned (Duarte et al., 2021). Superimposed on this long-term trend is a marine incursion during the 8.2 ka event (Obrist-Farner et al., 2022), highlighting the sensitivity of this low-lying lake to sea-level variations. This marine incursion resulted in an ecosystem shift, modifying the low-lying lake for  $\sim 4500$  years. A shorter sediment core from the southern side of the basin (PC in Fig. 3) spans the last 1400 years, revealing interesting hydroclimate changes during the Little Ice Age (LIA). In contrast to many records from Central America that suggest a drier hydroclimate during the LIA, evidence from Izabal suggests increased runoff (Obrist-Farner et al., 2023) and increased tropical forest cover after substantial human-mediated deforestation during ancient Maya times, which ended ca. 1000 years ago (Mongol et al.,

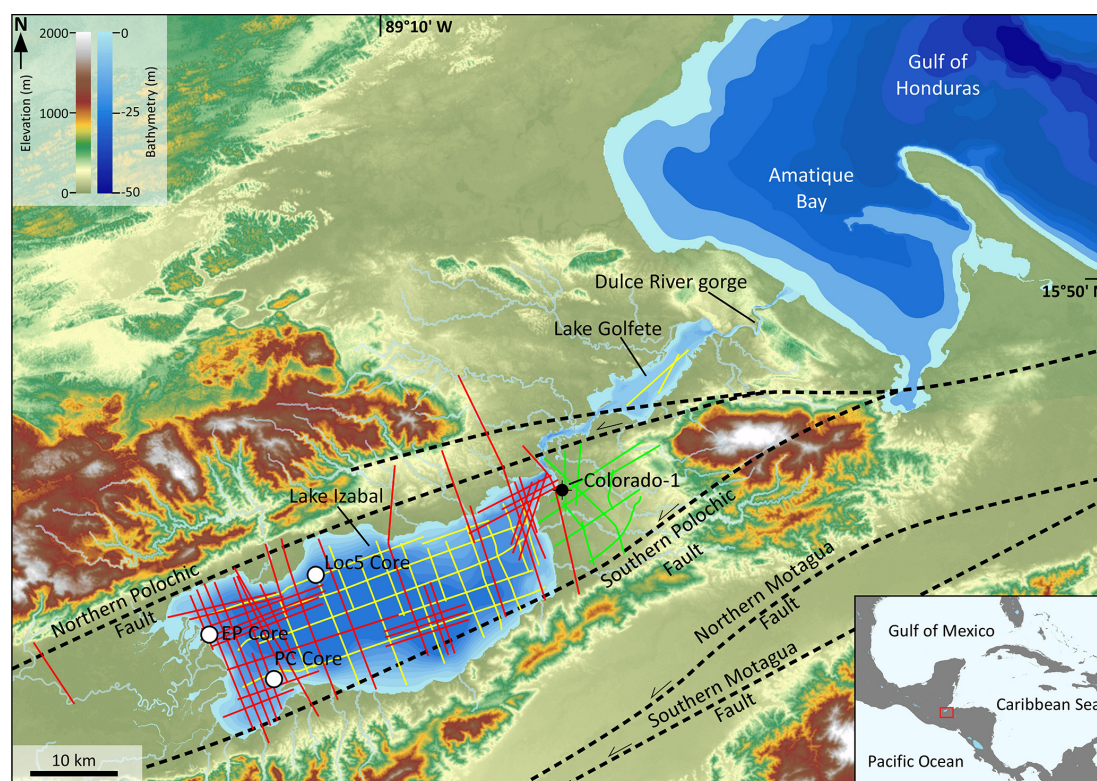


**Figure 3.** Topographic and bathymetric map of the Izabal region. White circles show existing coring locations discussed in the text. Yellow and green lines show the location of the 1978 Arco seismic lines, and red lines show the location of the 1991–1992 Shell seismic lines. Major faults are shown with thick dashed black lines. Inset shows a map of Central America and part of the Caribbean, with the location of the Izabal region in eastern Guatemala indicated by the red box.

2023). In addition, a shorter sediment core obtained near the Polochic Delta (EP core in Fig. 3) revealed several geochemical variations that indicate human disturbance of Lake Izabal during the last 100 years, including an increase in the lake's trophic status (Obrist-Farner et al., 2019) and metal contamination caused by mining activities in the catchment (Hernández et al., 2020). Together, these data sets indicate that the sedimentary archive of the LIB contains records of paleoseismic, paleoclimatic, and paleoenvironmental changes across various timescales.

#### 4 The Lake Izabal Basin – a world-class scientific drilling site

The LIBRE project is well positioned to address two science priorities identified by ICDP (Anselmetti et al., 2020), using an integrated scientific approach, as follows: (1) understanding the full chain from geologic hazard to risk (Theme 02: geohazards), and (2) exploring sedimentary archives to understand Earth's evolution (Theme 04: environmental change). Expanding on these two themes, the LIBRE workshop focused on defining scientific priorities and questions, logistics, drilling targets, and education and outreach

plans. The resulting discussions were synthesized into five scientific motivations and an outreach and education plan.

##### 4.1 Tectonic processes and seismic risk (ICDP Theme 02)

The LIB is an ideal scientific drilling site because it is a pull-apart basin that developed along the Polochic–Motagua Fault System (PMFS; Lodolo et al., 2009), a system comprised of four sub-parallel faults that separate the North American and Caribbean plates in Guatemala (Figs. 1, 2; Lyon-Caen et al., 2006). Through geologic time, basin depocenter migration and continued subsidence played a large role in the morphology of the basin. For example, the depocenter migrated  $\sim 70$  km at the speed of the transform (Bartole et al., 2019), recording the complex interplay between tectonic deformation and sedimentation. The area is also subject to intense seismic activity, as evidenced by the 1976 Motagua earthquake (Plafker, 1976) and by estimates of destruction and shaking during the estimated  $M_w$  7.6 Polochic earthquake in 1816 (White, 1985). In addition, high-resolution geophysical surveys of Lake Izabal's floor revealed contemporary surface fractures (Fig. 6). Despite evidence of contemporary deformation and potential for catastrophic earthquakes,





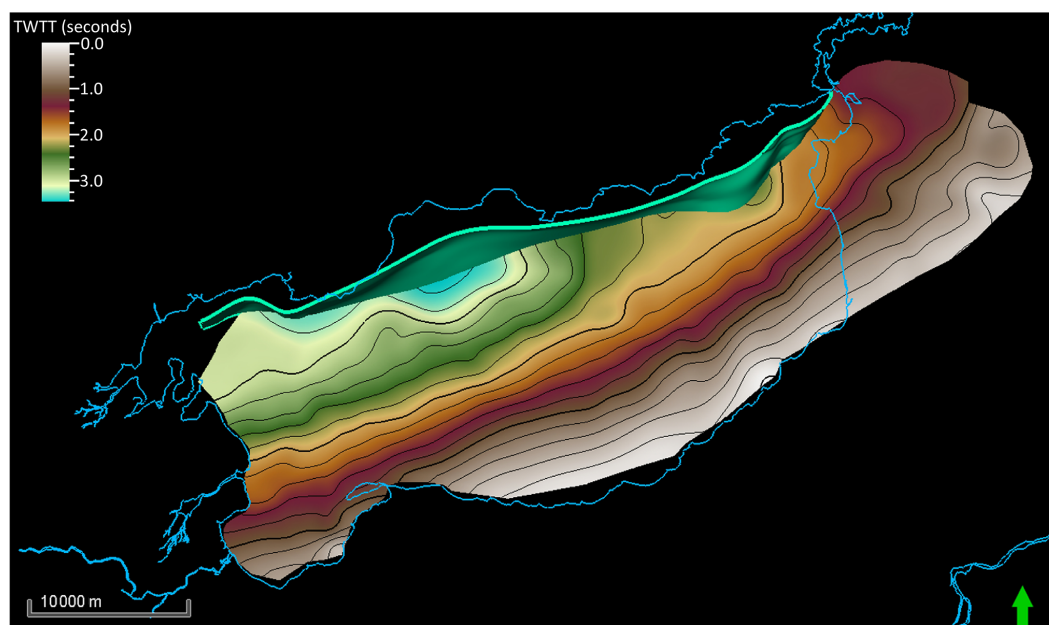


**Figure 5.** Basement contour map in two-way travel time (TWTT) of the Lake Izabal Basin (LIB). Green fault is the main principal deformation zone of the LIB. On the eastern side of the basin, the basement has been uplifted and is closer to the surface than it is on the western side, an area where more than 4 km of sediment has accumulated.

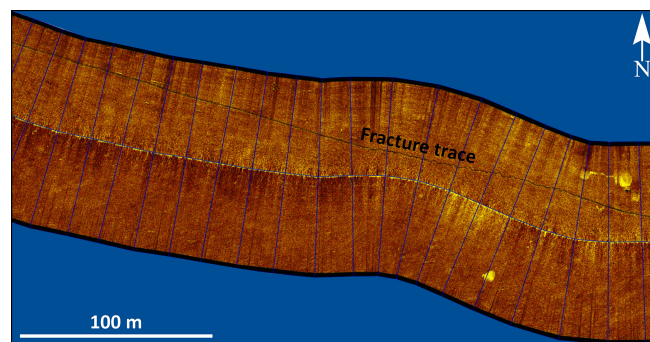


**Figure 6.** Side-scan sonar profile from the southwestern side of Lake Izabal showing a contemporary fracture trace. For location of the profile, see the blue square in Fig. 7.

through time and possible external controls on CAVA activity – information needed to better understand volcanic hazards in the region.

#### 4.3 Paleoclimatic reorganizations and analogs for modern climate change (ICDP Theme 04)

The sediments of the LIB record the response of terrestrial climate to tectonic, greenhouse gas, and orbital variations over the last ~ 12 Myr, providing a unique opportunity to investigate a hydroclimate record from the Neotropics that extends back to the late Miocene. A continental drilling project in the LIB will enable the study of climate evolution during the late Miocene, Pliocene, and through the Quaternary.

Expansion of  $C_4$  plants in regions such as North America, tropical Africa, and Indo-Asia during the late Miocene and Pliocene points to major ecosystem shifts (Strömberg and McInerney, 2011; Uno et al., 2011; Feakins et al., 2020). However, the expansion appears to have been region-specific (Strömberg, 2011) and likely the result of increased overall aridity and changes in the seasonality of precipitation (Pagan et al., 1999; Strömberg and McInerney, 2011). However, only sparse late Miocene to Pliocene paleoclimate data exist from the Neotropics to determine the regional expression of these changes. In addition, the paucity of long Central American paleoclimate records makes it difficult to resolve debates about the drivers of tropical climate change during the mid-Pliocene, a time of higher atmospheric  $CO_2$  and global warmth, and a prospective analog for present-day climate change (Burke et al., 2018).

Superimposed on long-term cooling, closure of the Central American Seaway (CAS) spanned ~ 7 to 4 Myr, with the last near-surface ocean connection closing by ca. 2.5 Ma (O’Dea et al., 2016; McGirr et al., 2020). CAS closure caused profound changes in the Atlantic Ocean, with a strengthening of the Atlantic Meridional Overturning Circulation (AMOC; Haug and Tiedemann, 1998; Auderset et al., 2019). Impacts of CAS closure on global climate are debated (Utescher et al., 2017 vs. Molnar, 2008) and model simulations suggest that southern Central America and northern South America became generally drier and colder (Fedorov et al., 2013, 2015; Brierley and Fedorov, 2016). On glacial and orbital timescales, the LIB offers an opportunity to extend paleoclimate records through the entire Quaternary; i.e.,

the past  $\sim 2.6$  Myr. The current lack of continuous Quaternary records precludes the evaluation of climate drivers during key time intervals, such as before and after the Mid-Pleistocene Transition (MPT)  $\sim 1.25$ – $0.70$  Ma, when global ice age cycles intensified and moved from 41 to 100 ka pacing (Chalk et al., 2017). Therefore, a long, continuous, and high-resolution record from the LIB will provide an unrivalled opportunity to reconstruct neotropical climate from the late Miocene to the present, enabling testing of hypotheses related to precipitation changes as a result of CAS closure, potential drying caused by reduced convection during the mid-Pliocene, and changes in hydroclimate as a result of the establishment of Northern Hemisphere glaciation.

#### 4.4 Paleoeological evolution and the American biotic exchange (ICDP Theme 04)

The LIBRE project offers the opportunity to explore the composition and structure of neotropical biological communities from the Miocene to present. Closure of the CAS marked one of the most important events in terms of the biogeography of the Neotropics (Jaramillo, 2018). Although species interchange between the Nearctic and Neotropical biogeographic realms started before the Miocene (Bacon et al., 2015), closure of the CAS accelerated migration rates, triggering ecological dynamics of community rearrangement. Before the complete emergence of the CAS, northern South America and southern Central America were mostly occupied by rainforests and mangroves, under a warm and wet climate regime (Graham, 1998; Salzmann et al., 2008; Jaramillo et al., 2020). A long sediment record from the LIB could help constrain how climate change after CAS closure modified the availability of environmental niches in the Neotropics, leading to the synthesis of novel ecosystems in the region (Correa-Metrio et al., 2012; Pérez et al., 2021).

Furthermore, a Quaternary record from the LIB can contribute to our understanding of how regional vegetation changed in response to glacial–interglacial dynamics. Palynological data suggest that during the Quaternary, vegetation changes in the northern Neotropics were characterized by relatively sparse forest cover, dominated by Nearctic elements during glacials and dense Neotropical forests during interglacials (Correa-Metrio et al., 2012). Thus, after the establishment of Northern Hemisphere glaciation, vegetation changes were likely associated with the formation/disappearance of corridors that promoted/impeded migration (Bacon et al., 2016). Differing migration patterns, together with climate variability, probably resulted in the synthesis of novel and “no-modern-analog” ecosystems in the region (Correa-Metrio et al., 2012; Perez et al., 2021). Long Quaternary records from the Izabal Basin will also enable us to understand vegetation changes in what is one of the currently wettest areas of Central America, and one that is influenced by climate drivers different from those that affect sites in the drier northeast lowlands of Central America and Mexico. For

instance, the Lake Izabal region is thought to have provided a haven for biodiversity (refugia) during past periods of climate change (Prance, 1982), and long sediment cores from the Quaternary will allow us to investigate the role of the region in maintaining regional ecosystems and biomes during times of climatic turmoil. Furthermore, we will be able to investigate relationships between the structure of aquatic and terrestrial ecosystems and sea-level variability (Obrist-Farner et al., 2022).

#### 4.5 Life in the deep biosphere: a continental lacustrine view (ICDP Theme 04)

The deep biosphere, microbial life that thrives in sediments down to several kilometers of depth, plays a major role in global biogeochemical cycles of carbon, nitrogen, and sulfur. Our knowledge of the community composition and abundance of the deep biosphere relies largely on studies carried out within the framework of the Integrated Ocean Discovery Program (IODP) and its predecessors over the past 3 decades (Parkes et al., 1994; D’Hondt et al., 2004). Such studies have provided a wealth of information on the nature and abundance of microbial life, showing that life can exist to  $\sim 10$  km below the surface and at temperatures that may reach  $> 120^\circ\text{C}$  (Inagaki et al., 2015; Heuer et al., 2020). They have also demonstrated that the genetic diversity of the deep biosphere and its abundance rivals that found in the overlying ocean waters (Kallmeyer et al., 2012), but data from continental settings are largely missing. In general, our understanding of the composition, abundance, and evolution of life in deeply buried lacustrine archives is sparse, hindering an understanding of the role of the continental deep biosphere in global biogeochemical cycles. With a Miocene-to-recent sediment record, Lake Izabal offers a unique opportunity to study the community composition of the continental deep biosphere at an unprecedented scale and resolution. It will also provide key insights into the vertical zonation and abundance of microbial cells. Given the generally higher productivity and organic matter preservation of lake systems compared to the marine realm, we expect that deeply buried lacustrine sediment sequences are oases of life and hot spots of microbial activity on the continents, but such deposits remain terra incognita. Furthermore, the sensitivity of Lake Izabal to sea-level variability (Obrist-Farner et al., 2022) offers an opportunity to understand how repeated marine incursions into Lake Izabal may have influenced the development of hot spots of microbial life in the deeply buried sediments.

#### 4.6 Increasing public engagement with geology in Guatemala

An important component of the LIBRE project is its education and outreach plan. During the workshop, participants focused on several ideas to build public interest in the drilling project. These include: (1) involvement of Guatemalan sci-

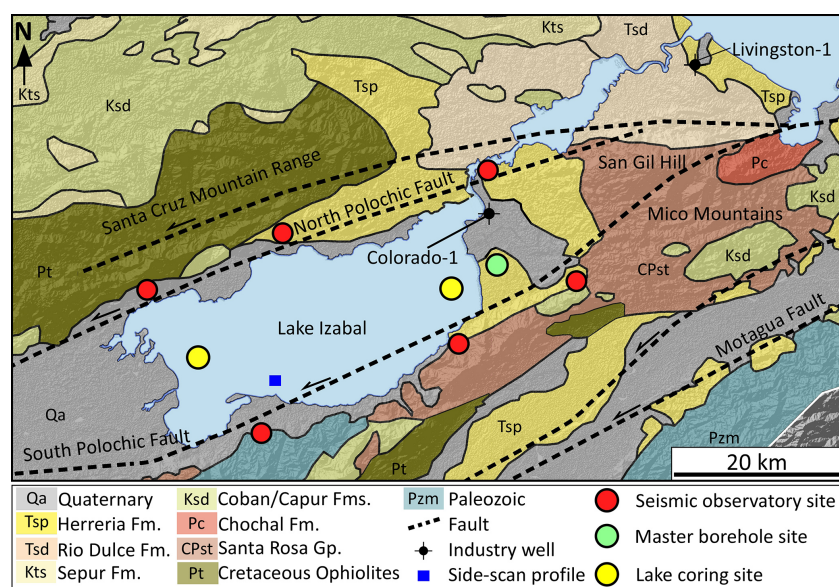


**Figure 7.** Geological map of the study area showing the proposed drilling and coring locations for the LIBRE project. Map modified from Bonis et al. (1970).

entists who have been working in Lake Izabal and on seismic hazard assessment in the country; (2) participation of Guatemalan geoscience undergraduate and graduate students; (3) collaboration with the Authority for the Sustainable Management of Lake Izabal (AMASURLI), the NGO Defensores de la Naturaleza, which is in charge of protecting the Izabal wetland, and the Guatemalan Institute for Seismology, Volcanology, Meteorology, and Hydrology (INSIVUMEH); (4) development of Earth Science stations at museums in Guatemala City and in the offices of AMASURLI and Defensores de la Naturaleza, near Lake Izabal; and (5) production of a book targeted to 10–13-year-old children that highlights the spectacular geology and environments of Guatemala, with the main focus related to the ICDP drilling project.

## 5 The LIBRE scientific drilling plan and site selection

The LIBRE workshop participants discussed drilling locations and operations within the framework of the scientific questions and generated specific drilling targets and borehole instrumentation plans. A consensus was reached on establishing a comprehensive three-component drilling plan that involves a network of instrumented boreholes and collection of long sediment cores, both on land and in Lake Izabal. These include a deep master borehole cored and instrumented onshore on the eastern side of the LIB, six instrumented seismic observatory onshore boreholes in the vicinity of Lake Izabal, and two coring sites offshore in Lake Izabal (Fig. 7). All drilling locations were selected and identified based on: (1) seismic data from the LIB; (2) stratigraphic cor-

relations between seismic lines and the reconstructed progradational infill of the basin (Bartole et al., 2019), ensuring stratigraphic overlap between coring sites and complete recovery of the sediment record to 8 Ma; (3) the velocity model and preliminary palynological work for the Colorado-1 well; and (4) the geologic map (Bonis et al., 1970) and revised stratigraphy for the Izabal region (Obrist-Farner et al., 2020; Fig. 4).

We discussed the drilling and coring of a master borehole on the alluvial plain along the eastern side of the LIB. The area is along seismic line 91-SF-50, 4 km from the location of the Colorado-1 well (Fig. 8) and near two crossing lines (lines 3 and 4; Figs. 7, 8). The master borehole will drill through 500 m of sediment without core recovery because this interval is most likely composed of sandstone and conglomerate, based on information from the Colorado-1 well. We discussed the possibility of then collecting a core from 500 to 1300 m, avoiding drilling deeper because of logistical challenges, available technology, and associated costs. Seismic interpretation (Fig. 8), in combination with the velocity model from the Colorado-1 well and preliminary palynological results, indicates that the 800 m core will contain thick mudstone intervals with minimal sandstone and will at least contain sediment from the Tortonian (~8 Ma) to the Messinian and Pliocene (~5 Ma). The borehole will then be used as a seismic observatory, with the installation of seismometers and strainmeters at multiple depths.

We identified two coring locations within Lake Izabal. The first site is in the eastern side of the lake, located along inline 91-SW-44 and near crossing line 91-SW-92 (Figs. 7, 9). The location is ~5 km from the master borehole site and is in an area where the lake is 15 m deep. A core will be collected to



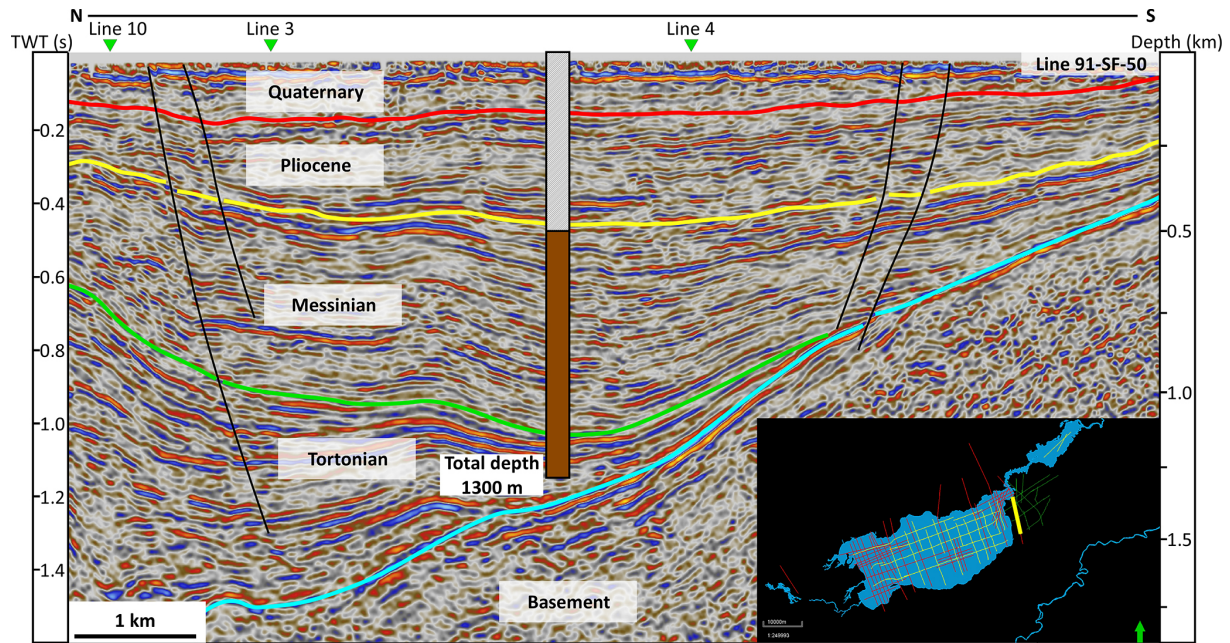


**Figure 8.** Interpreted seismic line 91-SF-50 showing the location and total depth of the master borehole (brown) and the proposed age of the sediment package. The inset map shows the location of profile 91-SF-50 on the eastern side of the Lake Izabal Basin.

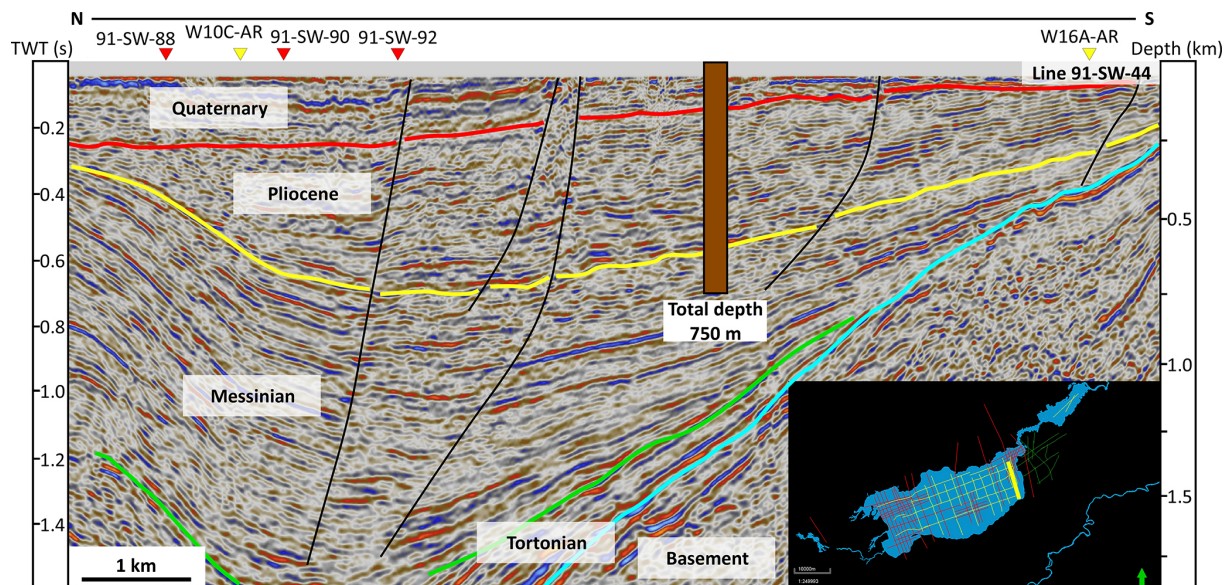


**Figure 9.** Interpreted seismic line 91-SW-44 showing the location and total depth of the eastern lake core (brown) and the proposed age of the sediment package. The inset map shows the location of profile 91-SW-44 on the eastern side of the Lake Izabal Basin.

a depth of  $\sim 750$  m and based on seismic interpretation will contain sediments deposited from the Messinian ( $\sim 6$  Ma) to the present. The second site is on the western side of Lake Izabal, located along inline 91-SW-66 and crossline 91-SW-21 (Figs. 7, 10). We plan to collect a 1000 m core from this site. Seismic interpretation indicates that the 1000 m core will contain a record from  $\sim 2.5$  Ma to the present, providing a highly resolved Quaternary record from the LIB.

Key to investigating the long record preserved in the LIB, obtained by drilling at three sites, is establishment of stratigraphic correlations and a robust chronology. Availability of industry seismic data provides the key to correlate the three planned long sediment cores. Furthermore, workshop participants discussed several suitable chronometric techniques and correlation strategies. We agreed that the LIBRE chronology will combine multiple well-developed techniques. For exam-



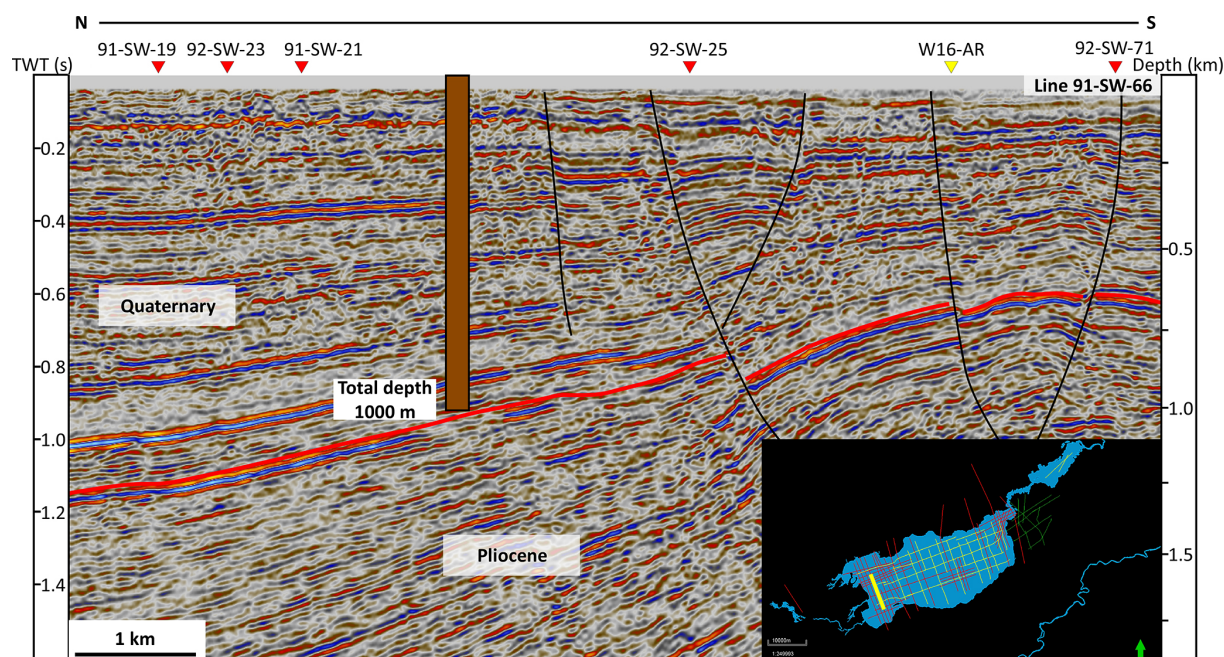


**Figure 10.** Interpreted seismic line 91-SW-66 showing the location and total depth of the eastern lake core (brown) and the proposed age of the sediment package. The inset map shows the location of profile 91-SW-66 on the western side of the Lake Izabal Basin.

ple, presence of CAVA tephra in outcrops surrounding Lake Izabal (Obrist-Farner et al., 2020) and in the broader region (Kutterolf et al., 2016) suggests that the recovered cores will contain sufficient tephra to establish anchor points for correlations. We will also utilize radiocarbon, optically stimulated luminescence, magnetic stratigraphy, U-series dating,  $^{40}\text{Ar}/^{39}\text{Ar}$  geochronology, and cosmogenic nuclide dating to establish correlations between core sites and a robust chronology for the LIB records.

Finally, workshop participants discussed the possibility of creating a set of fault observatory boreholes in the vicinity of Lake Izabal (Fig. 7). To establish a borehole-based observatory, drilling in bedrock is necessary to achieve coupling between the cemented borehole and the host rock. Discussions focused on drilling all boreholes in locations where bedrock is exposed at the surface (Fig. 3). All boreholes will be drilled to a depth of 200 m, cased, and instrumented with seismometers and strainmeters. Establishing a borehole-based observatory provides an excellent opportunity to monitor and record earthquake processes in close proximity to active faults. In particular, the borehole observatory will provide rich information for investigating and monitoring microseismicity and strain rates across the system (e.g., Prevedel et al., 2015) and be used to determine fault activity and geometries, which are essential input parameters for subsequent modeling studies that aim to assess the long-term hazards of the plate boundary.

**Data availability.** No data sets were used in this article.

**Team list.** The LIBRE Scientific Team: Alejandra Aguilar (University of Notre Dame, USA), Maritza Aguirre (Authority for the Sustainable Management of Lake Izabal, Guatemala), Linus Victor Anyanna (Missouri University of Science and Technology, USA), Cristina Arrieta (Missouri University of Science and Technology, USA), Maria Ask (Lulea University of Technology, Sweden), Rodrigo Barillas (Luis von Ahn Foundation, Guatemala), Thorsten Bauersachs (Christian-Albrechts-Universität, Germany), Melissa Berke (University of Notre Dame, USA), Juan Pablo Bernal (National Autonomous University of Mexico, Mexico), Broxton Bird (Indiana University–Purdue University Indianapolis, USA), Marco Bohnhoff (Helmholtz Centre Potsdam GFZ, Germany), Mark Brenner (University of Florida, USA), Erik Brown (University of Minnesota Duluth, USA), Matthias Buecker (TU Braunschweig, Germany), Caroline Burberry (University of Nebraska–Lincoln, USA), Alex Correa-Metrio (National Autonomous University of Mexico, Mexico), Andrew Cohen (University of Arizona, USA), Jason Curtis (University of Florida, USA), Peter Douglas (McGill University, Canada), Edward Duarte (Savoy Mont Blanc University, France), Paula Echeverría-Galindo (TU Braunschweig, Germany), Andreas Eckert (Missouri University of Science and Technology, USA), Jaime Escobar (Universidad del Norte, Colombia), Alejandro Fernandez (University of Minnesota, USA), Merle Fernandez (National Council for Protected Areas, Guatemala), Omar Flores (San Carlos University, Guatemala), Stephen Gao (Missouri University of Science and Technology, USA), Derek Gibson (Missouri University of Science and Technology, USA), Carla Gordillo (San Carlos University, Guatemala), Christoph Gruetzner (Jena University, Germany), Ulrich Harms (International Continental Scientific Drilling Program, Germany), Robert Hatfield (University of Florida, USA), Carlos Jaramillo (Smithsonian Tropical Research Institute, Panama), Bronwen Konecky (Washington

University, St. Louis, USA), Sebastian Krastel (Kiel University, Germany), Stephen Kuehn (Concord University, USA), Steffen Kutterolf (GEOMAR, Germany), Matthew Lachniet (University of Nevada, Las Vegas, USA), Emanuele Lodolo (National Institute of Oceanography and Experimental Geophysics, Italy), Silvia Lopez (National Forest Institute, Guatemala), Julio Luna (San Carlos University, Guatemala), Marta Marchegiano (Vrije University, Belgium), Javier Marquez (NGO Nature Defenders, Guatemala), Patricia Martinez-Garzon (Helmholtz Centre Potsdam GFZ, Germany), Jeremy Maurer (Missouri University of Science and Technology, USA), Trenton McEnaney (Missouri University of Science and Technology, USA), Jasper Moernaut (University of Innsbruck, Austria), Barbara Moguel (National Autonomous University of Mexico, Mexico), Sergio Moran (Northern Central University, Guatemala), Sydney Moser (Missouri University of Science and Technology, USA), Amy Myrbo (Amiable Consulting, USA), Tina Niemi (University of Missouri–Kansas City, USA), Anders Noren (Continental Scientific Drilling Office – University of Minnesota, USA), Francisca Oboh-Ikuenobe (Missouri University of Science and Technology, USA), Jonathan Obrist-Farner (Missouri University of Science and Technology, USA), Bessie Oliva (San Carlos University, Guatemala), Carlos Perez (San Carlos University, Guatemala), Liseth Perez (TU Braunschweig, Germany), Francisco Perez-Sabino (San Carlos University, Guatemala), Brittany Price (Northern Illinois University, USA), Fatima Reyes (Authority for the Sustainable Management of Lake Atitlan, Guatemala), Claudia Romero (University of the Valley of Guatemala, Guatemala), Joshua Rosenfeld (Geological consultant, USA), Daniel Ruiz-Carrascal (Columbia University, USA), Stephanie Scheidt (University of Cologne, Germany), Luca Smeraglia (Italian National Research Council, Italy), Sonia Solis (Luis von Ahn Foundation, Guatemala), Quin Stangeland (University of Minnesota Duluth, USA), Byron Steinman (University of Minnesota Duluth, USA), Jeffery Stone (Indiana State University, USA), Mathias Vinnepand (Leibniz Institute of Applied Geophysics, Germany), Mathew Waters (Auburn University, USA), Nigel Wattrus (University of Minnesota Duluth, USA), Robin Yani (National Institute of Seismology, Volcanology, Meteorology, and Hydrology, Guatemala), Christian Zeeden (Leibniz Institute of Applied Geophysics, Germany), Susan Zimmerman (Lawrence Livermore National Laboratory, USA).

**Author contributions.** JOF organized the workshop and wrote the first draft of the paper. AE, PMJD, LP, ACM, BLK, TB, SZ, StS, MB, SK, JM, OF, CMB, AN, AM, ML, NW, and DG and the entire LIBRE team co-wrote and edited the final version of the paper and provided intellectual input during the workshop.

**Competing interests.** The contact author has declared that none of the authors has any competing interests.

**Disclaimer.** Publisher's note: Copernicus Publications remains neutral with regard to jurisdictional claims in published maps and institutional affiliations.

**Acknowledgements.** We are most grateful to Vivian Paniagua from the Camino Real Hotel in Antigua and Ezequiel Insigna from the Nana Juana Hotel in Izabal for help with hotel accommodations and workshop organization. We also thank Maritza Aguirre and Edwin James from the Authority for the Sustainable Management of Lake Izabal for help with organizing the field excursion in Lake Izabal. This work was partially performed under the auspices of the US Department of Energy and by Lawrence Livermore National Laboratory under contract DE-AC52-07NA27344; this is LLNL-JRNL-844029. Finally, we thank editor Nadine Hallman and Bernd Zolitschka and an anonymous reviewer for comments that helped improve the paper.

**Financial support.** This research has been supported by the Directorate for Geosciences (grant no. 1939228) and the International Continental Scientific Drilling Program.

**Review statement.** This paper was edited by Nadine Hallmann and reviewed by Bernd Zolitschka and one anonymous referee.

## References

- Anselmetti, F., Ashwal, L., Ariztegui, D., Bohnhoff, M., Bomberg, M., Claeys, P., Echelberger, J., Ellsworth, W. L., Goodenough, K., Heubeck, C., Kelemen, P., Kipfer, R., Koeberl, C., Kopf, A., Miller, K., Nordgulen, O., Noren, A., Onstott, T., Pease, V., Philippot, P., Russell, J., Soreghan, G., Stein, M., Verschuren, D., and Yamada, Y.: ICDP Science Plan: 2020–2030, International Continental Scientific Drilling Program, Potsdam, <https://doi.org/10.2312/icdp.2020.001>, 2020.
- Auderset, A., Martínez-García, A., Tiedemann, R., Hasenfratz, A. P., Eglinton, T. I., Schiebel, R., Sigman, D. M., and Haug, G. H.: Gulf Stream intensification after the early Pliocene shoaling of the Central American Seaway, *Earth Planet. Sc. Lett.*, 520, 268–278, <https://doi.org/10.1016/j.epsl.2019.05.022>, 2019.
- Authemayou, C., Brocard, G., Teyssier, C., Suski, B., Cosenza, B., Morán-Ical, S., González-Véliz, C. W., Aguilar-Hengstenberg, M. A., and Holliger, K.: Quaternary seismo-tectonic activity of the Polochic Fault, Guatemala, *J. Geophys. Res.-Sol. Ea.*, 117, B07403, <https://doi.org/10.1029/2012JB009444>, 2012.
- Bacon, C. D., Silvestro, D., Jaramillo, C., Smith, B. T., Chakrabarty, P., and Antonelli, A.: Biological evidence supports an early and complex emergence of the Isthmus of Panama, *P. Natl. Acad. Sci. USA*, 112, 6110, <https://doi.org/10.1073/pnas.1423853112>, 2015.
- Bacon, C. D., Molnar, P., Antonelli, A., Crawford, A. J., Montes, C., and Vallejo-Pareja, M. C.: Quaternary glaciation and the Great American Biotic Interchange, *Geology*, 44, 375–378, <https://doi.org/10.1130/G37624.1>, 2016.
- Baldwin, J. W., Atwood, A. R., Vecchi, G. A., and Battisti, D. S.: Outsize influence of Central American orography on global climate, *AGU Advances*, 2, e2020AV000343, <https://doi.org/10.1029/2020AV000343>, 2021.
- Bartole, R., Lodolo, E., Obrist-Farner, J., and Morelli, D.: Sedimentary architecture, structural setting, and Late Cenozoic depocentre migration of an asymmetric transtensional basin:



- Lake Izabal, eastern Guatemala, *Tectonophysics*, 750, 419–433, <https://doi.org/10.1016/j.tecto.2018.12.004>, 2019.
- Beeson, J. W., Johnson, S. Y., and Goldfinger, C.: The transtensional offshore portion of the northern San Andreas fault: Fault zone geometry, late Pleistocene to Holocene sediment deposition, shallow deformation patterns, and asymmetric basin growth, *Geosphere*, 13, 1173–1206, <https://doi.org/10.1130/GES01367.1>, 2017.
- Ben-Avraham, Z. and Zoback, M. D.: Transform-normal extension and asymmetric basins: An alternative to pull-apart models, *Geology*, 20, 423–426, [https://doi.org/10.1130/0091-7613\(1992\)020<0423:TNEAAB>2.3.CO;2](https://doi.org/10.1130/0091-7613(1992)020<0423:TNEAAB>2.3.CO;2), 1992.
- Ben-Zion, Y., Beroza, G. C., Bohnhoff, M., Gabriel, A. A., and Mai, P. M.: A grand challenge international infrastructure for earthquake science, *Seismol. Res. Lett.*, 93, 2967–2968, <https://doi.org/10.1785/0220220266>, 2022.
- Bonis, S., Bohnenberger, O. H., and Dengo, G.: Mapa geológico de la República de Guatemala, Instituto Geográfico Nacional, 1970.
- Brierley, C. M. and Fedorov, A. V.: Comparing the impacts of Miocene–Pliocene changes in inter-ocean gateways on climate: Central American Seaway, Bering Strait, and Indonesia, *Earth Planet. Sc. Lett.*, 444, 116–130, <https://doi.org/10.1016/j.epsl.2016.03.010>, 2016.
- Brinson, M. M. and Nordlie, F. G.: II. Lakes. 8. Central and South America: Lake Izabal, Guatemala, *SIL Proceedings*, 1922–2010, 19, 1468–1479, <https://doi.org/10.1080/03680770.1974.11896206>, 1975.
- Burke, K. D., Williams, J. W., Chandler, M. A., Hayward, A. M., Lunt, D. J., and Otto-Bliesner, B. L.: Pliocene and Eocene provide best analogs for near-future climates, *P. Natl. Acad. Sci. USA*, 115, 13288–13293, <https://doi.org/10.1073/pnas.1809600115>, 2018.
- Chalk, T. B., Hain, M. P., Foster, G. L., Rohling, E. J., Sexton, P. F., Badger, M. P. S., Cherry, S. G., Hasenfratz, A. P., Haug, G. H., Jaccard, S. L., Martínez-García, A., Pälike, H., Pancost, R. D., and Wilson, P. A.: Causes of ice age intensification across the Mid-Pleistocene Transition, *P. Natl. Acad. Sci. USA*, 114, 13114–13119, <https://doi.org/10.1073/pnas.1702143114>, 2017.
- Colman, S. M.: Continental drilling and paleoclimate records: Recommendations from an international workshop, *PAGES Workshop Report Series*, GeoForschungsZentrum, Potsdam, 30 June–2 July 1995, Workshop Report, Series 96–4, [https://pastglobalchanges.org/sites/default/files/2022-12/1996\\_Continental\\_Drilling\\_PAGES\\_4\\_0.pdf](https://pastglobalchanges.org/sites/default/files/2022-12/1996_Continental_Drilling_PAGES_4_0.pdf) (last access: 20 March 2023), 1996.
- Correa-Metrio, A., Bush, M. B., Pérez, L., Schwalb, A., and Cabrera, K. R.: Pollen distribution along climatic and biogeographic gradients in northern Central America, Holocene, 21, 681–692, <https://doi.org/10.1177/0959683610391321>, 2011.
- Correa-Metrio, A., Bush, M. B., Cabrera, K. R., Sully, S., Brenner, M., Hodell, D. A., Escobar, J., and Guilderson, T.: Rapid climate change and no-analog vegetation in lowland Central America during the last 86 000 years, *Quaternary Sci. Rev.*, 38, 63–75, <https://doi.org/10.1016/j.quascirev.2012.01.025>, 2012.
- Crowell, J. C.: Introduction to geology of Ridge Basin, southern California, in: *Evolution of Ridge Basin, southern California: an interplay of sedimentation and tectonics*, edited by: Crowell, J. C., Geological Society of America Special Paper 367, 1–15, Boulder, Colorado, <https://doi.org/10.1130/0-8137-2367-1.1>, 2003.
- D'Hondt, S., Jørgensen, B. B., Miller, D. J., Batzke, A., Blake, R., Cragg, B. A., Cypionka, H., Dickens, G. R., Ferdelman, T., Hinrichs, K.-U., Holm, N. G., Mitterer, R., Spivack, A., Wang, G., Bekins, B., Engelen, B., Ford, K., Gettemy, G., Rutherford, S. D., Sass, H., Skilbeck, C. G., Aiello, I. W., Guérin, G., House, C. H., Inagaki, F., Meister, P., Naehr, T., Niitsuma, S., Parkes, R. J., Schippers, A., Smith, D. C., Teske, A., Wiegel, J., Padilla, C. N., and Acosta, J. L. S.: Distributions of microbial activities in deep seafloor sediments, *Science*, 306, 2216–2221, <https://doi.org/10.1126/science.1101155>, 2004.
- Drexler, J. W., Rose, W. I., Sparks, R. S. J., and Ledbetter, M. T.: The Los Chocoyos Ash, Guatemala: A major stratigraphic marker in Middle America and in three ocean basins, *Quaternary Res.*, 13, 327–345, [https://doi.org/10.1016/0033-5894\(80\)90061-7](https://doi.org/10.1016/0033-5894(80)90061-7), 1980.
- Duarte, E., Obrist-Farner, J., Correa-Metrio, A., and Steinman, B. A.: A progressively wetter early through middle Holocene climate in the eastern lowlands of Guatemala, *Earth Planet. Sc. Lett.*, 561, 116807, <https://doi.org/10.1016/j.epsl.2021.116807>, 2021.
- Ellis, A., DeMets, C., McCaffrey, R., Briole, P., Cosenza Murallés, B., Flores, O., Guzmán-Speziale, M., Hernández, D., Kostoglodov, V., LaFemina, P., Lord, N., Lasserre, C., Lyon-Caen, H., Rodríguez Maradiaga, M., Molina, E., Rivera, J., Rogers, R., Staller, A., and Tikoff, B.: GPS constraints on deformation in northern Central America from 1999 to 2017, Part 2: Block rotations and fault slip rates, fault locking and distributed deformation, *Geophys. J. Int.*, 218, 729–754, <https://doi.org/10.1093/gji/ggz173>, 2019.
- Feakins, S. J., Liddy, H. M., Tauxe, L., Galy, V., Tierney, J. E., Miao, Y., and Warny, S.: Miocene C<sub>4</sub> grassland expansion as recorded by the Indus Fan, *Paleoceanography and Paleoclimatology*, 35, e2020PA003856, <https://doi.org/10.1029/2020PA003856>, 2020.
- Fedorov, A. V., Brierley, C. M., Lawrence, K. T., Liu, Z., Dekens, P. S., and Ravelo, A. C.: Patterns and mechanisms of early Pliocene warmth, *Nature*, 496, 43–49, <https://doi.org/10.1038/nature12003>, 2013.
- Fedorov, A. V., Burls, N. J., Lawrence, K. T., and Peterson, L. C.: Tightly linked zonal and meridional sea surface temperature gradients over the past five million years, *Nat. Geosci.*, 8, 975–980, <https://doi.org/10.1038/ngeo2577>, 2015.
- Graham, A.: Studies in Neotropical paleobotany. XI. Late Tertiary vegetation and environments of southeastern Guatemala: palynofloras from the Mio-Pliocene Padre Miguel Group and the Pliocene Herrería Formation, *Am. J. Bot.*, 85, 1409–1425, <https://doi.org/10.2307/2446399>, 1998.
- Graham, A.: Late Cretaceous and Cenozoic history of Latin American vegetation and terrestrial environments, Missouri Botanical Garden Press, ISBN 9781930723689, 2010.
- Guzmán-Speziale, M. and Molina, E.: Seismicity and seismically active faulting of Guatemala: A review, *J. S. Am. Earth Sci.*, 115, 103740, <https://doi.org/10.1016/j.jsames.2022.103740>, 2022.
- Harms, U., Koeberl, C., and Zoback, M. D.: Continental scientific drilling: A decade of progress, and challenges for the future, Springer, <https://doi.org/10.1007/978-3-540-68778-8>, 2007.

- Haug, G. H. and Tiedemann, R.: Effect of the formation of the Isthmus of Panama on Atlantic Ocean thermohaline circulation, *Nature*, 393, 673–676, <https://doi.org/10.1038/31447>, 1998.
- Haug, G. H., Tiedemann, R., Zahn, R., and Ravelo, A. C.: Role of Panama uplift on oceanic freshwater balance, *Geology*, 29, 207–210, [https://doi.org/10.1130/0091-7613\(2001\)029<0207:ROPUOO>2.0.CO;2](https://doi.org/10.1130/0091-7613(2001)029<0207:ROPUOO>2.0.CO;2), 2001.
- Hernández, E., Obrist-Farner, J., Brenner, M., Kenney, W. F., Curtis, J. H., and Duarte, E.: Natural and anthropogenic sources of lead, zinc, and nickel in sediments of Lake Izabal, Guatemala, *J. Environ. Sci.*, 96, 117–126, <https://doi.org/10.1016/j.jes.2020.04.020>, 2020.
- Heuer, V. B., Inagaki, F., Morono, Y., Kubo, Y., Spivack, A. J., Viehweger, B., Treude, T., Beulig, F., Schubotz, F., Tonai, S., Bowden, S. A., Cramm, M., Henkel, S., Hirose, T., Homola, K., Hoshino, T., Ijiri, A., Imachi, H., Kamiya, N., Kaneko, M., Lagostina, L., Mannes, H., McClelland, H.-L., Metcalfe, K., Okutsu, N., Pan, D., Raudsepp, M. J., Sauvage, J., Tsang, M.-Y., Wang, D. T., Whitaker, E., Yamamoto, Y., Yang, K., Maeda, L., Adhikari, R. R., Glombitza, C., Hamada, Y., Kallmeyer, J., Wendt, J., Wörmer, L., Yamada, Y., Kinoshita, M., and Hinrichs, K.-U.: Temperature limits to deep seafloor life in the Nankai Trough subduction zone, *Science*, 370, 1230–1234, <https://doi.org/10.1126/science.abd7934>, 2020.
- Holt, B. G., Lessard, J.-P., Borregaard, M. K., Fritz, S. A., Araújo, M. B., Dimitrov, D., Fabre, P.-H., Graham, C. H., Graves, G. R., Jönsson, K. A., Nogués-Bravo, D., Wang, Z., Whitaker, R. J., Fjeldsø, J., and Rahbek, C.: An Update of Wallace's zoogeographic regions of the world, *Science*, 339, 74–78, <https://doi.org/10.1126/science.1228282>, 2013.
- Huntington, K. W. and Klepeis, K. A.: Challenges and opportunities for research in tectonics: Understanding deformation and the processes that link Earth systems, from geologic time to human time. A community vision document submitted to the U.S. National Science Foundation, University of Washington, 84 pp., <http://hdl.handle.net/1773/40754> (last access: 17 March 2023), 2018.
- Inagaki, F., Hinrichs, K. U., Kubo, Y., Bowles, M. W., Heuer, V. B., Hong, W. L., Hoshino, T., Ijiri, A., Imachi, H., Ito, M., Kaneko, M., Lever, M. A., Lin, Y. S., Methé, B. A., Morita, S., Morono, Y., Tanikawa, W., Bihan, M., Bowden, S. A., Elvert, M., Glombitza, C., Gross, D., Harrington, G. J., Hori, T., Li, K., Limmer, D., Liu, C. H., Murayama, M., Ohkouchi, N., Ono, S., Park, Y. S., Phillips, S. C., Prieto-Mollar, X., Purkey, M., Riedinger, N., Sanada, Y., Sauvage, J., Snyder, G., Susilawati, R., Takano, Y., Tasumi, E., Terada, T., Tomaru, H., Trembath-Reichert, E., Wang, D. T., and Yamada, Y.: Exploring deep microbial life in coal-bearing sediment down to ~2.5 km below the ocean floor, *Science*, 349, 420–424, <https://doi.org/10.1126/science.aaa6882>, 2015.
- Jaramillo, C.: Evolution of the Isthmus of Panama: biological, paleoceanographic and paleoclimatological implications, in: *Mountains, climate and biodiversity*, edited by: Hoorn, C., Perrigo, A., and Antonelli, A., Wiley-Blackwell, 323–338, ISBN 978-1-119-15988-9, 2018.
- Jaramillo, C., Sepulchre, P., Cardenas, D., Correa-Metrio, A., Moreno, J. E., Trejos, R., Vallejos, D., Hoyos, N., Martínez, C., Carvalho, D., Escobar, J., Oboh-Ikuenobe, F., Prámparo, M. B., and Pinzón, D.: Drastic vegetation change in the Guajira Peninsula (Colombia) during the Neogene, *Paleoceanography and Paleoclimatology*, 35, e2020PA003933, <https://doi.org/10.1029/2020PA003933>, 2020.
- Jordan, B. R., Sigurdsson, H., Carey, S., Lundin, S., Rogers, R. D., Singer, B., and Barquero-Molina, M.: Petrogenesis of Central American Tertiary ignimbrites and associated Caribbean Sea tephra, in: *Geologic and Tectonic Development of the Caribbean Plate Boundary in Northern Central America*, edited by: Mann, P., Geological Society of America, [https://doi.org/10.1130/2007.2428\(07\)](https://doi.org/10.1130/2007.2428(07)), 2007.
- Kallmeyer, J., Pockalny, R., Adhikari, R. R., Smith, D. C., and D'Hondt, S.: Global distribution of microbial abundance and biomass in seafloor sediment, *P. Natl. Acad. Sci. USA*, 109, 16213–16216, <https://doi.org/10.1073/pnas.1203849109>, 2012.
- Kutterolf, S., Freundt, A., and Pérez, W.: Pacific offshore record of Plinian arc volcanism in Central America: 2. Tephra volumes and erupted masses, *Geochem. Geophys. Geosy.*, 9, Q02S02, <https://doi.org/10.1029/2007GC001791>, 2008a.
- Kutterolf, S., Freundt, A., Pérez, W., Mörz, T., Schacht, U., Wehrmann, H., and Schmincke, H. U.: Pacific offshore record of Plinian arc volcanism in Central America: 1. Along-arc correlations, *Geochem. Geophys. Geosy.*, 9, Q02S01, <https://doi.org/10.1029/2007GC001631>, 2008b.
- Kutterolf, S., Schindlbeck, J. C., Anselmetti, F. S., Ariztegui, D., Brenner, M., Curtis, J., Schmid, D., Hodell, D. A., Mueller, A., Pérez, L., Pérez, W., Schwab, A., Frische, M., and Wang, K. L.: A 400-ka tephrochronological framework for Central America from Lake Petén Itzá (Guatemala) sediments, *Quaternary Sci. Rev.*, 150, 200–220, <https://doi.org/10.1016/j.quascirev.2016.08.023>, 2016.
- Lodolo, E., Menichetti, M., Guzmán-Speziale, M., Giunta, G., and Zanolli, C.: Deep structural setting of the North American-Caribbean plate boundary in eastern Guatemala, *Geophys. Int.*, 48, 263–277, 2009.
- Lyon-Caen, H., Barrier, E., Lasserre, C., Franco, A., Arzu, I., Chiquin, L., Chiquin, M., Duquesnoy, T., Flores, O., Galicia, O., Luna, J., Molina, E., Porras, O., Requena, J., Robles, V., Romero, J., and Wolf, R.: Kinematics of the North American–Caribbean–Cocos plates in Central America from new GPS measurements across the Polochic-Motagua fault system, *Geophys. Res. Lett.*, 33, L19309, <https://doi.org/10.1029/2006GL027694>, 2006.
- Mann, P. (Ed.): Overview of the tectonic history of northern Central America, in: *Geologic and tectonic development of the Caribbean plate boundary in northern Central America*, Geological Society of America Special Paper 428, 1–19, [https://doi.org/10.1130/2007.2428\(01\)](https://doi.org/10.1130/2007.2428(01)), 2007.
- McGirr, R., Seton, M., and Williams, S.: Kinematic and geodynamic evolution of the Isthmus of Panama region: Implications for Central American Seaway closure, *GSA Bulletin*, 133, 867–884, <https://doi.org/10.1130/B35595.1>, 2020.
- Molnar, P.: Closing of the Central American Seaway and the Ice Age: A critical review, *Paleoceanography*, 23, PA2201, <https://doi.org/10.1029/2007PA001574>, 2008.
- Mongol, E., Oboh-Ikuenobe, F., Obrist-Farner, J., Moreno, J. E., and Correa-Metrio, A.: A millennium of anthropic and climate dynamics in the Lake Izabal Basin, eastern lowland Guatemala, *Rev. Palaeobot. Palyno.*, 312, 104872, <https://doi.org/10.1016/j.revpalbo.2023.104872>, 2023.

- Mota-Vidaure, A. B.: Stratigraphy of the coal-bearing strata (Miocene) in the Carboneras Region, Izabal, Guatemala, Department of Geology and Geological Engineering, Colorado School of Mines, 104 pp., <https://hdl.handle.net/11124/172218> (last access: 17 March 2023), 1989.
- NASEM: National Academies of Sciences, E., and Medicine: A vision for NSF Earth Sciences 2020–2030: Earth in Time, The National Academies Press, <https://doi.org/10.17226/25761>, 2020.
- National Research Council (NRC): Scientific Ocean drilling: Accomplishments and challenges, The National Academies Press, Washington, DC, 158 pp., <https://doi.org/10.17226/13232>, 2011.
- Obrist-Farner, J., Brenner, M., Curtis, J. H., Kenney, W. F., and Salvinelli, C.: Recent onset of eutrophication in Lake Izabal, the largest water body in Guatemala, *J. Paleolimnol.*, 62, 359–372, <https://doi.org/10.1007/s10933-019-00091-3>, 2019.
- Obrist-Farner, J., Eckert, A., Locmelis, M., Crowley, J. L., Mota-Vidaure, B., Lodolo, E., Rosenfeld, J., and Duarte, E.: The role of the Polochic Fault as part of the North American and Caribbean Plate boundary: Insights from the infill of the Lake Izabal Basin, *Basin Res.*, 32, 1347–1364, <https://doi.org/10.1111/bre.12431>, 2020.
- Obrist-Farner, J., Brenner, M., Stone, J. R., Wojewódka-Przybył, M., Bauersachs, T., Eckert, A., Locmelis, M., Curtis, J. H., Zimmerman, S. R. H., Correa-Metrio, A., Schwark, L., Duarte, E., Schwalb, A., Niewerth, E., Echeverría-Galindo, P. G., and Pérez, L.: New estimates of the magnitude of the sea-level jump during the 8.2 ka event, *Geology*, 50, 86–90, <https://doi.org/10.1130/G49296.1>, 2022.
- Obrist-Farner, J., Steinman, B. A., Stansell, N. D., and Maurer, J.: Incoherency in Central American hydroclimate proxy records spanning the last millennium, *Paleoceanography and Paleoclimatology*, 38, e2022PA004445, <https://doi.org/10.1029/2022PA004445>, 2023.
- O'Dea, A., Lessios, H. A., Coates, A. G., Eytan, R. I., Restrepo-Moreno, S. A., Cione, A. L., Collins, L. S., de Queiroz, A., Farris, D. W., Norris, R. D., Stallard, R. F., Woodburne, M. O., Aguilera, O., Aubry, M.-P., Berggren, W. A., Budd, A. F., Cozzuol, M. A., Coppard, S. E., Duque-Caro, H., Finnegan, S., Gasparini, G. M., Grossman, E. L., Johnson, K. G., Keigwin, L. D., Knowlton, N., Leigh, E. G., Leonard-Pingel, J. S., Marko, P. B., Pyenson, N. D., Rachello-Dolmen, P. G., Soibelzon, E., Soibelzon, L., Todd, J. A., Vermeij, G. J., and Jackson, J. B. C.: Formation of the Isthmus of Panama, *Sci. Adv.*, 2, e1600883, <https://doi.org/10.1126/sciadv.1600883>, 2016.
- Pagani, M., Freeman, K. H., and Arthur, M. A.: Late Miocene atmospheric CO<sub>2</sub> concentrations and the expansion of C<sub>4</sub> grasses, *Science*, 285, 876–879, <https://doi.org/10.1126/science.285.5429.876>, 1999.
- Parkes, R. J., Cragg, B. A., Bale, S. J., Getliff, J. M., Goodman, K., Rochelle, P. A., Fry, J. C., Weightman, A. J., and Harvey, S. M.: Deep bacterial biosphere in Pacific Ocean sediments, *Nature*, 371, 410–413, <https://doi.org/10.1038/371410a0>, 1994.
- Pérez, L., Correa-Metrio, A., Cohuo, S., González, L. M., Echeverría-Galindo, P., Brenner, M., Curtis, J., Kutterolf, S., Stockhecke, M., Schenk, F., Bauersachs, T., and Schwalb, A.: Ecological turnover in neotropical freshwater and terrestrial communities during episodes of abrupt climate change, *Quaternary Res.*, 101, 26–36, <https://doi.org/10.1017/qua.2020.124>, 2021.
- Plafker, G.: Tectonic aspects of the Guatemala earthquake of 4 February 1976, *Science*, 193, 1201–1208, <https://doi.org/10.1126/science.193.4259.1201>, 1976.
- Powers, S.: Notes on the geology of eastern Guatemala and north-western Spanish Honduras, *J. Geol.*, 26, 507–523, 1918.
- Prance, G. T.: A review of the phytogeographic evidences for Pleistocene climate changes in the Neotropics, *An. MO Bot. Gard.*, 69, 594–624, <https://doi.org/10.2307/2399085>, 1982.
- Prevedel, B., Bulut, F., Bohnhoff, M., Raub, C., Kartal, R. F., Alver, F., and Malin, P. E.: Downhole geophysical observatories: best installation practices and a case history from Turkey, *Int. J. Earth Sci.*, 104, 1537–1547, <https://doi.org/10.1007/s00531-015-1147-5>, 2015.
- Salzmänn, U., Haywood, A. M., Lunt, D. J., Valdes, P. J., and Hill, D. J.: A new global biome reconstruction and data-model comparison for the Middle Pliocene, *Global Ecol. Biogeogr.*, 17, 432–447, <https://doi.org/10.1111/j.1466-8238.2008.00381.x>, 2008.
- Schindlbeck, J. C., Kutterolf, S., Freundt, A., Eisele, S., Wang, K. L., and Frische, M.: Miocene to Holocene marine tephrostratigraphy offshore northern Central America and southern Mexico: Pulsed activity of known volcanic complexes, *Geochim. Geophys. Geosci.*, 19, 4143–4173, <https://doi.org/10.1029/2018GC007832>, 2018.
- Sentman, L. T., Dunne, J. P., Stouffer, R. J., Krasting, J. P., Toggweiler, J. R., and Broccoli, A. J.: The mechanistic role of the Central American seaway in a GFDL Earth System model. Part 1: Impacts on global ocean mean state and circulation, *Paleoceanography and Paleoclimatology*, 33, 840–859, <https://doi.org/10.1029/2018PA003364>, 2018.
- Sigurdsson, H., Kelley, S., Leckie, R. M., Carey, S., Bralower, T., and King, J.: History of circum-Caribbean explosive volcanism: <sup>40</sup>Ar / <sup>39</sup>Ar dating of tephra layers, in: *Proceedings of the Ocean Drilling Program, Scientific Results*, edited by: Leckie, R. M., Sigurdsson, H., Acton, G. D., and Draper, G., 299–314, <https://doi.org/10.2973/odp.proc.sr.165.021.2000>, 2000.
- Soreghan, G. S. and Cohen, A. S.: Scientific drilling and the evolution of the earth system: climate, biota, biogeochemistry and extreme systems, *Sci. Drill.*, 16, 63–72, <https://doi.org/10.5194/sd-16-63-2013>, 2013.
- Strömberg, C. A. E.: Evolution of grasses and grassland ecosystems, *Annu. Rev. Earth Pl. Sc.*, 39, 517–544, <https://doi.org/10.1146/annurev-earth-040809-152402>, 2011.
- Strömberg, C. A. E. and McInerney, F. A.: The Neogene transition from C<sub>3</sub> to C<sub>4</sub> grasslands in North America: assemblage analysis of fossil phytoliths, *Paleobiology*, 37, 50–71, <https://doi.org/10.1666/09067.1>, 2011.
- Tsai, V. C., Hirth, G., Trugman, D. T., and Chu, S. X.: Impact versus fractional earthquake models for high-frequency radiation in complex fault zones, *J. Geophys. Res.-Sol. Ea.*, 126, e2021JB022313, <https://doi.org/10.1029/2021JB022313>, 2021.
- Uno, K. T., Cerling, T. E., Harris, J. M., Kunitatsu, Y., Leakey, M. G., Nakatsukasa, M., and Nakaya, H.: Late Miocene to Pliocene carbon isotope record of differential diet change among East African herbivores, *P. Natl. Acad. Sci. USA*, 108, 6509–6514, <https://doi.org/10.1073/pnas.1018435108>, 2011.
- Utescher, T., Dreist, A., Henrot, A.-J., Hickler, T., Liu, Y.-S., Mosbrugger, V., Portmann, F. T., and Salzmann, U.: Continental climate gradients in North America and West-



- ern Eurasia before and after the closure of the Central American Seaway, *Earth Planet. Sc. Lett.*, 472, 120–130, <https://doi.org/10.1016/j.epsl.2017.05.019>, 2017.
- Vaughan, T. W.: The biologic character and geological correlation of the sedimentary formations of Panama in their relation to the geologic history of Central America and the West Indies, U.S. National Museum Bulletin, 103, 547–612, 1919.
- Vinson, G. L.: Upper Cretaceous and Tertiary stratigraphy of Guatemala, *AAPG Bull.*, 46, 425–456, <https://doi.org/10.1306/BC743835-16BE-11D7-8645000102C1865D>, 1962.
- White, R. A.: Catalog of historic seismicity in the vicinity of the Chixoy-Polochic and Motagua faults, Guatemala, USGS Report 84-88, <https://doi.org/10.3133/ofr8488>, 1984.
- White, R. A.: The Guatemala earthquake of 1816 on the Chixoy-Polochic fault, *B. Seismol. Soc. Am.*, 75, 455–473, 1985.



## MagellanPlus Workshop: mission-specific platform approaches to assessing natural hazards that impact society

Hugh Daigle<sup>1</sup>, João C. Duarte<sup>2</sup>, Ake Fagereng<sup>3</sup>, Raphaël Paris<sup>4</sup>, Patricia Persaud<sup>5</sup>,  
Ángela María Gómez-García<sup>6,7</sup>, and the Lisbon MagellanPlus Workshop Participants<sup>+</sup>

<sup>1</sup>Center for Subsurface Energy and the Environment, The University of Texas at Austin,  
Austin, TX 78712, USA

<sup>2</sup>Instituto Dom Luiz, Faculty of Sciences, University of Lisbon, Lisbon 1749-016, Portugal

<sup>3</sup>School of Earth and Environmental Sciences, Cardiff University, Cardiff, CF10 3AT, UK

<sup>4</sup>Centre National de la Recherche Scientifique, Université Clermont-Auvergne,  
63178 Aubiere CEDEX, Clermont-Ferrand, France

<sup>5</sup>Department of Geosciences, University of Arizona, Tucson, AZ 85721, USA

<sup>6</sup>GEO3BCN, CSIC, Lluís Solé Sabarís/n, 08028 Barcelona, Spain

<sup>7</sup>GFZ German Research Centre for Geosciences, Telegrafenberg, 14473 Potsdam, Germany

<sup>+</sup>A full list of authors appears at the end of the paper.

**Correspondence:** Hugh Daigle (daigle@austin.utexas.edu)

Received: 11 April 2023 – Revised: 28 July 2023 – Accepted: 14 September 2023 – Published: 26 October 2023

**Abstract.** Oceanic natural hazards pose threats to coastal communities worldwide. These include earthquakes, tsunamis, submarine landslides, volcanic eruptions, and tropical cyclones. Scientific ocean drilling can contribute to our understanding and assessment of these hazards through rapid response measurements of hazardous events, learning from past hazard records, and sub-seafloor monitoring and observation. With the impending retirement of the D/V *JOIDES Resolution* and operational limitations of the D/V *Chikyu*, it is important to consider other options for achieving scientific ocean drilling goals. We convened a workshop in Lisbon, Portugal, in July 2022 to identify locations where natural hazards, or preferably several different hazards, can be addressed with mission-specific platform (MSP) drilling, with a consideration of further location-based workshops. Participants split into three working groups to develop hypotheses surrounding climate and tropical cyclones, slope failure, and processes at active margins that can be tested with MSP drilling and can be addressed using the unique capabilities of these platforms. We produced 13 questions or hypotheses with recommendations on specific areas or locations for drilling. Our hope is that the results of this workshop will lay the groundwork for future pre-proposals.

### 1 Introduction

Natural hazards associated with the ocean, including earthquakes, tsunamis, submarine landslides, volcanic eruptions, and tropical cyclones, can have a direct impact on coastal populations and even affect populations located far away from the coast (Koppers and Coggon, 2020). These hazards may interact, such as when tsunamis result in major direct damage and loss of life and also trigger submarine landslides, which themselves can produce tsunamis and dam-

age subsea infrastructure like communications cables, oil and gas pipelines, and offshore wind turbines. In addition to these events, sea level rise and warming sea temperatures are resulting in more damaging tropical cyclones (Walsh et al., 2016), severe and nuisance coastal flooding (Morris and Renken, 2020; Vega et al., 2021), and larger-scale disruptions to ocean and atmospheric circulation (Caesar et al., 2018). Tectonically and climatically driven hazards operate and interact over timescales that are societally relevant, from seasonal to decadal (Telesca, 2007), and their records are pre-

served in the geological record. Natural hazards can be investigated in locations threatened by only one hazard, or locations where several different hazards are present. While earthquakes and associated tsunamis more commonly originate on active margins, tsunamis triggered by submarine landslides can occur on oceanic islands and passive margins as well (Fig. 1). Submarine landslides can themselves be triggered by earthquakes even on passive margins (Schulten et al., 2019) or through cyclic loading by large waves during tropical cyclones, which primarily affect the tropics but also the European Atlantic coast (Sainsbury et al., 2020). The prevalence of various hazards throughout geological history could be investigated as well as linkages with longer-term trends in climate, ocean circulation, and tectonics. The paucity of warning systems for earthquakes and tsunamis (Fig. 1) demonstrates a particular opportunity for devising monitoring networks in other areas with a high natural hazard prevalence.

The International Ocean Discovery Program (IODP) 2050 *Science Framework* (Koppers and Coggon, 2020) lists investigating natural hazards impacting society as a strategic objective, with rapid response measurements of hazardous events, learning from past hazard records, and sub-seafloor monitoring and observation identified as areas where scientific ocean drilling can contribute to understanding. Assessing earthquake and tsunami hazards is specifically identified as a flagship initiative in the *Framework*, while climate-related hazards fall under the flagship initiative to ground-truth future climate change. Mission-specific platforms (MSPs) can provide a significant advantage over large drill ships in investigating natural hazards as they can potentially operate in shallower waters, in more restricted environments, or in sea ice; as MSPs can be specially tailored for deployment or monitoring of instrumentation; and as they have the potential for more rapid deployment in response to new events or repeat deployment over months or years to visit monitoring stations. They do have drawbacks as well, including limitations on water and coring depths as well as a restricted ability to perform shipboard analyses. MSPs are also usually smaller than the IODP vessels but are always able to carry out the minimum of IODP measurements. MSPs therefore have promise for advancing scientific ocean drilling, but the circumstances in which they can be used require definition.

MSPs are chosen by IODP to fulfill specific scientific objectives in certain conditions where the use of IODP vessels (D/V *JOIDES Resolution* or D/V *Chikyu*) is not appropriate. Whereas the *JOIDES Resolution* and *Chikyu* are dedicated drilling vessels, MSPs will be adapted to suit IODP needs as far as possible. Approaches for sample recovery of past MSPs include the use of wireline coring from geotechnical vessels or mining rigs on liftboats and of giant piston corer or seabed drills deployed from research vessels. There also exists the possibility of installing borehole observatories, though this has not been tested on MSPs to date. The

ECORD Science Operator (ESO) typically provides the necessary equipment for core curation and laboratory measurements onboard, usually in containerized facilities that are placed on deck for the length of the cruise. Overall, the science party for an MSP expedition is oftentimes smaller than on an IODP vessel and needs to be more flexible, as scheduling is more variable due to contracting of MSP vessels. After an MSP expedition, the majority of sampling and analysis takes place at the Onshore Science Party (OSP) Facility in Bremen, Germany, attended by the full science party.

MSP expeditions also aim at collecting in situ downhole logs. There are multiple approaches to collect downhole logs, with the standard one for MSP (and the *JOIDES Resolution*) being wireline logging, where tools are sent downhole connected to a cable, a winch, and acquisition equipment. Wireline logging allows real-time data acquisition against depth. The datasets acquired with this method on MSP expeditions can include borehole diameter, total and spectral gamma rays, formation resistivity or conductivity, magnetic susceptibility, acoustic velocity, borehole fluid properties, and borehole wall images. As with the MSP expeditions' flexibility for drilling platform and strategy, the logging equipment can be adapted to various operational setting and scientific objectives. For example, the European Petrophysics Consortium (EPC), part of ESO, has a set of wireline logging tools referred to as "slimline" and designed by ALT, Mount Sopris, Antares, and Geovista. These tools are relatively short (< 2.5 m), lightweight (< 20 kg), and narrow (4–6 cm diameter), and they can be run downhole as stand-alone sensors or combined into toolstrings of up to four tools and less than 40 kg. ESO–EPC provided wireline logging services on five MSP expeditions (see the methods section in Camoin et al., 2007; Mountain et al., 2010; Webster et al., 2011; Morgan et al., 2017; McNeill et al., 2019). Wireline logging services have also been provided by other service companies (see the methods section in Backman et al., 2006; Andr n et al., 2015). ESO also deployed logging-while-tripping slimline tools from seabed drills during Expedition 357 (see the methods section in Fr h-Green et al., 2017).

With the impending retirement of the D/V *JOIDES Resolution* and operational limitations of the D/V *Chikyu*, it is important to consider other options for ocean drilling research. To explore the potential to use MSPs to address natural hazards impacting society, we convened a workshop in Lisbon, Portugal, in July 2022 that brought together 28 researchers from around the world, including nine early-career researchers, both in person and virtually (Daigle et al., 2022).

## 2 Workshop objectives

The objectives of the workshop were (1) to form working groups that would develop plans to address key scientific questions discussed at the meeting, (2) to identify locations where tsunamis, submarine landslides, volcanic eruptions,



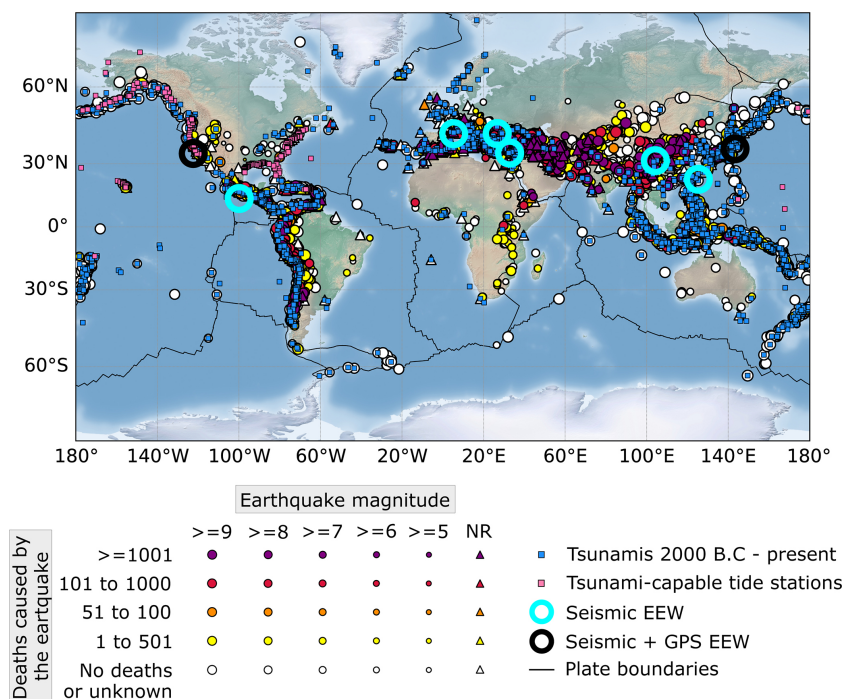


**Figure 1.** Historic earthquakes 2150 BCE–present (NGDC/WDS, 2023a), along with tsunami events 2000 BCE–present (NGDC/WDS, 2023b), tsunami-capable tide stations (NOS/CO-OPS, 2023), and earthquake early warning (EEW) systems (Minson et al., 2015). Earthquakes shown meet at least one of the following criteria: caused at least USD 1 million in damage, resulted in 10 or more deaths, had a magnitude of 7.5 or more, had a Modified Mercalli intensity of *X* or greater, or generated a tsunami.

and tropical cyclones, or preferably several of these hazards, can be addressed with MSP drilling, with a consideration of further location-based workshops, and (3) to develop a set of hypotheses that can be tested with MSP drilling which would lay the groundwork for future pre-proposals.

### 3 Working group discussions

During the workshop, we created three working groups that developed hypotheses and questions focused on three main topics: climate and tropical cyclones, slope failure, and processes at active margins. These hypotheses and questions can be used to develop drilling proposals for specific locations. Specific locations mentioned by the working groups are shown in Fig. 2.

#### 3.1 Working Group 1: climate and tropical cyclones

The climate and tropical cyclones working group agreed that the northern Gulf of Mexico presents the best location to address questions about climate change and its influence on tropical cyclone frequency and intensity. The Gulf of Mexico is ideal because of its overall thick sediment column (up to 20 km; Galloway, 2008) and well-preserved sedimentary sections in salt withdrawal minibasins, growth faults, river deltas, and basin-floor fans (Martin, 1978). The group

phrased two hypotheses of global significance that may be addressed in the Gulf of Mexico.

##### 3.1.1 Hypothesis 1

We hypothesize that past hurricane frequency and intensity in the Gulf of Mexico have responded to changes in the strength of ocean circulation patterns, most notably the strength of the Gulf Stream and the Atlantic Meridional Overturning Circulation (AMOC). Warm core eddies spun off the Loop Current can cause rapid intensification of hurricanes (e.g., Hurricane Katrina in 2005; Scharroo et al., 2005). The reconstruction of sea surface temperatures (SSTs) and storm frequency from sedimentary deposits in the Gulf of Mexico could be used to understand how much influence the variability in the Gulf Stream dynamics has on Gulf of Mexico storms.

*Drill site needs and potential outcomes.* MSPs could be used to collect very high-resolution storm and SST records in areas with continuous late Pleistocene to Holocene sedimentary sections. These time intervals contain many episodes of AMOC slowdown (Heinrich Events, Younger Dryas) that would allow us to understand the impact of AMOC variability on hurricane development in this region.

*Potential drill sites.* Salt withdrawal minibasins along the Gulf of Mexico's margin contain suitable deposits, typically representing a sediment thickness of 100–200 m.

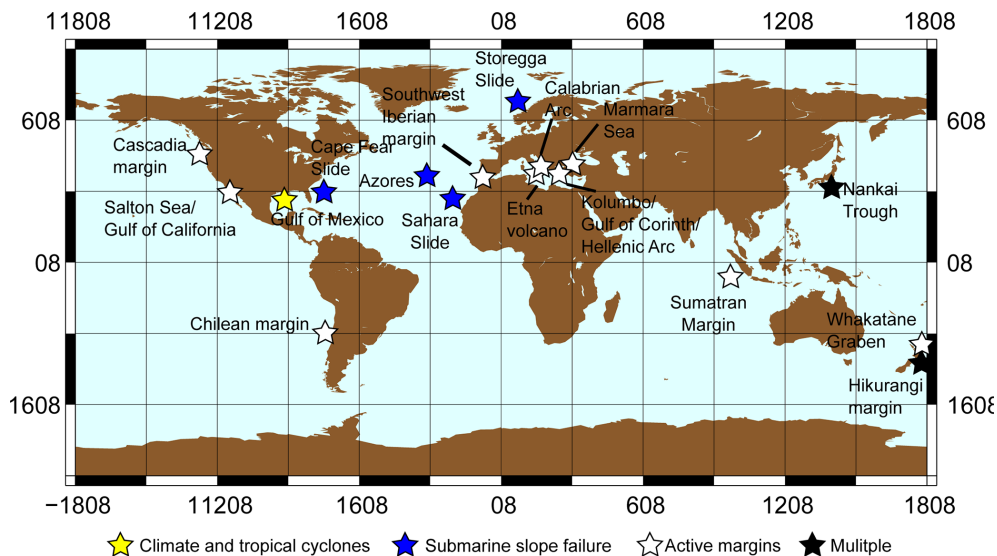


**Figure 2.** Locations recommended in the workshop color-coded by working group.

### 3.1.2 Hypothesis 2

Storm frequency has a strong influence on precipitation and streamflow in the western Gulf of Mexico and southwestern United States. Hurricane Harvey (2017) dropped more than 1500 mm of rain in parts of southeast Texas in less than a week and storm-related precipitation is expected to increase as climate warms over the 21st century (Bacmeister et al., 2018). Cores from the Gulf of Mexico have provided evidence for past occurrence of large flood events on the Mississippi River (e.g., deglacial meltwater pulses; Clark et al., 1996; Brown and Kennett, 1998).

*Drill site needs and potential outcomes.* Drill sites should be located offshore of rivers that provide sedimentary flux from catchments that are affected by tropical cyclones. These locations can provide information on flooding events, particularly those during past climate intervals warmer than the present day such as the mid-Holocene or previous interglacials. MSP drilling could include long cores, which could be combined with borehole or seafloor monitoring of the development of mud flow events to establish modern depositional system analogs and seismic surveys of the continental shelf to map potential sediment source areas.

*Potential drill sites.* Suitable locations can be found offshore of the mouths of the Rio Grande, Colorado River, Brazos River, Sabine River, and other rivers on the western Gulf of Mexico coast. Salt withdrawal minibasins offshore of the mouth of the Rio Grande may make the best locations as they tend to preserve more continuous sedimentary records.

### 3.2 Working Group 2: submarine slope failure

#### 3.2.1 Hypothesis 1: preconditioning factors cause repeat landslides

We hypothesize that through the Neogene, the presence of similar preconditioning factors has typically caused submarine landslides to occur repeatedly at the same location. Preconditioning factors can include sediment properties, pore fluid pressure, fluid chemistry, mechanical stratigraphy, and oversteepening/slope angle (Hampton et al., 1996). These can be investigated with hydraulic piston cores (equivalent to the *JOIDES Resolution* advanced piston coring (APC) tool) down to 1000 m water depth in most cases. Required measurements include core physical properties and pore fluid chemistry, in situ pore pressure and heat flow measurements, and anything that can provide evidence of changes in stresses, e.g., borehole breakouts or drilling-induced tensile fractures obtained from multi-axis caliper or borehole image logs. In situ observatories can help establish trends in pore pressure, heat flow, and stress over time.

*Drill site needs and potential outcomes.* Drill sites should be located near the headscarp of a submarine landslide. Core analysis, downhole measurements, and in situ observatories will provide evidence of the presence or absence of preconditioning factors, and how these change over time.

*Potential drill sites.* There are many locations that could be targeted on both active and passive margins. The Cape Fear Slide, Storegga Slide, and Sahara Slide are potential targets on passive margins, while active margins such as the Nankai Trough, the Sumatra Margin, and the Hikurangi Margin could be investigated.

### 3.2.2 Hypothesis 2: landslides are externally triggered

Preconditioning factors are necessary but not sufficient for submarine landslides, and in most cases an external trigger is needed. Triggers include earthquakes, storm wave loading, abrupt shifts in sedimentation, tectonic oversteepening, changes in ocean temperature, gas hydrate dissociation, volcanism, and salt diapirism (e.g., Urlaub et al., 2013). This hypothesis can be tested by recovering cores, fluid samples, and pore pressures to demonstrate that slope failure could occur in an area that would otherwise be stable. Note that, if hypothesis 1 is true, then one initiation can cause the area to be prone to failure for many years afterwards.

*Drill site needs and potential outcomes.* Ideal sites to test this hypothesis should be locations with no evidence of slope failure but near known submarine landslides. Measured properties could be used as inputs for models to predict conditions for slope failure.

*Potential drill sites.* This hypothesis could be tested at the same locations as the previous hypothesis, with the addition of volcanic islands such as the Azores.

### 3.2.3 Hypothesis 3: retrogressive failure leaves a signature

Retrogressive failure leaves a detectable perturbation of pore pressure and heat flow. The pore pressure perturbation is related to failure propagation upslope, and the heat flow perturbation is a leftover signature of it. Anomalously high heat flow also could be evidence of salt diapirism. This technique can also be used to infer gas hydrate (in)stability. This hypothesis would best be tested with in situ measurements and longer-term monitoring with dense spatial sampling. One particular location that should be targeted is the distal toe of a submarine landslide, although this may be deeper than MSP capabilities ( $\sim 1700$  m) in most locations. For example, the toe of the Cape Fear Slide is at about 5.4 km water depth (Popenoe et al., 1993), while that of the Storegga Slide is at 3–3.5 km water depth (Bugge et al., 1988).

*Drill site needs and potential outcomes.* Potential sites should be located at submarine landslides with known retrogressive failure. Long-term measurements of pore pressure and heat flow can provide evidence of the current state of the subsurface around submarine landslides and its response to external perturbations.

*Potential drill sites.* The Cape Fear Slide is a well-studied example of retrogressive failure that could be targeted to test this hypothesis.

### 3.2.4 Hypothesis 4: active margins have more earthquakes than landslides

Submarine landslides occur less frequently than earthquakes on active margins because of (a) seismic strengthening and (b) sediment accumulation rates. It is established that seismic shaking tends to increase the shear strength of sediments

(Sawyer and DeVore, 2015), so slope failure on an active margin would tend to require a large amount of sediment to accumulate between earthquakes.

*Drill site needs and potential outcomes.* To test this hypothesis, high-resolution seismic data, core data to understand strength and sedimentation rate, and a good paleoseismological record are required. A drilling strategy to test this hypothesis would consist of a transect across an accretionary prism with perched basins that preserved mass transport deposits.

*Potential drill sites.* The Nankai Trough or the Hikurangi Margin make excellent candidates to test this hypothesis due to the large volume of existing data.

## 3.3 Working Group 3: active margins

### 3.3.1 Hypothesis 1: major earthquakes have precursors

Transient events are observed at plate boundaries worldwide, but we currently do not understand how these relate to the timing of larger earthquakes. In a few cases, slow slip events at subduction zones have been observed in the weeks to months prior to great megathrust earthquakes (e.g., the Tōhoku-oki 2011 and Iquique 2014 earthquakes) (Ito et al., 2013; Ruiz et al., 2014). Resolving whether great earthquakes have precursors is a societally important question, critical for more effective, short-term earthquake forecasting. As most subduction zone earthquakes nucleate on offshore megathrusts, detailed offshore monitoring of potential transient deformation is required.

*Drill site needs and potential outcomes.* Drill sites should be located near active faults in areas with large earthquakes. Due to the high-noise ocean environment, the most viable tool to undertake this type of monitoring is borehole observatories, specifically detecting volumetric strain using changes in formation pore pressure as a proxy, as done in boreholes offshore subduction margins in Costa Rica, Japan, and New Zealand (Davis et al., 2015; Araki et al., 2017; Wallace et al., 2019).

*Potential drill sites.* Highly active transform faults that are the site of frequently recurring moderate to large-magnitude earthquakes, such as the Gofar transform fault with quasi-periodic  $M_w$  6–7 events every 5–6 years (McGuire, 2008), could be ideal targets to investigate potential precursors through the installation of borehole observatories. Amphibious experiments complementing the already existing infrastructure could be developed in both the Chilean Margin (Barrientos and the National Seismological Center (CSN) Team, 2018) and the Marmara Sea (MARSite; Özel et al., 2017). The Salton Sea and the Gulf of California may also be potential sites, as a southward extension of the U.S. Geological Survey Parkfield, CA, network, but are complicated by transtensional deformation (Brothers et al., 2009). In addition, the Hikurangi Margin, Hellenic Arc, and Southwest



Iberian Margin could be other locations targeted to test this hypothesis.

### 3.3.2 Hypothesis 2: rupture barriers are persistent

Several hypotheses exist to explain rupture terminations that appear to be persistent over the timescale of available earthquake records. These range from the presence of plate boundary transitions (Wallace et al., 2012), to changes in upper-plate/lower-plate properties and/or geometrical changes (Collot et al., 2004), stress heterogeneity (Huang, 2018), and the presence of positive relief structures such as seamounts or ridges (Sparkes et al., 2010). However, no conclusive evidence exists to confirm that these historical or recent rupture terminations are persistent over longer timescales. Potential boundary-breaking earthquake ruptures could lead to earthquakes that substantially exceed historical or instrumentally observed magnitudes (maybe even  $M > 10$ ) and that have recurrence intervals of several thousands of years or more (Goldfinger et al., 2013). This is much longer than the current length of available paleoseismic records along any subduction zone around the world, meaning we cannot reliably exclude their occurrence.

To evaluate the persistence of rupture/segment barriers and unveil (or discard) the existence of these larger-than-observed earthquakes, the available paleoseismic records need to be extended back in time. Long-term paleoseismic records are thus needed along the entire length of subduction margins. This requires sedimentary records in both the onshore (coastal and lake) and offshore realm and relies on the identification of secondary seismic effects such as shaking imprints (e.g., turbidites, soft-sediment deformation) and tsunami deposits. Identification of synchronous deposits along an entire subduction margin could hint at these extreme events, but the current limitations of dating accuracy do not allow distinguishing single, large events from short-term successions of ruptures (e.g., stress triggering). Therefore, key records at locations that are currently believed to form rupture barriers are essential to verify the existence of imprint stacks, resulting from rupture cascades, while the presence of a single deposit could hint at large, through-going ruptures.

*Drill site needs and potential outcomes.* Drill sites need to have historic earthquake records that show earthquake boundaries; a detailed understanding of sediment routing systems and several preferentially isolated depositional basins spanning the entire margin and containing high-resolution, continuous paleoseismic event deposit stratigraphies, for which sedimentary source areas can be well constrained to allow for the reconstruction of past rupture areas; and a straight margin to avoid complications of changes in fault geometry (unless testing the role of plate margin geometry on arresting earthquake rupture is desired). The outcome of drilling would ideally be a long-term extension of the paleoseismic record.

*Potential drill sites.* The South American subduction zone is a potential target to investigate this hypothesis. It generated the largest known earthquake (magnitude 9.6, in 1960), and it is potentially able to generate the largest earthquakes of any subduction zone (Graham et al., 2021). In addition, many lakes along the margin could be sampled by continental drilling to constrain the paleoseismic record (Bernhardt et al., 2015). Other potential locations include the Marmara Sea, the Salton Sea/Gulf of California, the Hikurangi Margin, Cascadia, the Hellenic Arc, and the Calabrian Arc.

### 3.3.3 Hypothesis 3: fault coupling characteristics are persistent in space and time

Subduction plate interfaces commonly have spatially variable interseismic coupling, where strongly coupled segments are most likely to produce large earthquakes and weakly coupled segments tend to slip aseismically (Fagereng, 2011; Saito and Noda, 2022). It is unclear whether geodetically constrained coupling patterns persist over multiple earthquake cycles and also to what extent poorly coupled regions may slip during earthquakes that nucleate in adjacent coupled areas. Controls on coupling could include fluid pressure (Moreno et al., 2014), downgoing plate roughness (Ruff, 1989; Wang and Bilek, 2011; van Rijnsingen et al., 2018), or rock physical properties at depth, including grain size, mineralogy, and fluid composition (Chen et al., 2013; Scholz, 2019).

*Drill site needs and potential outcomes.* Direct evidence for temporal variation in locking may be sought from the paleoseismic record by looking for evidence for past earthquakes and how their spatial pattern compares with current geodetic locking. This would require a margin where the current geodetic locking pattern is well characterized and where there are appropriate sites for paleo-seismicity (e.g., Chilean margin). The expectation, if coupling characteristics are persistent in time and space, would be that in locked regions, there is evidence for large earthquakes (where the meaning of “large” should be calculated from the size of the locked patch). These earthquakes should, however, not have propagated into poorly coupled segments. Another direct measure is variations in interseismic periods if observatories can be installed and maintained over multiple earthquake cycles.

*Potential drill sites.* Sites with existing reflection seismic and other data that could be used to test this hypothesis include the Chilean Margin, the Marmara Sea, the Hellenic Arc, the Salton Sea/Gulf of California, Cascadia, the Nankai Trough, the Hikurangi Margin, and Costa Rica Margin.

### 3.3.4 Hypothesis 4: subduction earthquakes are cyclic at multiple timescales

The 2011  $M_w$  9.0 Tōhoku-oki Japan earthquake occurred in an area where scientists thought large-magnitude earthquakes were less likely (Stein et al., 2012). In contrast, the

2010  $M_w$  8.8 Maule earthquake in Chile was somewhat expected but extended beyond the boundaries of the seismic gap that was believed to be present (Métois et al., 2012). These recent, very high-magnitude earthquakes painfully highlight how little we still know about megathrust earthquake recurrence along subduction zones, despite recent advances and widespread paleo-seismological studies. The concepts of seismic gaps and characteristic earthquakes are simplified and need further refining.

Mapping the spatiotemporal behavior of megathrust earthquakes thus forms a crucial step towards validation of physics-based earthquake cycle models but is currently not possible on sufficiently long timescales and/or spatial extents along any of the subduction zones. Instrumental and historical records are too short, and coastal records (tsunami deposits, uplifted terraces or corals, subsided paleosols) are affected by global eustatic sea level change and do not extend far beyond the last maximum sea level high stand of the Holocene.

*Drill site needs and potential outcomes.* Scientific ocean (and continental) drilling and coring of high-resolution marine and/or lacustrine paleoseismic archives extending well into the late Pleistocene and further back in time are the only reasonable approach to potentially deliver observational data on timescales long enough to robustly test the earthquake (super-)cycle hypothesis. Therefore, drill sites need to have well-preserved, continuous sedimentary sections.

*Potential drill sites.* Drilling to test this hypothesis could be conducted at the Chilean Margin, at the Hikurangi Margin, and in Cascadia.

### 3.3.5 Hypothesis 5: fault slip rates vary over multiple seismic cycles

Fault slip rates are critical for seismic hazard assessment and can be calculated over a range of different timescales from < 1 year to millions of years. Variations between short-term and long-term slip rates have been recorded, bringing into question the usefulness of slip rates calculated over a particular time period for seismic hazard assessment; i.e., are geological rates relevant to apply to modern seismic hazard estimates? Do modern satellite-derived slip rates (from GPS) give a good indication of the areas most at risk from earthquakes (e.g., Bell et al., 2011; Cowie et al., 2012; Fagereng and Biggs, 2019)? Our understanding of fault growth and fault slip is least well-constrained in the  $10^4$ – $10^6$ -year range (reviewed in Pan et al., 2022). There are a number of ways in which we can assess slip rates in the range of  $10^4$ – $10^6$  years using offshore MSP drilling/piston core data, including targeted giant piston coring or short drilled sections on either side of a fault (or one side of the fault only if horizons can be confidently correlated) to calculate offset and slip rate: using submarine paleo-seismology to identify evidence of individual earthquake slip events in high-resolution seismic data with ground-truthing of age and timing or using an onshore–

offshore approach for a comparison of slip rates over different timescales on an active normal fault.

*Drill site needs and potential outcomes.* Potential locations to study slip rates through time would ideally have the following: (i) high sedimentation rates, (ii) high slip rates (to give the greatest chance of slip rate variations being resolved), (iii) a constrained onshore record of uplift rates to compare with results of ocean/lake drilling, and (iv) high-resolution seismic reflection data imaging basin stratigraphy in the hanging wall and ideally also in the footwall.

*Potential drill sites.* Drilling to test this hypothesis could be conducted at active rift zones and potentially at suitable transform zones and subduction margins, e.g., the Corinth Rift (Greece), the Salton Sea/Gulf of California, the Marmara Sea, the Chilean Margin, and the Hikurangi Margin.

### 3.3.6 Hypothesis 6: faults grow rapidly to their full length

Seismological and geodetic data reveal that earthquake rupture patterns are complex and variable, often with temporal and spatial clustering of events (e.g., Wells and Coppersmith, 1994). In contrast, ancient normal faults commonly observed in high-resolution 3D seismic reflection datasets reveal strikingly consistent patterns of displacement accumulation along strike, commonly described as the classic “bell-shaped” cumulative displacement profile with greatest overall displacement in the center of the fault decreasing toward the tips (e.g., Cowie and Scholz, 1992). Other mature faults within extended systems have consistent slip rates along strike, potentially indicating linkage of segments at depth. Exactly how faults evolve in terms of how multiple earthquake cycles and aseismic slip accrue to produce the long-term fault geometry is unknown. Most work on this problem has focused on normal faults, as they are associated with a convenient marker of fault growth in the form of sediment thickness increases in the hanging wall when a fault is active at the Earth’s surface (i.e., it is a “growth fault”). Therefore, to address the question of “how faults grow” will likely require observations from active continental rifts. Understanding how faults develop has relevance to earthquake hazards because of how we interpret fault slip rates over different time periods (see Sect. 3.3.5 above) and how earthquake slip builds up to fault slip over longer timescales. One category of normal faults that is relatively understudied is outer rise normal faults at subduction zones. These faults, caused by flexure of the downbending subducting plate, are a significant tsunami hazard, and they are potential sites for investigating the normal fault evolution of this hypothesis.

*Drill site needs and potential outcomes.* It may be possible to investigate in detail how faults establish themselves and evolve both laterally and in terms of displacement accrual by identifying a study location where a very young fault exists at a shallow depth, which is well imaged by 3D or pseudo-3D high-resolution seismic reflection data. If age-constraints are available from drilling/piston coring, the interpretation of

high-resolution seismic reflection data will allow variations in sediment thickness between the hanging wall and footwall to be investigated at the millennial scale and hence how slip has accrued along different parts of the fault. This timescale links the supra-millennial scale of modern geological and seismological observation and the million-year-averaged observations from seismic reflection data in rifts.

*Potential drill sites.* Drilling to test this hypothesis could be conducted at the following locations: the Corinth Rift (Greece) (McNeill et al., 2019; Nixon et al., 2016), the Whakatane Graben (New Zealand) (Taylor et al., 2004), and outer rise normal fault systems at subduction margins.

### 3.3.7 Hypothesis 7: tectonic activity is linked to the timing of volcanic eruptions

Active submarine volcanoes are linked to several of the deadliest geohazards such as tsunami, earthquakes, landslides, pyroclastic material, and gas release. However, they pose difficult drilling conditions as they are covered by thin microbial crusts, and they have active hydrothermal systems and unstable slopes. MSP drilling presents an ideal way to sample these locations. Volcanic activity (frequency, volume, magma flux) is affected by tectonic activity at large length scales (e.g., plate tectonics) and smaller scales (e.g., development of preferential pathways for magma ascent due to local deformation). On the other hand, tectonic activity can also be affected by volcanism, for example in the case of magma ascent triggering localized seismic activity. This interconnection can be investigated through a high-resolution record of eruptive styles at individual centers that will give a characterization of their evolution in time, their intensity, and their spatial and temporal distribution. Large tectonic events recorded in sedimentary basins, like onlap surfaces, seismogenic turbidites, and homogeneities, can correlate with activation/deactivation of different volcanic centers, changes in eruptive style, and particularly large explosive eruptions.

*Drill site needs and potential outcomes.* Drilling should be conducted at sites with a well-preserved record of volcanism and tectonic events. Integration of paleoseismic and tephrochronological records need a good correlation between onshore and offshore records. Offshore geodesy would also be a priority to reconstruct the evolution of deformation around and within these volcanic centers. Possible correlations also exist with the paleoclimate record.

*Potential drill sites.* This hypothesis could be tested by drilling at the Chilean Margin, the Kolumbo submarine volcano northeast of Santorini (building on recent IODP drilling), Etna, the Hikurangi Margin, the Hellenic Arc, and the Calabrian Arc.

## 4 Conclusions

In this workshop, we defined questions and hypotheses about natural hazards that could be tested specifically with MSPs.

The unique characteristics of MSPs compared to IODP drill ships require some shifts in our thinking about how to interrogate the subsurface but also present opportunities in terms of long-term monitoring, drilling in shallow water, and amphibious proposals. The workshop discussions recognized the growing needs of highly populated regions along tectonically active or hazardous settings for a better assessment of earthquake, tsunami, volcanic, and climate hazards. A number of key questions/hypotheses, in combination with potential target locations and research strategies, were formulated that need to be tested in order to mitigate future risks.

MSP missions have the potential to contribute to the development of amphibious observatories, taking advantage of well-monitored onshore regions and leveraging partnerships with the continental drilling community. We considered that this strategy could be prioritized in the near future. The flexibility of an MSP and the relatively low costs in some cases make it worth the community effort in building a long-term infrastructure that allows us to monitor diverse geohazards from such observatories. The climate and tropical cyclones working group identified the Gulf of Mexico, where key questions can be answered by MSP drilling. The submarine slope failure working group identified areas on both passive and active margins where hypotheses can be tested, including the Cape Fear Slide, the Storegga Slide, the Sahara Slide; the Nankai Trough, the Sumatra Margin, and the Hikurangi Margin; and volcanic islands such as the Azores. Finally, the active margins working group selected priority sites for the near future including the Chilean margin, the Hikurangi Margin, the Marmara Sea, the Salton Sea/Gulf of California, Corinth Rift, and outer-rise normal fault systems. Other sites with high hazard exposure on active margins include regions around the Hellenic and Calabrian arcs, the Southwest Iberian, Cascadia, and the Sumatra and Hikurangi margins. We hope that this work serves as the foundation for future drilling proposals in the regions we identified or in other areas around the world.

**Data availability.** The datasets containing the historic earthquakes 2150 BCE–present (<https://doi.org/10.7289/V5TD9V7K>, NGDC/WGS, 2023a), the tsunami events 2000 BCE–present (<https://doi.org/10.7289/V5PN93H7>, NGDC/WGS, 2023b) and the tsunami-capable tide stations (<https://tidesandcurrents.noaa.gov/tsunami/>, NOS/CO-OPS, 2023) are available at the corresponding websites of the NOAA National Geophysical Data Center/World Data Service.

**Team list.** Tiago Alves (School of Earth and Environmental Sciences, Cardiff University, Cardiff, UK), Fernando Barriga (Instituto Dom Luiz, Faculty of Sciences, University of Lisbon, Lisbon, Portugal), Rebecca Bell (Department of Earth Science and Engineering, Imperial College London, London, UK), Julia Carvalho (Department of Earth Sciences, University of Pisa, Pisa, Italy; Department of Earth Sciences, University of Florence, Florence, Italy),



Yu-Chun Chang (Department of Earth and Environmental Sciences, University of Manchester, Manchester, UK), Gareth Davies (Geoscience Australia, Canberra, Australia), Davide Gamboa (Department of Geosciences, University of Aveiro, Aveiro, Portugal), Álvaro González (Centre de Recerca Matemàtica, Barcelona, Spain), Achim Kopf (MARUM, University of Bremen, Bremen, Germany), Holger Kuhlmann (MARUM, University of Bremen, Bremen, Germany), Lisa McNeill (School of Ocean and Earth Science, University of Southampton, Southampton, UK), Uisdean Nicholson (School of Energy, Geoscience, Infrastructure and Society, Heriot-Watt University, Edinburgh, UK), Paraskevi Nomikou (Faculty of Geology and Geo-Environment, University of Athens, Athens, Greece), Michael Strasser (Department of Geology, University of Innsbruck, Innsbruck, Switzerland), Mary Thompson (Department of Geology & Geophysics, Texas A&M University, College Station, TX, USA), Michael Toomey (United States Geological Survey, Reston, VA, USA), Caroline Ummenhofer (Woods Hole Oceanographic Institution, Woods Hole, MA, USA), Paola Vannucchi (Department of Earth Sciences, University of Florence, Florence, Italy), Laura Wallace (GNS New Zealand, Lower Hutt, New Zealand; Institute for Geophysics, The University of Texas at Austin, Austin, TX, USA), and Kathleen Wils (Department of Geology, Ghent University, Ghent, Belgium).

**Author contributions.** HD: conceptualization, funding acquisition, investigation, writing. JD: conceptualization, funding acquisition, investigation, resources, writing. AF: conceptualization, funding acquisition, investigation, writing. RP: conceptualization, funding acquisition, investigation, writing. PP: conceptualization, funding acquisition, investigation, writing. AMGG: investigation, visualization, writing. Workshop participants: investigation, writing.

**Competing interests.** The contact author has declared that none of the authors has any competing interests.

**Disclaimer.** Any use of trade, firm, or product names is for descriptive purposes only and does not imply endorsement by the U.S. Government.

**Publisher's note:** Copernicus Publications remains neutral with regard to jurisdictional claims made in the text, published maps, institutional affiliations, or any other geographical representation in this paper. While Copernicus Publications makes every effort to include appropriate place names, the final responsibility lies with the authors.

**Acknowledgements.** The authors wish to thank the students and staff of Instituto Dom Luiz for their assistance during the workshop, in particular Célia Lee.

**Financial support.** This workshop was funded by the European Consortium for Ocean Research Drilling (ECORD) and the International Continental Scientific Drilling Program (ICDP). Funding

for participation of US-based scientists was provided by the United States Science Support Program (USSSP).

**Review statement.** This paper was edited by Nadine Hallmann and reviewed by Ken Ikehara and one anonymous referee.

## References

- Andrén, T., Jørgensen, B. B., Cotterill, C., and the Expedition 347 Scientists: Expedition 347 summary, *Proc. IODP*, 347, 1–66, <https://doi.org/10.2204/iodp.proc.347.101.2015>, 2015.
- Araki, E., Saffer, D. M., Kopf, A. J., Wallace, L. M., Kimura, T., Machida, Y., Ide, S., Davis, E., and the Expedition 365 Scientists: Recurring and triggered slow-slip events near the trench at the Nankai Trough subduction megathrust, *Science*, 356, 1157–1160, <https://doi.org/10.1126/science.aan3120>, 2017.
- Backman, J., Moran, K., McInroy, D. B., Mayer, L. A., and the Expedition 302 Scientists: Expedition 302 summary, *Proc. IODP*, 302, 1–22, <https://doi.org/10.2204/iodp.proc.302.101.2006>, 2006.
- Bacmeister, J. T., Reed, K. A., Hannay, C., Lawrence, P., Bates, S., Truesdale, J. E., Rosenbloom, N., and Levy, M.: Projected changes in tropical cyclone activity under future warming scenarios using a high-resolution climate model, *Climatic Change*, 146, 547–560, <https://doi.org/10.1007/s10584-016-1750-x>, 2018.
- Barrientos, S. and the National Seismological Center (CSN) Team: The seismic network of Chile, *Seismol. Res. Lett.*, 89, 467–474, <https://doi.org/10.1785/0220160195>, 2018.
- Bell, R. E., McNeill, L. C., Henstock, T. J., and Bull, J. M.: Comparing extension on multiple time and depth scales in the Corinth Rift, Central Greece, *Geophys. J. Int.*, 186, 463–470, <https://doi.org/10.1111/j.1365-246X.2011.05077.x>, 2011.
- Bernhardt, A., Melnick, D., Hebbeln, D., Lückge, A., and Strecker, M. R.: Turbidite paleoseismology along the active continental margin of Chile – Feasible or not?, *Quaternary Sci. Rev.*, 120, 71–92, <https://doi.org/10.1016/j.quascirev.2015.04.001>, 2015.
- Brothers, D. S., Driscoll, N. W., Kent, G. M., Harding, A. J., Babcock, J. M., and Baskin, R. L.: Tectonic evolution of the Salton Sea inferred from seismic reflection data, *Nat. Geosci.*, 2, 581–584, <https://doi.org/10.1038/ngeo590>, 2009.
- Brown, P. A. and Kennett, J. P.: Megaflood erosion and meltwater plumbing changes during last North American deglaciation recorded in Gulf of Mexico sediments, *Geology*, 26, 599–602, [https://doi.org/10.1130/0091-7613\(1998\)026<0599:MEAMPC>2.3.CO;2](https://doi.org/10.1130/0091-7613(1998)026<0599:MEAMPC>2.3.CO;2), 1998.
- Bugge, T., Belderson, R. H., and Kenyon, N. H.: The Storegga Slide, *Philos. T. Roy. Soc. A*, 325, 357–388, <https://doi.org/10.1098/rsta.1988.0055>, 1988.
- Caesar, L., Rahmstorf, S., Robinson, A., Feulner, G., and Saba, V.: Observed fingerprint of a weakening Atlantic Ocean overturning circulation, *Nature*, 556, 191–196, <https://doi.org/10.1038/s41586-018-0006-5>, 2018.
- Camoin, G. F., Iryu, Y., McInroy, D. B., and the Expedition 310 Scientists: Methods, *Proc. IODP*, 310, 1–43, <https://doi.org/10.2204/iodp.proc.310.103.2007>, 2007.
- Chen, W. P., Yu, C. Q., Tseng, T. L., Yang, Z., Wang, C. yuen, Ning, J., and Leonard, T.: Moho, seismogenesis, and

- rheology of the lithosphere, *Tectonophysics*, 609, 491–503, <https://doi.org/10.1016/j.tecto.2012.12.019>, 2013.
- Clark, P. U., Alley, R. B., Keigwin, L. D., Licciardi, J. M., Johnsen, S. J., and Wang, H.: Origin of the first global meltwater pulse following the Last Glacial Maximum, *Paleoceanogr. Paleoclimatology*, 11, 563–577, <https://doi.org/10.1029/96PA01419>, 1996.
- Collot, J.-Y., Marcaillou, B., Sage, F., Michaud, F., Agudelo, W., Charvis, P., Graindorge, D., Gutscher, M.-A., and Spence, G.: Are rupture zone limits of great subduction earthquakes controlled by upper plate structures? Evidence from multichannel seismic reflection data acquired across the northern Ecuador–southwest Colombia margin, *J. Geophys. Res.-Sol. Ea.*, 109, B11103, <https://doi.org/10.1029/2004JB003060>, 2004.
- Cowie, P. A. and Scholz, C. H.: Displacement-length scaling relationship for faults: data synthesis and discussion, *J. Struct. Geol.*, 14, 1149–1156, [https://doi.org/10.1016/0191-8141\(92\)90066-6](https://doi.org/10.1016/0191-8141(92)90066-6), 1992.
- Cowie, P. A., Roberts, G. P., Bull, J. M., and Visini, F.: Relationships between fault geometry, slip rate variability and earthquake recurrence in extensional settings, *Geophys. J. Int.*, 189, 143–160, <https://doi.org/10.1111/j.1365-246X.2012.05378.x>, 2012.
- Daigle, H., Duarte, J., Fagereng, A., Paris, R., Persaud, P., Bell, R., Davies, G., Nomikou, P., Stewart, M., Toomey, M., Ummenhofer, C., Wallace, L., Alves, T., Carvalho, J., Chang, Y., Gamboa, D., Gómez-García, A. M., González, A., Kopf, A., Kuhlmann, H., Le Ber, E., McNeill, L., Nicholson, U., Strasser, M., Thompson, M., Vannucchi, P., and Wils, K.: MagellanPlus Workshop: Mission-specific platform approaches to assessing natural hazards that impact society, MagellanPlus workshop report, ECORD/ICDP, <https://www.ecord.org/?ddownload=16319> (last access: 29 September 2023), 2022.
- Davis, E. E., Villinger, H., and Sun, T.: Slow and delayed deformation and uplift of the outermost subduction prism following ETS and seismogenic slip events beneath Nicoya Peninsula, Costa Rica, *Earth Planet. Sci. Lett.*, 410, 117–127, <https://doi.org/10.1016/j.epsl.2014.11.015>, 2015.
- Fagereng, Å.: Wedge geometry, mechanical strength, and interseismic coupling of the Hikurangi subduction thrust, New Zealand, *Tectonophysics*, 507, 26–30, <https://doi.org/10.1016/j.tecto.2011.05.004>, 2011.
- Fagereng, Å. and Biggs, J.: New perspectives on “geological strain rates” calculated from both naturally deformed and actively deforming rocks, *J. Struct. Geol.*, 125, 100–110, <https://doi.org/10.1016/j.jsg.2018.10.004>, 2019.
- Früh-Green, G. L., Orcutt, B. N., Green, S. L., Cotterill, C., and the Expedition 357 Scientists: Expedition 357 summary, *Proc. IODP*, 357, 1–34, <https://doi.org/10.14379/iodp.proc.357.101.2017>, 2017.
- Galloway, W. E.: Depositional evolution of the Gulf of Mexico sedimentary basin, *Sediment. Basins World*, 5, 505–549, [https://doi.org/10.1016/S1874-5997\(08\)00015-4](https://doi.org/10.1016/S1874-5997(08)00015-4), 2008.
- Goldfinger, C., Ikeda, Y., Yeats, R. S. and Ren, J.: Superquakes and supercycles, *Seismolog. Res. Lett.*, 84, 24–32, <https://doi.org/10.1785/0220110135>, 2013.
- Graham, S. E., Loveless, J. P., and Meade, B. J.: A Global Set of Subduction Zone Earthquake Scenarios and Recurrence Intervals Inferred From Geodetically Constrained Block Models of Interseismic Coupling Distributions, *Geochem. Geophys. Geosyst.*, 22, e2021GC009802, <https://doi.org/10.1029/2021GC009802>, 2021.
- Hampton, M. J., Lee, H. J., and Locat, J.: Submarine landslides, *Rev. Geophys.*, 34, 33–59, <https://doi.org/10.1029/95RG03287>, 1996.
- Huang, Y.: Earthquake rupture in fault zones with along-strike material heterogeneity, *J. Geophys. Res.-Sol. Ea.*, 123, 9884–9898, <https://doi.org/10.1029/2018JB016354>, 2018.
- Ito, Y., Hino, R., Kido, M., Fujimoto, H., Osada, Y., Inazu, D., Ohta, Y., Iinuma, T., Ohzono, M., Miura, S., and Mishina, M.: Episodic slow slip events in the Japan subduction zone before the 2011 Tohoku-Oki earthquake, *Tectonophysics*, 600, 14–26, <https://doi.org/10.1016/j.tecto.2012.08.022>, 2013.
- Koppers, A. A. P. and Coggon, R. (Eds.): Exploring Earth by Scientific Ocean Drilling: 2050 Science Framework, International Ocean Discovery Program, College Station, TX, <https://doi.org/10.6075/JOW66J9H>, 2020.
- Martin, R. G.: Northern and eastern Gulf of Mexico continental margin: stratigraphic and structural framework, in: AAPG Studies in Geology 7: Framework, Facies, and Oil-Trapping Characteristics of the Upper Continental Margin, edited by: Coleman, J., Bouma, A. H., and Moore, G., American Association of Petroleum Geologists, Tulsa, OK, 21–42, <https://doi.org/10.1306/St7399C2>, 1978.
- McGuire, J.: Seismic cycles and earthquake predictability on East Pacific Rise transform faults, *B. Seismol. Soc. Am.*, 98, 1067–1084, <https://doi.org/10.1785/0120070154>, 2008.
- McNeill, L. C., Shillington, D. J., Carter, G. D. O., and the Expedition 381 Participants: Corinth Active Rift Development, *Proc. IODP*, 381, <https://doi.org/10.14379/iodp.proc.381.2019>, 2019.
- Métis, M., Socquet, A., and Vigny, C.: Interseismic coupling, segmentation and mechanical behavior of the central Chile subduction zone, *J. Geophys. Res.-Sol. Ea.*, 117, B03406, <https://doi.org/10.1029/2011JB008736>, 2012.
- Minson, S. E., Brooks, B. A., Glennie, C. L., Murray, J. R., Langbein, J. O., Owen, S. E., Heaton, T. H., Iannucci, R. A., and Hauser, D. L.: Crowdsourced earthquake early warning, *Sci. Adv.*, 1, e1500036, <https://doi.org/10.1126/sciadv.1500036>, 2015.
- Moreno, M., Haberland, C., Oncken, O., Rietbrock, A., Angiboust, S., and Heidbach, O.: Locking of the Chile subduction zone controlled by fluid pressure before the 2010 earthquake, *Nat. Geosci.*, 7, 292–296, <https://doi.org/10.1038/ngeo2102>, 2014.
- Morgan, J., Gulick, S., Mellett, C. L., Green, S. L., and the Expedition 364 Scientists: Chicxulub: Drilling the K-Pg impact crater, *Proc. IODP*, 364, <https://doi.org/10.14379/iodp.proc.364.2017>, 2017.
- Morris, J. T. and Renken, K. A.: Past, present, and future nuisance flooding on the Charleston peninsula, *PLOS One*, 15, e0238770, <https://doi.org/10.1371/journal.pone.0238770>, 2020.
- Mountain, G., Proust, J.-N., McInroy, D., Cotterill, C., and the Expedition 313 Scientists: New Jersey Shallow Shelf, *Proc. IODP*, 313, <https://doi.org/10.2204/iodp.proc.313.2010>, 2010.
- National Geophysical Data Center/World Data Service (NGDC/WDS): NCEI/WDS Global Significant Earthquake Database, NOAA National Centers for Environmental Information [data set], <https://doi.org/10.7289/V5TD9V7K>, 2023a.
- National Geophysical Data Center/World Data Service (NGDC/WDS): NGDC/WDS Global Historical Tsunami

- Database, NOAA National Centers for Environmental Information [data set], <https://doi.org/10.7289/V5PN93H7>, 2023b.
- National Ocean Service (NOS)/Center for Operational Oceanographic Products & Services (CO-OPS): Tsunami Capable Tide Stations, National Oceanic and Atmospheric Administration (NOAA) [data set], <https://tidesandcurrents.noaa.gov/tsunami/> (last access: 29 September 2023), 2023.
- Nixon, C. W., McNeill, L. C., Bull, J. M., Bell, R. E., Gawthorpe, R. L., Henstock, T. L., Christodoulou, D., Ford, M., Taylor, B., Sakellariou, D., Ferentinis, G., Papatheodorou, G., Leeder, M. R., Collier, R. E. L. I., Goodliffe, A. M., Sachpazi, M., and Kranis, H.: Rapid spatiotemporal variations in rift structure during development of the Corinth Rift, central Greece, *Tectonics*, 35, 1225–1248, <https://doi.org/10.1002/2015TC004026>, 2016.
- Özel, N. M., Necmioglu, O., Ergintav, S., Özel, O., Italiano, F., Favali, P., Bigarre, P., Akir, Z., Geli, L., Aochi, H., Bossu, R., Zulfikar, C., and Sesetyan, K.: MARSite-Marmara Supersite: accomplishments and outlook, EGU General Assembly 2017, 23–28 April 2017, Vienna, Austria, EGU2017-18891, 2017.
- Pan, S., Naliboff, J., Bell, R., and Jackson, C.: Bridging spatiotemporal scales of normal fault growth during continental extension using high-resolution 3D numerical models, *Geochem. Geophys. Geosyst.*, 23, e2021GC010316, <https://doi.org/10.1029/2021GC010316>, 2022.
- Popenoe, P., Schmuck, E. A., and Dillon, W. P.: The Cape Fear landslide: slope failure associated with salt diapirism and gas hydrate decomposition, in: *Submarine Landslides: Selected Studies in the U.S. Exclusive Economic Zone*, edited by: Schwab, W. C., Lee, H. J., and Twichell, D. C., U.S. Geological Survey, Washington, D.C., 40–53, <https://doi.org/10.3133/b2002>, 1993.
- Ruff, L. J.: Do trench sediments affect great earthquake occurrence in subduction zones?, *Pure Appl. Geophys.*, 129, 263–282, <https://doi.org/10.1007/BF00874629>, 1989.
- Ruiz, S., Metois, M., Fuenzalida, A., Ruiz, J., Leyton, F., Grandin, R., Vigny, C., Madariaga, R. and Campos, J.: Intense foreshocks and a slow slip event preceded the 2014 Iquique Mw 8.1 earthquake, *Science*, 345, 1165–1169, <https://doi.org/10.1126/science.1256074>, 2014.
- Sainsbury, E. M., Schiemann, R. K. H., Hodges, K. I., Shaffrey, L. C., Baker, A. J., and Bhatia, K. T.: How important are post-tropical cyclones for European wind-storm risk?, *Geophys. Res. Lett.*, 47, e2020GL089853, <https://doi.org/10.1029/2020GL089853>, 2020.
- Saito, T. and Noda, A.: Mechanically coupled areas on the plate interface in the Nankai Trough, Japan and a possible seismic and aseismic rupture scenario for megathrust earthquakes, *J. Geophys. Res.-Sol. Ea.*, 127, e2022JB023992, <https://doi.org/10.1029/2022JB023992>, 2022.
- Sawyer, D. E. and DeVore, J. R.: Elevated shear strength of sediments on active margins: evidence for seismic strengthening, *Geophys. Res. Lett.*, 42, 10216–10221, <https://doi.org/10.1002/2015GL066603>, 2015.
- Scharroo, R., Smith, W. H. F., and Lillibridge, J. L.: Satellite altimetry and the intensification of Hurricane Katrina, *Eos Trans. AGU*, 86, 366, <https://doi.org/10.1029/2005EO400004>, 2005.
- Scholz, C. H.: *The Mechanics of Earthquakes and Faulting*, 3rd edn., Cambridge University Press, Cambridge, UK, <https://doi.org/10.1017/9781316681473>, 2019.
- Schulten, I., Mosher, D. C., Piper, D. J. W., and Krastel, S.: A Massive Slump on the St. Pierre Slope, A New Perspective on the 1929 Grand Banks Submarine Landslide, *J. Geophys. Res.-Sol. Ea.*, 124, 7538–7561, <https://doi.org/10.1029/2018JB017066>, 2019.
- Sparkes, R., Tilmann, F., Hovius, N., and Hillier, J.: Subducted seafloor relief stops rupture in South American great earthquakes: Implications for rupture behaviour in the 2010 Maule, Chile earthquake, *Earth Planet. Sci. Lett.*, 298, 89–94, <https://doi.org/10.1016/j.epsl.2010.07.029>, 2010.
- Stein, S., Geller, R. J., and Liu, M.: Why earthquake hazard maps often fail and what to do about it, *Tectonophysics*, 562–563, 1–25, <https://doi.org/10.1016/j.tecto.2012.06.047>, 2012.
- Taylor, S. K., Bull, J. M., Lamarche, G., and Barnes, P. M.: Normal fault growth and linkage in the Whakatane Graben, New Zealand, during the last 1.3 Myr, *J. Geophys. Res.*, 109, B02408, <https://doi.org/10.1029/2003JB002412>, 2004.
- Telesca, L.: Time-clustering of natural hazards, *Nat. Hazards*, 40, 593–601, <https://doi.org/10.1007/s11069-006-9023-z>, 2007.
- Urlaub, M., Talling, P. J., and Masson, D. G.: Timing and frequency of large submarine landslides: implications for understanding triggers and future geohazard, *Quaternary Sci. Rev.*, 72, 63–82, <https://doi.org/10.1016/j.quascirev.2013.04.020>, 2013.
- van Rijnsingen, E., Lallemand, S., Peyret, M., Arcay, D., Heuret, A., Funicello, F., and Corbi, F.: How subduction interface roughness influences the occurrence of large interplate earthquakes, *Geochem. Geophys. Geosyst.*, 19, 2342–2370, <https://doi.org/10.1029/2018GC007618>, 2018.
- Vega, A. J., Miller, P. W., Rohli, R. V., and Heavilin, J.: Synoptic climatology of nuisance flooding along the Atlantic and Gulf of Mexico coasts, USA, *Nat. Hazards*, 105, 1281–1297, <https://doi.org/10.1007/s11069-020-04354-5>, 2021.
- Wallace, L. M., Barnes, P., Beavan, J., Van Dissen, R., Litchfield, N., Mountjoy, J., Langridge, R., Lamarche, G., and Pondard, N.: The kinematics of a transition from subduction to strike-slip: An example from the central New Zealand Plate boundary, *J. Geophys. Res.-Sol. Ea.*, 117, B02405, <https://doi.org/10.1029/2011JB008640>, 2012.
- Wallace, L. M., Saffer, D. M., Barnes, P. M., Pecher, I. A., Petronotis, K. E., LeVay, L. J., and the Expedition 372/375 Scientists: Hikurangi Subduction Margin Coring, Logging, and Observatories, *Proc. IODP*, 372B/375, <https://doi.org/10.14379/iodp.proc.372B375.2019>, 2019.
- Walsh, K. J. E., McBride, J. L., Klotzbach, P. J., Balachandran, S., Camargo, S. J., Holland, G., Knutson, T. R., Kossin, J. P., Lee, T., Sobel, A., and Sugi, M.: Topical cyclones and climate change, *WIREs Climate Change*, 7, 65–89, <https://doi.org/10.1002/wcc.371>, 2016.
- Wang, K. and Bilek, S. L.: Do subducting seamounts generate or stop large earthquakes?, *Geology*, 39, 819–822, <https://doi.org/10.1130/G31856.1>, 2011.
- Webster, J. M., Yokoyama, Y., Cotterill, C., and the Expedition 325 Scientists: Great Barrier Reef Environmental Changes, *Proc. IODP*, 325, <https://doi.org/10.2204/iodp.proc.325.2011>, 2011.
- Wells, D. L. and Coppersmith, K. J.: New empirical relationships among magnitude, rupture length, rupture width, rupture area, and surface displacement, *B. Seismol. Soc. Am.*, 84, 974–1002, 1994.





## Deep-time Arctic climate archives: high-resolution coring of Svalbard's sedimentary record – SVALCLIME, a workshop report

Kim Senger<sup>1</sup>, Denise Kulhanek<sup>2</sup>, Morgan T. Jones<sup>3</sup>, Aleksandra Smyrak-Sikora<sup>1</sup>, Sverre Planke<sup>3,4</sup>, Valentin Zuchuat<sup>5</sup>, William J. Foster<sup>6</sup>, Sten-Andreas Grundvåg<sup>7</sup>, Henning Lorenz<sup>8</sup>, Micha Ruhl<sup>9</sup>, Kasia K. Sliwiska<sup>10</sup>, Madeleine L. Vickers<sup>3</sup>, and Weimu Xu<sup>11</sup>

<sup>1</sup>Department of Arctic Geology, The University Centre in Svalbard, P.O. Box 156, 9171 Longyearbyen, Norway

<sup>2</sup>Institute of Geosciences, Kiel University, Ludewig-Meyn-Straße 14, 24118 Kiel, Germany

<sup>3</sup>Centre for Planetary Habitability (PHAB), University of Oslo, P.O. Box 1028 Blindern, 0315 Oslo, Norway

<sup>4</sup>Volcanic Basin Petroleum Research AS (VBPR), Blinderveien 5, 0361 Oslo, Norway

<sup>5</sup>Geological Institute, RWTH Aachen University, Wüllnerstraße 2, 52062 Aachen, Germany

<sup>6</sup>Institute for Geology, Universität Hamburg, 20146 Hamburg, Germany

<sup>7</sup>Department of Geosciences, UiT The Arctic University of Norway,  
P.O. Box 6050 Langnes, 9037 Tromsø, Norway

<sup>8</sup>Department of Earth Sciences, Uppsala University, Villavägen 16, 752 36 Uppsala, Sweden

<sup>9</sup>Department of Geology and SFI Research Centre in Applied Geosciences (iCRAG), Trinity College Dublin,  
The University of Dublin, College Green, Dublin 2, Ireland

<sup>10</sup>Geo-energy and Storage, Geological Survey of Denmark and Greenland (GEUS),  
Øster Voldgade 10, 1350 Copenhagen K, Denmark

<sup>11</sup>School of Earth Sciences and SFI Research Centre in Applied Geosciences (iCRAG),  
University College Dublin, Belfield, Dublin 4, Dublin, Ireland

**Correspondence:** Kim Senger (kims@unis.no)

Received: 24 April 2023 – Revised: 23 August 2023 – Accepted: 18 September 2023 – Published: 26 October 2023

**Abstract.** We held the MagellanPlus workshop SVALCLIME “Deep-time Arctic climate archives: high-resolution coring of Svalbard’s sedimentary record”, from 18 to 21 October 2022 in Longyearbyen, to discuss scientific drilling of the unique high-resolution climate archives of Neoproterozoic to Paleogene age present in the sedimentary record of Svalbard. Svalbard is globally unique in that it facilitates scientific coring across multiple stratigraphic intervals within a relatively small area. The polar location of Svalbard for some of the Mesozoic and the entire Cenozoic makes sites in Svalbard highly complementary to the more easily accessible mid-latitude sites, allowing for investigation of the polar amplification effect over geological time.

The workshop focused on how understanding the geological history of Svalbard can improve our ability to predict future environmental changes, especially at higher latitudes. This topic is highly relevant for the ICDP 2020–2030 Science Plan Theme 4 “Environmental Change” and Theme 1 “Geodynamic Processes”. We concluded that systematic coring of selected Paleozoic, Mesozoic, and Paleogene age sediments in the Arctic should provide important new constraints on deep-time climate change events and the evolution of Earth’s hydrosphere–atmosphere–biosphere system.

We developed a scientific plan to address three main objectives through scientific onshore drilling on Svalbard:

- a. Investigate the coevolution of life and repeated icehouse–greenhouse climate transitions, likely forced by orbital variations, by coring Neoproterozoic and Paleozoic glacial and interglacial intervals in the Cryogenian (“Snowball/Slushball Earth”) and late Carboniferous to early Permian time periods.

- b. Assess the impact of Mesozoic Large Igneous Province emplacement on rapid climate change and mass extinctions, including the end-Permian mass extinction, the end-Triassic mass extinction, the Jenkyns Event (Toarcian Oceanic Anoxic Event), the Jurassic Volgian Carbon Isotopic Excursion and the Cretaceous Weissert Event and Oceanic Anoxic Event 1a.
- c. Examine the early Eocene hothouse and subsequent transition to a coolhouse world in the Oligocene by coring Paleogene sediments, including records of the Paleocene–Eocene Thermal Maximum, the Eocene Thermal Maximum 2, and the Eocene–Oligocene transition.

The SVALCLIME science team created plans for a 3-year drilling programme using two platforms: (1) a lightweight coring system for holes of  $\sim 100$  m length (4–6 sites) and (2) a larger platform that can drill deep holes of up to  $\sim 2$  km (1–2 sites). In situ wireline log data and fluid samples will be collected in the holes, and core description and sampling will take place at The University Centre in Svalbard (UNIS) in Longyearbyen.

The results from the proposed scientific drilling will be integrated with existing industry and scientific boreholes to establish an almost continuous succession of geological environmental data spanning the Phanerozoic. The results will significantly advance our understanding of how the interplay of internal and external Earth processes are linked with global climate change dynamics, the evolution of life, and mass extinctions.

## 1 Introduction

The rate and magnitude of current global warming is unparalleled in the historical record and is forecast to disproportionately affect the polar regions, a process known as “polar amplification” (e.g. Holland and Bitz, 2003). Yet, climate models are known to have difficulty reproducing the latitudinal temperature gradients evidenced by deep-time palaeoclimate studies (e.g. Evans et al., 2018; Price et al., 2020), implying that this polar amplification effect may be even more severe than climate models predict. Detailed knowledge of Earth system dynamics is required to improve these climate models, and the only way to understand both long- and short-term feedback processes is through examination of the geological record of palaeoclimate change. Indeed, the Intergovernmental Panel on Climate Change (IPCC) assessment reports note that palaeoclimate proxy records “extend beyond the variability of recent decadal climate oscillations and thus provide an independent perspective on feedbacks between climate and carbon cycle dynamics” (IPCC, 2021), especially for times of global climate and environmental change. Thus, there is a critical need to study past climate archives in different parts of the globe.

Both the International Continental Scientific Drilling Program (ICDP) and the International Ocean Discovery Program (IODP) science plans highlight the study of past climate archives. Theme 4 (Environmental Change) of the ICDP 2020–2030 Science Plan specifically targets sedimentary archives to understand Earth’s evolution and future climate change. In particular, one key question addresses examining past greenhouse conditions to better understand future climate change. The IODP 2050 Science Framework (Koppers and Coggon, 2020) includes the strategic objectives “Earth’s Climate System”, “Feedbacks in

the Earth System”, and “Tipping Points in Earth’s History”, as well as the flagship initiative “Ground truthing future climate change”. Unfortunately with the plan to retire the R/V *JOIDES Resolution* in 2024, scientific ocean drilling will be limited to mission-specific platform and D/V *Chikyu* expeditions to address the 2050 Science Framework, making it even more critical to find alternative onshore targets, including Svalbard, to constrain palaeoclimate.

The Svalbard archipelago in the Norwegian high Arctic (Figs. 1 and 2) offers a series of unique, continuous, and high-quality sedimentary successions that include numerous global palaeoclimate change events from the last 650 million years (Myr). The outcropping geological successions record both temporally and spatially changing climatic and environmental conditions contemporaneous with Svalbard’s drift from the Southern Hemisphere in the Neoproterozoic to its current position at  $78^\circ$  N (Fig. 2). Although Svalbard’s palaeolatitudinal position varied over time, throughout the Phanerozoic it was located at the northern margin of major landmasses, with a rock record complementary to the more studied successions at lower latitude positions. Because Svalbard drifted to its present position during the Cenozoic, it naturally provides an opportunity to constrain the polar amplification effect in the geological past, e.g. during the Paleocene–Eocene Thermal Maximum (PETM). Evidence of past climatic variations include (i) tillites and carbonates related to the Cryogenian and Ediacaran glacial events; (ii) deposits illustrating the late Paleozoic tropical to subtropical climate transition and eustatic sea-level fluctuations caused by Gondwana glaciations; (iii) the record of the end-Permian mass extinction (EPME); (iv) Mesozoic climate and carbon cycle perturbations including the Dienerian Crisis, Carnian Pluvial Event, end-Triassic mass extinction, Jurassic oceanic anoxic events (OAEs), Weissert Event, Volgian Isotopic Carbon

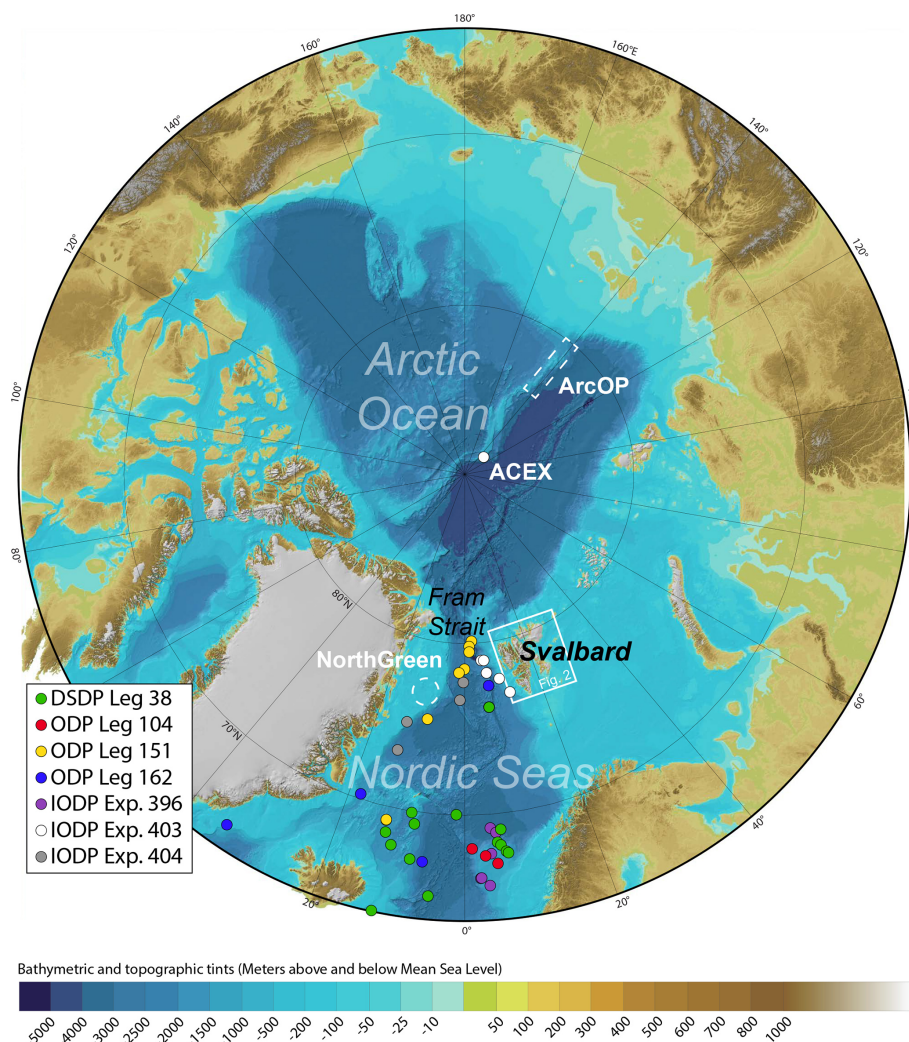


**Figure 1.** Location of Svalbard between the Arctic Ocean and the Nordic Seas and the position of scientific ocean drilling sites in the area. Sites from the most recent IODP expeditions (ACEX, 396, 403, and the cancelled 404) are marked. Potential site positions of the ArcOp and NorthGreen proposals are outlined with dashed white lines. Older DSDP and ODP sites in the Arctic Ocean and Nordic Seas area are indicated with coloured circles. Map from IBCAO (Jakobsson et al., 2012).

Excursion (VOICE), and OAE1a (Selli Event); (v) the Paleogene succession including rapid climate warming such as the PETM; and (vi) the remains of Quaternary to Holocene glaciations (Fig. 3).

Well-exposed outcrops in Svalbard provide excellent targets for analyses of past climate change, and several boreholes have already been drilled and fully cored in Svalbard (Fig. 1). Eight fully cored research boreholes were drilled as part of a CO<sub>2</sub> storage project that offer a total of 4.5 km of Triassic–Cretaceous core material (Olaussen et al., 2019), along with supplementary wireline logs. Hundreds of coal exploration boreholes have been drilled mainly within the Paleocene succession with a few providing high-resolution data across the PETM (Dypvik et al., 2011; Senger et al., 2019). Two shallow stratigraphic boreholes from Deltadalen (Zuchuat et al., 2020), with cores of

almost 100 m each, allowed for multidisciplinary analyses of the palaeoclimatic conditions across the Permian–Triassic boundary and the accompanying EPME at a resolution not yet undertaken elsewhere in the high Arctic. The Deltadalen research drilling campaign proved that cost- and time-effective stratigraphic drilling and full coring can be achieved with minimal environmental impact. Overall, the core data in combination with nearby outcrop data have formed the basis of numerous spin-off studies, including a re-evaluation of the global stratigraphic timescale. However, the large number of cored boreholes is limited to only a few stratigraphic intervals, have a small diameter (limiting sample material), and are heavily biased by commercial interests and priorities (see Fig. 3 in Senger et al., 2019, for an overview). In addition, many of the existing cores have been poorly stored,



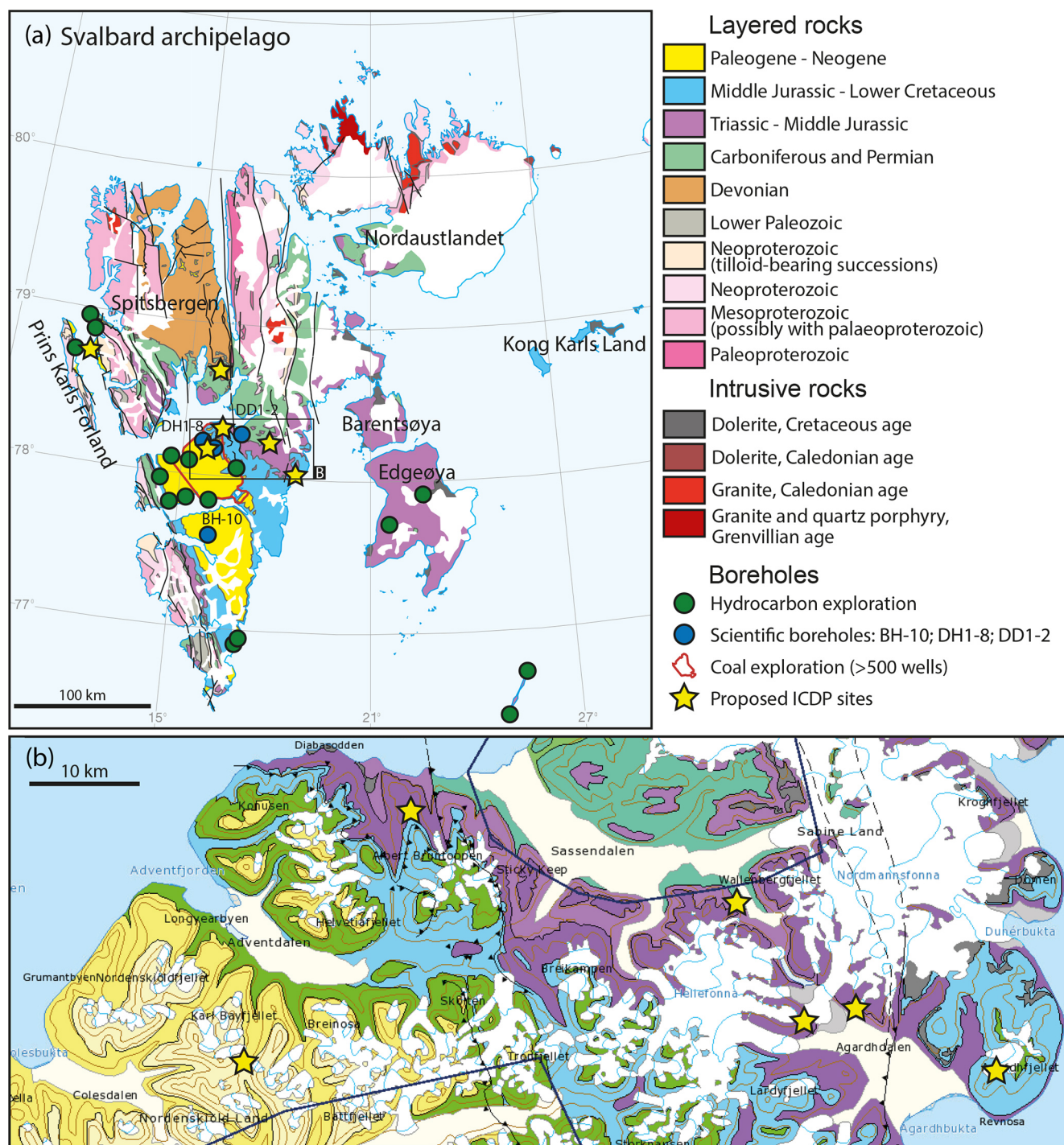


**Figure 2.** (a) Geological map of Svalbard, with locations of previous exploration and scientific wells, and proposed ICDP sites indicated. (b) A local map of central Spitsbergen showing the location of potential ICDP sites (maps from the Norwegian Polar Institute).

making them unusable for palaeoclimate and environmental proxy studies.

To take advantage of existing outcrop and core material and to design future deep-climate research programmes in Svalbard, we held a MagellanPlus ICDP/IODP workshop at

The University Centre in Svalbard (UNIS) in Longyearbyen from 18 to 21 October 2022. The main goal of the workshop was to develop new scientific drilling proposals to access Svalbard's unique and well-preserved high Arctic rock record. This overall goal was split into several specific

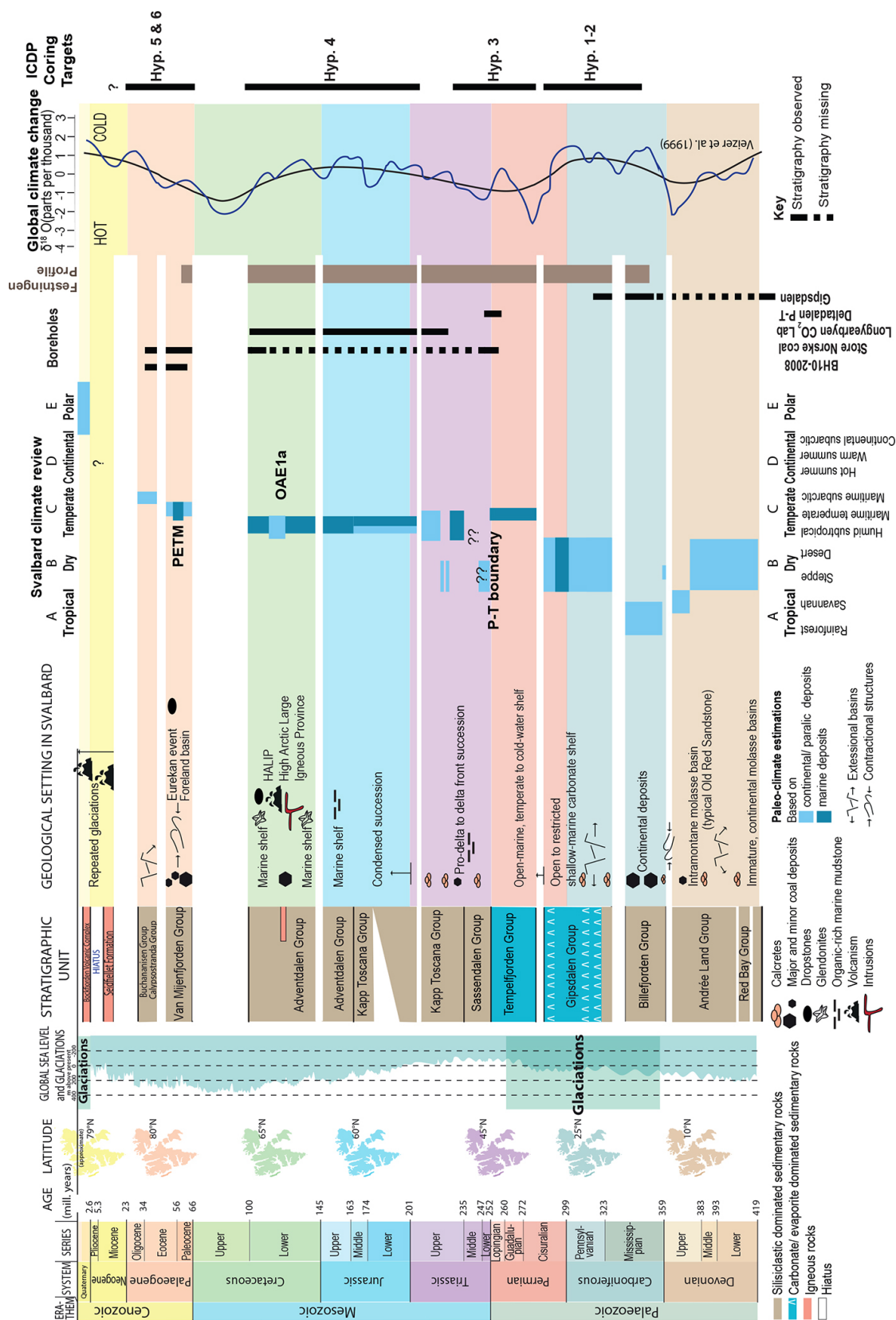


**Figure 3.** Stratigraphic column and climate summary of Svalbard, highlighting the nearly continuous sedimentary record from the Devonian to the Neogene (modified from Smyrak-Sikora et al., 2021). The stratigraphic coverage of research boreholes is indicated, with proposed ICDP drilling targets at right.

objectives related to the individual deep-time climatic events that require dedicated drilling efforts to acquire relevant drill cores, while others will benefit from pre-existing core material already acquired by the SVALCLIME proponents (Olaussen et al., 2019; Zuchuat et al., 2020).

The workshop (4 workshop days) was attended by 59 in-person participants (from 13 countries) and 33 virtual attendees (from a total of 17 countries), representing diversity in terms of expertise, career stage, gender, and country (see participant list in Appendix A). The workshop was organized with plenary presentations on the first 2 event days, followed by breakout group discussions covering different geological time intervals to identify knowledge gaps and objectives targeting globally significant climate change events. Each represents an objective of global significance that can only be fully achieved through scientific drilling to utilize high-resolution geochemical and non-destructive techniques (e.g. X-ray fluorescence (XRF) core scanning, hyperspectral and computed tomography (CT) imaging, multisensor core logger (MSCL) physical properties) that are not possible with weathered outcrop samples. Further work over the coming year, together with feedback from the ICDP Science Advisory Group (SAG) on a pre-proposal submitted in January 2023, will help to guide which objectives will become the focus of one or more full ICDP drilling proposals. The targets and objectives identified during the MagellanPlus workshop are outlined below by age.

The primary targets for potential future drilling include:

- a. Cryogenian–Ediacaran tillites and carbonates deposited during glacial or interglacial conditions,
- b. Carboniferous–Permian transition from coal-rich continental deposits to mixed carbonate–evaporite–siliciclastic rocks that record a shift from a tropical humid climate to an arid subtropical climate,
- c. Permian–Triassic siliciclastic deposits that record the EPME and its aftermath,
- d. Jurassic and Cretaceous rocks that record environmental changes associated with igneous intrusions of the High Arctic Large Igneous Province (HALIP; Early Cretaceous) and other LIPs that generated massive quantities of greenhouse gases through contact metamorphism, and
- e. Paleogene strata that record key climate perturbations such as the PETM and gradual change from hothouse to coolhouse conditions across the Eocene–Oligocene transition (EOT).

## 2 Previous onshore drilling on Svalbard: a brief synthesis

While some scientific boreholes under the auspices of DSDP, ODP, and IODP targeted areas near Svalbard (Fig. 1), no ICDP borehole campaign has yet been undertaken on Svalbard. In addition, shallow stratigraphic boreholes were drilled and fully cored off shore in the northern Barents Shelf for petroleum exploration (Lundschien et al., 2024).

Many onshore boreholes have been drilled on Svalbard for coal, petroleum, uranium, and gold exploration as well as scientific research (Table 1; Senger et al., 2019). The scientific boreholes provide drill cores suitable for deep-time palaeoclimate research and were presented during the SVALCLIME workshop. The deep petroleum exploration boreholes provide important constraints on stratigraphic thicknesses, lithology, and maturation and thus form an important foundation for subsequent research drilling. The Deltadalen campaign was undertaken using a helicopter-transportable drilling rig (Fig. 4; Zuchuat et al., 2020) and was completed in 1 week with minimal environmental impact, thus representing a model for some of the proposed sites within the SVALCLIME initiative.

## 3 Identified scientific drilling targets

During the workshop, we identified a number of climate events to target through systematic scientific drilling of key stratigraphic intervals on Svalbard. Here we outline these events by age from oldest to youngest, including testable hypotheses and supporting scientific questions developed for the more mature targets.

### 3.1 Neoproterozoic and Paleozoic

The Cryogenian (720–635 Ma; all ages hereunder are from the International Chronostratigraphic Chart June 2023) spans two of Earth's most extreme glacial intervals, the Sturtian and Marinoan as well as their intervening interglacial (Hoffman and Schrag, 2002; Rooney et al., 2015). Coring this time interval will help to improve age constraints for the Cryogenian using cyclostratigraphy and rhenium–osmium (Re–Os) dating. It would also allow us to further assess the C<sub>27</sub>–C<sub>29</sub> sterane transition (to distinguish biogenic sources of organic matter) that represents a major change in marine primary production from cyanobacteria to eukaryotic algae that occurred during the interglacial (Brocks et al., 2017). There are few cores globally spanning the Cryogenian and none from Svalbard, making this an important target to better understand this period in Earth's history when significant ice existed in tropical regions, as well as how the transition out of “Slushball Earth” impacted the evolution of life in the Ediacaran (635–538.8 Ma). However, the potential drill sites are in remote and largely protected sites; therefore, planning



**Table 1.** Synthesis of past onshore drilling on Svalbard and its relevance to deep-time palaeoclimate research.

Campaign	Time period	Stratigraphy	Coring?	Palaeoclimate studies?	Key references
Coal exploration boreholes	1950s–2013	Mostly Cenozoic	Yes	Yes (Charles et al., 2011; Cui, 2010; Dypvik et al., 2011)	Dypvik et al. (2011)
Petroleum exploration boreholes	1961–1994	Paleozoic to Cenozoic	Limited, many cores lost, some cutting samples available	Important for prediction of stratigraphy and maturation	Olaussen et al. (2023), Senger et al. (2019)
Uranium and coal exploration boreholes	1970s	Paleozoic	Partly	No	Senger et al. (2019)
Sysselembreen (BH10-2008)	2008	Cenozoic	Yes	Some	Johannessen et al. (2011), Grundvåg et al. (2014), Doerner et al. (2020)
Longyearbyen CO <sub>2</sub> lab	2007–2013	Mesozoic	Yes	Yes, mainly with $\delta^{13}\text{C}$ (Koevoets et al., 2016; Midtkandal et al., 2016; Jelby et al., 2020)	Braathen et al. (2012), Olaussen et al. (2019)
Deltadalen	2014	Permian–Triassic boundary	Yes	Yes (Zuchuat et al., 2020; Schobben et al., 2020; Rodríguez-Tovar et al., 2021)	Zuchuat et al. (2020)



**Figure 4.** Photographs of selected drill sites highlighting the large magnitude of the drilling operations. The Permian–Triassic research drilling in Deltadalen was conducted using a helicopter-transportable drill rig and took 1 week to finish. The Longyearbyen CO<sub>2</sub> lab boreholes in Adventdalen were drilled and fully cored with coal exploration drill rigs and took about a month to complete. The deepest onshore borehole on Svalbard, Ishøgda, was drilled (but not cored) on the shore of Van Mijenfjorden using a 900 t petroleum exploration drill rig brought in from Canada. Photo credits: Sverre Planke (Deltadalen), Geir Ove Titlestad (Longyearbyen CO<sub>2</sub> lab), and Carl A. Wendt (Ishøgda, kindly provided by Svalbard Museum). Refer to Senger et al. (2019) for details on all the boreholes.

for drilling these targets is not as mature as for the Paleozoic and younger sites.

The Late Paleozoic Ice Age (LPIA) was one of the biggest climatic events of the Phanerozoic as it significantly altered both climate and depositional systems on Earth (Montañez and Poulsen, 2013). It represents the only complete greenhouse–icehouse–greenhouse cycle on a vegetated Earth (cf. Isbell et al., 2008) and is considered a close analogue to present climate conditions with sustained low  $p\text{CO}_2$  within the range proposed for the near future (Montañez and Poulsen, 2013). The LPIA was characterized by discrete periods of glaciations separated by warm periods (Isbell et

al., 2008; Gastaldo et al., 1996; Montañez et al., 2007). The glaciations started during the Visean (346.7–330.9 Ma) and extended into the, most probably, late Permian for more than 100 Myr. During this time interval, Svalbard drifted from a tropical position into the northern subtropical arid zone (Torsvik and Cocks, 2019) and deposition gradually shifted from humid terrestrial to semi-arid terrestrial and finally to shallow marine (Steel and Worsley, 1984). The impact of the glaciations and deglaciation during the LPIA is most readily recognized in the Bashkirian (323.2–315.2 Ma; Pennsylvanian) to Sakamarian (293.52–290.1 Ma; Cisuralian) marine successions of the Gipsdalen

Group (Ahlborn and Stemmerik, 2015; Sorento et al., 2020; Smyrak-Sikora et al., 2021; Cutbill and Challinor, 1965). Over 130 cycles of sea-level variations could reveal the magnitude of glacioeustatic sea-level changes and the dynamics of the LPIA, especially the early Permian icehouse–greenhouse transition. Obtaining a fully cored record through these > 130 cycles would contribute to further development of the late Paleozoic timescale and the sensitivity of the planet to external forcings and feedbacks. Thus, we propose to collect ~ 1000 m of core through this interval to address the following hypotheses and specific scientific questions:

*Hypothesis 1.* The cycles present in the Gipsdalen Group record orbital cyclicity and its imprint on Earth's climate.

- 1a. Does the cyclicity relate to a long eccentricity cycle during the Pennsylvanian (Aretz et al., 2020, and references therein), as is inferred for other locations (e.g. China, United States, Ireland)?
- 1b. How do these cycles correlate with the North American cyclothems (and records from other regions), and what are the implications for the Carboniferous timescale?

*Hypothesis 2.* The far-field records of LPIA in Svalbard cover the transition across greenhouse–icehouse–peak-icehouse–greenhouse conditions.

- 2a. Does the gradual climate shift from humid to arid conditions recorded on Svalbard in the Visean represent the environmental and climatic far-field response to the onset of icehouse conditions?

### 3.2 Mesozoic

The Permian was marked by major supra-regional environmental perturbations including the Artinskian–Kungurian faunal turnover (~ 283.5 Ma; Lee et al., 2022), the Capitanian mass extinction (~ 262 Ma; Bond et al., 2020), and EPME (Wignall et al., 1998; Mørk et al., 1999). The subsequent Mesozoic saw enhanced volcanism due to the breakup of Pangea, resulting in major perturbations to the global carbon cycle that led to dramatic and short-lived global warming, significant changes in global hydrological cycling at times, enhanced development of oceanic anoxia especially in marginal marine basins, and extinction events (Schlanger and Jenkyns, 1976; Erba et al., 2015; Herrle et al., 2015; Jelby et al., 2020).

The environments and lithologies in which magmatic emplacement occurs are key factors for atmospheric volatile loading and global climate change. Svensen et al. (2004) showed that emplacement of magma into organic-rich sedimentary basins could create > 10 times the amount of greenhouse gases (CH<sub>4</sub> and CO<sub>2</sub>) than a comparable volume of lava degassing subaerially. For instance, emplacement of magma into the organic- and evaporite-rich Tunguska Basin in Siberia released large volumes of toxic halocarbons

through pipe structures called hydrothermal vent complexes, resulting in the largest known Phanerozoic extinction event, the EPME (Svensen et al., 2009). A similar scenario has been proposed for the EPME, whereby massive quantities of toxic and greenhouse gases were released from the Amazon, Parnaíba, and Solimões basins in South America (Ruhl and Kürschner, 2011; Heimdal et al., 2019).

The Svalbard stratigraphy provides a unique Arctic record to study both the long- and short-term climate variations associated with such global perturbations in the Mesozoic. Indeed, most of what is known about the EPME is based on records from China, southern Europe, and the Middle East, which all represent subtropical, Tethyan successions (e.g. China and central Europe; Jin et al., 2000; Farabegoli et al., 2007). Yet, the fossil record and modelling studies suggest that the impact of the climate crisis was greater at higher latitudes and along the Panthalassan margin of Pangea (Penn et al., 2018). During the late Permian and Triassic, Svalbard was located on the northern margin of Pangea between ~ 45 and 50° N (Elvevold et al., 2007). On Svalbard, the Permian strata of the Kapp Starostin Formation (Cutbill and Challinor, 1965) was deposited in a cold-water ramp setting (Bond et al., 2018). The conformably overlying Triassic succession consists of nine high-sedimentation-rate, fining-up transgressive, and coarsening-up regressive cycles (Mørk et al., 1989; Vigran et al., 2014) associated with progradational pulses of the “largest delta... in Earth's history” across the Barents Shelf (Klausen et al., 2019). Svalbard is unique compared to the equatorial, Tethyan successions in that it records diverse marine ecosystems but also silicified fauna (Foster et al., 2017) and faunal groups currently unknown from coeval shallow-marine settings, including radiolarians (Foster et al., 2023), hexactinellid sponges (Foster et al., 2023), red algae (Wignall et al., 1998), and bryozoans (Nakrem and Mørk, 1991). The absence of these groups from intensely studied equatorial shallow-marine successions from the Tethys and Panthalassa oceans suggests that their absence in these equatorial settings represents a biological signal and more habitable conditions in the Boreal Realm that can only be studied in difficult-to-access locations, including Arctic Canada, Greenland, and Russia.

The Permian–Triassic boundary succession was cored in two boreholes at Deltadalen (DD1-2; Fig. 2a; ~ 90 m each), providing a good record of the mass extinction event and its aftermath. However, the glauconitic, chert-rich, and often thoroughly bioturbated sandstone facies of the upper Permian Kapp Starostin Formation prevented detailed palynological, geochemical, and palaeoenvironmental analyses of pre-EPME conditions (Zuchuat et al., 2020). In addition, because of the high sedimentation rates, the 90 m core only covers the entire Induan (251.902–251.2 Ma) and the lower part of the Olenekian stages of the Lower Triassic. Therefore, most of the climatic events of the Triassic (including the Dienerian Crisis (upper Induan) or the Carnian Pluvial Event

~234 Ma; Ogg et al., 2016) are yet to be investigated (Fig. 2). We therefore propose to core a ~700 m succession spanning from the Upper Triassic strata into the Permian Kapp Starostin Formation from the top of and at the foot of Kropotkinfjellet, Friedrichfjellet, or Roslagenfjellet in Agardhdalen (Fig. 2b) to address the following hypothesis and key questions:

**Hypothesis 3.** The Svalbard sedimentary sequences record environmental changes from the Permian through Late Triassic associated with global perturbations in the carbon cycle resulting from major tectonic events, including the eruption and emplacement of the Siberian Traps Large Igneous Province (LIP) and the breakup of Pangea.

- 3a. How is the EPME expressed at higher latitudes relative to the equatorial regions?
- 3b. Are subsequent Triassic environmental perturbations and associated carbon isotope excursions (CIEs) present in low-latitude sections also found in Svalbard, suggesting a global nature?
- 3c. How do the progradational pulses of the delta migrating over the Barents Shelf recorded in the Triassic strata of Svalbard tie to concomitant global environmental perturbations, such as changes in regional or global hydrological cycling?

Mechanisms for the formation of Jurassic and Cretaceous OAEs are still debated, but the synchronicity between LIP emplacement and these events implies either a direct causal link (e.g. similar to the scenario above) or that greenhouse gas emissions from these LIPs drove global temperatures beyond a tipping point, and massive methane release from continental shelves drove extreme global climate change and ocean stratification (e.g. Hesselbo et al., 2000). Recent work from outcrops on Svalbard suggest that the subaerial HALIP volcanism may have played a more important role for at least the Northern Hemisphere changes than the larger, but submarine, Greater Ontong-Java Plateau LIP in the Pacific (e.g. Percival et al., 2021; Vickers et al., 2023). Furthermore, a heterogeneously distributed Upper Jurassic CIE (the VOICE event) was recently identified in Arctic regions and corroborated with one South American site; the causes and effects of this event are poorly understood (Jelby et al., 2020; Weger et al., 2022). We propose to core Triassic, Jurassic, and Cretaceous strata suitable for high-resolution proxy studies in key localities near the east coast of Spitsbergen where the thermal effects of the Paleogene fold-and-thrust belt are less severe than in the west to address the following hypothesis and specific questions:

**Hypothesis 4.** LIPs played a major role in global climate change and biotic crises during the Jurassic and Early Cretaceous.

- 4a. What are the Arctic climate responses to the Karoo LIP (~182 Ma) and the central Atlantic LIP (~201 Ma)?

- 4b. What are the mechanisms and drivers of the VOICE and associated Weissert Event in the Valanginian (~133 Ma)?

- 4c. What is the impact of HALIP intrusions on global carbon cycling and climate during OAE1a (~120 Ma)?

### 3.3 Paleogene

The Paleogene is a key interval for understanding the role of boreal environments in a changing global climate. This time interval is marked by fluctuations between warm-house and hothouse conditions from the Paleocene to mid-Eocene, followed by gradual cooling that culminated in the establishment of a coolhouse climate by the early Oligocene (Westerhold et al., 2020). The hothouse conditions included periods of transient hyperthermal events such as the PETM at ~56 Ma (Cramer et al., 2003). There is evidence of polar amplification for periods of extreme warmth, with temperate to subtropical flora identified in both marine (Sluijs et al., 2020) and terrestrial archives in the Arctic (Suan et al., 2017; Weijers et al., 2007; West et al., 2015; Willard et al., 2019). Despite the importance of polar regions in understanding global climate evolution through the Paleogene, the marine palaeoclimate record for the Arctic is severely underrepresented in global datasets. Integrated Ocean Drilling Program Exp. 302 (Arctic Coring Expedition, ACEX) to the Lomonosov Ridge (Backman et al., 2004) is currently the only scientific ocean drilling conducted in the Arctic Ocean to date. ACEX sites provide key marine archives for the Paleocene and early Eocene (Sluijs et al., 2020), but there is a considerable hiatus of ~26 Myr in ACEX cores (~44–18 Ma) that extends onto the Barents Shelf (Backman et al., 2008; Sangiorgi et al., 2008). An alternative age model by Poirier and Hillaire-Marcel (2011) suggests that the “hiatus” succession is heavily condensed. Subsequent efforts to redrill in the High Arctic (International Ocean Discovery Program (IODP) Expeditions 377 and 404) have recently been cancelled. As such, there is a major palaeoclimate data gap in this region, with no current drilling opportunities planned in the coming decade. The Svalbard archipelago is an ideal locality to address this knowledge gap. It has been located within the Arctic Circle during the last 60 Myr and contains an expanded and well-preserved succession of shallow marine to deltaic sediments of Paleocene (< 62 Ma) to Oligocene (~25 Ma) age (Helland-Hansen and Grundvåg, 2021). Continuous coring in strategic locations will allow us to test several critical hypotheses and pivotal research questions in Paleogene climate research.

The PETM is marked in the geological record by a large CIE ( $\delta^{13}\text{C}$ ), indicative of large atmospheric fluxes of  $\text{CO}_2$  that caused 4–6 °C of global warming (e.g. Inglis et al., 2020; Zachos et al., 2008). The sources of carbon required to instigate the PETM are intensely debated (e.g. Dickens et al., 1995; Lourens et al., 2005; Svensen et al.,



2004; Gutjahr et al., 2017). One potential candidate was the emplacement of the North Atlantic Igneous Province (NAIP). There is good temporal agreement between peak NAIP activity and the PETM, and both volcanic and contact metamorphic degassing are large potential carbon sources (Svensen et al., 2004; Jones et al., 2016). However, the exact relationship between the NAIP and the PETM is complicated by a lack of expanded successions that contain both volcanic and climatic proxies. The Central Spitsbergen Basin succession outcropping is an ideal candidate for resolving some of these uncertainties, as the  $\sim 2.5$  km thick sequence represents near-continuous deposition during the formation of a foreland basin. The relative proximity of Svalbard to the NAIP resulted in the co-preservation of multiple volcanic and climatic proxies. The PETM is within an expanded record of homogeneous siliciclastic mudstone deposited in a shallow to moderately deep marine setting (Dypvik et al., 2011). The lithological homogeneity and lack of extreme variations in sedimentation rates make the Svalbard strata an invaluable locality, as the vast majority of global PETM sites are affected by these factors. The relatively consistent sedimentation rates, high-latitude setting, and presence of some tephra layers mean that a robust geochronology can be attained by cyclostratigraphy, magnetostratigraphy, and radiometric dating. To date, only a single borehole (09/2005) has been studied in detail from the Central Spitsbergen Basin (e.g. Dypvik et al., 2011; Charles et al., 2011; Harding et al., 2011; Cui et al., 2021). Coring a new PETM interval at a location southeast of Longyearbyen (Fig. 2b) will allow for the implementation of state-of-the-art techniques, such as downhole imaging and logging that were unavailable for studies on core 09/2005, and also provides a detailed record of the cessation of elevated magmatic activity into the early Eocene. This new drill core will allow us to address the following hypothesis and key questions:

*Hypothesis 5.* NAIP activity was a potential driver of rapid and severe global climate change.

- 5a. Can a high-resolution record from Svalbard improve our understanding of what caused the initiation and long duration of the PETM hyperthermal?
- 5b. Can refined geochronology distinguish between various carbon sources, such as NAIP eruptions and thermogenic degassing from intrusions, during the evolution of the PETM?

The primary driver of global cooling beginning in the late Eocene is uncertain, with declining atmospheric  $\text{CO}_2$  and opening of tectonic gateways being the leading hypotheses (e.g. Hutchinson et al., 2021). Unlike the opening of the Tasman Gateway and Drake Passage (e.g. Toggweiler and Bjornsson, 2000; Stickley et al., 2004), there are significant uncertainties in the timing and nature of the opening of the Fram Strait (e.g. von Appen et al., 2015; Hossain et al., 2021). Recent studies suggest that the

Eocene–Oligocene transition from warm-house to coolhouse conditions ( $\sim 34$  Ma) may have been controlled by declining atmospheric  $\text{CO}_2$  concentration, with changing bathymetry of the northern gateways playing a secondary role (e.g. Hutchinson et al., 2019; Straume et al., 2022). The onset of glaciation on Antarctica at  $\sim 34$  Ma marked the beginning of the icehouse world at one pole. However, the onset of glaciation in the northern high latitudes is uncertain, with some studies arguing for the presence of Arctic sea ice from as early as the mid-Eocene (Stickley et al., 2009; Tripathi and Darby, 2018). The lack of marine sedimentary archives from the high Arctic region due to the  $\sim 26$  Myr data gap in the ACEX core precludes further testing of this hypothesis, along with a host of palaeoenvironmental data that would place Arctic climate evolution in a global context. Therefore, the recent cancellation of IODP Expedition 404 due to the planned decommissioning of the R/V *JOIDES Resolution* in 2024 dashed the hopes of the scientific community to acquire much needed data from the high Arctic; therefore, alternative targets must be sought.

The Eocene to Oligocene Forlandsundet Graben is a key locality for addressing this knowledge gap. Oblique extension and normal faulting on the western Svalbard margin formed a series of N–S trending basins, of which only the Forlandsundet Graben is, in part, subaerially exposed (Steel et al., 1985; Blinova et al., 2009; Kristoffersen et al., 2020; Schaaf et al., 2021). The activation of faulting and extension may represent a precursor of the Fram Strait and is therefore a key area to unravel the timing and sequence of events that established the seaway. The thickness of the Forlandsundet Graben infill is poorly constrained due to the tectonic complexity of the area and scattered outcrop sections but exceeds 4 km in places (Dallmann, 1999). Age estimates are also uncertain but ages as young as middle-to-late Oligocene have been proposed (Schaaf et al., 2021; Feyling-Hanssen and Ulleberg, 1984). An exploration well drilled near the centre of the graben penetrated  $> 1$  km of mostly marine mudstones and sandstones of Eocene and Oligocene age before reaching metamorphic basement (Senger et al., 2019; Schaaf et al., 2021). Unfortunately, only  $\sim 20$  m of the entire borehole were cored. Nevertheless, this borehole acts as a proof of concept that a continuous core of the Forlandsundet strata can be obtained to address the following hypothesis and key questions:

*Hypothesis 6.* The opening of the Fram Strait played a major role in global thermohaline circulation and the cooling of Earth's climate.

- 6a. Can the use of palaeoceanographic tracers in the Forlandsundet Graben establish when the deep-water connection from the Arctic to global oceans was initiated?
- 6b. Can drilling in the Forlandsundet Graben provide the first ever Eocene-to-Oligocene marine palaeoclimate archive in the high Arctic region?

## 4 From vision to drilling

Svalbard is the optimal logistical location for coring the Phanerozoic stratigraphy of the Arctic. Longyearbyen is a well-developed and accessible settlement (population 2400) with a university centre (UNIS), tourism infrastructure (e.g. hotels, boats, snowmobiles), and a natural polar logistics centre. Daily scheduled flights connect Longyearbyen to Norway (Oslo and Tromsø), and a mostly ice-free harbour serves weekly transport vessels arriving from the mainland. The archipelago has a more than 100-year-long record of year-round geological exploration and drilling with relatively limited impact on the environment.

Svalbard's legal status is governed by the Svalbard Treaty signed in 1920 and ratified in 1925. The Svalbard Treaty grants Norway full sovereignty over Svalbard, but it also prohibits discrimination against companies from outside Norway accessing Svalbard's natural resources. This is particularly reflected in the diverse international group of companies involved in petroleum exploration in Svalbard from the 1960s to the early 1990s (Senger et al., 2019).

However, environmental regulations have since become much stricter, with large-scale environmental protection implemented in 1973 (establishment of major natural parks and reserves in eastern Svalbard and the full protection of polar bears) and 2001 (through the passing of the Svalbard Environmental Protection Act), constraining the type of activities that are possible and their location. In the context of research drilling, coal exploration drilling around Nordenskiöld Land, deep drilling near Longyearbyen, and shallow drilling at Deltadalen in 2015 all illustrate the feasibility of acquiring high-quality cores with minimal environmental effects.

### 4.1 Existing data and site selection

An extensive geophysical and geological database exists for Svalbard, called Svalbox (Senger et al., 2022; <http://www.svalbox.no/map>, last access: 4 October 2023; Betlem et al., 2023; Fig. 5). Data available for SVALCLIME include (a) nearshore marine reflection seismic lines, covering almost all fjords, much of Spitsbergen's shoreline, and parts of the adjacent shelf; (b) onshore seismic reflection lines at key localities, such as Adventdalen, where they extend the offshore seismic lines to image the succession of the Central Spitsbergen Basin; (c) hydrocarbon exploration wells at a number of sites throughout Svalbard, between 200 m and > 3 km deep, mostly uncored; (d) ore exploration boreholes, mainly short intervals cored for coal and concentrated on relevant stratigraphic intervals; and (e) Longyearbyen CO<sub>2</sub> lab and Deltadalen drill cores and data (important for operational planning, including lessons learnt from drilling through permafrost and pressurized sections). The SVALCLIME coring targets are primarily stratigraphy that is (1) poorly or not exposed or is highly weathered where

exposed, (2) located away from outcrop localities, (3) less altered due to intrusive activity, and (4) is not already fully cored in an optimal location (considering thermal maturity, lithologies, sedimentation rate, basinal position, etc.).

### 4.2 Drilling platforms

During the workshop, we discussed drilling platforms and their suitability for the proposed SVALCLIME drilling targets, which can be divided into two groups: shallow, with a target depth of up to a couple of hundred metres, and deep. Deep targets include the Forlandsundet Graben at Sarstangen with > 1 km target depth (Hypothesis 6) and the Central Spitsbergen Basin near Longyearbyen with > 2 km target depth (Hypothesis 5); a third deep target on the southeastern shore of Sassenfjorden (~ 1.5 km; Hypothesis 1) can possibly be covered by multiple shallow holes. All other targets belong to the shallow group. Suitable drilling platforms are capable of continuous core drilling to target depth in at least N size (47.6 mm core diameter, 75.7 mm hole diameter with NQ drill bit) and sufficiently adaptable such that all required components can be mobilized to drill sites in comparatively remote Arctic environment without significant negative impact on the local environment. Certain sites for shallow boreholes are located on mountaintops and slopes, which requires transport by helicopter. We identified several potential drilling rigs that meet these requirements: (1) The University Centre in Svalbard (UNIS) operates a drill rig that can be used for short, uncomplicated coring down to 130 m. (2) SNSK (Store Norske, formerly Store Norske Spitsbergen Kulkompani AS, the Norwegian coal and service company on Svalbard) has used a drill rig operated by Arctic Drilling Company Oy Ltd for exploration locations that are only accessible by helicopter. The successor of this rig is expected to have a depth capacity of 200–300 m. (3) Other lightweight platforms for drilling to ~ 500 m (NQ: drill bit size; gives 47.6 mm core diameter) exist (e.g. underground exploration drill rigs) and could possibly be adapted to the requirements. (4) The Swedish National Research Infrastructure for Scientific Drilling “Riksrigger” can be used for deep core drilling in complicated, challenging environments. This platform is well known from previous ICDP projects (Eger Rift; Collisional Orogeny in the Scandinavian Caledonides (COSC); Lorenz et al., 2022; Fischer et al., 2022) and has a maximum drilling depth of 2.5 km (NQ). Riksrigger is comparatively large and heavy but still easily mobilized when compared to conventional rotary drilling equipment.

### 4.3 Operational and science planning and safety considerations

SVALCLIME operational planning is being done in collaboration with Riksrigger and SNSK, which became involved in the project during the MagellanPlus workshop.

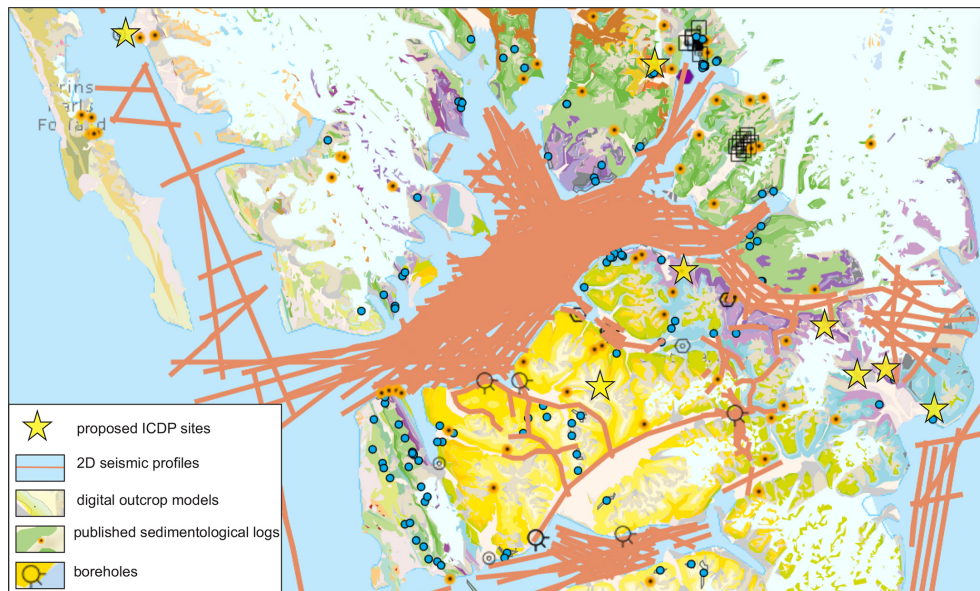


**Figure 5.** Database of existing geoscientific material including existing boreholes, seismic data, and high-resolution digital outcrop models as integrated in the Svalbox platform (Betlem et al., 2023; Senger et al., 2022). The interactive map is accessible at <http://www.svalbox.no/map>.

Major safety concerns, in addition to those expected in sedimentary basins, are linked to permafrost and the highly sensitive Arctic environment. Potential dangers, in particular during deep drilling, are fluid and gas overpressure below permafrost and at certain stratigraphic levels, semi-consolidated sediments and swelling clays in certain stratigraphic intervals, and the complications of drilling through multiple fault and décollement zones related to the West Spitsbergen Fold and Thrust Belt. Gas is also present regionally as shale gas in shale-dominated successions such as the Agardhfjellet and Botneheia formations, and this is well characterized in Adventdalen (Ohm et al., 2019). Much can be learnt from the analysis of the drilling reports from previous drilling projects, e.g. hydrocarbon exploration drilling and the Longyearbyen CO<sub>2</sub> lab.

In our ICDP pre-proposal submitted in January 2023, we proposed a 3-year drilling campaign using two different platforms. In the first year, shallow boreholes (~100 m) will be drilled with a lightweight drilling platform near Longyearbyen. With a similar approach but slightly deeper targets, four sites in more distal locations towards the east coast of Svalbard will be drilled during the second year. Finally, a large rig will be used at 1–2 sites during the third year, with expected drilling depths of between 1 km and more than 2 km. Final scheduling will depend on permitting, logistic, and economic considerations. On-site science will most likely be limited to producing knowledge required for managing the drilling and tasks that cannot be delayed. Scientific work on the drill core, such as high-resolution lithological descriptions, core scanning and logging, and initial sampling and analyses, will be conducted at existing

facilities in Longyearbyen. The downhole logging, testing, and sampling plan will ensure that the boreholes will be documented during the drilling phase to secure a maximum of information in case of an unexpected loss of the borehole and that a full scientific coverage to total depth is achieved with post-drilling surveys.

Of paramount importance is timely and sustained contact with the office of the governor of Svalbard, to inform them about the project, discuss targets, and get advice about regulations and restrictions, thus preparing for the permitting process and outreach to the local community.

## 5 Synergies to ongoing ICDP and IODP projects

The SVALCLIME initiative is ambitious in its multi-event approach while geographically constrained to Svalbard itself. As such, it is important to highlight how this broad approach is linked and complementary to other ongoing initiatives on deep-time climate in the region and globally (Table 2).

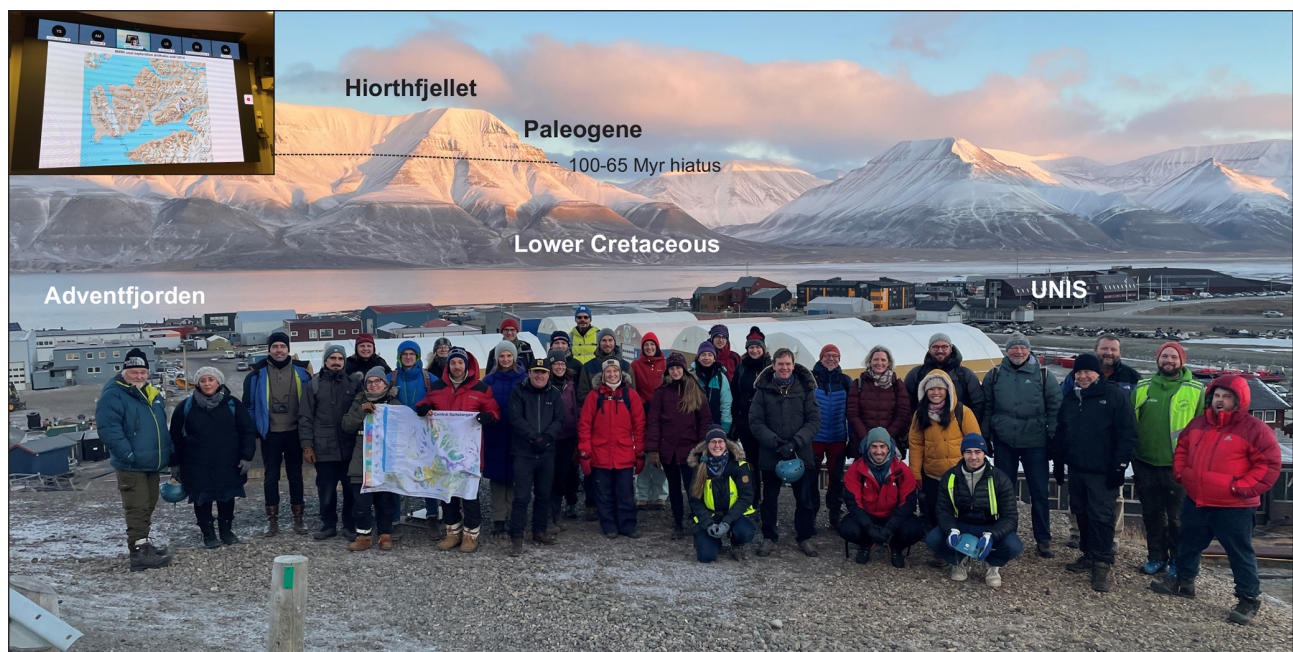
## 6 Outcomes and future plans

The outlined SVALCLIME workshop (Fig. 6) fulfilled its main objective by bringing together a broad, multidisciplinary, enthusiastic group of researchers spanning from MSc students to senior scientists and by formulating specific research questions that Svalbard's rock record can contribute to answering. An ICDP pre-proposal was submitted in January 2023 as a direct result of the workshop. A full ICDP drilling proposal will be developed during 2023 and submitted in January 2024, incorporating comments



**Table 2.** Summary of thematically or geographically complementary scientific projects with relevance to SVALCLIME.

Project	Stratigraphic target	Location	Comment	Reference
IODP X302 (ACEX)	Paleocene and early Eocene, with major hiatus	central Arctic Ocean	Completed in August–September 2004	Backman et al. (2004)
IODP X377 (ArcOP)	Cenozoic	Arctic Ocean	Cancelled due to geopolitics	
IODP X396	PETM, volcanoclastics	Norwegian Sea	Completed in August–October 2022	Berndt et al. (2019), Planke et al. (2023)
IODP X403	Cenozoic	Eastern Fram Strait	Scheduled June–August 2024	Lucchi et al. (2023)
IODP X404	Cenozoic	NE Atlantic	Cancelled due to <i>JOIDES Resolution</i> decommissioning	
NorthGreen	Cenozoic	NE Atlantic	Workshop held in November 2022	Pérez et al. (2023)
ICDP Deep Dust	Permian part of the LPIA	Paris Basin, France; Oklahoma Basin, USA	Multi-phase drilling planned, first in USA	Soreghan et al. (2020)
ICDP PVOLC	PETM	Northern Jutland, Denmark	Ready to drill, waiting for Denmark to become ICDP member	Berndt et al. (2019)
Bighorn Basin Coring Project (BBCP)	PETM, ETM2	Wyoming, USA	Completed	Clyde et al. (2013)
PETM	PETM	mid-Atlantic US coastal plain	Workshop held in 2022	NA

**Figure 6.** Group photograph of the SVALCLIME participants taken during an optional extended lunch break while walking from UNIS to outcrops exposing the Lower Cretaceous Carolinifjellet Formation on the road connecting Longyearbyen with Svalbard Airport.

from ICDP's Scientific Advisory Group on the pre-proposal and through further engagement of the international geoscientific community. In addition, we foresee systematic use of existing drill cores in research projects and in relevant courses at UNIS and other involved institutions to complement work on cores obtained through future ICDP drilling.

## Appendix A

**Table A1.** Participant list of the SVALCLIME workshop. Early-career researchers (ECRs) – representing MSc or PhD students and recent PhD graduates  $\leq 7$  years from PhD defence – are highlighted with an ×.

Name	Institution	Country	ECR
In-person attendees			
Aisha Al Suwaidi	Earth and Planetary Science Dept. Khalifa University	UAE	
Albina Gilmullina	University of Bergen	Norway	×
Aleksandra Smyrak-Sikora	UNIS	Svalbard	×
Anders Dahlin	UNIS	Svalbard	×
Anja Frank	Universität Hamburg	Germany	×
Anna Filipova	freelance artist	France	
Anna Marie Rose Sartell	University of Helsinki	Finland	×
Annie van der Boon	University of Oslo	Norway	
Carl Lie	UNIS	Svalbard	×
Chanakan Boonnawa	University of Bergen	Norway	×
Denise Kulhanek	Kiel University	Germany	
Erik Petter Johannessen	Consulting	Norway	
Farah Gagnier	University of Quebec in Montreal	Canada	×
Felix Elling	Kiel University	Germany	
Fenna Ammerlaan	Utrecht University	the Netherlands	×
Gerald Dickens	Trinity College Dublin	Ireland	
Grace Shephard	University of Oslo	Norway	
Greg Price	University of Plymouth	United Kingdom	
Henning Lorenz	Uppsala University	Sweden	
Isabel McDonald	University of Helsinki	Finland	×
Jack Whattam	University of Oslo	Norway	×
Jan Inge Faleide	University of Oslo	Norway	
Jennifer Galloway	Geological Survey of Canada	Canada	
Jonas Liebsch	Kiel University	Germany	×
Juan David Solano Acosta	Tallinn University of Technology (Taltech)	Estonia	×
Kasia K. Sliwinska	GEUS	Denmark	
Katrine Husum	Norwegian Polar Institute	Svalbard	
Kim Senger	UNIS	Svalbard	
Kristin Diane Bergmann	Massachusetts Institute of Technology	USA	
Lauri Malinen	University of Helsinki	Finland	×
Leandro Cesar Gallo	University of Oslo	Norway	×
Madeleine Vickers	University of Oslo	Norway	×



**Table A1.** Continued.

Name	Institution	Country	ECR
Mads E. Jelby	University of Copenhagen	Denmark	×
Marcos Tirado	University of Bergen	Norway	×
Maria Jensen	UNIS	Svalbard	
Marjolaine Verret	UNIS	Svalbard	
Matthijs Nuus	UNIS	Svalbard	×
Micha Ruhl	Trinity College Dublin, The University of Dublin	Ireland	
Monica Alejandra Gomez Correa	Universität Hamburg	Germany	×
Morgan Jones	University of Oslo	Norway	
Nickolas Bode	RWTH Aachen University	Germany	×
Nil Rodes	UNIS	Svalbard	×
Olaf Thiessen	Equinor	Norway	
Peter Betlem	UNIS	Svalbard	×
Philippe Claeys	Analytical, Environmental & Geo-Chemistry, Vrije Universiteit Brussel	Belgium	
Rafael Horota	UNIS	Svalbard	×
Sabina Kraatz	UNIS	Svalbard	×
Sara Cohen	UNIS	Svalbard	
Snorre Olaussen	UNIS	Svalbard	
Sten-Andreas Grundvåg	UiT The Arctic University of Norway	Norway	
Stephen Hesselbo	University of Exeter	United Kingdom	
Tatiana Sitnikova	University of Ottawa	Canada	×
Tereza Mosočiová	UNIS	Svalbard	×
Tom Birchall	Consulting	Norway	×
Tom Schaber	RWTH Aachen University	Germany	×
Valentin Zuchuat	RWTH Aachen University	Germany	×
Victoria Sjøholt Engelschiøn	Natural History Museum, University of Oslo	Norway	×
Weimu Xu	University College Dublin	Ireland	×
Digital attendees			
Anna van Yperen	University of Oslo	Norway	×
Bas van de Schootbrugge	Utrecht University	the Netherlands	
Boyang Zhao	Brown University	United States	
Cecilia Benavente	IANIGLA-CONICET, Facultad de Ciencias Exactas y Naturales UNCuyo, University of Mendoza	Argentina	
Christian Zeeden	Leibniz Institute for Applied Geophysics	Germany	
Clemens V Ullmann	University of Exeter	United Kingdom	
Anne-Christine Da Silva	Liege University	Belgium	

**Table A1.** Continued.

Name	Institution	Country	ECR
Leon J. Clarke	Manchester Metropolitan University	United Kingdom	
Huguet Arnaud	CNRS/Sorbonne University	France	
Ke Zhao	Camborne School of Mines, University of Exeter	United Kingdom	
Lara F. Perez	Geological Survey of Denmark and Greenland (GEUS)	Denmark	
Lutz Reinhardt	Federal Institute for Geosciences and Natural Resources (BGR)	Germany	
Maayke Koevoets-Westerduin	Geologische Dienst Nederland–Netherlands Organisation for Applied Scientific Research (TNO)	the Netherlands	
Maciej Jez	Institute of Geological Sciences, Polish Academy of Sciences	Poland	
Malte Jochmann	Store Norske Spitsbergen Kulkompani	Svalbard	×
Marcello Gugliotta	University of Bremen	Germany	×
Marjorie Cantine	Goethe University Frankfurt and University of Washington	Germany and United States	×
Matthew Staitis	University of East Anglia	United Kingdom	
Matthias Sinnesael	Paris Observatory	France	×
Meng Wang	Peking University	China	
Michel Crucifix	Université catholique de Louvain	Belgium	
Mingsong Li	Peking University	China	
Ricardo L. Silva	University of Manitoba	Canada	
Rüdiger Stein	MARUM – Center for Marine Environmental Sciences, Bremen University	Germany	
Salman Khan	Birbal Sahni Institute of Paleosciences	India	
Simona Pierdominici	Helmholtz-Zentrum Potsdam Deutsches GeoForschungsZentrum – GFZ	Germany	
Stella Buchwald	Universität Hamburg	Germany	×
Thomas Gibson	University of Exeter	United Kingdom	
Valentina M Rossi	National Research Council of Italy – Institute of Geosciences and Georesources	Italy	
Waliur Rahaman	National Centre for Polar and Ocean Research, Goa	India	
Weiqi Yao	Southern University of Science and Technology	China	
William Foster	Universität Hamburg	Germany	
Yvonne Spsychala	Leibniz University Hannover	Germany	×

## Appendix B: Abbreviations

ACEX	Arctic Coring Expedition (Integrated Ocean Drilling Program Exp. 302)
ArcOP	Arctic Ocean Paleoceanography
BBCP	Bighorn Basin Coring Project
CIE	carbon isotope excursion
COSC	Collisional Orogeny in the Scandinavian Caledonides
CT	computed tomography
DSDP	Deep Sea Drilling Project
EOT	Eocene–Oligocene transition
EPME	end-Permian mass extinction
HALIP	High Arctic Large Igneous Province
ICDP	International Continental Scientific Drilling Program
IODP	International Ocean Discovery Program
IPCC	Intergovernmental Panel on Climate Change
LIP	large igneous province
LPIA	Late Paleozoic Ice Age
MSCL	multisensor core logger
NAIP	North Atlantic Igneous Province
OAE	oceanic anoxic event
ODP	Ocean Drilling Program
PETM	Paleocene–Eocene Thermal Maximum
PVOLC	volcanic forcing and Paleogene climate change
Re-Os	rhenium–osmium
SAG	Science Advisory Group
NSNK	Store Norske (formerly Store Norske Spitsbergen Kulkompani AS, the Norwegian coal mining company on Svalbard)
UNIS	The University Centre in Svalbard
VOICE	Volgian isotopic carbon excursion
XRF	X-ray fluorescence

**Data availability.** No data sets were used in this article.

**Author contributions.** KS, ASS, MTJ, SP, VZ, and DK proposed and convened the workshop. All co-authors contributed to the text and figures that resulted in the submission of a preliminary ICDP proposal, led by DK. Participants at the workshop contributed intellectual input. All co-authors contributed to writing and reviewing the text of this article.

**Competing interests.** The contact author has declared that none of the authors has any competing interests.

**Disclaimer.** Publisher's note: Copernicus Publications remains neutral with regard to jurisdictional claims made in the text, published maps, institutional affiliations, or any other geographical representation in this paper. While Copernicus Publications makes ev-

ery effort to include appropriate place names, the final responsibility lies with the authors.

**Acknowledgements.** We sincerely appreciate the participants of the SVALCLIME workshop for their scientific expertise and enthusiasm to develop the SVALCLIME ICDP project. We also thank the UNIS student assistants Tereza Mosočiová, Nil Rodes, Carl Lie, and Matthijs Nuus for support during the workshop, for allowing digital participation, for organizing field excursions, and for the all-important catering.

Finally, we sincerely thank journal reviewers Matt O'Regan, Catalina Gebhardt, and Julie Brigham-Grette for their constructive feedback.

**Financial support.** This research has been supported by the Norges Forskningsråd (grant no. 331679). The SVALCLIME workshop was funded by MagellanPlus/ECORD and UNIS. The efforts built largely on the “Svalbard Rock Vault” and “Svalbox” projects, both funded by Svalbard Strategic Grants from the Research Council of Norway.

**Review statement.** This paper was edited by Nadine Hallmann and reviewed by Matt O'Regan, Catalina Gebhardt, and Julie Brigham-Grette.

## References

- Ahlborn, M. and Stemmerik, L.: Depositional evolution of the Upper Carboniferous–Lower Permian Wordiekkammen carbonate platform, Nordfjorden High, central Spitsbergen, Arctic Norway, *Norw. J. Geol.*, 95, 91–126, <https://doi.org/10.17850/njg95-1-03>, 2015.
- Aretz, M., Herbig, H.-G., Wang, X., Gradstein, F., Agterberg, F., and Ogg, J.: The carboniferous period, in: *Geologic time scale 2020*, Elsevier, 811–874, <https://doi.org/10.1016/B978-0-12-824360-2.00023-1>, 2020.
- Backman, J., Jakobsson, M., Løvlie, R., Polyak, L., and Febo, L. A.: Is the central Arctic Ocean a sediment starved basin?, *Quaternary Sci. Rev.*, 23, 1435–1454, <https://doi.org/10.1029/2007PA001476>, 2004.
- Backman, J., Jakobsson, M., Frank, M., Sangiorgi, F., Brinkhuis, H., Stickley, C., O'Regan, M., Løvlie, R., Pälike, H., Spofforth, D., Gattaceca, J., Moran, K., King, J., and Heil, C.: Age model and core-seismic integration for the Cenozoic Arctic Coring Expedition sediments from the Lomonosov Ridge, *Paleoceanography*, 23, PA1S03, <https://doi.org/10.1029/2007PA001476>, 2008.
- Berndt, C., Planke, S., Teagle, D., Huismans, R., Torsvik, T., Frieling, J., Jones, M. T., Jerram, D. A., Tegner, C., Faleide, J. I., Coxall, H., and Hong, W.-L.: Northeast Atlantic breakup volcanism and consequences for Paleogene climate change – MagellanPlus Workshop report, *Sci. Dril.*, 26, 69–85, <https://doi.org/10.5194/sd-26-69-2019>, 2019.
- Betlem, P., Rodes, N., Birchall, T., Dahlin, A., Smyrak-Sikora, A., and Senger, K.: The Svalbox Digital Model Database:



- a geoscientific window to the High Arctic, *Geosphere*, <https://doi.org/10.1130/GES02606.1>, online first, 2023.
- Blinova, N. V., Stejskal, J., Trchová, M., Sapurina, I., and Ćirić-Marjanović, G.: The oxidation of aniline with silver nitrate to polyaniline–silver composites, *Polymer*, 50, 50–56, <https://doi.org/10.1016/j.polymer.2008.10.040>, 2009.
- Bond, D. P., Blomeier, D. P., Dustira, A. M., Wignall, P. B., Collins, D., Goode, T., Groen, R. D., Buggisch, W., and Grasby, S. E.: Sequence stratigraphy, basin morphology and sea-level history for the Permian Kapp Starostin Formation of Svalbard, Norway, *Geol. Mag.*, 155, 1023–1039, <https://doi.org/10.1017/S0016756816001126>, 2018.
- Bond, D. P., Wignall, P. B., and Grasby, S. E.: The Capitanian (Guadalupian, Middle Permian) mass extinction in NW Pangea (Borup Fiord, Arctic Canada): A global crisis driven by volcanism and anoxia, *GSA Bull.*, 132, 931–942, <https://doi.org/10.1130/B35281.1>, 2020.
- Braathen, A., Bælum, K., Christiansen, H. H., Dahl, T., Eiken, O., Elvebakk, H., Hansen, F., Hanssen, T. H., Jochmann, M., Johansen, T. A., Johnsen, H., Larsen, L., Lie, T., Mertes, J., Mørk, A., Mørk, M. B., Nemec, W. J., Olausen, S., Oye, V., Rød, K., Titlestad, G. O., Tveranger, J., and Vagle, K.: Longyearbyen CO<sub>2</sub> lab of Svalbard, Norway – first assessment of the sedimentary succession for CO<sub>2</sub> storage, *Norw. J. Geol.*, 92, 353–376, 2012.
- Brocks, J. J., Jarrett, A. J., Sirantoine, E., Hallmann, C., Hoshino, Y., and Liyanage, T.: The rise of algae in Cryogenian oceans and the emergence of animals, *Nature*, 548, 578–581, <https://doi.org/10.1038/nature23457>, 2017.
- Intergovernmental Panel on Climate Change (IPCC): Global Carbon and Other Biogeochemical Cycles and Feedbacks, in: *Climate Change 2021 – The Physical Science Basis: Working Group I Contribution to the Sixth Assessment Report of the Intergovernmental Panel on Climate Change*, Cambridge, Cambridge University Press, 673–816, <https://doi.org/10.1017/9781009157896.007>, 2023.
- Charles, A. J., Condon, D. J., Harding, I. C., Pälike, H., Marshall, J. E., Cui, Y., Kump, L., and Croudace, I. W.: Constraints on the numerical age of the Paleocene–Eocene boundary, *Geochem. Geophys. Geos.*, 12, Q0AA17, <https://doi.org/10.1029/2010GC003426>, 2011.
- Clyde, W. C., Gingerich, P. D., Wing, S. L., Röhl, U., Westerhold, T., Bowen, G., Johnson, K., Baczynski, A. A., Diefendorf, A., McInerney, F., Schnurrenberger, D., Noren, A., Brady, K., and the BBCP Science Team: Bighorn Basin Coring Project (BBCP): a continental perspective on early Paleogene hyperthermals, *Sci. Dril.*, 16, 21–31, <https://doi.org/10.5194/sd-16-21-2013>, 2013.
- Cramer, B. S., Wright, J. D., Kent, D. V., and Aubry, M. P.: Orbital climate forcing of  $\delta^{13}\text{C}$  excursions in the late Paleocene–early Eocene (chrons C24n–C25n), *Paleoceanography*, 18, 1097, <https://doi.org/10.1029/2003PA000909>, 2003.
- Cui, Y.: Carbon addition during the Paleocene–Eocene Thermal Maximum: model inversion of a new, high-resolution carbon isotope record from Svalbard, MSc thesis, Pennsylvania State University, [https://etda.libraries.psu.edu/files/final\\_submissions/6907](https://etda.libraries.psu.edu/files/final_submissions/6907) (last access: 4 October 2023), 2010.
- Cui, Y., Diefendorf, A. F., Kump, L. R., Jiang, S., and Freeman, K. H.: Synchronous marine and terrestrial carbon cycle perturbation in the high arctic during the PETM, *Paleoceanography and Paleoclimatology*, 36, e2020PA003942, <https://doi.org/10.1029/2020PA003942>, 2021.
- Cutbill, J. and Challinor, A.: Revision of the stratigraphical scheme for the Carboniferous and Permian rocks of Spitsbergen and Bjørnøya, *Geol. Mag.*, 102, 418–439, 1965.
- Dallmann, W. K. (Ed.): *Lithostratigraphic Lexicon of Svalbard. Upper Palaeozoic to Quaternary Bedrock, Review and Recommendations for Nomenclature Use*, Committee on the Stratigraphy of Svalbard/Norsk Polarinstitutt, p. 320, ISBN 82-7666-166-1, 1999.
- Dickens, G. R., O’Neil, J. R., Rea, D. K., and Owen, R. M.: Dissociation of oceanic methane hydrate as a cause of the carbon isotope excursion at the end of the Paleocene, *Paleoceanography*, 10, 965–971, 1995.
- Doerner, M., Berner, U., Erdmann, M., and Barth, T.: Geochemical characterization of the depositional environment of Paleocene and Eocene sediments of the Tertiary Central Basin of Svalbard, *Chem. Geol.*, 542, 119587, <https://doi.org/10.1016/j.chemgeo.2020.119587>, 2020.
- Dypvik, H., Riber, L., Burca, F., Rütther, D., Jargvoll, D., Nagy, J., and Jochmann, M.: The Paleocene–Eocene thermal maximum (PETM) in Svalbard – clay mineral and geochemical signals, *Palaeogeogr. Palaeoclimatol.*, 302, 156–169, 2011.
- Elvevold, S., Dallmann, W., and Blomeier, D.: *Geology of Svalbard*, Norwegian Polar Institute, Tromsø, Norway, 38 pp., <https://brage.npolar.no/npolar-xmlui/bitstream/handle/11250/173141/GeologyOfSvalbard.pdf?sequence=1&isAllowed=y> (last access: 4 October 2023), 2007.
- Erba, E., Duncan, R. A., Bottini, C., Tiraboschi, D., Weissert, H., Jenkyns, H. C., and Malinverno, A.: Environmental consequences of Ontong Java Plateau and Kerguelen plateau volcanism, The origin, evolution, and environmental impact of oceanic large igneous provinces, *Geol. Soc. Am. Spec. Pap.*, 511, 271–303, [https://doi.org/10.1130/2015.2511\(15\)](https://doi.org/10.1130/2015.2511(15)), 2015.
- Evans, D., Sagoo, N., Renema, W., Cotton, L. J., Müller, W., Todd, J. A., Saraswati, P. K., Stassen, P., Ziegler, M., and Pearson, P. N.: Eocene greenhouse climate revealed by coupled clumped isotope–Mg/Ca thermometry, *P. Natl. Acad. Sci. USA*, 115, 1174–1179, <https://doi.org/10.1073/pnas.1714744115>, 2018.
- Farabegoli, E., Perri, M. C., and Posenato, R.: Environmental and biotic changes across the Permian–Triassic boundary in western Tethys: the Bulla parastratotype, Italy, *Global Planet. Change*, 55, 109–135, <https://doi.org/10.1016/j.gloplacha.2006.06.009>, 2007.
- Feyling-Hanssen, R. W. and Ulleberg, K.: A Tertiary–Quaternary section at Sarsbukta, Spitsbergen, Svalbard, and its foraminifera, *Pol. Res.*, 2, 77–106, <https://doi.org/10.1111/j.1751-8369.1984.tb00487.x>, 1984.
- Fischer, T., Hrubcová, P., Dahm, T., Woith, H., Vylita, T., Ohrnberger, M., Vlček, J., Horálek, J., Dědeček, P., Zimmer, M., Lipus, M. P., Pierdominici, S., Kallmeyer, J., Krüger, F., Hanemann, K., Korn, M., Kämpf, H., Reinsch, T., Klicpera, J., Vollmer, D., and Daskalopoulou, K.: ICDP drilling of the Eger Rift observatory: magmatic fluids driving the earthquake swarms and deep biosphere, *Sci. Dril.*, 31, 31–49, <https://doi.org/10.5194/sd-31-31-2022>, 2022.
- Foster, W. J., Danise, S., and Twitchett, R. J.: A silicified Early Triassic marine assemblage from Svalbard, *J. Syst. Palaeontol.*,

- 15, 851–877, <https://doi.org/10.1080/14772019.2016.1245680>, 2017.
- Foster, W. J., Asatryan, G., Botting, J., Rauzi, S., Lazarus, D. B., Buchwald, S. Z., Isson, T., Renaudie, J., and Kiessling, W.: Response of siliceous marine organisms to Permian-Triassic climate crisis based on new findings from central Spitsbergen, Svalbard, ESS Open Archive, <https://doi.org/10.22541/essoar.169447472.26881234/v1>, 2023.
- Gastaldo, R. A., DiMichele, W. A., and Pfefferkorn, H. W.: Out of the icehouse into the greenhouse: a late Paleozoic analogue for modern global vegetational change, *GSA today*, <https://rock.geosociety.org/net/gsatoday/archive/6/10/pdf/gt9610.pdf> (last access: 4 October 2023), 1996.
- Grundvåg, S. A., Helland-Hansen, W., Johannessen, E. P., Olsen, A. H., and Stene, S. A.: The depositional architecture and facies variability of shelf deltas in the Eocene Battfjellet Formation, Nathorst Land, Spitsbergen, *Sedimentology*, 61, 2172–2204, 2014.
- Gutjahr, M., Ridgwell, A., Sexton, P. F., Anagnostou, E., Pearson, P. N., Pälike, H., Norris, R. D., Thomas, E., and Foster, G. L.: Very large release of mostly volcanic carbon during the Palaeocene–Eocene Thermal Maximum, *Nature*, 548, 573–577, <https://doi.org/10.1038/nature23646>, 2017.
- Harding, I. C., Charles, A. J., Marshall, J. E. A., Pälike, H., Roberts, A. P., Wilson, P. A., Jarvis, E., Thorne, R., Morris, E., Moremon, R., Pearce, R. B., and Akbari, S.: Sea-level and salinity fluctuations during the Paleocene–Eocene thermal maximum in Arctic Spitsbergen, *Earth Planet. Sc. Lett.*, 303, 97–107, <https://doi.org/10.1016/j.epsl.2010.12.043>, 2011.
- Heimdal, T. H., Callegaro, S., Svensen, H. H., Jones, M. T., Pereira, E., and Planke, S.: Evidence for magma–evaporite interactions during the emplacement of the Central Atlantic Magmatic Province (CAMP) in Brazil, *Earth Planet. Sc. Lett.*, 506, 476–492, <https://doi.org/10.1016/j.epsl.2018.11.018>, 2019.
- Helland-Hansen, W. and Grundvåg, S. A.: The Svalbard Eocene–Oligocene (?) Central Basin succession: Sedimentation patterns and controls, *Basin Res.*, 33, 729–753, 2021.
- Herrle, J. O., Schröder-Adams, C. J., Davis, W., Pugh, A. T., Galloway, J. M., and Fath, J.: Mid-Cretaceous High Arctic stratigraphy, climate, and oceanic anoxic events, *Geology*, 43, 403–406, 2015.
- Hesselbo, S. P., Gröcke, D. R., Jenkyns, H. C., Bjerrum, C. J., Farimond, P., Morgans Bell, H. S., and Green, O. R.: Massive dissociation of gas hydrate during a Jurassic oceanic anoxic event, *Nature*, 406, 392–395, 2000.
- Hoffman, P. F. and Schrag, D. P.: The snowball Earth hypothesis: testing the limits of global change, *Terra Nova*, 14, 129–155, <https://doi.org/10.1046/j.1365-3121.2002.00408.x>, 2002.
- Holland, M. M. and Bitz, C. M.: Polar amplification of climate change in coupled models, *Clim. Dynam.*, 21, 221–232, <https://doi.org/10.1007/s00382-003-0332-6>, 2003.
- Hossain, A., Knorr, G., Jokat, W., and Lohmann, G.: Opening of the Fram Strait led to the establishment of a modern-like three-layer stratification in the Arctic Ocean during the Miocene, *Arktos*, 7, 1–12, <https://doi.org/10.1007/s41063-020-00079-8>, 2021.
- Hutchinson, D. K., Coxall, H. K., O'Regan, M., Nilsson, J., Caballero, R., and de Boer, A. M.: Arctic closure as a trigger for Atlantic overturning at the Eocene–Oligocene Transition, *Nat. Commun.*, 10, 3797, <https://doi.org/10.1038/s41467-019-11828-z>, 2019.
- Hutchinson, D. K., Coxall, H. K., Lunt, D. J., Steinthorsdottir, M., de Boer, A. M., Baatsen, M., von der Heydt, A., Huber, M., Kennedy-Asser, A. T., Kunzmann, L., Ladant, J.-B., Lear, C. H., Moraweck, K., Pearson, P. N., Piga, E., Pound, M. J., Salzmann, U., Scher, H. D., Sijp, W. P., Śliwińska, K. K., Wilson, P. A., and Zhang, Z.: The Eocene–Oligocene transition: a review of marine and terrestrial proxy data, models and model–data comparisons, *Clim. Past*, 17, 269–315, <https://doi.org/10.5194/cp-17-269-2021>, 2021.
- Inglis, G. N., Bragg, F., Burls, N. J., Cramwinckel, M. J., Evans, D., Foster, G. L., Huber, M., Lunt, D. J., Siler, N., Steinig, S., Tierney, J. E., Wilkinson, R., Anagnostou, E., de Boer, A. M., Dunkley Jones, T., Edgar, K. M., Hollis, C. J., Hutchinson, D. K., and Pancost, R. D.: Global mean surface temperature and climate sensitivity of the early Eocene Climatic Optimum (EECO), Paleocene–Eocene Thermal Maximum (PETM), and latest Paleocene, *Clim. Past*, 16, 1953–1968, <https://doi.org/10.5194/cp-16-1953-2020>, 2020.
- Isbell, J. L., Fraiser, M. L., and Henry, L. C.: Examining the Complexity of Environmental Change during the Late Paleozoic and Early Mesozoic, *PALAIOS*, 23, 267–269, <https://doi.org/10.2110/palo.2008.S03>, 2008.
- Jakobsson, M., Mayer, L., Coakley, B., Dowdeswell, J. A., Forbes, S., Fridman, B., Hodnesdal, H., Noormets, R., Pedersen, R., Rebesco, M., Schenke, H. W., Zarayskaya, Y., Accettella, D., Armstrong, A., Anderson, R. M., Bienhoff, P., Camerlenghi, A., Church, I., Edwards, M., Gardner, J. V., Hall, J. K., Hell, B., Hestvik, O., Kristoffersen, Y., Marcussen, C., Mohammad, R., Mosher, D., Nghiem, S. V., Pedrosa, M. T., Travaglini, P. G., and Weatherall, P.: The International Bathymetric Chart of the Arctic Ocean (IBCAO) Version 3.0, *Geophys. Res. Lett.*, 39, L12609, <https://doi.org/10.1029/2012GL052219>, 2012.
- Jelby, M. E., Śliwińska, K. K., Koevoets, M. J., Alsen, P., Vickers, M. L., Olausson, S., and Stemmerik, L.: Arctic reappraisal of global carbon-cycle dynamics across the Jurassic–Cretaceous boundary and Valanginian Weissert Event, *Palaeogeogr. Palaeoclimatol.*, 555, 109847, <https://doi.org/10.1016/j.palaeo.2020.109847>, 2020.
- Jin, Y., Wang, Y., Wang, W., Shang, Q., Cao, C., and Erwin, D. H.: Pattern of marine mass extinction near the Permian-Triassic boundary in South China, *Science*, 289, 432–436, 2000.
- Johannessen, E. P., Henningsen, T., Bakke, N. E., Johansen, T. A., Ruud, B. O., Riste, P., Elvebakk, H., Jochmann, M., Elvebakk, G., and Woldengen, M. S.: Palaeogene clinoform succession on Svalbard expressed in outcrops, seismic data, logs and cores, *First Break*, 29, 35–44, 2011.
- Jones, M. T., Jerram, D. A., Svensen, H. H., and Grove, C.: The effects of large igneous provinces on the global carbon and sulphur cycles, *Palaeogeogr. Palaeoclimatol.*, 441, 4–21, <https://doi.org/10.1016/j.palaeo.2015.06.042>, 2016.
- Klausen, T. G., Nyberg, B., and Helland-Hansen, W.: The largest delta plain in Earth's history, *Geology*, 47, 470–474, <https://doi.org/10.1130/G45507.1>, 2019.
- Koevoets, M. J., Abay, T. B., Hammer, Ø., and Olausson, S.: High-resolution organic carbon–isotope stratigraphy of the Middle Jurassic–Lower Cretaceous Agardhfjellet Formation of cen-

- tral Spitsbergen, Svalbard, *Palaeogeogr. Palaeoclimatol.*, 449, 266–274, <https://doi.org/10.1016/j.palaeo.2016.02.029>, 2016.
- Koppers, A., and Coggon, R.: Exploring earth by scientific ocean drilling: 2050 Science Framework, International Ocean Drilling Programme, <https://www.iodp.org/2050-science-framework> (last access: 4 October 2023), 2020.
- Kristoffersen, Y., Ohta, Y., and Hall, J. K.: On the the origin of the Yermak Plateau north of Svalbard, Arctic Ocean, Norw. J. Geol./Norsk Geologisk Forening, 100, 202006, <https://doi.org/10.17850/njg100-1-5>, 2020.
- Lee, S., Shi, G. R., Nakrem, H. A., Woo, J., and Tazawa, J.-I.: Mass extinction or extirpation: Permian biotic turnovers in the northwestern margin of Pangea, *GSA Bull.*, 134, 2399–2414, <https://doi.org/10.1130/b36227.1>, 2022.
- Lorenz, H., Rosberg, J.-E., Juhlin, C., Klonowska, I., Lescoutre, R., Westmeijer, G., Almqvist, B. S. G., Anderson, M., Bertilsson, S., Dopson, M., Kallmeyer, J., Kück, J., Lehnert, O., Menegon, L., Pascal, C., Rejkjær, S., and Roberts, N. N. W.: COSC-2 – drilling the basal décollement and underlying margin of palaeocontinent Baltica in the Paleozoic Caledonide Orogen of Scandinavia, *Sci. Dril.*, 30, 43–57, <https://doi.org/10.5194/sd-30-43-2022>, 2022.
- Lourens, L. J., Sluijs, A., Kroon, D., Zachos, J. C., Thomas, E., Röhl, U., Bowles, J., and Raffi, I.: Astronomical pacing of late Palaeocene to early Eocene global warming events, *Nature*, 435, 1083–1087, <https://doi.org/10.1038/nature03814>, 2005.
- Lucchi, R. G., St. John, K., and Ronge, T. A.: Expedition 403 Scientific Prospectus: Eastern Fram Strait Paleo-Archive (FRAME), International Ocean Discovery Program, <https://doi.org/10.14379/iodp.sp.403.2023>, 2023.
- Lundschien, B. A., Mattingsdal, R., Johansen, S. K., and Knutsen, S.-M.: North Barents Composite Tectono-Sedimentary Element, Geological Society, London, Memoirs, 57, M57–2021–2039, <https://doi.org/10.1144/M57-2021-39>, 2024.
- Midtkandal, I., Svensen, H. H., Planke, S., Corfu, F., Polteau, S., Torsvik, T. H., Faleide, J. I., Grundvåg, S.-A., Selnes, H., and Kürschner, W.: The Aptian (Early Cretaceous) oceanic anoxic event (OAE1a) in Svalbard, Barents Sea, and the absolute age of the Barremian-Aptian boundary, *Palaeogeogr. Palaeoclimatol.*, 463, 126–135, <https://doi.org/10.1016/j.palaeo.2016.09.023>, 2016.
- Montañez, I. P. and Poulsen, C. J.: The Late Paleozoic ice age: an evolving paradigm, *Annu. Rev. Earth Pl. Sc.*, 41, 629–656, 2013.
- Montañez, I. P., Tabor, N. J., Niemeier, D., DiMichele, W. A., Frank, T. D., Fielding, C. R., Isbell, J. L., Birgenheier, L. P., and Rygel, M. C.: CO<sub>2</sub>-forced climate and vegetation instability during Late Paleozoic deglaciation, *Science*, 315, 87–91, 2007.
- Mørk, A., Embry, A. F., and Weitschat, W.: Triassic transgressive-regressive cycles in the Sverdrup Basin, Svalbard and the Barents Shelf, in: Correlation in Hydrocarbon Exploration, edited by: Collinson, J. D., Springer, Dordrecht, [https://doi.org/10.1007/978-94-009-1149-9\\_11](https://doi.org/10.1007/978-94-009-1149-9_11), 1989.
- Mørk, A., Dallmann, W., Dypvik, H., Johannessen, E., Larssen, G., Nagy, J., Nøttvedt, A., Olaussen, S., Pchelina, T., and Worsley, D.: Mesozoic lithostratigraphy, Lithostratigraphic lexicon of Svalbard. Upper Palaeozoic to Quaternary bedrock. Review and recommendations for nomenclature use, Norwegian Polar Institute, 127–214, ISBN 82-7666-166-1, 1999.
- Nakrem, H. A. and Mørk, A.: New early Triassic Bryozoa (Trepostomata) from Spitsbergen, with some remarks on the stratigraphy of the investigated horizons, *Geol. Mag.*, 128, 129–140, <https://doi.org/10.1017/S001675680001832X>, 1991.
- Ogg, J. G., Ogg, G. M., and Gradstein, F. M.: A concise geologic time scale: 2016, Elsevier, ISBN 9780444637710, 2016.
- Ohm, S. E., Larsen, L., Olaussen, S., Senger, K., Birchall, T., Demchuk, T., Hodson, A., Johansen, I., Titlestad, G. O., and Karlsen, D. A.: Discovery of shale gas in organic-rich Jurassic successions, Adventdalen, Central Spitsbergen, Norway, *Norsk Geol. Tidsskr.*, 99, 349–376, <https://doi.org/10.17850/njg007>, 2019.
- Olaussen, S., Senger, K., Braathen, A., Grundvåg, S. A., and Mørk, A.: You learn as long as you drill; research synthesis from the Longyearbyen CO<sub>2</sub> Laboratory, Svalbard, Norway, *Norw. J. Geol.*, 99, 157–187, <https://doi.org/10.17850/njg008>, 2019.
- Olaussen, S., Grundvåg, S.-A., Senger, K., Anell, I., Betlem, P., Birchall, T., Braathen, A., Dallmann, W. M., Johannessen, E. P., Lord, G., Mørk, A., Osmundsen, P. T., Smyrak-Sikora, A., and Stemmerik, L.: Svalbard Composite Tectono-Stratigraphic Element, High Arctic Norway Geological Society of London Memoirs, <https://doi.org/10.1144/M57-2021-36>, 2023.
- Penn, J. L., Deutsch, C., Payne, J. L., and Sperling, E. A.: Temperature-dependent hypoxia explains biogeography and severity of end-Permian marine mass extinction, *Science*, 362, eaat1327, <https://doi.org/10.1126/science.aat1327>, 2018.
- Percival, L., Tedeschi, L. R., Creaser, R., Bottini, C., Erba, E., Giraud, F., Svensen, H., Savian, J., Trindade, R., and Coccioni, R.: Determining the style and provenance of magmatic activity during the Early Aptian Oceanic Anoxic Event (OAE 1a), *Global Planet. Change*, 200, 103461, <https://doi.org/10.1016/j.gloplacha.2021.103461>, 2021.
- Pérez, L. F., Knutz, P. C., Hopper, J., Seidenkrantz, M.-S., and O'Regan, M.: Scientific drilling in Northeast Greenland: Greenland Ice Sheet sensitivity to polar amplification and long-term ice-ocean-tectonic interactions, EGU General Assembly 2023, Vienna, Austria, 24–28 April 2023, EGU23-11575, <https://doi.org/10.5194/egusphere-egu23-11575>, 2023.
- Planke, S., Berndt, C., Alvarez Zarikian, C. A., and Expedition 396 Scientists: Proceedings of the International Ocean Discovery Program Volume 396 – Mid-Norwegian Margin Magmatism and Paleoclimate Implications, International Ocean Discovery Program, <https://doi.org/10.14379/iodp.proc.396.2023>, 2023.
- Poirier, A. and Hillaire-Marcel, C.: Improved Os-isotope stratigraphy of the Arctic Ocean, *Geophys. Res. Lett.*, 38, L14607, <https://doi.org/10.1029/2011GL047953>, 2011.
- Price, G. D., Bajnai, D., and Fiebig, J.: Carbonate clumped isotope evidence for latitudinal seawater temperature gradients and the oxygen isotope composition of Early Cretaceous seas, *Palaeogeogr. Palaeoclimatol.*, 552, 109777, <https://doi.org/10.1016/j.palaeo.2020.109777>, 2020.
- Rodríguez-Tovar, F., Dorador, J., Zuchuat, V., Planke, S., and Hammer, Ø.: Response of macrobenthic trace maker community to the end-Permian mass extinction in Central Spitsbergen, Svalbard, *Palaeogeogr. Palaeoclimatol.*, 581, 110637, <https://doi.org/10.1016/j.palaeo.2021.110637>, 2021.
- Rooney, A. D., Strauss, J. V., Brandon, A. D., and Macdonald, F. A.: A Cryogenian chronology: Two long-lasting synchronous Neoproterozoic glaciations, *Geology*, 43, 459–462, 2015.
- Ruhl, M. and Kürschner, W. M.: Multiple phases of carbon cycle disturbance from large igneous province forma-



- tion at the Triassic-Jurassic transition, *Geology*, 39, 431–434, <https://doi.org/10.1130/g31680.1>, 2011.
- Sangiorgi, F., Brumsack, H. J., Willard, D. A., Schouten, S., Stickley, C. E., O'Regan, M., Reichert, G. J., Sinninghe Damsté, J. S., and Brinkhuis, H.: A 26 million year gap in the central Arctic record at the greenhouse-icehouse transition: Looking for clues, *Paleoceanography*, 23, PA1S04, <https://doi.org/10.1029/2007PA001477>, 2008.
- Schaaf, N. W., Osmundsen, P. T., Van der Lelij, R., Schönnenberger, J., Lenz, O. K., Redfield, T. F., and Senger, K.: Tectono-sedimentary evolution of the eastern Forland-sundet Graben, Svalbard, Norw. *J. Geol.*, 100, 202021, <https://doi.org/10.17850/njg100-4-4>, 2021.
- Schlanger, S. O. and Jenkyns, H.: Cretaceous oceanic anoxic events: causes and consequences, *Geol. Mijnbouw*, 55, 179–184, 1976.
- Schobben, M., Foster, W. J., Sleveland, A. R., Zuchuat, V., Svensen, H. H., Planke, S., Bond, D. P., Marcelis, F., Newton, R. J., and Wignall, P. B.: A nutrient control on marine anoxia during the end-Permian mass extinction, *Nat. Geosci.*, 13, 640–646, <https://doi.org/10.1038/s41561-020-0622-1>, 2020.
- Senger, K., Brugmans, P., Grundvåg, S.-A., Jochmann, M. M., Nøttvedt, A., Olausen, S., Skotte, A., and Smyrak-Sikora, A.: Petroleum, coal and research drilling onshore Svalbard: a historical perspective, *Norw. J. Geol.*, 99, 30 pp., <https://doi.org/10.17850/njg99-3-1>, 2019.
- Senger, K., Betlem, P., Birchall, T., Gonzaga Jr, L., Grundvåg, S.-A., Horota, R. K., Laake, A., Kuckero, L., Mørk, A., and Planke, S.: Digitising Svalbard's Geology: the Festningen Digital Outcrop Model, *First Break*, 40, 47–55, 2022.
- Sluijs, A., Frieling, J., Inglis, G. N., Nierop, K. G. J., Peterse, F., Sangiorgi, F., and Schouten, S.: Late Paleocene–early Eocene Arctic Ocean sea surface temperatures: reassessing biomarker paleothermometry at Lomonosov Ridge, *Clim. Past*, 16, 2381–2400, <https://doi.org/10.5194/cp-16-2381-2020>, 2020.
- Smyrak-Sikora, A., Nicolaisen, J. B., Braathen, A., Johannessen, E. P., Olausen, S., and Stemmerik, L.: Impact of growth faults on mixed siliciclastic-carbonate-evaporite deposits during rift climax and reorganisation – Billefjorden Trough, Svalbard, Norway, *Basin Res.*, 33, 2643–2674, <https://doi.org/10.1111/bre.12578>, 2021.
- Soreghan, G. S., Beccaletto, L., Benison, K. C., Bourquin, S., Feulner, G., Hamamura, N., Hamilton, M., Heavens, N. G., Hinnov, L., Huttenlocker, A., Looy, C., Pfeifer, L. S., Pochat, S., Sardar Abadi, M., Zambito, J., and the Deep Dust workshop participants: Report on ICDP Deep Dust workshops: probing continental climate of the late Paleozoic icehouse–greenhouse transition and beyond, *Sci. Dril.*, 28, 93–112, <https://doi.org/10.5194/sd-28-93-2020>, 2020.
- Sorento, T., Olausen, S., and Stemmerik, L.: Controls on deposition of shallow marine carbonates and evaporites – lower Permian Gipshuken Formation, central Spitsbergen, Arctic Norway, *Sedimentology*, 67, 207–238, <https://doi.org/10.1111/sed.12640>, 2020.
- Steel, R., Gjølberg, J., Helland-Hansen, W., Kleinspehn, K., Nøttvedt, A., and Rye-Larsen, M.: The Tertiary strike-slip basins and orogenic belt of Spitsbergen, in: *Strike-Slip Deformation, Basin Formation, and Sedimentation*, edited by: Biddle, K. T. and Christie-Blick, N., SEPM Society for Sedimentary Geology, <https://doi.org/10.2110/pec.85.37.0319>, 1985.
- Steel, R. J. and Worsley, D.: Svalbard's post-Caledonian strata – an atlas of sedimentational patterns and palaeogeographic evolution, in: *Petroleum Geology of the North European Margin*, edited by: Spencer, A. M., Graham & Trotman, London, 109–135, [https://doi.org/10.1007/978-94-009-5626-1\\_9](https://doi.org/10.1007/978-94-009-5626-1_9), 1984.
- Stickley, C. E., Brinkhuis, H., Schellenberg, S. A., Sluijs, A., Röhl, U., Fuller, M., Grauert, M., Huber, M., Warnaar, J., and Williams, G. L.: Timing and nature of the deepening of the Tasmanian Gateway, *Paleoceanography*, 19, PA4027, <https://doi.org/10.1029/2004PA001022>, 2004.
- Stickley, C. E., St John, K., Koç, N., Jordan, R. W., Passchier, S., Pearce, R. B., and Kearns, L. E.: Evidence for middle Eocene Arctic sea ice from diatoms and ice-rafted debris, *Nature*, 460, 376–379, <https://doi.org/10.1038/nature08163>, 2009.
- Straume, E. O., Nummelin, A., Gaina, C., and Nisancioglu, K. H.: Climate transition at the Eocene–Oligocene influenced by bathymetric changes to the Atlantic–Arctic oceanic gateways, *P. Natl. Acad. Sci. USA*, 119, e2115346119, <https://doi.org/10.1073/pnas.2115346119>, 2022.
- Suan, G., Popescu, S.-M., Suc, J.-P., Schnyder, J., Fauquette, S., Baudin, F., Yoon, D., Piepjohn, K., Sobolev, N. N., and Labrousse, L.: Subtropical climate conditions and mangrove growth in Arctic Siberia during the early Eocene, *Geology*, 45, 539–542, <https://doi.org/10.1130/G38547.1>, 2017.
- Svensen, H., Planke, S., Malthe-Sørenssen, A., Jamtveit, B., Myklebust, R., Rasmussen Eidem, T., and Rey, S. S.: Release of methane from a volcanic basin as a mechanism for initial Eocene global warming, *Nature*, 429, 542–545, 2004.
- Svensen, H., Planke, S., Polozov, A. G., Schmidbauer, N., Corfu, F., Podladchikov, Y. Y., and Jamtveit, B.: Siberian gas venting and the end-Permian environmental crisis, *Earth Planet. Sc. Lett.*, 277, 490–500, <https://doi.org/10.1016/j.epsl.2008.11.015>, 2009.
- Toggweiler, J. and Björnsson, H.: Drake Passage and palaeoclimate, *J. Quaternary Sci.*, 15, 319–328, 2000.
- Torsvik, T. H. and Cocks, L. R. M.: The integration of palaeomagnetism, the geological record and mantle tomography in the location of ancient continents, *Geol. Mag.*, 156, 242–260, 2019.
- Tripathi, A. and Darby, D.: Evidence for ephemeral middle Eocene to early Oligocene Greenland glacial ice and pan-Arctic sea ice, *Nat. Commun.*, 9, 1038, <https://doi.org/10.1038/s41467-018-03180-5>, 2018.
- Vickers, M. L., Jelby, M. E., Śliwińska, K. K., Percival, L. M., Wang, F., Sanei, H., Price, G. D., Ullmann, C. V., Grasby, S. E., and Reinhardt, L.: Volcanism and carbon cycle perturbations in the High Arctic during the Late Jurassic–Early Cretaceous, *Palaeogeogr. Palaeoclimatol.*, 613, 111412, <https://doi.org/10.1016/j.palaeo.2023.111412>, 2023.
- Vigran, J. O., Mangerud, G., Mørk, A., Worsley, D., and Hochuli, P. A.: Palynology and geology of the Triassic succession of Svalbard and the Barents Sea, *Norges geologiske undersøkelse, Geological Survey of Norway Special Publication*, 14, ISBN 978-82-7385-156-7, 2014.
- von Appen, W.-J., Schauer, U., Somavilla, R., Bauerfeind, E., and Beszczynska-Möller, A.: Exchange of warming deep waters across Fram Strait, *Deep-Sea Res. Pt. I*, 103, 86–100, <https://doi.org/10.1016/j.dsr.2015.06.003>, 2015.
- Weger, R. J., Eberli, G. P., Rodriguez Blanco, L., Tenaglia, M., and Swart, P. K.: Finding a VOICE in the Southern Hemisphere: A

- new record of global organic carbon?, *Geol. Soc. Am. Bull.*, 135, 2107–2120, <https://doi.org/10.1130/B36405.1>, 2022.
- Weijers, J. W., Schouten, S., Sluijs, A., Brinkhuis, H., and Damsté, J. S. S.: Warm arctic continents during the Palaeocene–Eocene thermal maximum, *Earth Planet. Sc. Lett.*, 261, 230–238, <https://doi.org/10.1016/j.epsl.2007.06.033>, 2007.
- West, C. K., Greenwood, D. R., and Basinger, J. F.: Was the Arctic Eocene “rainforest” monsoonal? Estimates of seasonal precipitation from early Eocene megafloras from Ellesmere Island, Nunavut, *Earth Planet. Sc. Lett.*, 427, 18–30, <https://doi.org/10.1016/j.epsl.2015.06.036>, 2015.
- Westerhold, T., Marwan, N., Drury, A. J., Liebrand, D., Agnini, C., Anagnostou, E., Barnet, J. S., Bohaty, S. M., De Vleeschouwer, D., and Florindo, F.: An astronomically dated record of Earth’s climate and its predictability over the last 66 million years, *Science*, 369, 1383–1387, <https://doi.org/10.1126/science.aba6853>, 2020.
- Wignall, P., Morante, R., and Newton, R.: The Permo-Triassic transition in Spitsbergen:  $\delta^{13}\text{C}_{\text{org}}$  chemostratigraphy, Fe and S geochemistry, facies, fauna and trace fossils, *Geol. Mag.*, 135, 47–62, <https://doi.org/10.1017/S0016756897008121>, 1998.
- Willard, D. A., Donders, T. H., Reichgelt, T., Greenwood, D. R., Sangiorgi, F., Peterse, F., Nierop, K. G., Frieling, J., Schouten, S., and Sluijs, A.: Arctic vegetation, temperature, and hydrology during Early Eocene transient global warming events, *Global Planet. Change*, 178, 139–152, <https://doi.org/10.1016/j.gloplacha.2019.04.012>, 2019.
- Zachos, J. C., Dickens, G. R., and Zeebe, R. E.: An early Cenozoic perspective on greenhouse warming and carbon-cycle dynamics, *Nature*, 451, 279–283, <https://doi.org/10.1038/nature06588>, 2008.
- Zuchuat, V., Sleveland, A. R. N., Twitchett, R. J., Svensen, H. H., Turner, H., Augland, L. E., Jones, M. T., Hammer, Ø., Hauksson, B. T., Haflidason, H., Midtkandal, I., and Planke, S.: A new high-resolution stratigraphic and palaeoenvironmental record spanning the End-Permian Mass Extinction and its aftermath in central Spitsbergen, Svalbard, *Palaeogeogr. Palaeoclimatol.*, 554, 109732, <https://doi.org/10.1016/j.palaeo.2020.109732>, 2020.

## Benefits of U.S. Scientific Ocean Drilling Include Science, Policy, and Economy

Beth Christensen, Rowan University, Department of Environmental Science

The International Ocean Discovery Program (IODP) will end in 2024 and so far, the US has not committed to formally continuing the international collaboration that has allowed global geoscience to flourish for decades. Scientific ocean drilling has been uncovering the mysteries of Earth's operating systems for more than 50 years, and the global earth, atmosphere, ocean, and microbiological scientific communities have developed a visionary science plan<sup>1</sup> to continue to unravel the fundamental workings of earth systems at a time when scientific guidance to society is more critical than ever. Over its ~50 years, 12,262 papers related to scientific ocean drilling have been published, with more than half in high impact journals<sup>2</sup>. Yet IODP delivers much more than high-impact science. IODP discoveries inform decision-makers about some of the most important environmental issues facing society today while building intellectual capacity through the promotion of international collaboration, education, and training across universities and governmental agencies in 21 different nations. This scientist-driven endeavor takes a lean approach to facility science, drawing great minds from around the world to study Earth together and leverage global talents for mutual benefit. However, only ECORD and Japan are actively engaged in collaborative planning for the next iteration of this scientist-led and globally significant endeavor. The U.S. geoscience community may soon be isolated from the global collaboration that has for decades provided invaluable scientific insights with practical applications, societal and policy benefits, and desirable economic impacts.

The U.S. operates a globally-ranging research vessel and, in collaboration with Japan and Europe, who operate their

own platforms, drives a global network of ocean drilling capability that greatly benefits U.S. scientists and its citizens.<sup>2,3</sup> U.S.-IODP supports researchers and institutions across the U.S. and, like a James Webb Space Telescope for Earth, delivers spectacular discoveries. IODP results support U.S. science and policy goals such as leveraging international collaboration to provide otherwise inaccessible samples and data to U.S. scientists and improving gender and race balance in the field sciences. The research that can only be performed using scientific ocean drilling materials aligns with the Ocean Policy Committee 2022–2023 Action Plan<sup>4</sup>, providing spatial data necessary for ocean stewardship and management; ensuring a diverse community of ocean drilling scientists and widening opportunities to broaden participation; and, closing knowledge gaps around U.S. EEZ resources such as gas hydrates and freshwater aquifers<sup>5,6</sup>. Scientific ocean drilling has for over 50 years, connected “scientists from more than 600 U.S. institutions, community colleges, industry partners, government labs, museums, and more, representing 50 states...”<sup>2</sup> Since 2015 alone, it directly supported research by scientists and universities in 46 states. Education and outreach connects scientific ocean drilling across the U.S. reaching ~12,500 students annually in ~40 colleges, 100 high schools, and 100 middle schools. In just 2013–2021, 286 different U.S. scientists ranging from graduate students to senior scientists sailed on IODP expeditions with excellent gender balance.

The U.S. further benefits from job creation and other positive economic impacts. The U.S.-IODP, funded by NSF, creates jobs and economic activity across the country.<sup>7</sup> The roughly \$37 million annual budget for U.S.-IODP program activities (separate from the cost of a \$37 million contract for research vessel operation) likely generated an estimated \$66 million of direct, indirect, and induced labor-related economic benefits in 2021 and nearly 900 direct, indirect, and induced jobs across the U.S. Considering further economic impacts associated with additional transactions by related businesses, the near-term value added

by ocean drilling could rise to more than \$100 million. Moreover, these estimates do not reflect additional long-term benefits associated with allied scientific investigations or potential jobs and impact arising from construction of a new vessel. Nor do these estimates include the jobs arising from federal R&D spending on post-expedition investigations.

Through its international cooperation in IODP, the U.S. benefits from enhanced global research opportunities and data needed to build a full understanding of earth systems and the potential impacts on the U.S. and the lives of its citizens. NSF-funded U.S. scientific ocean drilling using its unique research vessel will cease operations in September 2024. While NSF is developing plans for a U.S.-only program, there is not yet any clarity on how that program will operate, or a commitment or planning for a replacement vessel. The discontinuation of the U.S. partnership in global IODP will have far-reaching impacts on U.S. science and society including economy, policy, planning, and scientific outreach and education.

### References and Endnotes

1. <https://www.iodp.org/2050-science-framework>
2. [https://us-soda.org/wp-content/uploads/2022/05/2022-05-16.US-SODA.letter.NSF\\_FINAL.pdf](https://us-soda.org/wp-content/uploads/2022/05/2022-05-16.US-SODA.letter.NSF_FINAL.pdf)
3. [iodp.org](https://www.iodp.org)
4. <https://www.noaa.gov/sites/default/files/2022-06/OPC2022ActionPlan-Summary.pdf>
5. <https://www.state.gov/u-s-extended-continental-shelf-project/>
6. <https://www.federalregister.gov/documents/2019/11/22/2019-25618/ocean-mapping-of-the-united-states-exclusive-economic-zone-and-the-shoreline-and-nearshore-of-alaska>
7. Economic impact analysis provided by Carissa Christensen, a science and technology analyst. Details of this analysis are available upon request.



## ICDP 25<sup>+2</sup> years International Continental Drilling Program

Almost for three decades drilling related to international Earth sciences on the continents is being coordinated by the ICDP. Accordingly, it is time to re-consider accomplishments, look into future scientific targets, and to critically examine the organizational structure of the ICDP.

The IV. International Conference of Continental Scientific Drilling “ICDP in the Second Quarter of its First Century” was convened at the German Research Center for Geosciences GFZ in Potsdam, Germany, July 21-23. 139 invited attendees from 23 countries took part representing the entire range of Earth science disciplines and career stages, including PIs of completed, ongoing and future ICDP drilling projects, members of ICDP panels, representatives from partner organizations and funding agencies, as well as 30 international early-career researchers. Highlights of the past years were presented and the future scientific and programmatic orientation of ICDP was discussed.

The conference program was divided into nine sessions with a mixture of contributions on the four core research themes of the ICDP (Geodynamics, Geohazards, Georesources, Environmental Change) with outlines of achievements and short presentations on new plans and projects, as well as five ‘cross-topics’ on the future organizational direction of the ICDP, funding of major drilling projects, organization of operational support, major new research initiatives related to ICDP, and outreach activities with a focus on early career researchers.

The conference aimed to highlight achievements of the past years and to discuss the scientific outlook and the organization of our program, which included 1) actions to implement the objectives defined in the ICDP Science

Plan 2020-2030, 2) strengthening and expanding ties among member countries and partner organizations, and 3) initiating new measures for a better integration and involvement of early-career researchers in ICDP.

The recommendations of the conference discussions are currently being compiled so that critical suggestions such as improving involvement of early career scientists will be considered and decided on at forthcoming ICDP board meetings.

## Ocean Drilling Legacy Assets Projects (LEAPs): New Proposal Opportunity

Ocean Drilling Legacy Assets Projects (LEAPs) are a new type of project for international and interdisciplinary collaborations under the umbrella of the scientific ocean drilling programs. They are standalone research endeavors that: (1) address at least one aspect of the 2050 Science Framework, and (2) have objectives that maximize the return on the legacy assets of current and past scientific ocean drilling programs without new drilling. Examples of legacy assets are cores, samples, data, open boreholes, and downhole observatories from current and past scientific ocean drilling programs.

Avenues of LEAP research could include, for example, the production of new data from samples, integration of data across multiple expeditions and/or multiple boreholes, incorporation of legacy borehole data with new data, application of a new method or technology that was not available when the legacy assets were collected, or measurements in legacy drillholes to address new problems in innovative and creative ways.

LEAPs do not replace other research mechanisms (e.g., individual proposals to funding agencies for sample requests or data analysis); instead, they are intended to provide a new avenue to facil-

itate collaboration at scales larger than conventional single or multi-proponent research projects. The definition for LEAPs is deliberately broad to provide flexibility for new approaches, integrations, and technology uses that foster coordinated multidisciplinary and international research efforts. LEAPs also provide an opportunity through which researchers can increase the visibility of their research and results.

The proposal deadline is November 1, 2023. For more information on LEAPs and the proposal process, please visit: <https://www.iodp.org/call-for-leap-proposals>.

## Workshop on the future of Scientific Ocean Drill- ing: Towards submission of drilling proposals for IODP<sup>3</sup>

ECORD and Japan, the current IODP platform providers and core members in IODP3, have initiated a process of information on the development of IODP3 and encouragement of new scientific collaborations among the scientific communities of ECORD and Japan together with international partners through a 2-phase Workshop including all Scientific Ocean Drilling partners and covering all scientific themes described in 2050 Science Framework.

The Phase-1 Workshop, conceived as a scientific brokerage event, was held online-only in January 2023, with a participation of up to 191 scientists from all over the world. Break-out session discussion addressed the themes Climate Change and Ocean Health, Deep Earth, Geohazards, Deep Life. It resulted in identification of a large number of scientific topics suitable for new MSP and Chikyu scientific drilling proposals (<https://www.ecord.org/workshop-on-the-future-of-scientific-ocean-drilling/>).

The Phase-2 Workshop will be held in person and virtual (hybrid) from 18 to 20 March 2024 in Nachikatsuura, Kii Peninsula, Japan, jointly organized by J-DESC and ESSAC, and hosted by J-DESC.

<https://www.ecord.org/workshop-on-the-future-of-scientific-ocean-drilling-with-msps-and-chikyu-phase-2/>

The aim is to gather researchers representing promising drilling ideas that emerged during and after Phase-1 Workshop to present and discuss their scientific and operational plans to prepare for MSP and Chikyu drilling proposals to be submitted to IODP3.

The Workshop is open to ~100 in-person participants from any country. The involvement of researchers with project ideas for Land-to-Sea drilling proposals to be implemented jointly with ICDP is particularly welcome.

Pre-registrations are open. Follow the ECORD and J-DESC web pages for updates.

<https://www.ecord.org/>

<https://j-desc.org/eng/>

Angelo Camerlenghi and Masa Kinoshita (Co-Chairs)

Sanny Saito and Hanno Kinkel (ESSAC and J-DESC PMO representatives)

The whole Steering Committee

## The International Ocean Drilling Programme (IODP<sup>3</sup>)

The International Ocean Drilling Programme (IODP3) will start on January 1st 2025, soon after the conclusion of the current International Ocean Discovery Program.

IODP3 will consist of a fully international scientific collaboration inspired by the '2050 Science Framework: Exploring Earth by Scientific Ocean Drilling'.

IODP3 will adopt a transparent, open, flexible and international modus operandi, adopting program-wide standard

policies and guidelines, sustainable management and publicly accessible knowledge-based resources.

IODP3 will be open to participation of any entities that can access IODP3 through three membership levels involving various financial contributions:

- Core Members that are represented by platform providers (currently ECORD and JAMSTEC).

- Associate Members that will make regular cash contributions to IODP3 ( $\pm 1$  M€) and not regularly provide scientific ocean drilling platform(s) to IODP3; Associate Members may increase their participation rights by providing additional cash and/or in-kind contributions.

- Temporary Members that will provide cash and/or project-based in-kind contributions (minimum  $\pm 0.5$  M€) to access IODP expedition(s) and/or other service(s), and not regularly providing scientific ocean drilling platform(s) to IODP3.

IODP3 will conduct offshore expeditions of flexible duration that will be implemented by the ECORD Science Operator (ESO) and/or JAMSTEC-MarE3, following an expanded Mission Specific Platform (MSP) concept. A wide array of drilling and coring technologies (riser and riserless drilling, lift boats/barges deploying land-based drilling technology, seabed drilling, long piston coring) will be applied to all drilling environments, as determined by scientific priorities, operational efficiency and better value for money. Offshore operations will include land-to-sea transects that will be implemented in collaboration with the International Continental scientific Drilling Program (ICDP).

IODP3 will also fund Scientific Projects using Ocean Drilling ARCHives (SPARCs) that are international and multidisciplinary large-scale research projects that may address any aspect of the 2050 Science Framework and have objectives originating from, or that are based on ocean drilling archives (i.e.,

cores, samples and data).

Drilling/coring and SPARC proposals will be evaluated by the Science Evaluation Panel before being potentially selected and scheduled by the MSP Facility Board.

The overall size of the Science Parties for offshore expeditions and SPARCs will be flexible and be adapted to project needs, thus providing additional scientific and participation opportunities.

Gilbert Camoin,

Director of the ECORD Managing Agency

Nobu Eguchi,

Director of Operations Dept MarE3 JAMSTEC

On behalf of the

ECORD-Japan Scientific Ocean Drilling Working Groups

## Schedules

**IODP** – Expedition schedule <http://www.iodp.org/expeditions/>



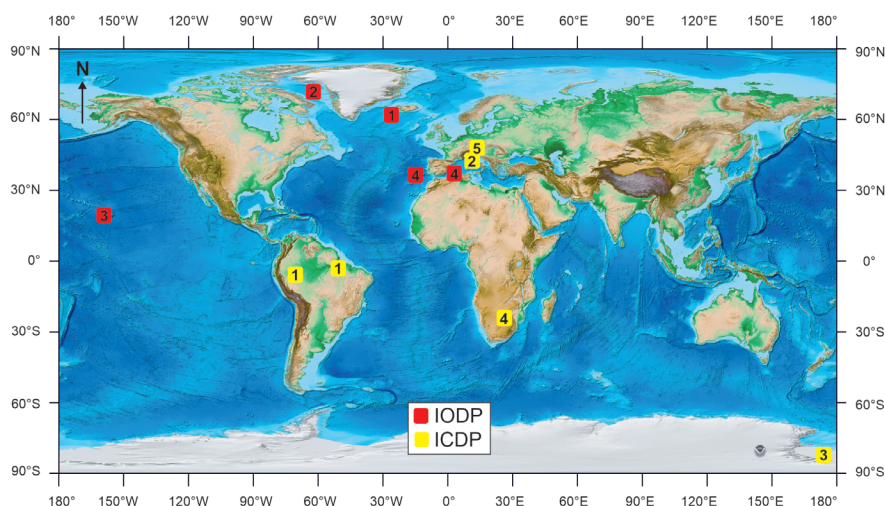
USIO operations	Platform	Dates	Port of origin
<b>1</b> Reykjanes Mantle Convection and Climate (Exp 395)	JOIDES Resolution	Jun 12–Aug 12, 2023	Ponta Delgada
<b>2</b> NW Greenland Glaciated Margin (Exp 400)	JOIDES Resolution	Aug 12–Oct 12, 2023	Reykjavik
<b>3</b> Hawaiian Drowned Reefs (Exp 389)	MSP	Aug 29–Oct 31, 2023	Honolulu
<b>4</b> Mediterranean-Atlantic Gateway Exchange (Exp 401)	JOIDES Resolution	Dec 10, 2023–Feb 9, 2024	Amsterdam



**ICDP** – Project schedule <http://www.icdp-online.org/projects/>

ICDP project	Drilling dates	Location
<b>1</b> Trans-Amazon Drilling Project (TADP)	Jun 2023–Feb 2024	Brazil (Acre and Marajo Basins)
<b>2</b> Drilling the Ivrea-Verbano ZonE (DIVE)	Oct–Dec 2023	Northern Italy (Megolo)
<b>3</b> Sensitivity of the West Antarctic Ice Sheet to 2 Degrees Celsius (SWAIS 2C)	Dec 2023–Feb 2025	Western Antarctica (Ross Ice Shelf)
<b>4</b> Bushveld Drilling Project (BVDP)	Nov 2023–Aug 2024	South Africa (Mpumalanga, Limpopo)
<b>5</b> Eger Rift Drilling Project (EGER)	Spring 2024	Germany (Neualbenreuth)

## Locations



Topographic/bathymetric maps courtesy of NOAA (Amante, C. and B.W. Eakins, 2009. ETOPO1 1 Arc-Minute Global Relief Model: Procedures, Data Sources and Analysis. NOAA Technical Memorandum NESDIS NGDC-24. National Geophysical Data Center, NOAA. doi:10.7289/V5C8276M).